

## **Copyright Notices**

### **Notice 1**

Under the Copyright Act 1968, this thesis must be used only under the normal conditions of scholarly fair dealing. In particular no results or conclusions should be extracted from it, nor should it be copied or closely paraphrased in whole or in part without the written consent of the author. Proper written acknowledgement should be made for any assistance obtained from this thesis.

### **Notice 2**

I certify that I have made all reasonable efforts to secure copyright permissions for third-party content included in this thesis and have not knowingly added copyright content to my work without the owner's permission.

**GENERATION AND CHARACTERISATION  
OF A HUMAN EMBRYONIC STEM CELL-  
DERIVED DEVELOPMENTAL MODEL OF  
THE HUMAN FEMALE REPRODUCTIVE  
TRACT EPITHELIUM**

Louie Ye

Bachelor of Applied Science (Honours I)

The Ritchie Centre

Monash Institute of Medical Research

Department of Obstetrics and Gynaecology

Monash University

Melbourne, Australia

**Submitted to fulfil the requirements for the degree of Doctor of Philosophy**

**August 2011**

# Table of Contents

ABSTRACT .....	VIII
GENERAL DECLARATION .....	X
STRUCTURE OF THESIS .....	XI
LIST OF PUBLICATIONS AND ABSTRACTS .....	XII
ACKNOWLEDGMENTS .....	XIII
ABBREVIATIONS .....	XIV
<b>CHAPTER 1 INTRODUCTION .....</b>	<b>1</b>
1.1 DEVELOPMENT OF THE MÜLLERIAN DUCT AND UTERUS .....	1
1.1.1 <i>Origin of the Müllerian Ducts</i> .....	1
1.1.2 <i>Three phases of the Müllerian duct formation</i> .....	2
1.1.3 <i>Formation of the uterus from Müllerian ducts</i> .....	4
1.1.4 <i>Maturation of the uterus</i> .....	5
1.1.4.1 Laboratory rodents .....	6
1.1.4.2 Domestic Animals .....	7
1.1.4.3 Humans .....	7
1.2 MOLECULAR GENETICS OF MÜLLERIAN DUCT FORMATION .....	8
1.2.1 <i>Homeodomain transcription factors</i> .....	8
1.2.2 <i>Signalling molecules</i> .....	9
1.3 MOLECULAR GENETICS OF MÜLLERIAN DUCT DIFFERENTIATION: REGION SPECIFIC CELL FATE DETERMINATION .....	12
1.3.1 <i>Hox genes and Müllerian duct differentiation</i> .....	12
1.3.2 <i>Wnt signalling pathway</i> .....	13
1.4 POSTNATAL ENDOMETRIAL DEVELOPMENT AND REMODELLING .....	15
1.4.1 <i>ECM components and regulation</i> .....	15
1.4.1.1 Glycoaminoglycans .....	15
1.4.1.2 Matrix metalloproteinase and Connective tissue growth factor .....	15
1.4.2 <i>Mesenchyme derived growth factors</i> .....	16
1.4.2.1 FGF, HGF and IGF .....	16
1.4.2.2 Wnt signalling pathway .....	17

1.4.2.3	Bone morphogenetic proteins.....	17
1.4.3	<i>Hormones</i> .....	18
1.5	BIOLOGY OF THE ADULT HUMAN ENDOMETRIUM: STRUCTURE, HORMONE REGULATION AND CYCLIC REGENERATION.....	19
1.5.1	<i>Menstrual stage specific endometrial morphological and biochemical features</i> .....	20
1.5.2	<i>Ovarian hormone receptors in the human endometrium</i> .....	21
1.5.3	<i>Endometrial regeneration</i> .....	22
1.5.3.1	Endometrial Stem/Progenitor Cells.....	22
1.5.3.2	Persistent expression of developmental factors.....	22
1.6	UTERINE ABNORMALITIES WITH FETAL ORIGINS .....	24
1.7	THE NEED FOR A DEVELOPMENTAL MODEL OF HUMAN FEMALE REPRODUCTIVE TRACT.....	26
1.7.1	<i>Tissue recombination and in vivo modelling</i> .....	26
1.7.1.1	Tissue recombination methods .....	27
1.7.2	<i>Technological advances in tissue recombination</i> .....	28
1.8	PLURIPOTENT STEM CELLS: HUMAN EMBRYONIC STEM CELLS .....	30
1.8.1	<i>Cultivation of hESC</i> .....	31
1.8.1.1	Current hESC culture systems.....	31
1.8.1.2	Embryoid body formation .....	32
1.8.2	<i>Lineage Specific Differentiation of hESC</i> .....	32
1.8.3	<i>Pathways of Mesoderm induction</i> .....	34
1.8.3.1	Molecular pathways regulating mesoderm formation.....	34
1.8.4	<i>Role BMP and Wnt family molecules in animal models and mESC differentiation systems</i> .....	36
1.8.4.1	BMP ligands .....	36
1.8.4.2	Wnt family ligands .....	36
1.8.4.3	Activin/Nodal .....	37
1.8.4.4	Interaction between signalling pathways.....	37
1.8.4.5	Role of ECM and mesoderm induction .....	38
1.8.5	<i>Primitive streak and mesoderm induction in hESC differentiation systems</i> .....	38
1.9	HYPOTHESES AND AIMS .....	41
1.9.1	<i>Hypotheses</i> .....	41
1.9.2	<i>Aims</i> .....	41



## **CHAPTER 2 DEVELOPMENT OF A METHOD TO GENERATE HUMAN FEMALE REPRODUCTIVE TRACT EPITHELIUM FROM HUMAN EMBRYONIC STEM CELLS 42**

2.1	INTRODUCTION .....	42
2.2	METHODS .....	44
2.2.1	<i>Animals</i> .....	44
2.2.2	<i>Micro-dissection of neonatal uterine mesenchyme</i> .....	44
2.2.3	<i>hESC culture</i> .....	45
2.2.4	<i>Generation of heterotypic tissue recombinants</i> .....	45
2.2.5	<i>Kidney capsule transplantation, in vivo imaging and tissue processing</i> .....	46
2.2.6	<i>Immunocytochemistry</i> .....	46
2.3	RESULTS .....	48
2.3.1	<i>Pluripotency of MEL-1 cells</i> .....	48
2.3.2	<i>Tissue recombination in vitro: MEL-1 with nMUM</i> .....	48
2.3.3	<i>Morphological analysis of the MEL-1/nMUM recombinant graft</i> .....	50
2.3.4	<i>Tissue recombination of nMUM with ENVY</i> .....	53
2.3.5	<i>Efficiency and macroscopic appearance of recombinant grafts</i> .....	56
2.3.6	<i>Real time imaging of ENVY grafts</i> .....	59
2.4	DISCUSSION .....	60
2.4.1	<i>Instructive interaction between nMUM and hESC</i> .....	60
2.4.2	<i>Off target differentiation</i> .....	60
2.4.3	<i>Immune rejection and cell death</i> .....	61
2.4.4	<i>Other strategies to increase efficiency and reproducibility of the in vivo model</i> .....	62
2.4.5	<i>Conclusion</i> .....	63

## **CHAPTER 3 GENERATION OF HUMAN FEMALE REPRODUCTIVE TRACT EPITHELIUM FROM HUMAN EMBRYONIC STEM CELLS..... 66**

3.1	SUPPLEMENTARY FIGURES .....	77
-----	-----------------------------	----

## **CHAPTER 4 LIM1/LIM1 IS EXPRESSED IN DEVELOPING AND ADULT MOUSE AND HUMAN ENDOMETRIUM ..... 83**

4.1	INTRODUCTION .....	84
4.2	METHODS .....	86
4.2.1	<i>Animals</i> .....	86

4.2.2	<i>Tissue recombination and graft transplantation</i> .....	86
4.2.3	<i>Human and Mouse tissue collection</i> .....	86
4.2.4	<i>Tissue culture</i> .....	87
4.2.5	<i>Immunofluorescence</i> .....	87
4.2.6	<i>Quantification of LIM1<sup>+</sup> cells in human endometrium</i> .....	88
4.2.7	<i>Quantitative real time-PCR</i> .....	88
4.2.8	<i>Statistical Analysis</i> .....	89
4.3	RESULTS .....	90
4.3.1	<i>LIM1 expression in the human developmental reproductive tract model</i> .....	90
4.3.2	<i>LIM1 expression in human uterine tissue</i> .....	91
4.3.3	<i>Lim1 expression in mouse uterine tissue</i> .....	92
4.3.4	<i>LIM1 expression in human endometrial cancer tissue and cell lines</i> .....	94
4.4	DISCUSSION .....	95
4.5	SUPPLEMENTARY INFORMATION .....	97

<b>CHAPTER 5 IDENTIFICATION OF MESENCHYME-DERIVED GROWTH FACTORS</b>		
<b>DIRECTING HESC DIFFERENTIATION .....</b>		<b>100</b>
5.1	INTRODUCTION .....	100
5.2	METHODS .....	102
5.2.1	<i>Animals</i> .....	102
5.2.2	<i>Tissue Recombination, RNA extraction and Microarray</i> .....	102
5.2.3	<i>Microarray analysis</i> .....	103
5.2.4	<i>Gene ontology (GO)</i> .....	104
5.2.5	<i>PCR</i> .....	104
5.2.6	<i>Immunohistochemistry</i> .....	105
5.2.7	<i>Statistical Analysis</i> .....	105
5.3	RESULTS .....	106
5.3.1	<i>Genes upregulated in mesenchyme during hESC differentiation</i> .....	106
5.3.2	<i>Endogenous CTGF is expressed in hESC derived embryoid body</i> .....	110
5.3.3	<i>Role of exogenous CTGF on EB differentiation</i> .....	113
5.4	DISCUSSION .....	115
5.4.1	<i>Genes coding for mesenchyme-derived growth factors</i> .....	115
5.4.2	<i>Expression and role of CTGF in hESC differentiation</i> .....	116
5.4.3	<i>Limitations and future studies</i> .....	117

5.4.4 Conclusion.....	118
5.5 SUPPLEMENTARY INFORMATION .....	119
<b>CHAPTER 6 GENERAL DISCUSSION .....</b>	<b>121</b>
6.1 DEVELOPMENT OF METHODS TO DIFFERENTIATE HUMAN FRT EPITHELIUM FROM hESC .	123
6.2 GENERATION OF HUMAN FEMALE REPRODUCTIVE TRACT EPITHELIUM FROM hESC .....	125
6.3 EXPRESSION OF TRANSCRIPTION FACTOR LIM1/LIM1 IN MOUSE AND HUMAN ENDOMETRIUM .....	126
6.4 IDENTIFICATION OF MESENCHYME-DERIVED GROWTH FACTORS INVOLVED IN hESC DIFFERENTIATION .....	127
6.5 LIMITATIONS OF THIS INVESTIGATION .....	128
6.6 FUTURE APPLICATIONS AND FURTHER STUDIES .....	131
6.7 CONCLUSION .....	133
<b>BIBLIOGRAPHY.....</b>	<b>134</b>

## **Figures**

FIGURE 1.1 COELOM FORMATION FROM THE LATERAL PLATE.....	2
FIGURE 1.2 THREE PHASE MODEL FOR MÜLLERIAN DUCT DEVELOPMENT .....	3
FIGURE 1.3 HUMAN MÜLLERIAN DUCT AND WOLFFIAN DUCT.....	3
FIGURE 1.4 MAMMALIAN FEMALE REPRODUCTIVE TRACT .....	4
FIGURE 1.5 DIFFERENTIATION AND MATURATION OF THE MOUSE MÜLLERIAN DUCTS .....	5
FIGURE 1.6 TIME LINE HIGHLIGHTING KEY EVENTS DURING POSTNATAL UTERINE ADENOGENESIS IN MAMMALS .....	6
FIGURE 1.7 HOX GENE EXPRESSIONS IN FRT .....	13
FIGURE 1.8 THE CHANGING STRUCTURE OF THE HUMAN UTERUS DURING THE MENSTRUAL CYCLE. ...	19
FIGURE 1.9 CILIATED ENDOMETRIAL EPITHELIUM .....	21
FIGURE 1.10 DERIVATION OF HUMAN EMBRYONIC STEM CELLS AND VARIOUS DIFFERENTIATION STRATEGIES .....	33
FIGURE 1.11 ESC DIFFERENTIATION <i>IN VITRO</i> .....	35
FIGURE 2.1 ASSESSMENT OF PLURIPOTENCY OF MEL-1 hESCs .....	49
FIGURE 2.2 TISSUE RECOMBINATION OF MEL-1 hESC WITH nMUM .....	50
FIGURE 2.3 MORPHOLOGICAL ANALYSIS OF MEL-1 nMUM/hESC RECOMBINANT GRAFTS.....	52

FIGURE 2.4 CYSTIC GROWTHS FROM ENVY-DERIVED EMBRYOID BODIES TRANSPLANTED UNDER THE CAPSULE OF NOD.SCID MOUSE KIDNEY .....	53
FIGURE 2.5 MORPHOLOGICAL ANALYSIS OF ENVY/NMUM TISSUE RECOMBINANTS .....	54
FIGURE 2.6 WORK FLOW: FROM TISSUE RECOMBINATION TO ANALYSIS .....	56
FIGURE 2.7 MACROSCOPIC APPEARANCE OF VARIOUS GRAFTS .....	58
FIGURE 2.8 NON-INVASIVE <i>IN VIVO</i> IMAGING OF TRANSPLANTED ENVY hESC .....	59
FIGURE 4.1 LIM1 EXPRESSION IN hESC-DERIVED HUMAN FEMALE REPRODUCTIVE EPITHELIUM.....	90
FIGURE 4.2 LIM1 EXPRESSION IN NORMAL ADULT HUMAN ENDOMETRIAL TISSUE .....	92
FIGURE 4.3 LIM1 EXPRESSION IN NEONATAL AND ADULT MOUSE UTERINE TISSUE .....	93
FIGURE 4.4 LIM1 EXPRESSION IN HUMAN ENDOMETRIAL CANCER CELL LINES.....	94
FIGURE 5.1 SCHEMATIC DIAGRAM OF EXPERIMENTAL DESIGN: PART 1 .....	103
FIGURE 5.2 EUCLIDIAN DISTANCE HIERARCHICAL CLUSTERING OF SAMPLES.....	107
FIGURE 5.3 EXPRESSION OF CTGF IN RECOMBINANT MESENCHYME .....	109
FIGURE 5.4 SCHEMATIC DIAGRAM OF EXPERIMENTAL DESIGN: PART 2 .....	110
FIGURE 5.5 ENDOGENOUS EXPRESSION OF CTGF IN DIFFERENTIATING EBS .....	111
FIGURE 5.6 FOLD CHANGE OF IN GENE EXPRESSION IN DIFFERENTIATING EBS FOLLOWING ANTI-CTGF ANTIBODY TREATMENT.....	113
FIGURE 5.7 GENE EXPRESSION OF DIFFERENTIATING EBS FOLLOWING TREATMENT WITH CTGF .....	114

## **TABLES**

TABLE 1.1 GENES INVOLVED IN FORMATION AND PATTERNING OF THE MÜLLERIAN DUCTS.....	11
TABLE 2.1 TECHNICAL CONSIDERATIONS OF hESC LINES USED .....	55
TABLE 2.2 MACROSCOPIC DESCRIPTIONS OF GRAFT TYPES.....	57
TABLE 5.1 NUMBER OF DIFFERENTIALLY UPREGULATED GENES BETWEEN TIME POINTS .....	108
TABLE 5.2 CANDIDATE MOUSE GENES EXPRESSED IN GENE ONTOLOGY TERMS ASSOCIATED WITH GROWTH FACTORS, PROTEINACEOUS EXTRACELLULAR MATRIX AND CELL DIFFERENTIATION ..	108

## **Supplementary Information**

SUPPLEMENTARY FIGURE 3.1.1 .....	77
SUPPLEMENTARY FIGURE 3.1.2 .....	78
SUPPLEMENTARY FIGURE 3.1.3 .....	78
SUPPLEMENTARY FIGURE 3.1.4 .....	79
SUPPLEMENTARY FIGURE 3.1.5 .....	80
SUPPLEMENTARY FIGURE 3.1.6 .....	81
SUPPLEMENTARY FIGURE 4.5.1 .....	98
SUPPLEMENTARY FIGURE 4.5.2 .....	99
SUPPLEMENTARY TABLE 4.5.1 PRIMARY ANTIBODY .....	97
SUPPLEMENTARY TABLE 5.5.1 CANDIDATE GENES EXPRESSED IN GENE ONTOLOGY TERMS ASSOCIATED WITH GROWTH FACTOR ACTIVITY IN nMUM ALONE GROUP .....	119
SUPPLEMENTARY TABLE 5.5.2 PRIMER SEQUENCES .....	120

## **Abstract**

Following the discovery of human embryonic stem cells (hESC), much effort has focused on their *in vitro* differentiation to therapeutically relevant cell types. Tissue recombination technology enabled recombination of embryonic stem cells with organ specific mouse mesenchyme for organogenesis *in vivo*. These differentiation strategies have also enabled researchers to gain an insight into human organ development previously not possible. The aim of this study was to establish a model of human female reproductive tract (FRT) epithelium to gain a better understanding of its development.

A two-stage method was developed that recombined hESC with neonatal mouse uterine mesenchyme (nMUM) for development *in vitro* and then *in vivo*. *In vitro* recombination experiments showed that hESC-derived embryoid bodies (EBs) from two separate human embryonic stem cell lines (ENVY and MEL-1) fused together with nMUM as a recombinant structure *in vitro*. Following transplantation of the recombinant grafts *in vivo* into NOD.SCID mice, nMUM was able to direct hESCs to differentiate into epithelial structures (simple columnar ciliated epithelium) within small teratoma-like growths. The established model required further modifications to improve success rate. More importantly, a detailed characterisation was required to confirm the identity of the hESC derived epithelium.

To increase the reproducibility of the established model, exogenous growth factors (BMP4 and Activin A) were added *in vitro* to enhance hESC survival. A new strain of severely immunodeficient mice was used for hosting recombinant grafts to increase viability of hESC *in vivo*. A comprehensive characterisation of the established model was carried out from the earliest stage of hESC differentiation (day 3 *in vitro*) to 8 weeks after transplantation by immunohistochemical and molecular methods. The expression of a panel of morphological (cilia, columnar/cuboidal morphology, CK18) and functional markers (Estrogen receptor, Ki-67 and Glycodelin A) confirmed that by week 8 of *in vivo* incubation, hESC derived FRT-like epithelium (surrounded by mouse uterine stroma) had characteristics similar to human adult upper FRT epithelium of the oviduct or endometrium. At early *in vivo* stages (week 2 and 4), temporally regulated expression of developmental homeodomain transcription factors (HOXA10, PAX2) recapitulated key events during FRT organogenesis. Moreover, nMUM was demonstrated for the first time to induce formation of primitive streak-like cells and upregulate

mesoderm/endoderm gene expression in differentiating hESC-derived embryoid bodies (EBs) *in vitro*.

Using the established hESC-derived FRT model, the ontogeny of a particular transcription factor, LIM1 was examined. The expression of the LIM1 protein in the hESC-derived FRT model instigated a novel investigation into the expression of LIM1 into human adult uterine tissue as well as human endometrial cancer cell lines. The findings of this investigation contradicts a previous notion that Lim1 is not expressed in adult FRT. Interestingly, the evolutionarily conserved expression of Lim1 was also detected in neonatal and adult mouse uterus using immunofluorescence and real time polymerase chain reaction (PCR) methods.

Based on evidence of the inductive capabilities of the nMUM mentioned above, a microarray investigation was conducted to identify genes coding for mesenchyme-derived growth factors involved in hESC differentiation. Connective tissue growth factor (CTGF) was identified and confirmed by immunofluorescence and real time PCR in the nMUM. The presence of endogenous CTGF in the recombinant EBs, however, further complicated the investigation. Functional analysis into endogenous CTGF in the EB and the action of exogenous CTGF revealed that the production of the growth factor is dependent on initial formation of primitive streak-like cells in the EBs. Furthermore, CTGF may be involved in epithelial-mesenchymal transition (EMT) as well as mesoderm differentiation in EBs.

The model established in this study provides a platform for future studies to explore various aspects of human FRT development, or as an alternative strategy for hESC differentiation using organ specific animal mesenchyme. The model may one day be used to study the detrimental effects of endocrine disruptors on human FRT development. Furthermore, the presence of the Lim1/LIM1 in adult reproductive tract shows the persistent expression of yet another developmental homeodomain transcription factor in the adult mouse and human uterus, further highlighting the complex transcriptional factor network regulating adult endometrial remodelling.

## **General Declaration**

### **Monash University**

Monash Research Graduate School

Declaration for thesis based or partially based on conjointly published or unpublished work

**In accordance with Monash University Doctorate Regulation 17/ Doctor of Philosophy and Master of Philosophy (MPhil) regulations the following declarations are made:**

**I hereby declare that this thesis contains no material which has been accepted for the award of any other degree or diploma at any university or equivalent institution and that, to the best of my knowledge and belief, this thesis contains no material previously published or written by another person, except where due reference is made in the text of the thesis.**

This thesis includes 1 original paper published in peer reviewed journals and 1 unpublished publication. The core theme of the thesis is generation of human female reproductive tract epithelium from human embryonic stem cells. The ideas, development and writing up of all the papers in the thesis were the principal responsibility of myself, the candidate, working within the Ritchie Centre for Women's Health, Monash Institute of Medical Research under the supervision of Associate Professor Caroline Gargett.

**The inclusion of co-authors reflects the fact that the work came from active collaboration between researchers and acknowledges input into team-based research.**

In the case of Chapter 3 and 4, my contribution to the works involved the following:

Thesis chapter	Publication title	Publication status	Nature and extent of candidate's contribution
Chapter 3	Generation of human female reproductive tract epithelium from human embryonic stem cells	Published	Design, performing all experiments, collecting and analysing data for all figures, manuscript writing
Chapter 4	Lim1/LIM1 is expressed in developing and adult mouse and human endometrium	Submitted	Design, performing all experiments, collecting and analysing data for all figures, manuscript writing

Signed: .....

Date: .....



## **Structure of Thesis**

In compliance with Monash University Doctorate Regulation, this thesis consists of published and unpublished works relating to “A human embryonic stem cell- derived developmental model of the human female reproductive tract epithelium”.

**Chapter 1** – *Introduction*. Written as a chapter

**Chapter 2** - *Development of a method to generate human female reproductive tract epithelium from human embryonic stem cells*. Written as a chapter

**Chapter 3** - *Generation of human female reproductive tract epithelium from human embryonic stem cells*. Presented as a published manuscript in PloS One

**Chapter 4** - *Lim1/LIM1 is expressed in developing and adult mouse and human endometrium*.  
Written as a manuscript, submitted for publication

**Chapter 5** - *Identification of mesenchyme-derived growth factors directing hESC differentiation*.  
Written as a chapter

**Chapter 6** - *Discussion*. Written as a chapter

## ***List of Publications and abstracts***

### **Peer reviewed publication relating to the thesis**

**Ye, L.**, Mayberry, R., Lo, C., Britt, K., Stanley, E., Elefanty, A., Gargett, C. Generation of human female reproductive tract epithelium from human embryonic stem cells. PloS One. 2011. 6(6): p. e21136.

### **Submitted**

**Ye, L.**, Gargett, C. Lim1/LIM1 is expressed in developing and adult mouse and human endometrium. Submitted to The Journal of Histochemistry and Cell Biology

### **Conference Abstracts**

#### ***International***

**Ye, L.**, Mayberry, R., Lo, C., Stanley, E., Elefanty, A., Gargett, C. Differentiation of human embryonic stem cells to Mullerian tissue. 8<sup>th</sup> annual meeting of the International Society for Stem Cell Research. June 2010. (poster presentation)

#### ***National***

**Ye, L.**, Mayberry, R., Lo, C., Stanley, E., Elefanty, A., Gargett, C. Differentiation of human embryonic stem cells to Mullerian tissue. Endocrine Society of Australia (ESA) & Society of Reproductive Biology (SRB) annual scientific meeting, August 2010. (oral presentation)

**Ye, L.**, Mayberry, R., Lo, C., Stanley, E., Elefanty, A., Gargett, C. In Vivo Differentiation of Human Embryonic Stem Cells to Uterine Tissue. Endocrine Society of Australia (ESA) & Society of Reproductive Biology (SRB) annual scientific meeting. August 2009. (oral presentation)

### **Other peer reviewed publications during PhD**

Kaitu'u-Lino, T., **Ye, L.**, Gargett, C. Re-epithelialization of the uterine surface arises from endometrial glands: evidence from a functional mouse model of breakdown and repair. Endocrinology, July 2010, 151 (7):3386-3395

## ***Acknowledgments***

There are a number of people that I would like to thank for their help and support over the years, without whom, I would not have succeeded in finishing.

First and foremost, my mentor and supervisor, Associate Professor Caroline Gargett, thank you for introducing the world of cutting edge biomedical research to me. I am most grateful for your advice and guidance during my candidature. The duration of my PhD was short but I have learnt from you will be with me for a life time.

Secondly, I like to thank my partner Amita Surti, and my parents for unconditional support throughout my PhD. And the Father's Club for the weekend laughs. You were the light in my darkest hours.

I owe special thanks to many people from several laboratories; Monash Immunology & Stem Cell Laboratory (MISCL), Robyn Mayberry for provision of human embryonic stem cells, Professor Andrew Elefanty and Professor Ed Stanley for their contribution in experiment design and manuscript corrections. From Monash Imaging, Dr. Camden Lo for his work on image stacking and all the great tips on immunohistochemistry. From Department of Anatomy and Developmental Biology, Dr Renea Taylor for the most crucial tips on setting up the model described in this thesis and Dr Kara Britt for her help with microarray analysis. Over at the Monash Institute of Medical Research (MIMR), I would like to thank those from the Centre for Reproduction/Development (CRD), including Karen Jones for teaching me the art of stem cell culture and Dr Paul Verma for initially providing facilities/equipments to culture human embryonic stem cells. Also from the Cancer Research Centre (CRC) Dr Elizabeth Williams for the use of in vivo imaging machine.

Last but not least, I want thank everyone from my laboratory past and present. First, Dr. Tu'uheva ha Kaituulino for the best advice on all things. Dr. Rachel Chan for teaching me mouse uterine dissection, Dr. Sonya Hubbard, lessons on kidney capsule transplantation, Charmaine Tan, Hong Ngyuen and Dr. Hirotaka Masuda for tips on tissue culture. Also Isabella Ciurej for administrative support throughout my PhD.

## ***Abbreviations***

3D	Three dimensional
°C	Degrees Celsius
$\alpha$ SMA	Alpha smooth muscle actin
$\beta$ -catenin	beta-catenin
$\Delta\Delta C_t$	delta-delta Comparative threshold
$\mu$ g	microgram
$\mu$ l	microlitre
Ab	Antibody
ASCs	Adult Stem Cells
AMH	Anti-Müllerian Hormone
AMHR2	Anti-Müllerian Hormone Receptor 2
BMSC	Bone Marrow Stromal Cell
BMP	Bone morphogenetic protein
BPA	Bisphenol-A
BrdU	Bromodeoxyuridine
BSA	Bovine Serum Albumin
CA	Cancer Antigen
CD44	Cell surface glycoprotein 44
cDNA	complimentary Deoxyribonucleic acid
CK	Cytokeratin
CTGF/Ctgf	Connective tissue growth factor
Dlgh1	discs, large homolog 1
DES	Diethylstilbestrol
DMEM	Dulbecco's Modified Eagle Medium

DNA	Deoxyribonucleic Acid
DNAse	Deoxyribonuclease
DPBS	Dulbecco's Phosphate Buffered Saline
EB	Embryoid Body
ECAD	E-Cadherin
ER	Estrogen receptor
ECM	Extracellular Matrix
EMX2	Empty spiracles-like protein 2
EMT	Epithelial-Mesenchymal Transition
ESC	Embryonic stem cell
FBS	Fetal Bovine Serum
FCS	Fetal Calf Serum
FGF	Fibroblast growth factor
FITC	Fluorescein isothiocyanate
FOXA2	Forkhead box protein A2
FRT	Female reproductive tract
GAGs	Glycoaminoglycans
GdA	Glycodelin A
GDF	Growth differentiation factors
GFP	Green fluorescent protein
GSC	Goosecoid
GAPDH	Glyceraldehyde 3-phosphate dehydrogenase
H <sub>2</sub> O	Water
H <sub>2</sub> O <sub>2</sub>	Hydrogen Peroxide
H&E	Haematoxylin and Eosin

hESC	Human embryonic stem cell
HGF	Hepatocyte growth factor
HNF1	Hepatocyte nuclear factor 1 homeobox B
HOXA10	Homeobox A10
Hoxb1	Homeobox B1
HPO	Hypothalamus-pituitary-ovary
hrs	Hours
Ig	Immunoglobulin
IGF	Insulin-like growth factor
IGFBP	Insulin-like growth factor binding protein
IL	Interleukin
KDR	Kinase insert domain receptor
LIF	Leukemia Inhibitory Factor
LIM1	Lim homeobox protein 1
Lrp5/6	Low density lipoprotein receptor-related protein
MEF	Mouse embryonic fibroblast
mESC	mouse embryonic stem cells
mg	milligram
ml	millilitre
MIXL1	MIX1 homeobox-like protein 1
MMPs	Metalloproteinases
MMMT	Mixed Müllerian Malignant Tumour
MRKH	Mayer Rokitansky Kuster Hauser syndrome
nMUM	Neonatal mouse uterine mesenchyme
MHC	Major histocompatibility complex class

Msx1	homeo box, msh-like 1
MUC1	Mucin 1, cell surface associated
n	number of samples
NOD/SCID	Non-Obese Diabetic/Severe Combined Immunodeficiency
NSG	NOD.SCID gamma
OCT4 (POU5F1)	Octamer-binding transcription factor 4
OSR1	Odd-skipped-1
P1	Postnatal Day 1
PAX2	Paired box gene 2
PBS	Phosphate Buffer Saline
PFA	Paraformaldehyde
PDGFR	Platelet-derived growth factor receptor
PR	Progesterone receptor
PS	Primitive streak
PRL	Prolactin
PCR	Polymerase chain reaction
RAR	Retionic acid receptor
rH	recombinant Human
RNase	Ribonuclease
SCC	Spermatogonial Stem Cells
SCF	Stem cell factor
SCID	Severe combined immunodeficiency
SEM	Standard Error Mean
SiRNA	Small interfering RNA
SNAI1	Snail homolog 1

SLUG	Snail homolog 2
Sry	Sex determining region Y
SSEA	Stage specific embryonic antigen
TBP	TATA box binding protein
TCF2 (HNF1)	Transcription factor 2
TGF- $\beta$	Transforming growth factor beta
TIMPs	Tissue inhibitors of metalloproteinases
VIM	Vimentin
VEGF	Vascular endothelial growth factor
vs	Versus
Wg	Wingless



## CHAPTER 1 Introduction

### ***1.1 Development of the Müllerian duct and uterus***

The Müllerian ducts give rise to the uterus late in gestation. Little is known about the events preceding the formation of the Müllerian ducts. Much of what is known about fetal and postnatal Müllerian duct and uterine development comes from animal models. Few studies have examined the development of the human Müllerian ducts.

#### **1.1.1 Origin of the Müllerian Ducts**

A series of events during early embryogenesis lead to the formation of precursors of the Müllerian ducts. At one of the earliest developmental stages, during gastrulation, the primitive streak gives rise to the lateral plate mesoderm [1]. The lateral plate mesoderm separates into somatic and splanchnic mesoderm, the former subsequently contributes to the formation of the coelomic epithelium of pericardium, pleura and the peritoneum whilst the latter contributes to formation of internal organs [2]. After folding of the embryo, the parietal peritoneum of coelomic mesothelial origin covers part of the intermediate mesoderm that gives rise to the pronephros, mesonephros and metanephros Figure 1.1 [1, 3].

Previously, it was thought that the Müllerian ducts derived entirely from the Mesonephric ducts (Wolffian ducts) [4-6]. Recent studies using both lineage tracing in chicken and mouse explants [7], as well as genetic fate mapping in mice [8], indicated that the Müllerian ducts was in fact a derivative of the coelomic epithelium as illustrated in Figure 1.1-1.2. Similarly, in human, endometrial epithelial cells expresses a coelomic epithelial marker Cancer Antigen 125 (CA125), suggesting that human female reproductive tract (FRT) epithelium is also a coelomic epithelial derivative [9]. In contrast to the Wolffian ducts (an intermediate mesoderm derivative), the Müllerian ducts are therefore a lateral plate mesodermal derivative because the coelomic epithelium (mesothelium) is formed from the lateral plate mesoderm.

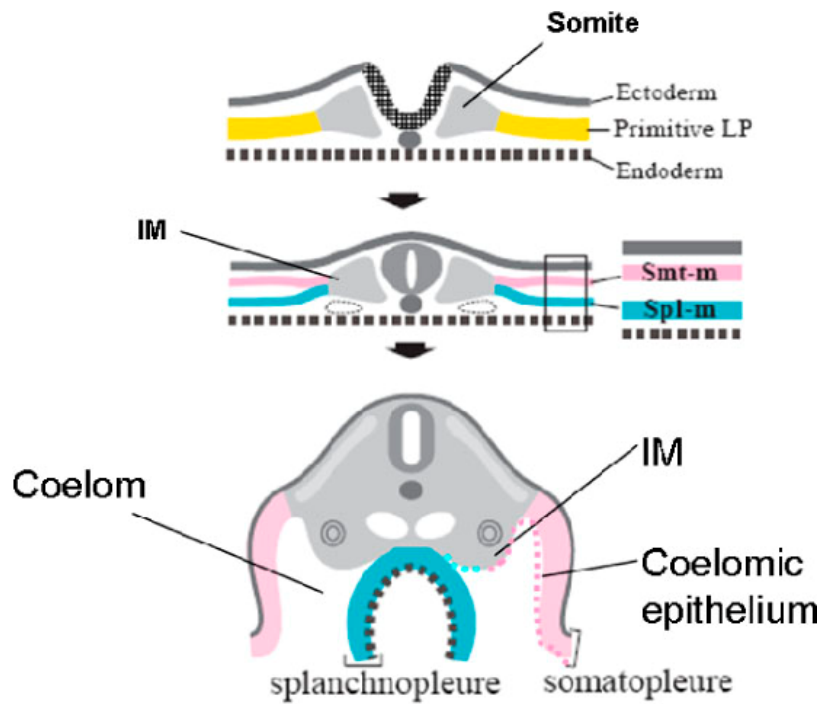


**Figure 1.1 Coelom formation from the lateral plate**

The primitive lateral plate (yellow) mesoderm are a group of mesenchymal cells is located lateral to the somite/intermediate mesoderm (IM) (grey) and between the ectoderm and the endoderm. Subsequently it splits into the two cell layers: the somatopleural (somatic) mesoderm (Smt-m; pink) underlying the ectoderm and the splanchnopleural (splanchnic) mesoderm (Spl-m; blue) adjacent to the endoderm. After folding of the embryo, the lateral-most portions of the lateral plates eventually close at the ventral midline. The somatopleure (lateral ectoderm + Smt-m) forms the outer body wall, whereas the splanchnopleure (lateral endoderm + Spl-m) develops to produce internal organs. The space between the somatopleure and splanchnopleure is the coelom. The coelomic epithelium (pink dotted line) covers the intermediate mesoderm (IM). Adapted from Funayama et al 2007 [2] with permission from The Company of Biologists.

### 1.1.2 Three phases of the Müllerian duct formation

Development of the Müllerian ducts comprises of three stages [8], consisting of 1) initiation, 2) invagination and 3) elongation stages (Wolffian ducts dependent) Figure 1.2. During the initiation phase, the coelomic epithelial cells adopt a Müllerian fate as a result of *Lim* homeobox protein 1 (*Lim1*) expression in the epithelium [10]. The specified epithelium then invaginates caudally towards the Wolffian ducts [10, 11].

The Wolffian ducts are essential for the elongation of the Müllerian ducts after invagination of the coelomic epithelium. Interruption or degeneration of the Wolffian ducts disrupts Müllerian duct development [12-14]. Anatomical evidence further demonstrates the dependence of the Müllerian ducts on the Wolffian ducts for elongation. Following invagination, the Müllerian epithelium extends caudally in close association with the Wolffian epithelium. At the caudal tip

of the Müllerian epithelium, both epithelia are in physical contact separated only by the basement membrane [8]. Similar observations were made in human fetal tissue where the basement membranes of the two ducts are also in close contact (Figure 1.3) [15]. Despite the reliance on the Wolffian ducts for elongation, the Müllerian duct cells proliferated as shown by Brdu uptake and histone H3 immunostaining indicating that Müllerian duct extension was achieved by proliferating cells rather than migrating cells from the surrounding tissue [7, 8].

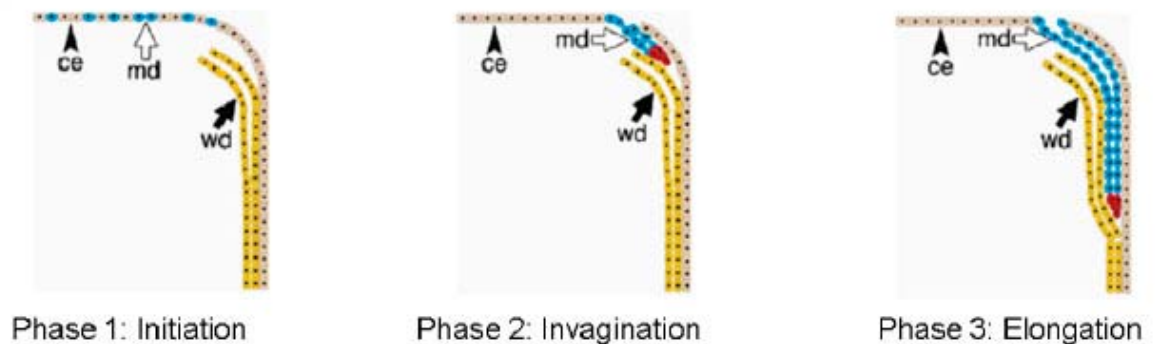


### Figure 1.2 Three phase model for Müllerian duct development

Phase 1, the coelomic epithelial cells are specified to become the Müllerian duct cells. Phase 2, the coelomic epithelial cells invaginate caudally towards the Wolffian ducts. Phase 3, the Müllerian duct meets the Wolffian duct and extends further caudally under the Wolffian duct's guidance towards the urogenital sinus. Blue cells; the mesoepithelial Müllerian duct cells, red cells; proliferating Müllerian duct precursor cells, brown cells; the coelomic epithelial cells, yellow cells; the Wolffian epithelial cells. Abbreviations: ce; coelomic epithelium, md; Müllerian duct, wd, Wolffian duct. Adapted from Orvis et al 2007 [8] with permission from Elsevier.

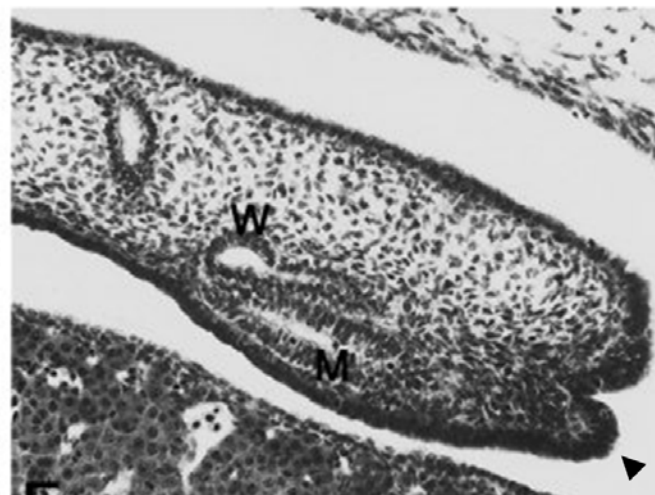


### Figure 1.3 Human Müllerian duct and Wolffian duct

Sagittal sections of a male Carnegie stage 18 embryo showing the caudal end of the Müllerian duct. The Müllerian and Wolffian ducts are enclosed by a common basement membrane. M, Müllerian duct; W, Wolffian duct. Arrow head points to coelomic epithelium. Adapted from Hashimoto 2003 [15] with permission from John Wiley and Sons.

### 1.1.3 Formation of the uterus from Müllerian ducts

The process of elongation ends when the proliferating tip of the Müllerian duct joins the urogenital sinus. Both the Wolffian and Müllerian ducts are found in developing embryos. In male embryos, the regression of the Müllerian ducts is governed by the activation of the Sex determining region Y (*Sry*) gene on the Y chromosome which functions to develop testes from undifferentiated male gonads. Sertoli cells in the testes secrete testicular hormones such as the anti-Müllerian hormone (AMH) also known as Müllerian inhibiting substance (MIS) which triggers the regression of the Müllerian ducts [16]. By contrast, in females, without the Y chromosome or *Sry* gene activation, the ovaries develop in place of testes. The Wolffian duct degenerates in the absence of testicular hormones whilst the Müllerian ducts develop into the oviducts, uterus, cervix and upper segment of the vaginal canal [17].

There is substantial variation in the anatomical features of mammalian FRT [17, 18]. This difference is mainly attributed to the level of fusion of the Müllerian ducts during development (Figure 1.4). The human Müllerian ducts fuse at more anterior regions (at the uterine level) forming a simplex uterus (Figure 1.4C), whilst mouse and pig Müllerian ducts fuse at more posterior regions (at the cervical/vaginal level) and form a bipartite uterus (Figure 1.4B). In larger quadrupeds such as cows and horses, the Müllerian ducts fuse in a region between that of human and rodents, resulting in the formation of a bicornuate uterus (Figure 1.4D) [17]. In all cases, the fused region forms the utero-vaginal duct consisting of the uterus, cervix and vagina. The non-fused region of the Müllerian ducts differentiates into oviducts and infundibulum.

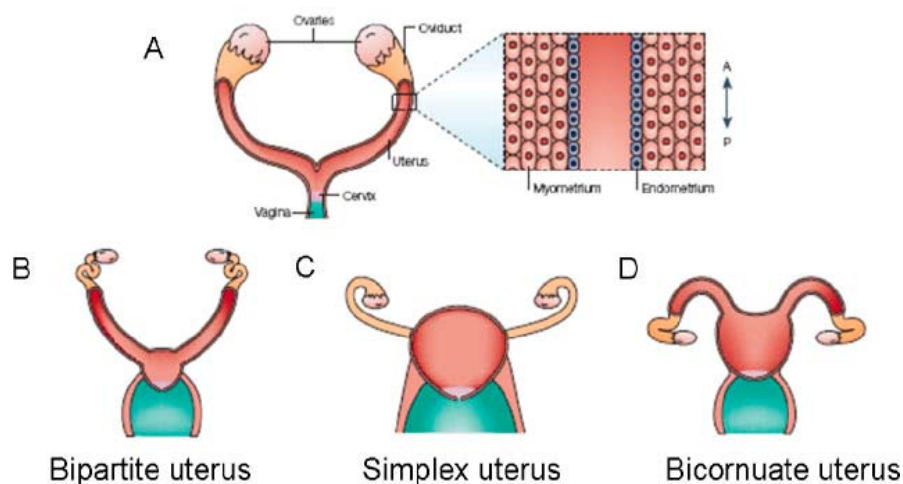


**Figure 1.4 Mammalian female reproductive tract**

Adapted from Kobayashi et al 2003 [17] with permission from Nature Publishing Group.

Much of what is known about regional differentiation of the FRT during development derives from rodent models. During the prenatal stage of FRT development in rodents, the Müllerian ducts undergo unique cytodifferentiation along its anterior – posterior axis (molecular mechanism regulating this is discussed in the following section), however, each region remains morphologically indistinguishable at around E16 – 18 and only begin to show histological differences during the postnatal development (Figure 1.5) [19].

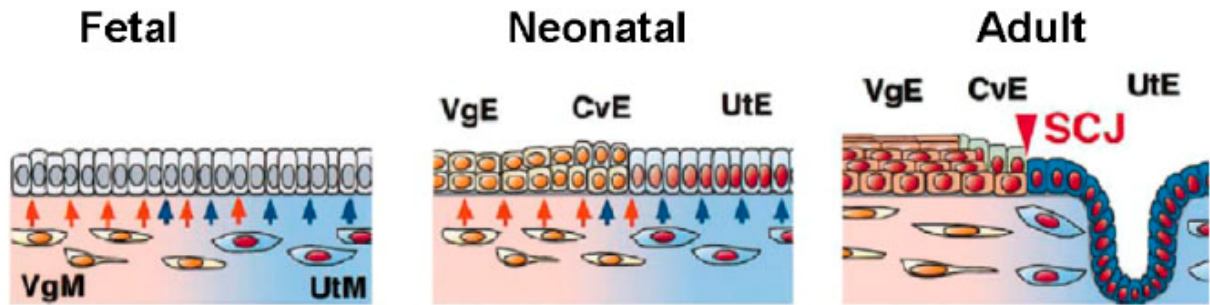


**Figure 1.5 Differentiation and maturation of the mouse Müllerian ducts**

During fetal development, the Müllerian duct appears uniform and undifferentiated. The vaginal mesenchyme (VgM) secretes factors (red arrows) to induce the Müllerian duct epithelial cells to commit to a vaginal epithelial cell fate. The uterine mesenchyme (UtM) secretes factors (blue arrows) to induce the Müllerian duct epithelial cells to commit to a uterine epithelial cell fate. In the neonate, mesenchyme-derived growth factors continue (red and blue arrows) to induce epithelial differentiation. Epithelial cells begin to show morphological features specific to the vaginal epithelium (VgE), cervical epithelium (CvE) and uterine epithelium (UtE). In the adult, the boundary between these different regions is clearly defined. The squamo-columnar junction (SCJ) (red arrowhead) defines the junction between the UtE and VgE/CvE. Adapted from Kurita et al 2001 [19] with permission from Elsevier.

#### 1.1.4 Maturation of the uterus

In addition to anatomical differences in the FRT between mammalian species, the maturation of the uterus (in particular the process of adenogenesis) also differs significantly between species. The maturation of the Müllerian ducts, in particular, the uterine segment of the FRT, is summarised in detail for several species in the following section and illustrated in Figure 1.6.

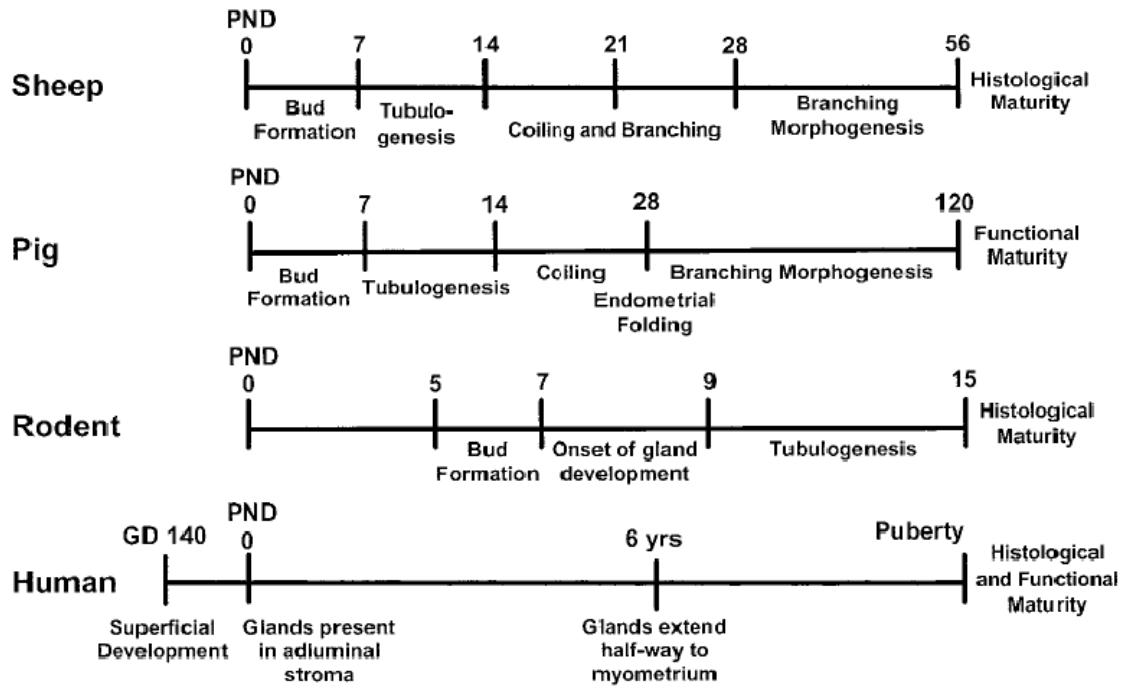


**Figure 1.6 Time line highlighting key events during postnatal uterine adenogenesis in mammals**

Abbreviations: GD, gestational day; PND, post natal day. Adapted from Spencer et al 2005 [20] with permission from Springer.

#### 1.1.4.1 Laboratory rodents

Maturation of the Müllerian ducts in rodents (mice and rats) occurs soon after birth and is completed before the onset of puberty. From postnatal day 1 (P1), regional patterning of the utero-vaginal tube occurs and is demonstrated by the expression of distinct markers in the epithelium of each segment (uterus, cervix and upper vagina), under the control of mesenchymal paracrine signals [19, 21-23]. In the neonatal uterus, there are 3 layers of undifferentiated mesenchymal cells destined to form the endometrial stroma (radially orientated inner mesenchymal layer), inner circular and outer longitudinal myometrial layers [24]. Uterine adenogenesis is the process of gland formation in the uterus which occurs concurrently with uterine mesenchymal differentiation [25]. Rodent uterine adenogenesis begins between P5-7, characterised by the formation of glandular epithelial buds invaginating from the uterine luminal epithelium into the underlying stroma. Formation of simple tubular endometrial glands is complete by P15 in rodents [26, 27]. Morphological features defining the region anterior to the uterus occurs from P5-10, where ciliated epithelial cells are observed in the oviductal epithelia. The mucous secretory cells differentiate from P23 [28, 29].

#### **1.1.4.2 Domestic Animals**

Similar to rodents, neither pigs nor ruminants (sheep, cattle, and goats) have a fully developed uterus at birth. Porcine and ovine endometrial glands are not visible until P7 [25, 30, 31]. However, the ovine vagina, cervix and oviducts exhibit histological maturity at birth [32-34]. After glandular epithelial budding around P7, coiling of the nascent glands occur followed by branching. The branching morphogenesis of the uterine glands continues until functional maturity at P120 in the pig and histological maturity at P56 in the sheep [25].

#### **1.1.4.3 Humans**

Unlike rodents and domestic animals, much of the human Müllerian duct epithelial differentiation is complete at birth [35]. Ultra-structural and light microscopy analyses of human fetal tissue suggest that endometrial glands can be found in the uterine mucosa from as early as 16-20 weeks of gestation. In addition, epithelial features resembling the adult endometrium were also observed, including pseudostratification and ciliation [36-38]. At birth, endometrial glands are sparse and limited to the adluminal stroma [25]. Complete maturation of the human endometrium is not reached until puberty.

## **1.2 Molecular genetics of Müllerian duct formation**

The formation of the Müllerian ducts occurs in three stages (Section 1.1.2); specification, invagination and elongation (Figure 1.2) [8]. Numerous homeodomain transcription factors and signalling molecules critical to each stage of the Müllerian duct formation have been described in mouse and human female reproductive tract (Table 1.1).

### **1.2.1 Homeodomain transcription factors**

Lim homeobox protein 1 (*Lim1*) encodes for a homeodomain transcription factor required for Müllerian duct formation since *Lim1*-null mutant mice lacked Wolffian and the Müllerian ducts [10]. During FRT development, *Lim1* is first expressed in the invaginating coelomic epithelium on the surface of the mesonephros around E11.5 [10]. Female mouse chimera assays revealed that cell-autonomous expression of *Lim1* is required for Müllerian duct formation [10]. However, the persistent expression of *Lim1* in the presumptive oviducts and uterine segments during late embryogenesis suggest it may also have a role in Müllerian duct differentiation [10]. Conditional inactivation of *Lim1* in the Wolffian duct epithelium triggers its degeneration, ultimately disrupting development of the Müllerian ducts indicating its involvement in the maintenance and elongation of the Müllerian ducts [12].

Paired box gene 2 (*Pax2*) encodes for a homeodomain transcription factor found in the epithelium of both the Wolffian ducts and Müllerian ducts. *Pax2*-null mutant mice lack kidneys and the FRT [14]. In contrast to the *Lim1*-null mutant mice phenotype, both the Wolffian and Müllerian ducts are initially formed in the *Pax2*-null mutants. In fact, the Müllerian ducts in *Pax2*-null mutants extended to the same level caudally as the Müllerian ducts in wild type embryos around E13.5. Lack of FRT seen in the *Pax2* knockout mouse model is a result of degeneration around E16.5 indicating its role in elongation and maintenance of the Müllerian ducts [14]. Similar to *Pax2*, Empty spiracles-like protein 2 (*Emx2*) encodes for another homeodomain transcription factor expressed in both the Müllerian and Wolffian duct epithelium. *Emx2*-null mutant mice lack both sexual ducts as a result of their degeneration, indicating a similar role for *Emx2* in Müllerian duct elongation [13].

Recently, another transcription factor has been implicated in Müllerian duct formation. Hepatocyte nuclear factor 1-beta (*Hnf1b*) or *Tcf2*, encodes for a homeodomain transcription factor found in the epithelium of many organs during development including the kidney [39].



Numerous reports have documented FRT malformation (bicornuate and didelphys uterus, Müllerian aplasia) in patients with renal anomalies showing mutations in the *TCF2* gene indicating its role in Müllerian duct development [40-42]. In addition to those mentioned above, the transcription cofactors Dachshund homolog 1/2 (*Dach 1/Dach2*) have been detected in the developing Müllerian ducts. The combined *Dach1/Dach2* knockout mouse model demonstrated defects in the Müllerian development associated with abnormal expression of *Lim1*, indicating their involvement in Müllerian duct development [43].

### 1.2.2 Signalling molecules

*Wnt* genes encode for secreted glycoproteins homologous to the *Drosophila* segment polarity gene *wingless* (Wg). Wnt proteins have pivotal roles in embryogenesis, tissue growth, differentiation and epithelial-mesenchymal interaction in many organs including the FRT [44-46]. Wnt signalling is mediated via activation of cell surface receptors known as Frizzled (Fz) followed by downstream cytoplasmic events that result in accumulation of nuclear  $\beta$ -catenin which regulates gene transcription [47]. Recent studies have demonstrated its role in fetal and postnatal development of FRT in various mammalian species [48-51].

*Wnt4* is expressed in the coelomic epithelium and mesenchyme surrounding the Müllerian ducts [11, 52]. *Wnt4*-null mice (both sexes) contain a normal male reproductive tract whilst missing a FRT indicating a role for Wnt4 signalling in Müllerian duct formation [11]. Coincidentally, a female patient presenting with FRT agenesis also had a mutation in the *Wnt4* gene [53]. Furthermore, *Lim1*<sup>+</sup> coelomic epithelial cells in *Wnt4*-null mutant mice failed to invaginate suggesting that during development, *Wnt4* is required for invagination rather than specification of coelomic epithelial cells into a Müllerian fate [10]. *Wnt9b* plays a minor but critical role in the elongation of the Müllerian ducts. It is expressed in the Wolffian duct epithelium in both sexes from E9.5-14.5. Whilst, the Wolffian duct phenotype appears to be normal in *Wnt9b* mutant mice, Müllerian duct elongation is interrupted, suggesting that the Wolffian ducts guides Müllerian ducts extension via *Wnt9b* signals [54].

In addition to Wnt signalling, other developmental signalling molecules such as retinoic acid (RA) and the gene, discs, large homolog 1 (*Dlgh1*) have been implicated in Müllerian duct formation. Whilst RA $\alpha\beta$  receptor (RAR) double mutants lacked Müllerian ducts [55], *Dlgh1*-null mutants exhibited vaginal aplasia suggesting its role in Müllerian duct elongation [56]. Finally, it

has recently been shown that the PI3K/AKT signalling pathway is also involved in elongation of the Müllerian duct emphasising the complexity of the Müllerian duct development [57].

In summary homeodomain transcription factors and signalling molecules play crucial roles in the formation of the Müllerian ducts in the mouse embryo. Similar molecular pathways also contribute to functional differentiation of the developing Müllerian ducts.

**Table 1.1 Genes involved in formation and patterning of the Müllerian ducts**

Abbreviations: CE, coelomic epithelium; FRT, female reproductive tract; GE, glandular epithelium; H, human; M, mouse; MD, Müllerian ducts; ME, Müllerian epithelium; MM, Müllerian mesenchyme; NE, not expressed; UE, uterine epithelium; UM, uterine mesenchyme; US, uterine stroma

Spatial/temporal expression of genes in mouse and human						
Gene Symbol	Fetal (M)	Neonatal (M)	Adult (M)	Adult (H)	Knockout phenotype	References
Lim1	CE, WE, ME	-	NE	-	No FRT	[10, 12, 58]
Pax2	CE, WE, ME	-	-	UE	No FRT	[14, 59]
Emx2	WE, ME	-	-	-	No FRT	[13, 60]
Foxa2	N/A	-	GE	-	Infertile, lack uterine glands	[61]
Dach1	MD, WD		-		Malformed FRT, disorganised uterus lack lumen and gland,	[43]
Dach2	MD				vaginal aplasia	[43]
Wnt4	CE, MM	UM	UM	-	No FRT	[11, 52]
Wnt5a	ME, MM	UM	UM	-	Malformed posterior FRT, lack uterine glands	[52, 62]
Wnt7a	ME	UE	UE	-	Posterior homeotic transformation of the uterus, lack uterine glands	[63-67]
Wnt9b	WE		-		Lack uterus and upper vaginal canal	[54]
Wnt11	-	UE	UE	-	-	[48, 50]
Wnt16	-	UM	UM	-	-	[48, 50]
RAR $\alpha,\beta,\gamma$		-			Lacked Müllerian ducts ( $\alpha\beta$ mutants), uterine body and cranial vaginal canal ( $\alpha\beta$ and $\alpha\gamma$ mutants)	[68]
Dlgh1	WE	NE	-	-	Cervix and vagina aplasia	[56]
Hoxa10	Co-linear expression along the Anterior-Posterior axis of ME/MM			UE/US	Anterior homeotic transformation of the uterus	[69, 70]
Hoxa11				UE/US	Partial anterior homeotic transformation of the uterus, reduced uterine gland	[70-72]
Hoxa13				-	Lack caudal FRT	[70, 73]

### **1.3 Molecular genetics of Müllerian duct differentiation: region specific cell fate determination**

Much of what is known about the differentiation of the Müllerian ducts comes from mouse models [17]. Compartmentalisation or region-specific patterning of the Müllerian ducts along the anterior-posterior (A-P) axis requires interaction between the Müllerian duct epithelium and the adjacent mesenchyme. Governing this process of segmental patterning during the mammalian Müllerian duct differentiation are the Hox and Wnt gene families.

#### **1.3.1 Hox genes and Müllerian duct differentiation**

The *Hox* gene family consist of 39 genes organised in four clusters (*Hoxa* to *Hoxd*) encoding for homeodomain transcription factors involved in establishment of metazoan body plan during embryonic development and differentiation [74]. Specific cell fates along the FRT are dictated by the positional information encoded in the Hox genes. As illustrated in Figure 1.7, the *Abdominal-B (Abd-B) like Hox* gene family (including *Hoxa* 9-13 and *Hoxd* 9-13) are “colinearly” expressed in the mouse Müllerian mesenchyme along the A-P axis with overlapping regions during differentiation [70]. Genetic studies in mice demonstrated that inactivation of any one of these genes led to alterations in regional identity. For instance, the uterus in *Hoxa10*-null mutant mice displayed coiled morphology resembling the oviducts, suggestive of an anterior homeotic transformation [69]. Anatomical changes suggestive of anterior homeotic transformation also occurred in the uterus of *Hoxa11*-null mutant mice [71]. When *Hoxa11* was replaced with *Hoxa13*, a posterior homeotic transformation of the uterine epithelium to vaginal-like epithelium was observed [75]. Furthermore, *Hoxa13*-null mutant mice lacked the distal portion the Müllerian ducts suggesting its involvement in duct formation [73].

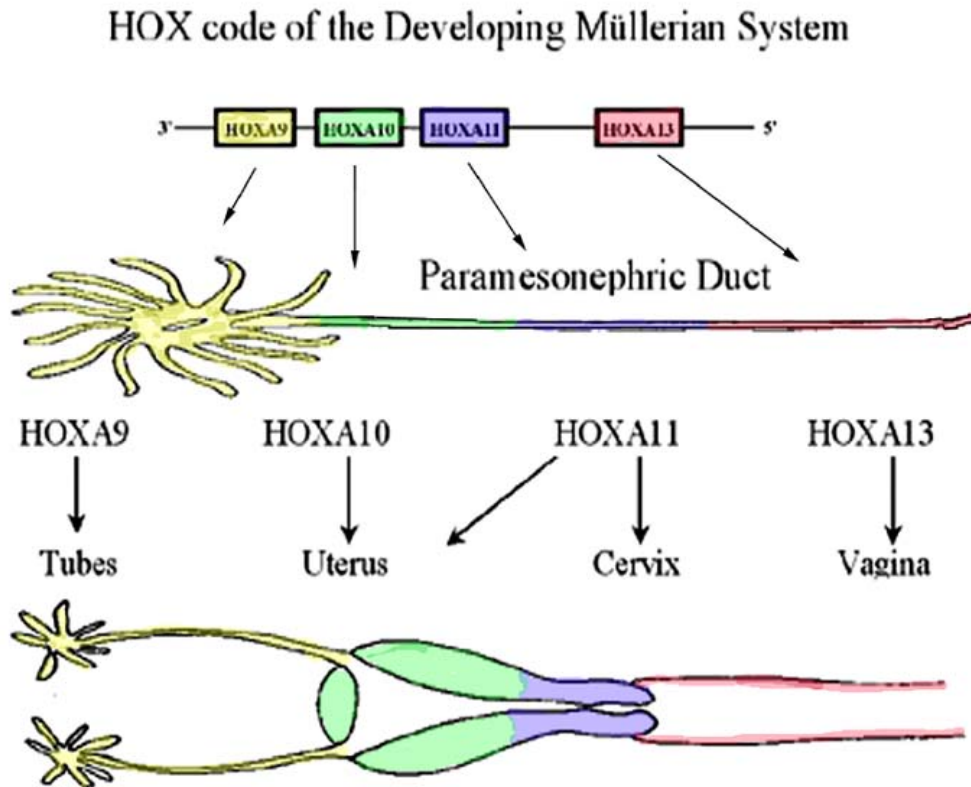


**Figure 1.7 Hox gene expressions in FRT**

Adapted from Du and Taylor 2004 [76] with permission from John Wiley and Sons.

### 1.3.2 Wnt signalling pathway

In addition to Müllerian duct formation, the Wnt signalling pathways also plays a critical role in Müllerian duct cell fate determination and postnatal uterine development. *Wnt5a*-null mutant mice have a malformed uterus and therefore dispensable for cell fate specification of the Müllerian ducts but required for proper differentiation into the uterine phenotype [62]. Neonatal uterine columnar epithelial cells in *Wnt7a*-null mutant mice exhibit uterine differentiation markers indicating that *Wnt7a* is also dispensable for uterine cell fate determination [35, 66, 77]. However, the absence of *Wnt7a* in the neonatal uterine epithelium results in down regulation of several key transcription factor and signalling genes including *Hoxa10/11*, *Wnt5a*, forkhead box protein A2 (*Foxa2*), Leukemia Inhibitory Factor (*Lif*), homeo box, msh-like 1 (*Msx1*) and *Wnt16* in the neonatal uterus ultimately leading to abnormal epithelial and stromal development [62, 63, 65]. Morphologically, no uterine glands were observed in *Wnt7a*-null mutant mice and *Wnt7a* conditional knockout model. Furthermore, a gradual posterior homeotic transformation occurred over time in these models where uterine epithelium transformed into squamous epithelium [63,

65]. Squamous metaplasia of the uterine epithelium may also be triggered by the ovarian steroid hormone, estrogen, experiments in *postaxial hemimelia* mice (a spontaneous *Wnt7a*-null mutant strain) further underscored the role *Wnt7a* in “stabilisation” of the uterine epithelial cell fate [35]. Furthermore, conditional inactivation of  $\beta$ -catenin in the uterus induced expression of p63 (marker of vaginal basal epithelial cells [78]) in the uterine epithelium of adult mice [79]. Similarly, conditional inactivation of *Wnt4* also induced p63 expression implicating the canonical Wnt/ $\beta$ -catenin signalling pathway in the maintenance of uterine epithelial identity [80].

In contrast to the mouse, no mechanistic studies have ever been conducted on fetal human FRT tissue to dissect the molecular mechanisms involved in the development of the human Müllerian ducts. With advent of genetic technologies, numerous genes have been associated with particular phenotypes ranging from vaginal atresia, persistent Müllerian ducts in the male, formation of vaginal septum to the most severe case of complete uterine aplasia seen in human patients. These genes include *TCF2*, *LIM1*, *AMH*, *Anti-Müllerian hormone receptor 2 (AMHR2)* and *HOXA13* [40, 81-83].

In summary, a number of important molecular pathways control Müllerian duct formation and patterning. There are complex interactions between Hox transcription factors and Wnt signalling pathways that ensure proper region-specific cytodifferentiation during development and for maintenance of the normal phenotype in mature FRT. Despite the anatomical differences in the FRT between mammals, the genetic blueprint for the FRT appears to be well conserved between mammalian species [17]. However, human studies need to be conducted to verify the role of these molecular pathways in human FRT development.

## **1.4 *Postnatal endometrial development and remodelling***

A series of elegant tissue recombination studies using mouse FRT tissue have demonstrated the significance of epithelial-stromal tissue interaction in the differentiation and maturation of the Müllerian duct epithelium [19, 22, 78, 84-86]. The conclusions drawn from these studies suggest that mesenchyme directs and patterns the epithelium of the FRT. The epithelium reciprocates by facilitating endometrial stromal and myometrial smooth muscle development. Similarly, endometrial gland morphogenesis in other mammalian species (ovine, porcine, primate) is also regulated via epithelial-stromal tissue interaction [31, 33, 87-89]. Mechanisms controlling these tissue interactions include alterations in the extracellular matrix (ECM) components as well as intrinsic growth factor signalling pathways [18].

### **1.4.1 ECM components and regulation**

#### **1.4.1.1 Glycoaminoglycans**

ECM components have been implicated in endometrial gland development. Both sulphated and non-sulfated (hyaluronate) glycosaminoglycans (GAGs) have been identified in the ovine/porcine fetal and neonatal uterine tissue. Whilst, the sulphated GAGs are associated with structural stabilisation, the expression of non-sulfated GAGs in morphogenetically active areas of endometrial glands suggest its involvement in endometrial gland remodelling/development [25, 31, 90]. Furthermore, recent studies have detected prominent expression of hyaluronate receptor (CD44) in the secretory human endometrium during the window of implantation indicating the role of non-sulfated GAGs in gland remodelling in the adult human endometrium [91-93]. However, no information is available on the role of ECM components during human FRT development.

#### **1.4.1.2 Matrix metalloproteinase and Connective tissue growth factor**

The Matrix metalloproteinase (MMP) and their inhibitors regulate ECM remodelling in adult human and primate endometrium [94, 95]. The MMP system is also involved in endometrial adenogenesis in postnatal mouse endometrium. The mRNA expression of several MMPs (MMP-

2, MMP-10, MMP-11, MMP-14, MMP-23) and tissue inhibitors of metalloproteinases (TIMP-1, TIMP2, TIMP3) have been localised in the neonatal mouse endometrium during critical stages of endometrial adenogenesis [26, 96]. Furthermore, *TIMP-1*-null mutant adult mice exhibited unopposed expression of several MMPs resulting in abnormal endometrial luminal morphology compared to wild-type highlighting the importance of ECM in maintaining normal phenotypes [97]. Member of the CNN gene family, connective tissue growth factor (CTGF) can also influence ECM availability therefore the process of tissue remodelling [98, 99]. The role of CTGF in neonatal endometrial adenogenesis has not been reported, however, its expression in the endometrium during embryo implantation suggest a role in endometrial remodelling [100].

## **1.4.2 Mesenchyme derived growth factors**

### **1.4.2.1 FGF, HGF and IGF**

Postnatal uterine epithelial proliferation and differentiation depends not only on changes in ECM components, but also on the expression of mesenchyme derived growth factors including Fibroblast growth factor 7 (FGF7) (also known as keratinocyte growth factor), FGF10, and Hepatocyte growth factor (HGF) are found in mesenchyme(s) both within and outside the FRT [33, 101-105]. They act in a paracrine manner in stimulating epithelial proliferation and differentiation. Similarly, Insulin-like growth factors (IGF) play a critical role in mammalian uterine development and postnatal cell proliferation, and differentiation [18]. In rodents, IGF-I has been detected in neonatal rat uterine stroma/myometrium, whilst IGF-II and number of IGF binding proteins have also been identified in the neonatal mouse stroma/myometrium during early stages of endometrial adenogenesis [26, 106]. Similarly, both IGF-I and IGF-II mRNAs have been detected in the neonatal ovine uterine stroma, whilst IGF-IR but not IGF-IIR is localised in all uterine cell types particularly the endometrial glandular epithelium [105]. Disruption of the “IGF system” in the endometrium by estrogen caused aberrant expression of IGFs, their receptors as well as IGF binding proteins and growth reduction in the postnatal ovine endometrium highlighting the importance of IGFs in mammalian endometrial gland development [32, 107, 108]. The “IGF system” has also been characterised in cycling adult human endometrium where mRNAs of IGF-I and IGF-II are found in the endometrial stroma, and their receptors and binding proteins ubiquitously distributed throughout the endometrium [109].



Collectively, these studies suggest that the “IGF system” may be crucial to endometrial adenogenesis in the developing human FRT.

#### **1.4.2.2 Wnt signalling pathway**

A large cohort of *Wnt* genes have been identified in the neonatal uterus. Only those located in the mesenchyme will be discussed in this section. By in situ hybridisation, both *Wnt4* and *Wnt5a* are restricted to the postnatal uterine mesenchyme [50, 65]. In addition to *Wnt4* and *Wnt5a*, recent in situ hybridisation identified *Wnt16* in the neonatal uterine mesenchyme [50]. Its function in neonatal uterine adenogenesis remains to be determined. Although WNT16B stimulates cell proliferation and extended clonogenicity of primary human epidermal keratinocytes *in vitro* indicating that it may act as a stromal paracrine signal regulating neonatal uterine adenogenesis [110]. The precise contribution of *Wnt4* in adenogenesis is unknown. On the other hand, genetic and tissue recombination studies have demonstrated the involvement of *Wnt5a* in Müllerian duct differentiation and uterine adenogenesis [62, 111]. By contrast, neonatal ovine endometrial *Wnt5a* is predominantly expressed in the epithelium rather than mesenchyme [49].

In the adult mouse endometrium, there is a persistent expression of *Wnt4*, *Wnt5a* and *Wnt16b* in the peri-implantation mouse uterine stroma, highlighting the critical roles developmentally regulated *Wnt* genes may play in decidualisation of the endometrium [48]. *Wnt* genes have also been identified by a several studies in the adult human endometrium [51, 112]. The expression and function of *Wnt* genes in the developing human endometrium remains to be investigated.

#### **1.4.2.3 Bone morphogenetic proteins**

The transforming growth factor beta (TGF- $\beta$ ) super family includes 4 sub-families; TGF- $\beta$ , Activins, Bone Morphogenetic proteins (BMPs) and Growth Differentiation factors (GDFs). Limited literature exists on the role of TGF- $\beta$  family growth factors in FRT development and postnatal uterine differentiation compared the large number of studies conducted in adult rodent and human endometrium [113-118]. However, it has been shown that BMP2 is differentially expressed in the neonatal mouse uterine stroma between P9 and 12 suggesting its role in endometrial adenogenesis [26]. The role of BMP ligands in embryonic development of Müllerian ducts have not been investigated, their role in postnatal adenogenesis has been shown in mice [119]. The role of BMPs in developing human FRT remains to be investigated.

### 1.4.3 Hormones

Mesenchyme derived paracrine growth factors from various molecular pathways discussed in Sections 1.5.1.1-1.5.1.3 are crucial during postnatal uterine adenogenesis. Systemic factors such as steroid hormones also regulate the postnatal uterine adenogenesis. For instance, Prolactin (PRL) is a major regulator of endometrial adenogenesis in the neonatal ovine uterus [120]. Circulating levels of prolactin (PRL) peak in neonatal ewes at the time of uterine bud formation and tubulogenesis [89, 120]. Restricted expression of PRL receptors in the glandular epithelial buds indicates a role for PRL in adenogenesis [89]. Furthermore, postnatal ewes treated with recombinant PRL and PRL inhibitor resulted in a dramatic increase and reduction in glandular formation respectively [120]. Whilst a large body of evidence exists on the role of PRL in adult human endometrium [121], no studies have examined its role during the fetal and neonatal human endometrial adenogenesis.

Circulating factors derived from the ovaries and adrenal glands may also stimulate uterine growth but do not appear to have a role in endometrial adenogenesis [122-125]. Jost first conceptualised that prenatal FRT development is an ovary-independent process [126]. This concept has been further corroborated by a number of animal studies showing the development of the FRT in the absence of estrogen or its receptors [125, 127]. Similarly, ovarian hormones are not required for adenogenesis in neonatal porcine or rodent endometrium [123, 124, 128]. The ovarian hormone estrogen is, however, required for uterine growth [125]. Fetal uterine tissue lacks expression of estrogen receptors compared to oviduct epithelium which had detectable expression at 38 weeks of gestation [129]. In the light this evidence, human endometrial adenogenesis observed previously may have occurred independently of circulating fetal or maternal ovarian hormones [36-38]. The influence of ovarian hormones on human endometrial adenogenesis during development remains to be investigated.

### 1.5 *Biology of the adult human endometrium: structure, hormone regulation and cyclic regeneration*

Whilst little is known about the biology and the role of ovarian hormones on human FRT development, ovarian hormones are primary regulators of adult human endometrial physiology. The adult human endometrium comprises of the upper functionalis and lower basalis layer (Figure 1.8). Before puberty, the human endometrium is relatively unremarkable and underdeveloped due to a suppressed hypothalamus-pituitary-ovary (HPO) axis. As the HPO axis matures, a positive feedback mechanism is created which provides the basis for an ovarian estradiol-triggered surge of luteal hormones leading to ovulation and establishment of regular menses [130].

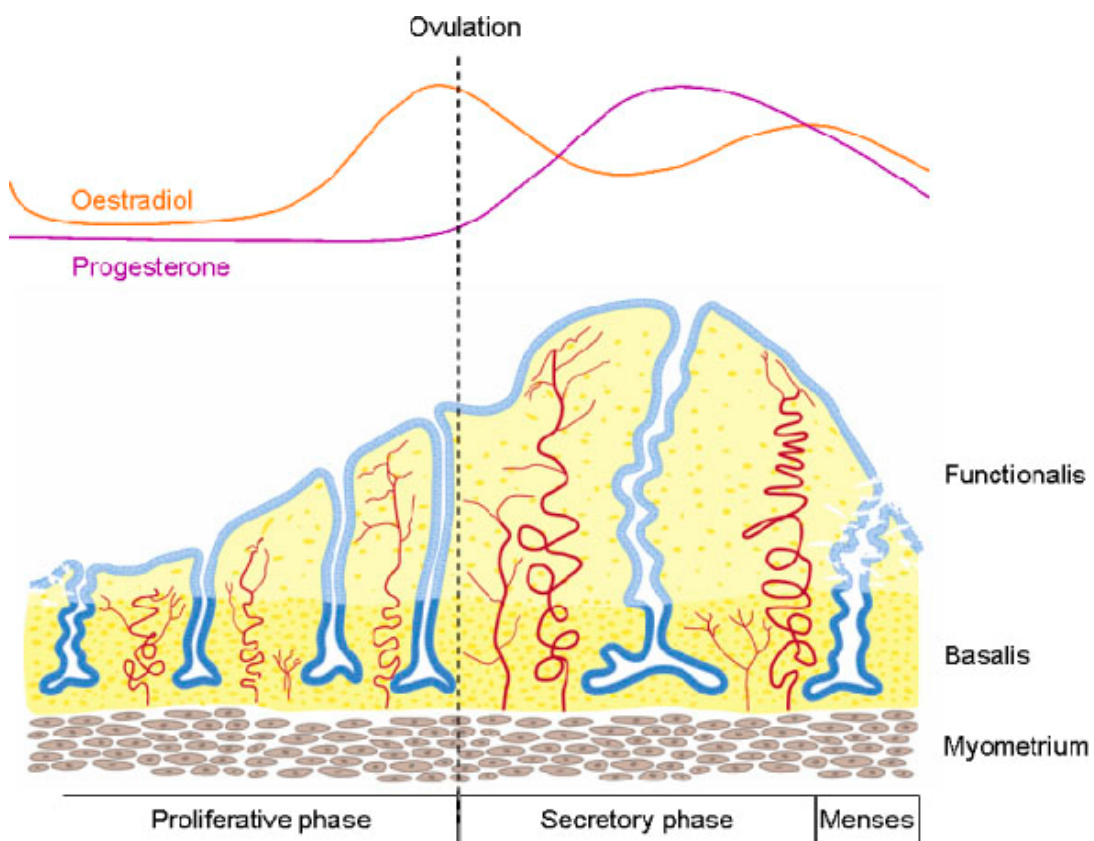


**Figure 1.8 The changing structure of the human uterus during the menstrual cycle.**  
Adapted from Gargett et al 2008 [131] with permission from Elsevier.

### **1.5.1 Menstrual stage specific endometrial morphological and biochemical features**

The menstrual cycle can be divided into 3 phases; menstrual, proliferative (follicular) and secretory (luteal) where estrogen and progesterone dominate, respectively. A number of hallmark morphological and biochemical features of endometrium emerge during the menstrual cycle.

During the early proliferative phase (days 5-7), the endometrial glands are lined by columnar epithelium, and appear straight and undifferentiated. By contrast, during the mid-proliferative phase (days 11-14) tortuous longer glands can be observed, lined by pseudostratified epithelium. The tortuosity of the glands is prominent in the late proliferative phase with glandular cells appearing as tall pseudostratified columnar cells. The morphology of the luminal epithelium is also under the influence of estrogen.

In the secretory phase, progesterone regulates endometrial differentiation of both the stromal and epithelial cells in preparation for embryo implantation, as well as antagonising estrogenic effects. During the early secretory phase, the glandular epithelium initially appears pseudostratified with basally located nuclei which is also a feature seen in late proliferative phase. As the secretory stage progresses, the subnuclear vacuoles displace cell nuclei more centrally, and the glandular cells appear taller and less pseudostratified. By mid-secretory phase, there is increased tortuosity of the glands which marks a short period of time known as the 'window of receptivity' where embryo implantation may take place. As glandular cells release their glycogen-rich products into the lumen, the glandular lumen size increases whilst the epithelial cells contain little secretory product by the end of the secretory phase, and appear low columnar to cuboidal, with smaller nuclei and indistinct cytoplasm [132]. At the end of each cycle (menses), the functionalis is shed whilst the basalis remains intact.

The search for a reliable marker for endometrial receptivity has been elusive, although a combination of markers (both morphological and biochemical) may be useful; formation of pinopods, secretion of glycoproteins including Glycodelin A (GdA), Mucin 1, cell surface associated (MUC1), expression of homeodomain transcription factor HOXA10, and the presence of a range of adhesion/antiadhesion molecules, calcium-associated proteins as well as growth factors/cytokines [133, 134].

Presence of motile cilia on the surface of both endometrial luminal and glandular epithelial cells is a key feature of the human endometrium epithelium (Figure 1. 9), a characteristic it shares with only several organs; airways, choroid plexus, ependymal, oviducts and testes [132, 135]. The number of ciliated cells increases as the cycle progresses but decreases dramatically during withdrawal of estrogen at the end of the cycle [136, 137].



**Figure 1.9 Ciliated endometrial epithelium**

Scanning electron microscopy (SEM) of human endometrial biopsy day LH + 6. Single ciliated epithelial cells separated endometrial cells with flattened surfaces and short microvilli. Adapted from Bentin-Ley et al 1999 [138] with permission from Oxford University Press.

### 1.5.2 Ovarian hormone receptors in the human endometrium

Like morphological and biochemical markers, dynamic expression pattern of ovarian hormone receptors are observed in the endometrial epithelium across the menstrual cycle. This is reflected in the dramatic cyclical morphological changes that occur in the endometrium (Figure 1.8), driven by changing levels of circulating estrogen and progesterone which bind to specific high-affinity nuclear receptors found in endometrial cells.

The location and function of estrogen and progesterone receptors has been studied extensively in the human body. In adult human endometrium during the proliferative phase, estrogen receptor  $\alpha$  (ER $\alpha$ ) and the progesterone receptors (PR) are expressed in both the epithelium and stroma

[131]. Stromal ER $\alpha$  responds to estrogen and growth factors inducing extensive proliferation of glandular epithelial cells by juxtacrine mechanisms. Similar to estrogen receptors, PR-A and PR-B are also be found in glandular epithelium.

During the proliferative phase, both progesterone receptors are upregulated by estrogen, but downregulated by its own ligands in secretory phase. By mid-secretory phase only PR-B is expressed [134]. In addition to ER and PR, an early developmental receptor found in the Müllerian ducts, the AMHR2 has been located in normal and malignant adult human endometrium [139].

### **1.5.3 Endometrial regeneration**

Another key feature of a functional endometrium is its ability to regenerate the entire functionalis layer following shedding that occurred during menses (Figure 1.8). The concept of endometrial regeneration by resident adult stem cells dates back several decades [88, 140-142].

#### **1.5.3.1 Endometrial Stem/Progenitor Cells**

Recent studies identified small populations of adult human endometrial epithelial and stromal cells with adult stem cell properties [143, 144]. Furthermore, a series of studies using the label retaining technique have also identified adult stem cells in the mouse uterus [145-147]. Human endometrial side population have also been shown to have stem cell properties [148]. The exact mechanism by which endometrial adult stem/progenitor cells regenerate the endometrium remains unknown.

#### **1.5.3.2 Persistent expression of developmental factors**

Whilst the presence of adult stem/progenitor cells in the endometrium is consistent with its ability to regenerate, the persistent expression of developmental factors may explain how it maintains developmental plasticity required for cyclic tissue regeneration.

Most of the homeodomain transcription factors listed in Table 1.1 are expressed in the adult human endometrium. *HOXA10* and *EMX2* gene expression has been detected in adult endometrium at different stages of the menstrual cycle [76]. *EMX2* is negatively regulated by *HOXA10* in the secretory phase [133]. *HOXA10* expression peaks in both secretory endometrial stromal and epithelial cells in response to progesterone stimulation, indicating its role in implantation [76, 133]. Recently, *PAX2* has also been identified in the normal human adult female reproductive tract and gynaecological tumours [59]. The expression of *LIM1* in human FRT remains unknown. The exact contribution of these homeodomain transcription factors on human endometrial regeneration remains to be determined.

On the other hand, WNT and BMP signalling have been implicated in stem cell regulation in several systems including embryonic stem cells, neural stem cells, mesenchymal stem cells, hematopoietic stem cells, and intestinal stem cells [149]. Persistent expression of members of WNT and BMP signalling pathways in the adult human endometrium underscores the potential roles of these developmental pathways in endometrial regeneration and their role in resident stem cell regulation [51, 113]. By contrast, aberrant activation of WNT pathways has been linked to genesis of endometrial tumours [150].

## **1.6 Uterine abnormalities with fetal origins**

Amongst the various aetiologies of adult endometrial lesions, exposure to chemicals *in utero* during FRT development is a major risk factor. The impact of a synthetic estrogen, diethylstilbestrol (DES) on FRT carcinogenesis in humans had been known for decades. DES was first prescribed to reduce the risk of miscarriage and other pregnancy associated complications between years 1938-71. *In utero* exposure to DES therapy was subsequently associated with adenocarcinoma of the endocervix found in daughters whose mothers had undergone DES therapy [151]. Recent epidemiologic studies revealed other FRT abnormalities in women exposed to DES in utero including a “T shaped” uterus and increased risk of clear cell adenocarcinoma of the vagina and cervix as well as enhanced risk incidence of spontaneous abortion, ectopic pregnancy and preterm delivery [152, 153].

Several animal studies have revealed the mechanisms associated with endocrine disruption. The action of estrogen or estrogen-mimetic is mediated via estrogen receptors [127, 154]. In absence of ER $\alpha$ , as seen in ER $\alpha$  knockout mouse models, female mice are infertile and have a hypoplastic uterus [127]. Exposure of the neonatal ovine uterus to estrogen stimulation during critical periods of uterine adenogenesis actually reduced gland formation [107]. Over stimulation of the uterus with non-steroidal estrogen-mimetic such as DES, or Bisphenol-A (BPA) during development (prenatal and postnatal) can lead to a range of irreversible abnormalities ultimately leading to malignancy in mouse uterine tissue [155-158].

In recent years, various studies have investigated the impact of other chemicals with estrogenic activity in mouse models. Genistein, a non-steroidal phytoestrogen usually found in soy products is one of the compounds. Exposure to genistein in neonatal mice increased the risk of uterine adenocarcinoma [159]. Similarly, neonatal exposure to BPA also led to the appearance of endometrial cystic hyperplasia in adult mice [160]. Furthermore, fetal and postnatal exposure to DES transiently represses and deregulates key developmental pathways such as *Hox* and *Wnt* in the mouse uterus, whilst permanently altering other genes including Lactotransferrin, Complement C3, Cyclin D1 [50, 64, 161, 162]. Coincidentally, some of the aberrantly expressed genes associated with DES treatment also overlap with those found in human uterine adenocarcinoma [162].



Overall, these studies demonstrate that abnormal exposure to natural or synthetic compounds with estrogenic activity during critical periods of FRT development may have a long term impact of reproductive health. Often, the detrimental effects of endocrine disruptors are well disguised until later in life. During the last few decades, the release of large quantities of chemicals with estrogenic activity into the environment and our diet may have detrimental consequences for human FRT development in the future. A developmental model of the human FRT could provide a platform for novel investigations into the action of various environmental agents (including estrogen mimetics) during human Müllerian duct development.

## **1.7 The need for a developmental model of human female reproductive tract**

Animal models have played vital roles in informing our current understandings of the development of FRT. Due to ethical and legal restrictions, human Müllerian duct tissues are almost inaccessible to most investigators. Past studies using human Müllerian duct tissue have been observational in nature [15, 36-38]. A model of the human FRT would allow investigations into human FRT development, the impact of various endocrine disruptors on the developing human FRT and facilitate the characterisation of human uterine stem cells.

The discovery of human embryonic stem cell (hESC) marked the beginning of a new era where human cell/tissue types can be generated in the laboratory for regenerative medicine purposes as well as understanding basic biology of human embryonic development. The most accessible source of pluripotent stem cells today are mouse and human embryonic stem cells. Since the discovery of human embryonic stem cells (hESC) in 1999 [163], protocols have been developed for their differentiation into any type of cells in the human body. In recent years, with advances in cell culture techniques and fewer legal restrictions in some countries, hESCs have become easier to handle and more readily available for research.

Lineage specific differentiation of hESC *in vitro* using exogenous factors has been an intense area of research activity. The most successful differentiation protocol systems today use hESC to produce wide variety of clinically relevant cells/tissues including connective tissue [164], haemopoietic cells [165], cardiomyocytes [166-168], neuronal and non-neuronal ectodermally derived tissue [169, 170], hepatocytes [171], pancreatic cells [172], and respiratory epithelial cells [173] cell types *in vitro* for regenerative medicine. Whilst *in vitro* hESC differentiation systems using chemically defined conditions have been successful (ie. by addition of exogenous growth factors), others have showed innovative ways to use hESC to create models in order to study basic human developmental mechanisms in other fields.

### **1.7.1 Tissue recombination and in vivo modelling**

The principle behind co-culture models where hESC are cultured with an organ specific mesenchyme is that epithelial-stromal interaction is pivotal for organ development. In a world

first hESC-derived prostate model, hESC was recombined with embryonic mouse urogenital mesenchyme [174]. It was shown that the mouse urogenital mesenchyme induced hESC to develop into functional human prostate epithelial tissue *in vivo*. Others showed that rat bladder mesenchyme can induce differentiation of mouse embryonic stem cells (mESC) into mouse bladder epithelium [175]. These studies involved both tissue recombination and *in vivo* modelling techniques.

### 1.7.1.1 Tissue recombination methods

Tissue recombination techniques and *in vivo* modelling complement each other, and have traditionally been used to investigate stromal-epithelial cell interaction in a number of visceral organs, in particular those in the urogenital system [22, 176-179].

*In vivo* modelling includes several different approaches. One type of experiment involves transplantation of differentiated cell types into a host stromal niche to study their interaction [180, 181]. Tissue fragments or cells have also been grafted into an animal host to study their development *in vivo* [182-184]. Some *in vivo* models use tissue recombination technology where defined epithelial and stromal cells are constructed *in vitro* and subsequently transplanted as a xenograft into various sites in an animal host. Sub-renal capsule sites is one of many sites where grafts could be transplanted, even though it is technically more demanding, it is preferred over orthotopic and subcutaneous sites by the virtue of its vascularity [185].

Many studies investigating stromal-epithelial interactions in the female reproductive organs used tissue recombination technology coupled with *in vivo* modelling [19, 22, 184, 186]. Traditionally, tissue recombination involved the separation of epithelial from stromal cells using microdissection and enzymatic methods [187, 188]. Generally speaking, tissue recombinants are generated from mesenchymal and epithelial cells from the same tissue are referred to as homotypic, whilst those from different tissue are referred to as heterotypic [185]. Furthermore, homospecific refers to mesenchymal and epithelial cells belonging to the same species whilst heterospecific refers to cells from different species [185]. The conservation of signalling pathways between different species is particularly important for the viability and validity of heterospecific recombinants. The ability of neonatal mouse uterine mesenchyme (nMUM) to support human adult uterine epithelium and the epithelium inducing myometrial differentiation

from nMUM suggested that a robust level of conservation exist between mouse and human signalling pathways regulation endometrial growth and development [184]. Whilst it is advantageous to transplant heterospecific recombinants for identification of species specific cell types during analysis, both human and out-bred mice tissue are immunogenic in mouse hosts. Therefore the use of severe combined immunodeficiency (SCID) mouse hosts is required for heterospecific tissue recombinants.

Tissue recombination studies focus on understanding the interaction between epithelial and stromal cells. In general, the interaction is classified as permissive or instructive [176]. A permissive effect refers to the support of a predetermined developmental program [189]. By contrast, an instructive effect refers to initiation of a new program of differentiation [189]. Both the permissive and instructive capabilities of nMUM have been documented in the past [22, 184, 190]. One of the earliest tissue recombination experiments demonstrated the instructive capacity of the neonatal uterine mesenchyme, which altered the phenotype of the vaginal epithelium to that of the uterine epithelium [22]. The permissive nature of the nMUM was demonstrated when nMUM was shown to support the adult human endometrial epithelium [184]. Recently, the instructive nature of nMUM was again shown when it transdifferentiated mouse spermatogonial stem cells (SCC) into the mouse uterine epithelium [190]. Despite overwhelming evidence indicating the inductive capacity of nMUM, the soluble factors involved in various induction experiments have not been characterised [128].

### **1.7.2 Technological advances in tissue recombination**

The advent of genetic technology in recent times has increased the flexibility of tissue recombination methods. Researchers can now manipulate a target gene by over-expressing or silencing it in primary animal cells prior to recombination with another tissue [191]. Alternatively, mesenchyme from gene knockout mice has been used in tissue recombination studies [186, 192-194]. These approaches have allowed investigators to dissect the molecular pathways involved in normal organogenesis as well as those involved in disease initiation and progression.

In summary, *in vivo* modelling and tissue recombination are powerful tools for investigation of epithelial-mesenchymal interactions. The technique is applicable to a variety of cell types, from

different species, from different developmental lineage (i.e. mesoderm, endoderm), and at different developmental states (i.e. embryonic, neonatal). Tissue recombination may help to create a model of human FRT from hESC.

### **1.8 Pluripotent stem cells: human embryonic stem cells**

Human embryonic stem cells (hESCs) are cells derived from the inner cell mass of blastocyst-stage human embryo [195]. Unlike adult stem cells (ASCs), hESCs are pluripotent, capable of forming all tissue types of the human body [196], and undergo self-renewal *in vitro* and can be maintained as undifferentiated colonies indefinitely [197]. These properties make hESCs ideal for both research and possible future clinical applications [195, 198].

There are some 300 hESC lines available since Thomson et al derived the first human embryonic stem cell line [163, 199]. A recent study employing gene expression analysis showed there may be significant differences in the developmental potential between hESC lines [200]. The study highlighted an important issue overshadowing hESC research; differentiation protocols developed for one hESC line may not yield the same results when applied to another.

Early experiments demonstrated that hESC transplanted alone into immunodeficient mice spontaneously differentiated into a teratoma containing cells from three germ lineages i.e. mesoderm, endoderm, ectoderm, which presented a major obstacle for any clinical use of hESC [195]. In order to avoid transplanting undifferentiated cells and avoid teratoma formation, researchers have differentiated hESC towards specific tissue types *in vitro* prior to transplantation into animal models. Genetic manipulations by transfection of hESC with DNA constructs produced hESC with reporter genes, which allows purification of cells of interest following *in vitro* differentiation [43]. Electroporation of hESC has also been used to genetically manipulate hESC. Green fluorescent protein (GFP) has been introduced into the HES3 cell line creating the “ENVY” cell line robustly expressing GFP in all embryoid bodies and their differentiated progenies [201]. The “ENVY” cell line has been an invaluable tool for both transplantation experiments and *in vitro* studies [181, 202]. It allows identification of hESC unequivocally amidst foreign mouse tissue long after transplantation [181]. In addition to ENVY, other hESC reporter cell lines have been generated to aid research efforts investigating early *in vitro* hESC differentiation [43, 203-206].

In summary, hESC are pluripotent stem cells that can self-renew indefinitely *in vitro*, with great variation in the developmental potential of cell lines. Advances in genetic technology have allowed modifications of hESC to incorporate fluorescent proteins that enables tracking the

development of hESC under both *in vitro* and *in vivo* conditions especially where there are other species of mammalian cells present. The propensity of hESC to develop uncontrollably into a teratoma *in vivo* have impeded their use under clinical setting for cell therapies, as a result, hESC remains predominantly a research tool. Recently, however, a world first Phase I clinical trial have commenced using hESC-derived cells for spinal cord injuries [207].

### 1.8.1 Cultivation of hESC

The laboratory cultivation of hESC *in vitro* is technically demanding because of the propensity of hESC to undergo spontaneous differentiation. Under laboratory settings, hESC are maintained in a pluripotent state (undifferentiated) by co-culture with mitotically inactivated mouse embryonic fibroblasts (MEF) in medium supplemented with 20% fetal bovine serum (FBS) [163]. hESC is frequently passaged by manual micro-dissection, followed by transfer of individual colonies onto fresh MEFs. This method is still widely used but present two major disadvantages: 1) contamination with animal pathogens through the use of MEFs and FBS and 2) inconsistency of hESC growth resulting from variations between MEF and FBS batched used. Alternatively, enzymatic passaging techniques have reduced preparation time while continue to maintain karyotypic stability [208, 209].

#### 1.8.1.1 Current hESC culture systems

Recently, new and improved culture systems have been designed to eliminate the use of MEF and FBS. hESC can now be propagated using serum-free media [210]. Alternatively undifferentiated hESC can be maintained using Matrigel matrix combined with 100% MEF-conditioned medium [211]. Others have used a variety of human supportive cells such as embryonic fibroblasts, adult fallopian tube epithelium, and foreskin fibroblasts [212-214]. More sophisticated systems incorporate defined serum replacement medium containing growth factors and a matrix replacing the feeder layer [215, 216]. Without a functional supportive layer such as the MEF or the more advanced serum and feeder layer replacement systems, hESC attached onto a culture plate can undergo more rapid spontaneous differentiation in the centre and along the border of the flat colonies [195]. These colonies contain cells representing all three germ layers; ectoderm, mesoderm and endoderm [217].

### 1.8.1.2 Embryoid body formation

hESCs cultured in non-attachment conditions, or plated in the absence either feeder-layer or anti-differentiation factors will spontaneously form embryoid bodies (EB) [218]. EBs are three-dimensional (3D) structures with a tri-layer shell covering the ectodermal tissue which lines the outer layer and internal structures comprising cells from endoderm and mesoderm lineages [219].

Several methods have been described for the formation of EBs from embryonic stem cells. These methods generally fall into five categories; 1) suspension culture in bacteriological dish, 2) methycellulose culture, 3) hanging drop culture, 4) suspension culture on low adherent plates 5) and spinner flask and bioreactor culture [220]. Each method was designed independently to suit the goals of particular experiments. The conditions vary between methods, and as a result, the size and shape of EB produced may also vary. Formation of heterogeneous EBs has been linked to difference in size and shape of the EB [221]. The lack of homogeneity in the EB results in asynchronous differentiation of the cells within. Most current methods aim to produce homogenous or uniform EBs. One method in particular, allows for small-scale production of uniform EB, where hESCs are centrifuged in the wells of 96-well round-bottom well plates to generate EBs [222].

### 1.8.2 Lineage Specific Differentiation of hESC

The hESCs are differentiated as either as an EB structure or flat colonies *in vitro*. As hESC differentiate, they become less pluripotent, eventually becoming a precursor to a specific type of tissue. Depending on the environmental cues these progenitors will terminally differentiate and resemble their endogenous counterparts.

The 3D structure of the EB allows multi-cellular interaction in a physiologically relevant manner, i.e. cell-cell contact which is crucial in directing cell fate. Signalling between cells is believed to generate concentration gradients of morphogens consequently leading to differentiation. Much of EB development recapitulates events observed in early embryogenesis. For this reason, EBs are often used to initiate *in vitro* differentiation [220]. *In vitro* differentiation methods often attempt to alter the concentration gradient within the EB by adding



exogenous soluble biochemicals in the media to influence or direct cells towards specific fates [219]. More advanced methods involve EB dissociation and isolation of cells bearing particular antigenic markers by flow cytometric methods for further differentiation under different *in vitro* conditions [195].

Several type of assays have been described for differentiation of hESC towards a particular lineage *in vitro*; co-culture of hESC with cell types capable of lineage induction [166, 223], exposure of hESC to one or a combination of growth factors and /or their antagonists [165], culture of ESC with extracellular matrix proteins [224], and other complicated protocols involving sequential addition of growth factors at different stages of *in vitro* differentiation [172]. There is a growing list of clinically relevant cell types derived from hESC (Figure 1.10). The progress in differentiation of hESC towards the ectodermal and endodermal lineages is beyond the scope of this thesis. The focus will instead be on the knowledge relevant to mesoderm induction from hESC.

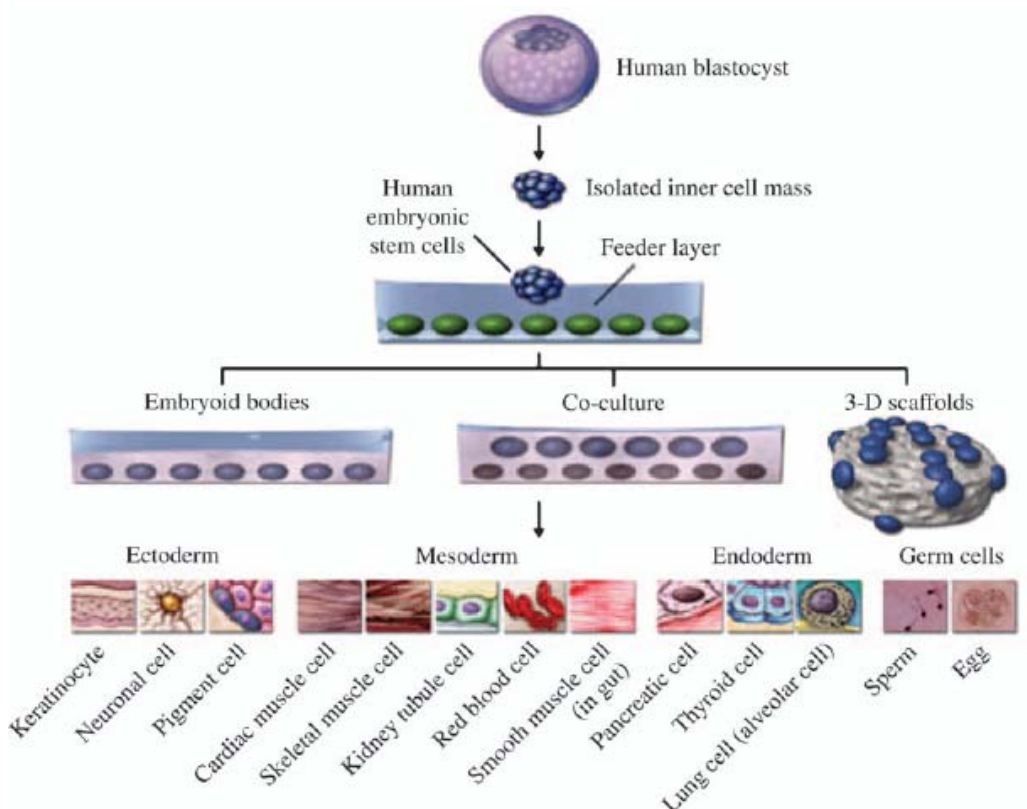


**Figure 1.10 Derivation of human embryonic stem cells and various differentiation strategies**

Adapted from Mountford 2008 [199] with permission from John Wiley and Sons.

### 1.8.3 Pathways of Mesoderm induction

In mouse embryos, the formation of a transient structure known as the primitive streak (PS) marks the beginning of gastrulation [225]. The PS is formed in a region of the epiblast destined to become the posterior end of the embryo. Specific regions of the PS give rise to the mesoderm during embryogenesis [1].

#### 1.8.3.1 Molecular pathways regulating mesoderm formation

Molecular analyses and lineage mapping studies have delineated different regions of the PS, based on level of gene expression and developmental potential as illustrated in Figure 1.11 [226]. The anterior PS expresses high levels of *Foxa2* and *Goosecoid* (*GSC*) compared to the posterior PS which preferentially expresses homeobox B1 (*Hoxb1*) and even skipped homeotic gene 1 homolog (*Evx1*). Genes commonly found throughout the PS include *Brachyury* and MIX1 homeobox-like protein 1 (*Mixl1*). The specification of subpopulations of mesoderm and endoderm from the PS during gastrulation is regulated both temporally and spatially beginning with migration of cells from the posterior PS to form embryonic mesoderm which gives rise to mesodermally derived cardiac, and vascular cell types. Cell migration continues through the anterior end of the PS resulting in the formation of axial, intermediate and lateral mesoderm. Further development of both the lateral and intermediate mesoderm contributes to generation of urogenital organs (i.e. kidney and reproductive tracts) [2, 227, 228]. Cells migrating through the most anterior region of the PS form the definitive endoderm.

The ability of PS cells to migrate is attributed to the complex process of epithelial-to-mesenchymal transition (EMT) that occurs during gastrulation in the mouse embryo [225]. Similarly, in human cells, several studies have identified the upregulation of EMT related genes including Snail homolog 1 (*SNAI1*), Snail homolog 2 (*SLUG*), Vimentin in hESC derived endoderm and mesoderm progenitor cells, underscoring the critical nature of the EMT process for mesoderm formation during the mammalian embryogenesis [229, 230].

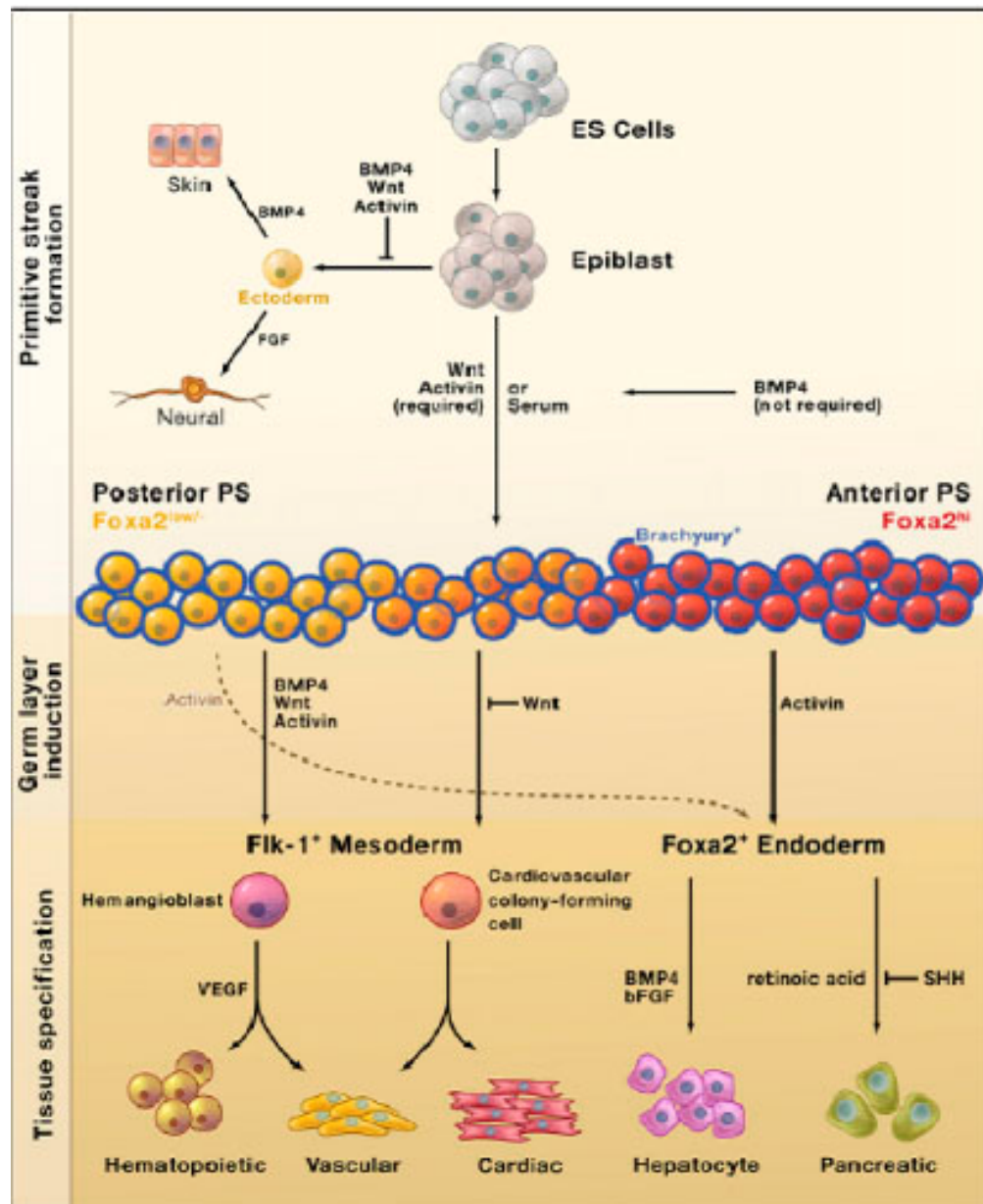


**Figure 1.11 ESC differentiation *in vitro***

A model illustrating the mechanisms regulating primitive streak (PS) formation, primary germ layer induction and tissue specification from differentiated mouse embryonic stem cells. The initial step in the differentiation pathway involves development of epiblast-like cells. Upon exposure to Wnt, activin, BMP4, these epiblast-like cells differentiate to form the PS-like population (row of cells outlined in blue). In the absence of these inductive molecules, the epiblast cells will differentiate into ectoderm lineage. The presence of the aforementioned signalling pathways block ectoderm differentiation. Following PS induction, the anterior streak cells (dark orange) are fated to generate *Foxa2*<sup>+</sup> cells belonging the definitive endoderm. In contrast, the posterior PS cells (yellow) become Flk-1<sup>+</sup> mesoderm cells. Reproduced from Murry and Keller 2008 [226] with permission from Elsevier

### **1.8.4 Role BMP and Wnt family molecules in animal models and mESC differentiation systems**

The specification of cell fate through the PS during gastrulation is influenced by both temporal/spatial factors. A number of key regulatory molecular signalling pathways involved in the process of cell fate specification include members of the TGF- $\beta$  family, BMP4 and Nodal, and Wnt family [231].

#### **1.8.4.1 BMP ligands**

Studies in mouse embryonic development have shown that Bmp4 is essential for gastrulation and mesoderm formation [232-234]. In the absence of BMP inhibitors such as Noggin and Chordin, anterior neural patterning is disrupted by Bmp4 thus allowing formation of the PS. In the absence of Bmp4, there is expansion of the anterior ectoderm and definitive endoderm [235]. The evidence from mESC differentiation studies correlates with observations made in early mouse embryos. Neuronal differentiation of mESC *in vitro* is disrupted in the presence of Bmp4 and increased by the addition of Noggin [236, 237]. Several studies using the mESC differentiation system have shown that Bmp4 in serum free medium may be dispensable for PS induction [238], but is critical in specification of the posterior mesoderm which has the potential to give rise to haemopoietic progenitor cells [236, 239-243]. Other members of the BMP family including Bmp2 and Bmp7 also influence mesodermal differentiation, promoting mESC to become renal progenitors at the expense of haemopoietic progenitors [244, 245].

#### **1.8.4.2 Wnt family ligands**

Like BMPs, ligands from the Wnt pathway are heavily involved in gastrulation and PS formation. The PS and mesoderm fail to form in embryos of *Wnt3*-null mutant mice [246]. In a mutation study targeting the frizzled co-receptors *Lrp-5* and *Lrp-6*, it was demonstrated that *Wnt3* is not only required for proper migration of cells from the PS, but also for inhibition of neuroectoderm and anterior PS formation [247]. *Wnt4* was recently shown to play an important role in formation of haemopoietic cells in a *Xenopus* study [248]. Recent findings suggest that Wnt pathway is indispensable for formation of a primitive streak-like region in the self-

organising mouse EB [238]. Similarly, in a mESC differentiation system, blocking Wnt in serum-stimulated culture reduced the number of mesodermal cells whilst enhancing neuroectoderm formation [249-251]. Conversely, addition of Wnt3 to cultures triggered formation of the PS population and promoted cardiac mesoderm development in a biphasic manner [251, 252]. Wnt3 in serum-free culture preferentially induced posterior PS population [253]. Furthermore, cell lines generated with GFP targeting the *Brachyury* gene and human CD4 cDNA targeting the *Foxa2* gene allowed isolation of the PS and its subpopulations [253].

#### **1.8.4.3 Activin/Nodal**

Mouse embryo studies showed that Activin and Nodal are indispensable in formation of PS but may be redundant in producing posterior mesodermal cells [254]. Loss of function of the *Nodal* gene resulted in failure of PS development [255]. Notwithstanding the failure of PS development, posterior mesodermal cells formed, however, they failed to migrate which suggested a role for nodal in spatial orientation of mesodermal cells.[255].

Studies in mESC differentiation systems often use Activin A as a surrogate for Nodal since both bind to the same receptors and thus initiate the same signalling events [256]. The addition of recombinant human Activin A in serum-free culture induced formation of endoderm and mesodermal cells in a dose-dependent manner [239, 257]. The lower level of activin A resulted in paraxial mesoderm which gave rise to skeletal muscles. In contrast higher levels induced formation of definitive endoderm [257]. In summary, studies have indicated the importance of BMP, Wnt and Activin/Nodal in early embryonic development both *in vivo* and *in vitro*. They have also shown that the signalling pathways are inextricably linked.

#### **1.8.4.4 Interaction between signalling pathways**

Collectively, the studies mentioned above suggest the BMP, Wnt and Activin/Nodal signalling pathways are critical in normal development of the PS and mesoderm in both mouse embryo and mESC differentiation systems. Evidence from mouse embryo studies also indicates the complex interactions between the signalling pathways. For example, in a gene mutation study, a mathematically modelled network showed that where Nodal promotes expression of endogenous Bmp4 from extra-embryonic sources which subsequently led to activation of Wnt3 and

amplification of Nodal expression to promote mesoderm formation [258]. Both Wnt and Nodal are simultaneously required for formation of PS [253]. Combination of Wnt, Activin and Bmp4 led to induction PS and *Flk1*+ mesoderm, however the effect of Bmp4 may be indirect through endogenous activation of Wnt and Nodal, similar to the Ben Haim's model [241, 258].

#### **1.8.4.5 Role of ECM and mesoderm induction**

In addition to soluble factors, extracellular matrix (ECM) proteins form part of the niche that determines cell fate during ESC differentiation. Loss of  $\beta 1$  integrin receptor (a cell membrane receptors involved in signalling between ESC and the ECM) resulted in delayed induction of cardiac-specific genes and functions in differentiating ESC [259, 260]. Furthermore, another study using the same  $\beta 1$  integrin deficient ESC observed an accelerated neuroectodermal commitment at the expense of mesodermal tissue in differentiating ESC which also paralleled an upregulation of *Wnt-1* levels and downregulation of *Bmp4* levels [261]. ESC was also demonstrated to differentiate preferentially towards a mesodermal and endodermal lineage when grown as an aggregate in the presence of exogenous ECM. In contrast, a reduction in endogenous ECM caused disaggregation of ESC highlighting the role of ECM in their differentiation [224].

#### **1.8.5 Primitive streak and mesoderm induction in hESC differentiation systems**

The developmental fate of differentiating hESC depends on a complex cocktail of soluble growth factors, signalling molecules, and ECM proteins that make up the developmental niche. Although, there are fundamental differences in the developmental processes mESC and hESC [163, 217], the signalling pathways responsible for early developmental stages of PS and mesoderm formation are evolutionarily conserved between mammalian species.

In hESC systems, BMP4 also induces PS and mesoderm formation. Several studies using hESC showed that a combination of cytokines including stem cell factor (SCF), granulocyte colony-stimulating factor, Flt3-ligand, interleukin 3 (IL-3) and interleukin 6 (IL-6), vascular endothelial

growth factor (VEGF) with BMP4 promoted haemopoietic development *in vitro* [165, 262]. Studies using both wild-type and modified hESC with GFP targeting the *MIXL1* gene showed that addition of BMP4 in culture lead to an increased number of cells expressing both *Brachyury* and *MIXL1* followed by formation of KDR<sup>+</sup> and PDGFR<sup>+</sup> mesodermal subpopulations [204, 222, 263-265]. More interestingly, hESC exposed to BMP4 for shorter periods resulted in mesoderm induction, where as longer treatment of hESC with BMP4 resulted in trophoblast and extra-embryonic endoderm differentiation [266]. The importance of Wnt signalling in PS and mesoderm formation was further demonstrated in hESC culture by blocking Wnt ligands in serum-containing cultures which diminished the development of haemopoietic progenitor cells [267]. The combined action and interaction of the major signalling pathways involved in mesoderm development has been demonstrated in hESC differentiation systems; combination of Activin A and BMP4 induces cardiac mesoderm [168]. Through the use of small molecule inhibitors which blocked PS and mesoderm formation despite the presence of BMP4, it was demonstrated that BMP4 relies on Activin/Nodal as well as FGF to induce mesoderm formation [266].

The addition of ECM protein complex consisting of laminin and nidogen increases differentiation of mesodermally derived hematoendothelial cell types in differentiating human EBs compared to untreated EBs further highlighting the role ECM may have on mesodermal lineage commitment [268]. Collectively, these studies demonstrate that there are similarities between the development of mESC and hESC, and strategies used in mESC differentiation system can also be applied in hESC culture.

The standard combination of growth factors used for mesoderm induction in current protocols for hESC differentiation culture often includes BMP4 and Activin A along with a variety of other growth factors including vascular endothelial growth factor (VEGF), FGF, and TGF- $\beta$ 1. A recent study showed that a combination of factors is capable of inducing the formation of a multipotent mesoderm-committed progenitor population *in vitro* [229]. Whilst, a large number of investigations focus on differentiating hESC towards ectodermally- and endodermally-derived organs, mesodermally derived organs and cells types of the haemopoietic, and cardiac lineages have also been an intense focus of research [206, 269]. By contrast, little effort has been directed towards differentiation of hESC into other mesodermally derived organs; urogenital organs. There are only two published studies in which the authors examined the possibility of

differentiating hESC towards early renal progenitors *in vitro* [270, 271]. Differentiation of hESC towards other urogenital organs such as the human FRT remains to be attempted.



## **1.9 Hypotheses and Aims**

### **1.9.1 Hypotheses**

1. Neonatal mouse uterine mesenchyme induces hESC to differentiate towards a mesodermal lineage *in vitro* and will subsequently develop into human FRT epithelium *in vivo*
2. The development of a hESC-derived FRT will recapitulate sequence of events observed during normal mammalian FRT development
3. A model of hESC-derived FRT will facilitate identification of molecules involved in human FRT development
4. The earlier stage of mesenchyme and hESC interaction will reveal mesenchyme- derived growth factors involved in hESC differentiation towards Müllerian duct precursors

### **1.9.2 Aims**

1. Generate human FRT epithelium by recombining hESC with neonatal mouse uterine mesenchyme in a xenograft tissue recombinant model.
2. Characterise and stage the development of hESC-derived Müllerian duct epithelium
3. Using hESC-derived FRT epithelium to investigate the dynamic expression of LIM1 and examine its expression in adult human endometrium
4. Identify neonatal mouse uterine mesenchyme-derived growth factors involved in hESC differentiation.

## **CHAPTER 2 Development of a method to generate human female reproductive tract epithelium from human embryonic stem cells**

### **2.1 Introduction**

Human embryonic stem cells (hESC) are derived from the inner cell mass of blastocyst stage embryos [163]. These pluripotent cells differentiate into any cell types in the body. Much effort has focused on differentiating hESC into various clinically relevant cell types by addition of exogenous growth factors or co-culture with various murine and human feeder layers *in vitro* [226, 272]. *In vitro* culture system, however, can not match the complexity of an *in vivo* environment. *In vivo* models are therefore important tools to expand the understanding of complex interaction between cell types during normal development.

*In vivo* modelling uses several different approaches. Differentiated cell types (i.e. epithelial, stromal) can be transplanted into a host stromal niche to study epithelial-stromal interactions [180, 181]. Alternatively, tissue fragments can be grafted into an animal host to study their development *in vivo* [182, 183]. Finally, there are *in vivo* models that use tissue recombination technology where defined stromal and epithelial cells are brought together *in vitro* and subsequently transplanted into an animal host as a xenograft. Commonly used transplantation sites include sub-renal capsule or subcutaneous locations. Sub-renal capsule sites are technically more demanding however are better vascularised than subcutaneous sites resulting in higher take rates [185].

In a seminal study, Taylor et al applied tissue recombination methods in an *in vivo* model of prostate organ development using murine fetal and postnatal urogenital /seminal vesicle mesenchyme to direct the differentiation of hESC [174]. Similarly, mouse embryonic stem cells (mESC) were differentiated into bladder epithelium *in vivo* following tissue recombination with fetal rat bladder mesenchyme [175]. These experiments suggested that *in vivo* organ development models can be established by combining undifferentiated ESC with organ specific mesenchyme.

The use of neonatal mouse uterine mesenchyme (nMUM) in tissue recombination experiments has been instrumental in increasing understanding of female reproductive tract (FRT) biology [19, 22, 26, 184, 186, 194, 273, 274]. Unlike other visceral organs (ie. pancreas, liver), the tubular nature of the fetal/neonatal mouse uterus allows easy separation of the stroma from the epithelium. Cunha et al first described the method of uterine epithelial-stromal separation using an enzymatic digestion coupled with micro-dissection [23, 188]. Later it was shown by tissue recombination that nMUM supports adult human uterine epithelium *in vivo* [184]. Recently, the nMUM transdifferentiated mouse spermatogonial stem cells (SCC) into the mouse uterine epithelium further highlighting the instructive capacity of the nMUM [190]. We therefore hypothesized the nMUM will also support differentiation of hESC *in vivo*.

Tissue recombination involving ESC and embryonic mesenchyme required impeccable timing with regards to obtaining both types (ESC and mesenchyme) for differentiation. The amount of embryonic tissue available for experiments is also a limiting factor for establishing *in vivo* models. The aims of the current investigation was to establish a 2 step differentiation protocol utilising nMUM to direct the differentiation of hESC by 1) making heterospecific/heterotypic tissue recombinants from differentiating hESC *in vitro* and 2) transplanting the recombinant graft *in vivo* for further development into human FRT epithelium.

## **2.2 Methods**

### **2.2.1 Animals**

Animals were obtained from Monash Animal Services. Day 0-3 nMUM was obtained from female C57BL/6JAsmu (F1) mice. Female NOD.CB17-prkdcscid/Asmu (NOD.SCID) mice 4-6 weeks old were housed under controlled environmental conditions at 20°C with 12-hour dark/light cycles and unlimited access to food and water. All animal handling and procedures were carried out in accordance with National Health and Medical Research Council of Australia guidelines for the Care and Use of Laboratory Animal Act and approval was obtained from the Monash University Animal Ethics Committee at Monash Medical Centre – A (MMC-A), Clayton, Australia. The approval numbers are 2006/44 and 2010/41.

### **2.2.2 Micro-dissection of neonatal uterine mesenchyme**

nMUM tissue collection was modified based on methods previously reported [23, 188]. The uterus from donor 0-3 day old F1 mice were separated into two horns, 6 pieces each measuring 0.5mm (each piece contained approximately  $8 \times 10^5$  cells) from each uterine horn were then placed into 1% Trypsin (Gibco, Invitrogen) in Dulbecco's Phosphate Buffer Saline (DPBS)(Invitrogen). After one hour digestion at room temperature, the tissue pieces were washed briefly with Dulbecco's modified Eagle's medium (DMEM)(Invitrogen) to inactivate the trypsin reaction. The uterine pieces were then further treated with dextranase I (DNase) (4mg/ml) (Worthington Biochemical Corporation, Lakewood, NJ) to enhance separation of epithelium and mesenchyme. Separation was performed mechanically with fine surgical forceps in a modified watch glass (Maximov depression slides (Fisher, Pittsburgh, PA) using a Zeiss dissecting microscope (Stemi-2000C, Zeiss). The mesenchyme was rinsed again in DMEM followed by a final rinse with DPBS to remove residual DMEM and DNase I in the tissue before recombination with hESC.

### 2.2.3 hESC culture

The International Stem Cell Initiative Registry listed hESC line, MEL-1 (The International Stem Cell Initiative, 2007) was obtained from Australian Stem Cell Centre (ASCC, Australia) and cultured in Dr Paul Verma's laboratory according to previously published methods (Centre of Reproduction and Development, Monash Institute of Medical Research) [275]. Approval was obtained from Southern Health Standing Committee on Ethics in Research Involving Humans (approval number: CF08/1793 – 2008000889) The MEL-1 cell line was maintained on mitotically inactivated mouse embryonic fibroblasts (MEF) in gelatin-coated culture dishes in hESC medium: Dulbecco's modified Eagles's medium (DMEM) supplemented with 1% nonessential amino acids, 1mM L-glutamine, 1% Insulin-Transferrin-Selenium (ITS), 4 ng/ml basic fibroblast growth factor (bFGF), 0.1 mM 2-mercaptoethanol (all from Invitrogen, Mount Waverly, VIC, Australia) and 20% fetal calf serum (FCS; Hyclone, Melbourne, Australia) under a humidified atmosphere of 5% CO<sub>2</sub> in air at 37°C. For passage, the cells were dissociated by treatment with 4 mg/ml Dispase (Invitrogen) in DMEM for 10 min at 37°C, centrifuged at 100g for 10 min, and then seeded onto MEF feeder layers. To check pluripotency of the hESC, cells were seeded at high density onto gelatin coated chamber slides for attachment overnight. Cells were fixed briefly in 4% PFA on the following day and then rinsed for storage or immunocytochemistry for pluripotency markers.

### 2.2.4 Generation of heterotypic tissue recombinants

To form embryoid bodies (EBs), MEL-1 colonies were microdissected and the cell clumps were resuspended in hESC medium without bFGF. The cell clumps were cultured together with nMUM in non-adherent cell inserts (Millicell, Millipore) placed in individual wells of 24 well plates. One genetically modified hESC lines; the constitutively GFP<sup>+</sup> line, ENVY [201] was used. T25 culture flasks from Stem Core were purchased (ASCC, Australia). The pluripotency and karyotype of the hESCs were regularly tested by the staff at Stem Core and Monash Cytogenetics department respectively. hESCs were harvested from the culture flask using TrypLE Select (Invitrogen) and cells were force aggregated to form embryoid body (EB) by centrifugation in 96 well plates in serum-free medium (SFM) according to previously reported protocols for 24 hours before nMUM was added to culture [205, 222]. Tissue recombinants for grafting were cultured *in vitro* for a total of 42 hours for MEL-1 recombinants and 72 hours for

ENVY recombinants at 37°C in hESC medium (without bFGF) or SFM respectively, prior to transplantation into NOD.SCID mice.

### **2.2.5 Kidney capsule transplantation, in vivo imaging and tissue processing**

Prior to transplantation, culture media was removed from each well containing tissue recombinants, and tissue recombinants were re-suspended in 10µl of neutralised rat tail collagen (a generous gift from Dr. Renea Taylor, Department of Anatomy and Developmental Biology, Monash University, Australia) and placed on the surface of a non-adherent Petri-dish and incubated without medium for 10-15 minutes at 37°C for gel solidification. Medium was then added and recombinants were incubated for 15 minutes at 37°C prior to transplantation.

The tissue recombinants were grafted under the renal capsule of adult female NOD.SCID mice as previously described [175]. Briefly, vertical skin incision was made along the dorsal midline and the kidney was exteriorised with gentle pressure. A capsulotomy was performed to create a subcapsular space. Grafts were then placed underneath the renal capsule. Two grafts were placed into each kidney which was reintroduced back into the mouse. Surgical incisions were closed with staples. All mice were ovariectomized at the time of grafting.

Four weeks after grafting, mice were anesthetized, abdominal hair was removed to prevent auto-fluorescence, and the fluorescence emitted from the ENVY hESC was detected using LAS3000 (Fuji, Tokyo, Japan) Imaging Systems (courtesy of Dr Elizabeth Williams, MIMR) and digitally captured as previously described [276]. At the time of harvest, mice were sacrificed by CO<sub>2</sub> asphyxiation. Grafts were harvested together with the kidney, fixed in 4% paraformaldehyde (PFA) overnight. After fixation, the grafts were imaged and measured. Specimens were processed, paraffin embedded, and serial sections cut at 3µm for H&E and Hoechst staining. Hoechst Dye 33258 was placed on sections for 30 seconds (Molecular Probes, Eugene, Oregon, USA) and rinsed with distilled water and allowed to air dry before mounting.

### **2.2.6 Immunocytochemistry**

hESCs cultured on chamber slides were permeabilized with 0.5% Triton-X 100 in PBS for 15 min. The endogenous peroxidase activity was blocked with 3% H<sub>2</sub>O<sub>2</sub> in methanol for 10 min at

RT followed by 3 rinses with PBS. Protein Block was applied to sections to minimise non-specific antibody binding (Serum-free protein block, DAKO, Denmark) for 10 min at room temperature. Antibodies of the same IgG isotype as the primary antibody were incubated on the same slide at a matched concentration as a negative control. Cells were incubated with primary antibodies to Oct-3/4 (Santa Cruz sc-9081), SSEA-3 (MAB4303; Millipore), SSEA-4 (MAB4304; Millipore), TRA-160 (MAB4360; Millipore), and TRA-181 (MAB4381; Millipore) overnight at 4°C. Slides were then washed thoroughly with PBS, and cells were incubated with the appropriate Alexa Fluor secondary antibody (Invitrogen) for 30-60 minutes at RT. Slides were washed, air dried in the dark and mounted with fluorescent mounting medium (DAKO). Fluorescent images were captured with a Leica DMR upright fluorescence microscope (Leica). Alkaline phosphatase activity of hESC was analyzed using the Vector Red Alkaline Phosphatase Substrate Kit (Cat. No. SK-5100; Vector Laboratories) according to manufacturer's specifications and the reaction product was visualized using bright field. Images were captured with an Olympus upright microscope (Olympus).

## **2.3 Results**

### **2.3.1 Pluripotency of MEL-1 cells**

MEL-1 hESCs were cultured on mouse embryonic fibroblast (MEF) feeder layers to prevent differentiation and maintain their pluripotency for continuous passaging. Expression of a panel of commonly used pluripotent markers were assessed for manually passaged colonies of MEL-1 cells (Figure 2.1A). Robust expression of pluripotency markers including Oct4, SSEA-4, TRA-181, and TRA-160 was observed. Strong alkaline phosphatase activity was also detected, consistent with previous studies [277, 278]. However, weaker expression of SSEA-3 suggests some differentiation may have already occurred in the hESC colonies, nevertheless, the majority of the colonies remained pluripotent. The pluripotency of the manually passaged MEL-1 cells was further checked by intramuscular injection of hESCs into the legs of the immunodeficient NOD.SCID mice. The pluripotent MEL-1 cells formed teratoma consisting of tissues from the three germ layers (Figure 2.1B) consistent with previous studies [279, 280].

### **2.3.2 Tissue recombination in vitro: MEL-1 with nMUM**

It had been shown previously that the viability of embryonic stem cells (ESCs) is markedly reduced if they are prepared as single cells [281, 282]. No attempts were made to recombine dissociated single hESC with nMUM despite a previous study showing that single mESC successfully recombined with rat bladder mesenchyme [175]. Rather than single cells, embryoid bodies (EB) were created from hESC for tissue recombination with nMUM. Non-attached hESCs in suspension culture form EB [220]. Heterospecific/heterotypic recombinant tissues consisting of nMUM and hESC derived EBs formed after 48 hours *in vitro* culture (Figure 2.2, n>20) consistent with previous reports on the ability of mouse mesenchyme to form tissue recombinants with ES cells *in vitro* [174, 175, 283]. The hESC were distinguished from nMUM by the more transparent nature of the hESC under bright field microscopy, in contrast to the denser connective tissue that made up the nMUM. In summary, microdissected nMUM formed heterospecific recombinants with MEL-1 derived EB under serum conditions in suspension culture *in vitro*.



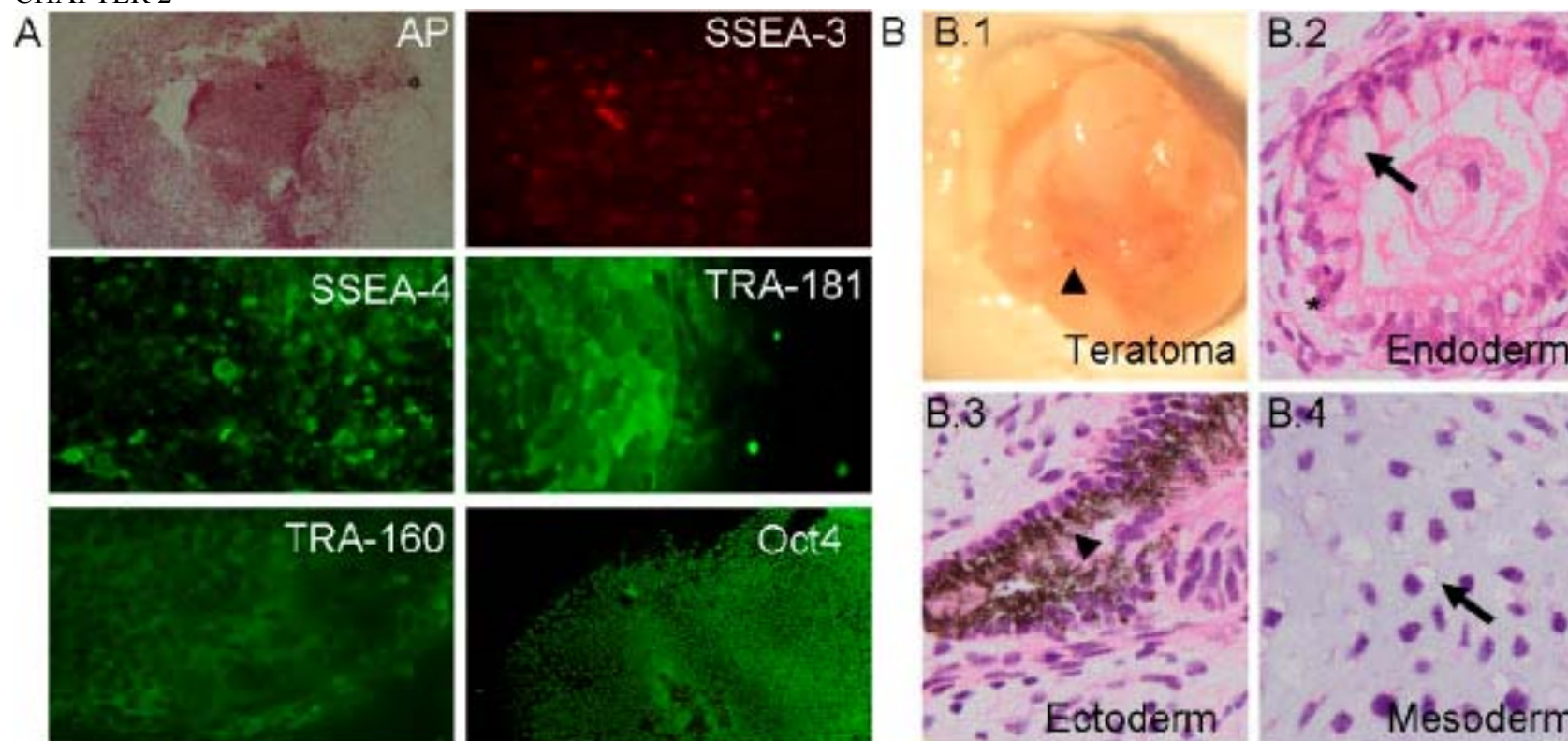


**Figure 2.1 Assessment of pluripotency of MEL-1 hESCs**

(A) Co-Expression of pluripotency markers in cultured MEL-1 colonies (B) representative photograph of a MEL-1 derived teratoma (n=1) (arrow head shows pigmented tissue). (B.1-4 photomicrograph of representative H&E sections showing tissue types found within the teratoma. (B.1) photograph of a teratoma (arrow head points to pigmented tissue) (B.2) endodermally derived gut-like epithelium (asterix indicate a Paneth cell, arrow points to a mucous cell). (B.3) ectodermally derived tissue (arrow head points to pigmented epithelial tissue). (B.4) mesodermally derived cartilage (arrow points to chondrocytes in lacunae).

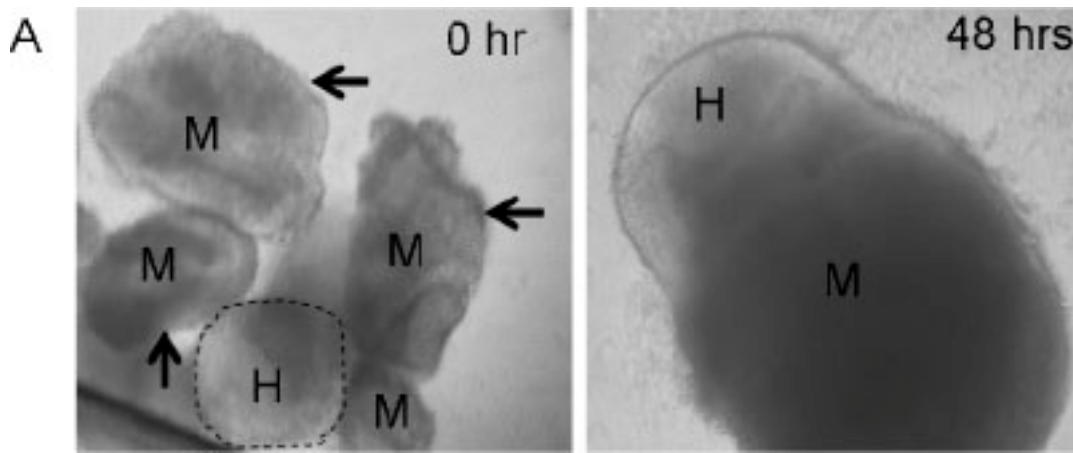


**Figure 2.2 Tissue recombination of MEL-1 hESC with nMUM**

(A) Photomicrograph showing MEL-1 cell clump in culture with day 1 nMUM at 0 and 48 hours (arrows point to epithelial-free nMUM). Abbreviations: H, MEL-1 hESC; M, nMUM.

### 2.3.3 Morphological analysis of the MEL-1/nMUM recombinant graft

After 8 weeks of *in vivo* incubation, recombinant grafts had developed into teratoma-like tissue consistent with previous studies [174, 175]. Whole grafts were sectioned and representative serial sections (3 $\mu$ m) at every 60 $\mu$ m intervals were used to search for hESC derived epithelium surrounded by mouse stromal cells using Hoechst and H&E stains (Figure 2.3).

hESC-derived epithelium surrounded by mouse stromal cells was identified in recombinant grafts (n=2) in the presence of other tissue types (Figure 2.3). The mouse stromal cells were distinguished from human cells by their speckled nuclear chromatin pattern (Figure 2.3E-F) in Hoechst stained sections as previously described [284]. In one case, a mouse uterine gland was detected in the recombinant graft in the vicinity of the hESC derived hybrid epithelium possibly due to remnants of uterine epithelium not removed during enzymatic separation in microdissected neonatal mouse uterus (Figure 2.3G), a technical difficulty also reported in a previous study [184].

Examining the recombinant glandular structures surrounded by mouse stromal cells in sections stained with H&E revealed a number of morphological features of the upper FRT epithelium of the oviduct or uterus. Ciliation and basal vacuolation of epithelium with cuboidal/columnar morphology were observed (Figure 2.3D) [285]. To our knowledge, no studies have reported spontaneous differentiation of FRT epithelium in ESC derived teratomas, although spontaneous differentiation of hESC towards glandular tissue has been documented [280]. The FRT-like

morphology of the recombinant glandular structure was not found in control grafts comprising of hESC EB xenografts (n=4). Consistent with a previous report, no hESC derived epithelial structures in controls were surrounded by host stromal cells [286].

Collectively, these data suggest that tissue recombinants consisting of nMUM and hESC transplanted under the kidney capsule for further differentiation and development generated a recombinant glandular structure consisting of hESC-derived epithelium with underlying mouse uterine stroma.

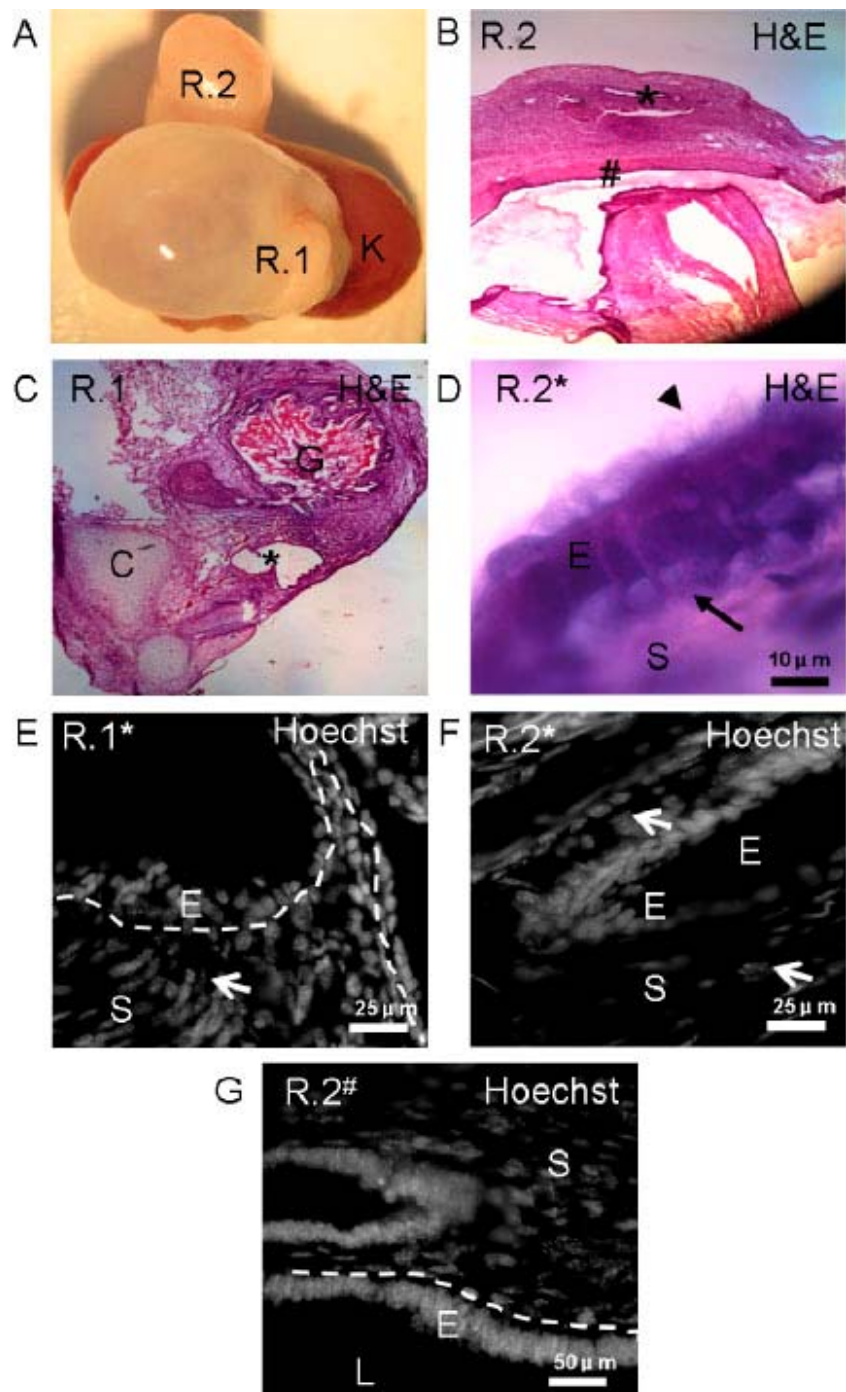


**Figure 2.3 Morphological analysis of MEL-1 nMUM/hESC recombinant grafts**

(A) Two 8 week recombinant grafts comprising MEL-1/nMUM on top of a mouse kidney after 8 weeks of incubation. (B-C) representative H&E sections that correspond to R.1 and R.2 labelled in the top left panel (asterix marks the hESC derived epithelial structure surrounded by mouse stromal cells, hash marks the mouse uterine epithelium surrounded by mouse stroma). (D) is a high power view showing ciliation on the recombinant epithelium (arrowhead points to cilia, arrow point to basal vacuolation). (E-F) are serial sections at higher magnification following sections depicted in (C, B respectively) stained with the Hoechst dye (arrows point to mouse stromal cells with speckled nuclei). Note epithelium have smooth nuclei indicating human cells. (G) Contaminant mouse uterine epithelium with stroma correspond to area with hash symbol in (B). **Abbreviations:** C, cartilage; E, epithelium; G, glandular structure; K, kidney; L, lumen; S, stroma; R, recombinant.

### 2.3.4 Tissue recombination of nMUM with ENVY

A recent gene expression analysis revealed that there are significant differences in the developmental potential between human embryonic stem cell lines [200]. In order to show that nMUM was able to support the differentiation of multiple hESC lines, ENVY cells were purchased from Stem Core (Monash University). The ENVY hESC is a green fluorescent protein-tagged hES cell line [201].

Unlike MEL-1, ENVY cells were supplied with minimal laboratory preparation. Following established protocols of embryoid body formation [205, 222], embryoid bodies were created by force aggregation for tissue recombination with nMUM under serum free conditions. The ability of embryoid bodies to form teratoma structures *in vivo* was tested first. Consistent with a previous study [222], the minimum number of cells required for tumour formation was 3000 cells (Figure 2.4A), no tumours formed using embryoid bodies developed from <3000 cells ( $n>20$ ). It appeared that as the number of cells increased, the size of the tumour growth also increased (Figure 2.4B).

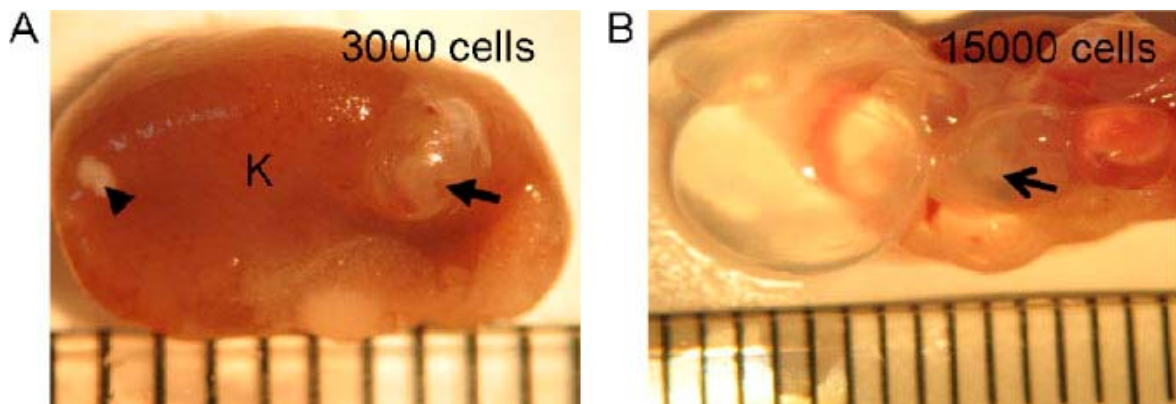


**Figure 2.4 Cystic growths from ENVY-derived embryoid bodies transplanted under the capsule of NOD.SCID mouse kidney**

(A) Representative photograph of a 4 week cystic growth on the mouse kidney developed from a single 3000 cell embryoid body (arrow points to the EB-derived growth, arrowhead points to a patch of collagen gel, a sign of failed EB growth). (B) Representative photograph of 4 week cystic growth on the mouse kidney developed from a single 15,000 cell embryoid body (arrow points to area of solid tumour). Measuring units of the ruler depicted in the photograph is 1mm. **Abbreviation:** K, kidney.



Initially, nMUM (2-4 pieces) were cultured with EB on Day 0 of EB formation. After 48 hours of culture, it appeared that nMUM prevented aggregation of the embryoid body (Figure 2.5A). In subsequent experiments, hESCs were aggregated first to form EBs for 24 hours before culturing with nMUM. With this strategy, EBs formed tissue recombinants with nMUM (Figure 2.5B). Following *in vivo* incubation under the renal capsule between 4-8 weeks, ENVY derived epithelium surrounded by mouse stromal cells was detected in recombinant grafts (Figure 2.5C) with similar features described for hESC derived epithelial structure in MEL-1 derived grafts.

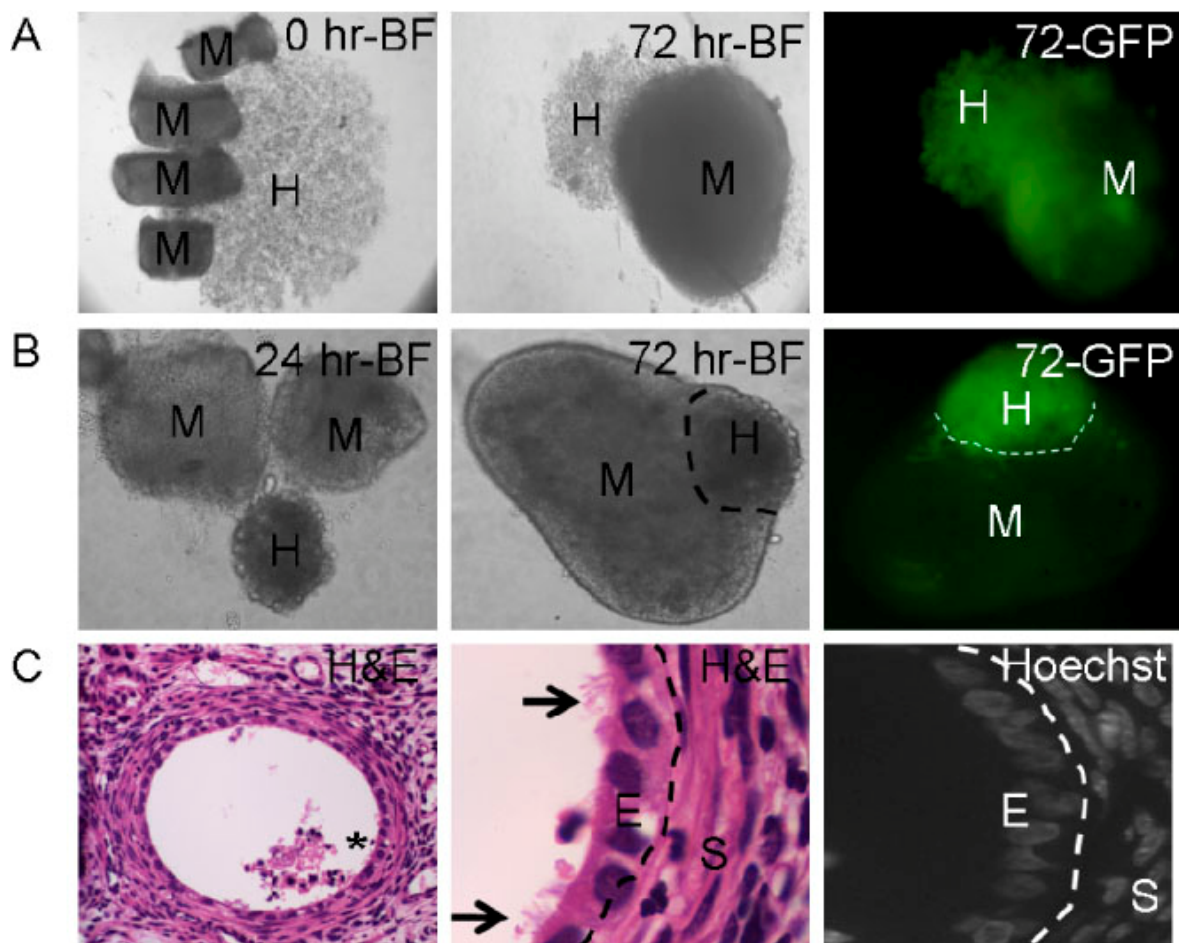


**Figure 2.5 Morphological analysis of ENVY/nMUM Tissue recombinants**

(A) representative photomicrographs showing the development of a tissue recombinant at two time points in vitro using the first strategy where nMUM was added at 0 hr of EB formation (n=20). (B) second strategy where nMUM was added 24 hrs after EB formation (n>150). (C) Far left panel is a representative photomicrograph of H&E section of a single 8 week ENVY derived recombinant graft, middle panel is a magnified view of the asterisk area in the recombinant glandular structure depicted in first panel (arrows show cilia), far right panel is Hoechst stained serial section corresponding to the recombinant structure showing hESC-derived epithelium with smooth nuclei and mouse stromal cells with speckled nuclei (representative of n=6). **Abbreviations:** BF, brightfield; E, epithelium; GFP, green fluorescent protein; H, ENVY hESC; M, nMUM; S, stroma.

At this point, a comparison was made between the two cell lines in terms of accessibility, costs and future applications (Table 2.1). It was decided that ENVY cells would be ideal for future experiments. The work flow using ENVY cells to create tissue recombinants is depicted in Figure 2.6.

**Table 2.1 Technical considerations of hESC lines used**

	<b>MEL-1 [275, 287]</b>	<b>ENVY [181, 201, 202]</b>
Source	ASCC/Dr Paul Verma's Laboratory (CRD, MIMR)	ASCC/Stem Core
Manual Passage	Every 2-3 days	N/A
Availability of cells	Usually weekly, variable, depends on MEF and passage	Usually available twice per week (Tuesday or Thursday)
Cells harvested for experiment	4-5 pieces (averaging 5000 – 10,000 cells)	T25 (1-2 million cells)
Cost	Costs of general laboratory consumables + hESC culture media (with growth factors)	\$30 for cells and services
Pluripotency/Karyotype	Self assessed periodically	Checked by Stem Core
Genetic modification	-	Stable transfection of Green Fluorescent Protein (GFP)

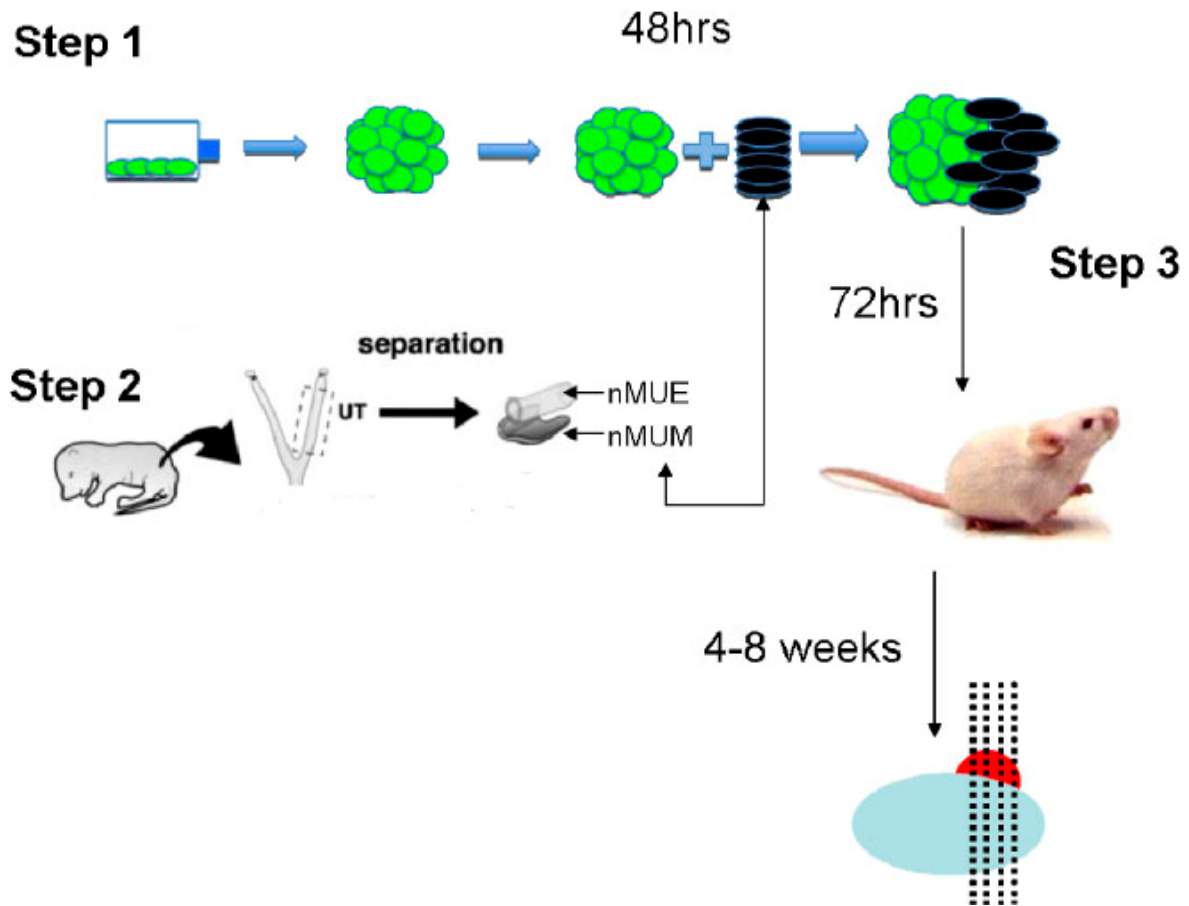


**Figure 2.6 Work flow: from tissue recombination to analysis**

Schematic diagram illustrating the work flow of the method used in the current study. Step 1 illustrates the formation embryoid bodies from ENVY hESC (green circles). Step 2 involves the collection of nMUE (image modified from Kurita et al 2001 [19] with permission from Elsevier). Step 3 involves the transplantation of recombinant grafts for *in vivo* development. **Abbreviations:** nMUE, neonatal mouse uterine epithelium; nMUM, neonatal mouse uterine mesenchyme.

### 2.3.5 Efficiency and macroscopic appearance of recombinant grafts

In total, 114 ENVY/nMUM recombinant grafts were transplanted under the renal capsule of 58 mice, and only 6 grafts contained recombinant glandular structure. In the remaining 108 grafts, either or both of the cell types transplanted perished *in vivo*. Unique macroscopic appearance made it possible to distinguish failed recombinant grafts from successful grafts (Table 2.2, Figure 2.7) thus facilitated quicker analysis without the necessity of processing and sectioning failed grafts.



In these experiments, the nMUM always survived *in vivo* transplantation, in contrast, to hESCs which rarely survived the procedure. A recombinant graft where neither cell types survived was detected by the remnants of a collagen patch under the renal capsule (Figure 2.4A, 2.7B). A recombinant graft containing hESC derived structures were smaller cystic/solid growth compared to EB transplanted alone (Figure 2.7A-B). The presence of hESC derived structure is evident by areas of cartilage or bone like growth, pigmented areas and small areas of cystic sacs (Figure 2.7B, 2.7D). In a failed recombinant graft, where nMUM/remnant epithelial cells developed exclusively into uterine gland, the macroscopic appearance was a small well vascularised smooth growth on top of the kidney. In contrast, in recombinant grafts where hESC have survived, the surface was always irregular. In summary, ENVY hESCs can also be recombined with nMUM and will undergo further differentiation *in vivo*, albeit with a dismal take rate.

**Table 2.2 Macroscopic descriptions of graft types**

Appearance of grafts under the renal capsule at 4-8 weeks				
	Size	Surface	Fluid filled sacs	Pigmented/Cartilage Tissue
EB (control)	Large	Irregular	Numerous	Occasional
Recombinant	Small	Irregular	Occasional	Occasional
Failed grafts (cells death)	-	Flat collagen patch under capsule	-	-
Failed grafts (uterine gland formation )	Small	Smooth, half sphere	none	none

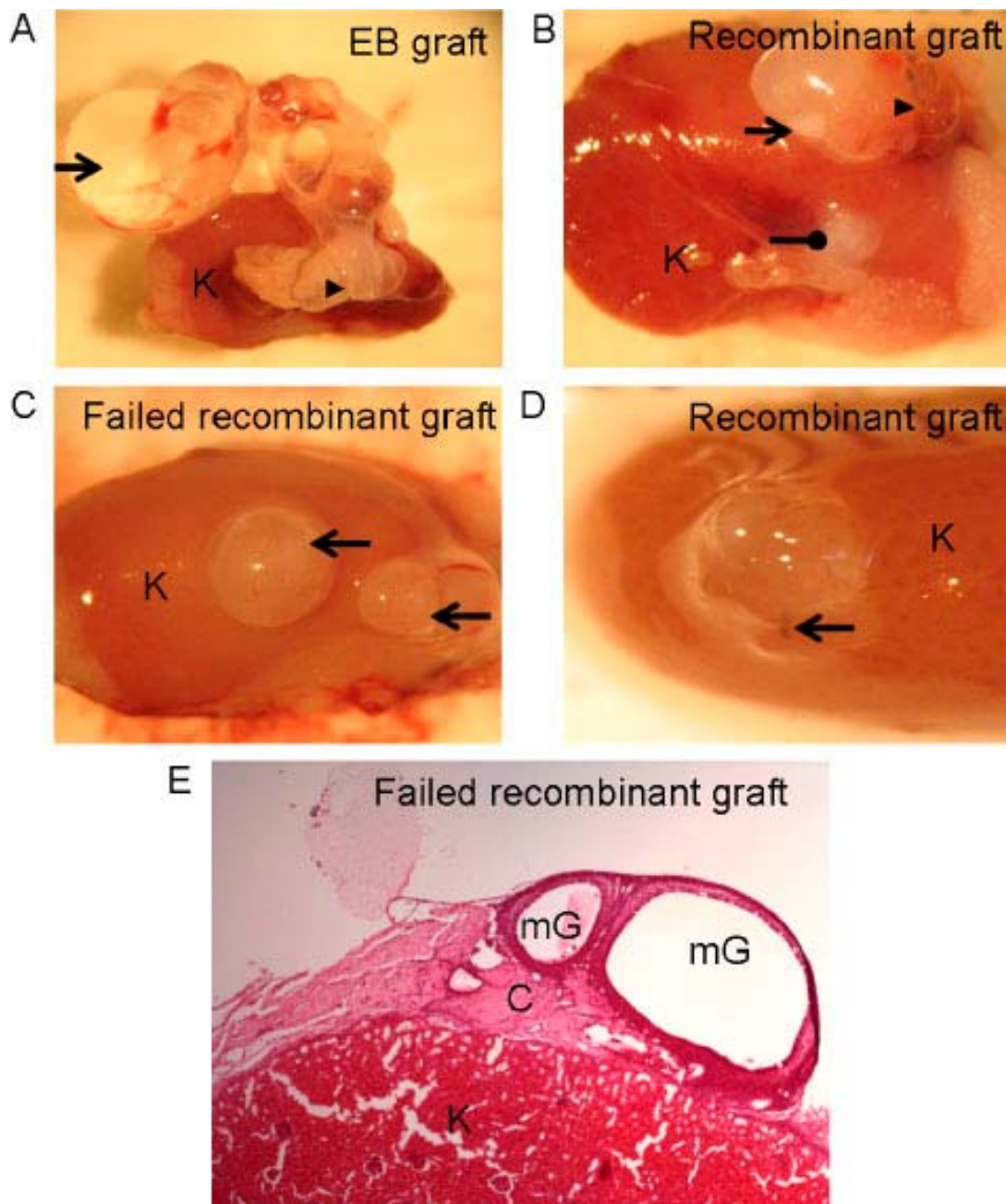


**Figure 2.7 Macroscopic appearance of various grafts**

(A-D) representative photograph of various grafts harvested at 4 weeks. (A) Cystic teratoma developed from EB alone (arrowhead points to area solid tissue growth at the base of the graft, nearest to the kidney parenchyma, arrow points to a fluid filled sac). (B) teratoma like growth developed from a recombinant graft (arrowhead points to fluid filled sacs, arrow points to cartilage-like growth at the base of the growth, circle points to patch of collagen). (C) Smooth, vascularised growth typically seen in grafts containing mouse uterine gland only. (D) Small solid growth with irregular surface (arrow points to pigmented tissue). (E) Representative photomicrograph of H&E section of recombinant graft containing only mouse uterine gland. **Abbreviations:** C, collagen; K, kidney; mG, mouse uterine gland.

### 2.3.6 Real time imaging of ENVY grafts

Due to the high failure rate of recombinant grafts, it was decided that *in vivo* imaging would enable detection of failed grafts at earlier time points, allowing non – invasive monitoring over longer incubation time points (ie. 8 weeks). It has been shown previously that GFP expression can be captured by high sensitivity cameras [288]. It was hypothesized that *in vivo* imaging for GFP expression would be sufficient and reliable method to detect ENVY cell survival *in vivo* under the renal capsule since ENVY hESCs constitutively express green fluorescent protein (GFP) [201]. Fluorescent signal from an area corresponding to the location of the host kidney where ENVY cells were grafted was detected (Figure 2.8A, C). Similarly, signal in a region of the hind leg where single hESCs were injected was also detected (Figure 2.8B). These were verified by when animals were sacrificed.

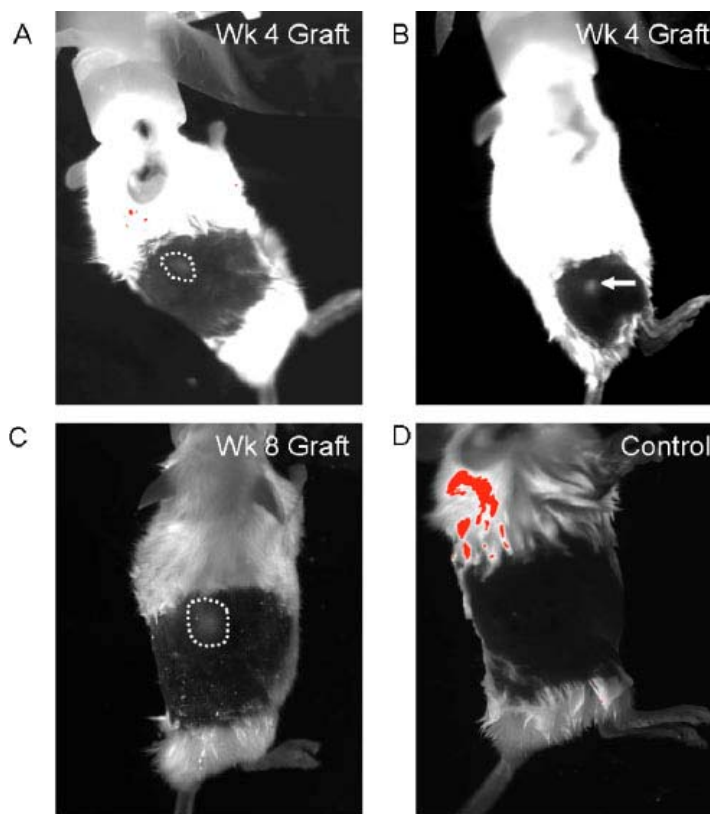


**Figure 2.8 Non-invasive *in vivo* imaging of transplanted ENVY hESC**

(A-C) Photographs demonstrate GFP signal detected in NOD/SCID mouse hosts carrying renal recombinant grafts at two different time points; (A) one animal at week 4 and (C) one animal at week 8 after grafting (dotted lines encircle detected GFP signal). (B) one animal with GFP signal detected in the leg where hESC were injected intramuscularly (arrows point to GFP signal). (D) Photograph of a control animal that did not receive any grafts or cells

## **2.4 Discussion**

Differentiation of ESC into clinically relevant tissue or cell types *in vitro* holds promises for future regenerative therapies. Few studies have used tissue recombination methods to establish *in vivo* models of organogenesis [60, 175]. Using *in vivo* models to study human organ development is a powerful approach to understand human development previously not possible. *In vivo* modelling coupled with tissue recombination would allow dissection of complex pathways involved in fate specification by the utilisation of transgenic and gene knockout technologies [191]. In the current study, I have established an *in vivo* model of human organ development using tissue recombination technology forming heterospecific/heterotypic recombinant grafts using nMUM with two separate hESC cell lines; MEL-1 and ENVY.

### **2.4.1 Instructive interaction between nMUM and hESC**

Interactions between epithelial and stromal cells are classified as permissive or instructive [176]. Both the permissive and instructive effects of the nMUM have been documented in the past [22, 184, 190]. The former refers to the support of a predetermined developmental program, the latter refers to the initiation of a new program for differentiation. The interaction between nMUM and hESCs reported in the current study is instructive because nMUM specified the fate of undifferentiated hESCs. Notwithstanding the propensity of hESC to spontaneously differentiate towards a certain type of tissue [200], a small percentage of both MEL-1 and ENVY hESCs used in this study faithfully followed the instructions of nMUM to form glandular epithelial structures with FRT-like morphological features. This is consistent with the concept that most developmental pathways are evolutionarily conserved between human and mouse [184]. Further characterisation is, however, required for the hESC derived FRT-like epithelium.

### **2.4.2 Off target differentiation**

Similar to previous studies, a considerable degree of ‘off target differentiation’ was observed in the current study where hESC formed teratoma-like growths that consisted of tissue types from various lineages [174, 175]. Whilst a reduction of hESC numbers reduced the tumour size in the current and a previous study [175], it may also reduce the viability of hESC *in vivo* [281]. An alternative strategy could be to partially differentiate hESC by addition of exogenous growth

factors to form progenitor or more mature cell types prior to recombination or transplantation [180]. Although to differentiate hESC into fully mature FRT epithelial cells prior to transplantation would relegate the nMUM to a purely permissive role since much of the hESC fate specification would have been completed by growth factors *in vitro*. Such a differentiation strategy may still be too futuristic since little is known about the growth factors involved in fate specification and differentiation of the Müllerian duct during development despite the discovery of the major molecular pathways involved [17]. A more realistic strategy would be to partially differentiate hESC to form pre-Müllerian progenitors found at different stages of embryogenesis. For example, the primitive streak cells, lateral plate mesodermal cells and coelomic epithelial cells [2]. Primitive streak cells are the obligate intermediate for both mesoderm and endodermally derived tissue, there is a large collection of literature documenting efficient differentiation strategies for formation of mesoderm and endodermally derived tissue using a wide range of growth factors [226, 272]. Such pre-differentiation strategies could potentially reduce ‘off target’ outcomes by increasing differentiation of hESC, thereby reducing pluripotency of the stem cells.

### 2.4.3 Immune rejection and cell death

As hESC differentiate, they express low levels of the major histocompatibility complex class I (MHC-I) antigens suggesting that hESC derivatives may elicit an immune response when transplanted *in vivo* across histocompatibility barriers [289, 290]. Interestingly, it was originally thought that ESC had immune privileges because embryos consisting of paternal material are usually not rejected by maternal hosts. Results from a number of studies offer conflicting evidence of hESC survival in xenogeneic hosts. Whilst some showed that both mESC and hESC evade immune recognition in immunocompetent mice [291, 292], others showed some level of rejection of both undifferentiated hESC and its derivatives from the host [293, 294]. Ultimately, the rejection was attributed to T cell recognition of the MHC-I on hESC and its derivatives [293]. Immunocompromised mice such as the NOD.SCID has impaired T and B lymphocyte development and was therefore able to host xenografts containing hESC without rejection [174, 293]. A recent study showed a new strain of NOD/SCID/gamma(null) (NOG) mice without T, B or NK cell activity were superior hosts for cynomolgus ES cells compared with NOD.SCID mice [281, 295, 296]. In contrast to previous studies, the current study had an extremely low take rate with transplantation of recombinants containing hESCs. Unlike these previous studies, less than

0.5% of the total number of cells (3,000 cells vs  $1 \times 10^6$  cells in previous study) transplanted in the past studies was used in the current study [281, 293]. Communication with the author of a similar study [174] where approximately only 1,500 hESC were transplanted in tissue recombinants revealed a similar disappointing take rate in their recombinant grafts. Whilst residual immunogenic response from NOD/SCID hosts may play a small part in low hESC survival rate, hESC cell death noted in the current study is likely due to the extremely low number of cells transplanted into the host. However, to ensure that any residual immunogenic response on hESC survival was avoided, we have imported another strain of immunocompromised mice known as NOD/Scid II-2R Gamma (NSG) for future studies. The NSG mouse is the most immunocompromised strain available today. Even though cell survival is important, low number is pivotal for reduction of teratoma size in order to achieve a homogenous differentiation of ESC *in vivo* [174, 175].

#### **2.4.4 Other strategies to increase efficiency and reproducibility of the *in vivo* model**

The *in vivo* incubation time of recombinant grafts in the current study ranged from 4 to 8 weeks, during which time, the fate of hESC can not be assessed due graft site location. In contrast, injection of large numbers of hESC into hind legs of mice allows for palpation after several weeks of *in vivo* incubation. Today, the most advanced systems of *in vivo* imaging of hESC detect both bioluminescence and GFP signal since each have their unique advantages [297, 298]. However, for the purpose of cell detection, GFP signal emitted from recombinant grafts was sufficient.

Maintaining hESC in any laboratory is a costly affair. Since both MEL-1 and ENVY were able to form FRT-like epithelium when transplanted with nMUM *in vivo*, to reduce cost in laboratory consumables and time, it was decided that ENVY hESCs was a much more cost effective way for experiments conducted in the following Chapters of this thesis. The scheduled delivery of ENVY cells allowed experiments to be planned ahead and harvesting of neonatal uterine mesenchyme to be co-ordinated with the creation of EBs in an orderly and efficient manner.

### 2.4.5 Conclusion


The methods developed in the current study include the recombination of nMUM with hESC (MEL-1 and ENVY), transplantation of heterotypic/heterospecific recombinant grafts, macro- and microscopic analysis, and real time imaging of recombinant grafts. The recombinant glandular epithelium described in this *in vivo* model required in depth morphological and functional characterisation which is described in the following Chapter. In Chapter 3, the addition of growth factors to pre-differentiate hESC prior to recombination was also attempted to reduce “off target” differentiation and NSG mice used to enhance survival of transplanted hESCs.

**Declaration****Monash University****PART B: Suggested Declaration for Thesis Chapter****Declaration by candidate**

In the case of Chapter 3, the nature and extent of my contribution to the work was the following:

<b>Nature of contribution</b>	<b>Extent of contribution (%)</b>
I was involved in designing and performing the experiments, collecting and analysing the data for all figures and tables. I wrote the manuscript.	100%

The following co-authors contributed to the work. Co-authors who are students at Monash University must also indicate the extent of their contribution in percentage terms:

<b>Name</b>	<b>Nature of contribution</b>	<b>Extent of contribution (%) for student co-authors only</b>
<b>Robyn Mayberry</b>	Provision of human embryonic stem cells	
<b>Ed Stanley</b>	Conception and design of experiments, editing of the manuscript	
<b>Andrew Elefanty</b>	Conception and design of experiments, editing of the manuscript	
<b>Kara Britt</b>	Analysed microarray data (data not shown)	
<b>Camden Lo</b>	Analysed data required to produce Figure 4K	
<b>Caroline Gargett</b>	Conception and design of experiments, editing of the manuscript, responsible for final approval of the manuscript	
<b>Candidate's Signature</b>		<b>Date: 4/8/11</b>

**Declaration by co-authors**

The undersigned hereby certify that:

- (1) the above declaration correctly reflects the nature and extent of the candidate's contribution to this work, and the nature of the contribution of each of the co-authors.
- (2) they meet the criteria for authorship in that they have participated in the conception, execution, or interpretation, of at least that part of the publication in their field of expertise;
- (3) they take public responsibility for their part of the publication, except for the responsible author who accepts overall responsibility for the publication;
- (4) there are no other authors of the publication according to these criteria;
- (5) potential conflicts of interest have been disclosed to (a) granting bodies, (b) the editor or publisher of journals or other publications, and (c) the head of the responsible academic unit; and



(6) the original data are stored at the following location(s) and will be held for at least five years from the date indicated below:

Location(s)

**Monash Immunology and Stem Cell Laboratories (MISCL), Monash University,  
Clayton  
Monash Institute of Medical Research (MIMR), Monash University, Clayton**

[Please note that the location(s) must be institutional in nature, and should be indicated here as a department, centre or institute, with specific campus identification where relevant.]

Name	Nature of contribution	Date
Robyn Mayberry	[REDACTED]	4/8/11
Ed Stanley	[REDACTED]	4/8/11
Andrew Elefanty	[REDACTED]	4/8/11
Kara Britt	[REDACTED]	4/8/11
Camden Lo	[REDACTED]	4/8/11
Caroline Gargett	[REDACTED]	4/8/11

.....

# Generation of Human Female Reproductive Tract Epithelium from Human Embryonic Stem Cells

Louie Ye<sup>1</sup>, Robyn Mayberry<sup>2</sup>, Camden Y. Lo<sup>3</sup>, Kara L. Britt<sup>4</sup>, Edouard G. Stanley<sup>2</sup>, Andrew G. Elefanty<sup>2</sup>, Caroline E. Gargett<sup>1\*</sup>

**1** The Ritchie Centre, Monash Institute of Medical Research and Department of Obstetrics and Gynecology, Monash University, Melbourne, Australia, **2** Monash Immunology and Stem Cell Laboratories, Monash University, Melbourne, Australia, **3** Monash Micro Imaging, Monash University, Melbourne, Australia, **4** Anatomy and Developmental Biology, Monash University, Melbourne, Australia

## Abstract

**Background:** Recent studies have identified stem/progenitor cells in human and mouse uterine epithelium, which are postulated to be responsible for tissue regeneration and proliferative disorders of human endometrium. These progenitor cells are thought to be derived from Müllerian duct (MD), the primordial female reproductive tract (FRT).

**Methodology/Principal Findings:** We have developed a model of human reproductive tract development in which inductive neonatal mouse uterine mesenchyme (nMUM) is recombined with green fluorescent protein (GFP)-tagged human embryonic stem cells (hESCs); GFP-hESC (ENVY). We demonstrate for the first time that hESCs can be differentiated into cells with a human FRT epithelial cell phenotype. hESC derived FRT epithelial cells emerged from cultures containing *MIXL1*<sup>+</sup> mesendodermal precursors, paralleling events occurring during normal organogenesis. Following transplantation, nMUM treated embryoid bodies (EBs) generated epithelial structures with a typical MD phenotype that expressed the MD markers PAX2, HOXA10. Functionally, the hESCs derived FRT epithelium responded to exogenous estrogen by proliferating and secreting uterine-specific glycidol A (GdA).

**Conclusions/Significance:** These data show nMUM can induce differentiation of hESC to form the FRT epithelium. This may provide a model to study early developmental events of the human FRT.

**Citation:** Ye L, Mayberry R, Lo CY, Britt KL, Stanley EG, et al. (2011) Generation of Human Female Reproductive Tract Epithelium from Human Embryonic Stem Cells. PLoS ONE 6(6): e21136. doi:10.1371/journal.pone.0021136

**Editor:** Zhongjun Zhou, The University of Hong Kong, Hong Kong

**Received:** February 15, 2011; **Accepted:** May 20, 2011; **Published:** June 15, 2011

**Copyright:** © 2011 Ye et al. This is an open-access article distributed under the terms of the Creative Commons Attribution License, which permits unrestricted use, distribution, and reproduction in any medium, provided the original author and source are credited.

**Funding:** The authors have no support or funding to report.

**Competing Interests:** The authors have declared that no competing interests exist.

\* E-mail: caroline.gargett@monash.edu

## Introduction

During embryogenesis, the mesoderm emerges from the primitive streak and gives rise to coelomic epithelium. The Müllerian Duct (MD) arises from invagination of coelomic epithelium during fetal development. Subsequently, the MD gives rise to the human female reproductive tract (FRT) that further differentiates to form the oviduct, uterus and upper vaginal canal. The mucosal lining of the uterus is known for its remarkable regenerative capacity during a female's reproductive years. Recently, the regenerative capacity of the endometrium has been attributed to a small population of resident stem/progenitor cells. Our laboratory discovered these cells in both the stroma and epithelium of the adult human and murine uterus [1,2,3]. We have identified cell surface markers that enrich for endometrial mesenchymal/stromal stem/progenitor cells, and ongoing investigations now focus on finding definitive markers for the epithelial stem/progenitor cells. Identifying and characterising these stem/progenitor cells will provide a better understanding of the normal cyclical regenerative processes in human endometrium and the pathophysiology of human endometrial proliferative diseases, such as endometriosis, endometrial hyperplasia and endometrial cancer.

Recent studies have shown that creating developmental models from embryonic stem cells (ESCs) is a tractable approach to track and potentially identify adult stem/progenitor cells [4,5]. In this context, we believe a hESC based model of human MD development will facilitate the identification and characterization of female reproductive tract stem/progenitor cells. Tissue recombination is a powerful tool for studying stromal-epithelial interactions. For example, neonatal mouse uterine mesenchyme (nMUM) had been recombined with human and mouse uterine epithelial cells in previous tissue recombination experiments [6,7,8,9]. nMUM also transdifferentiates pluripotent spermatogonial stem cells into murine uterine epithelial tissue [10] and a number of studies have shown that specific stromal populations can direct ESC differentiation towards derivatives of their corresponding epithelia, including bladder, prostate and oocytes [4,5,11]. We hypothesized that nMUM might provide inductive cues capable of directing hESCs to differentiate into human FRT epithelium. We adopted established methods for hESC differentiation to form embryoid bodies (EB) from green fluorescent protein-tagged hESCs; GFP-hESCs (ENVY). EBs were then combined with nMUM and the resultant recombinant subsequently grafted into immunocompromised mice. We demonstrated that nMUM induced differentiation of

hESCs to form human FRT epithelium in a process that paralleled known stages of human FRT organogenesis.

## Results

### Neonatal mouse uterine mesenchyme directed hESCs to form human female reproductive tract epithelium in vivo

No single marker defines the adult FRT epithelium which includes the oviduct, uterus and upper vaginal canal. Therefore we used a previously established combination of a morphological marker (cilia) and the immunohistochemical markers cancer antigen 125 (CA125), Glycodelin A (GdA) and estrogen receptor alpha (ER- $\alpha$ ) to identify the FRT epithelium [12,13]. As a prelude to experiments utilising nMUM mesenchyme, we first tested the ability of differentiating hESCs to spontaneously differentiate into human FRT epithelium following transplantation. To this end, we grafted ovariectomized mice with two types of controls; EBs formed in the absence of growth factors ( $n = 4$ ) or EBs treated with BMP4/ACTIVIN A ( $n = 4$ ), growth factors known to induce hESCs to differentiate towards mesendoderm, an obligate intermediate during FRT development. Lack of ovarian hormones does not impair ciliogenesis or development of the female reproductive tract [14,15,16], but the absence of these hormones enables distinction of reproductive and respiratory tract epithelia. Specifically, under these conditions, normal human uterine epithelium is a ciliated simple columnar epithelium (Figure 1A), in contrast, respiratory epithelium is ciliated and pseudostratified (data not shown). We found no evidence of ciliated simple columnar epithelium in either control group, however, we detected ciliated pseudostratified columnar epithelium resembling respiratory epithelium similar to that described in a previous report [17]. In addition to these hESC controls, we also grafted nMUM alone and found no evidence of epithelial differentiation, consistent with previous studies (data not shown) [7,10]. In the experimental groups, we detected ciliated simple columnar epithelium in each graft derived from both the non-growth factor treated ( $n = 2$ ) (data not shown) and growth factor treated EB/nMUM recombinant tissues ( $n = 30$ ) (Figure 1B, C). Grafts derived from these samples were smaller than those arising from EBs formed in the absence of nMUM and/or growth factors, (Figure S1A), consistent with previous studies showing that differentiated hESC had reduced the potential for teratoma formation [5,17]. We also found the viability of hESC differed between immunodeficient host mouse strains and that NOD.Scid gamma (NSG) mice were ideal for hESC cell development compared to NOD.Scid mice (data not shown) consistent with a previous study [18].

In order to confirm that ciliated structures were indeed hESC derived epithelium, we used a combination of Hoechst stain and anti-GFP antibody staining (Figure 1C–F, Figure S6A). This analysis enabled GFP<sup>+</sup> ENVY-derived human epithelial cells containing smooth Hoechst-stained nuclei to be distinguished from GFP<sup>−</sup> mouse cells with speckled nuclei [19]. In week 8 recombinant grafts, ciliated simple columnar epithelium was only observed when surrounded by mouse stromal cells (Figure 1C). In GF-treated week 8 recombinant grafts, we found epithelial tissue made up a small percentage of the total area ( $4.8 \pm 2.3\%$ ), and that ciliated simple columnar human epithelium accounted for  $33.8 \pm 22.6\%$  of all epithelial structures ( $n = 4$ , mean  $\pm$  s.e.m.). Consistent with a previous report, our data showed that a considerable portion of each graft consisted of non-epithelial tissue and fluid filled cavities (Figure S1C) [17]. In addition, the proportion of ciliated simple columnar epithelial structures in recombinant grafts varied; for instance, in one graft, the only epithelial structure present was ciliated whilst the rest of the graft consisted of fluid-filled cavities (Figure S1C). In other grafts, several hESC derived

FRT epithelial structures were present (Figure S1B, Figure S1D). Despite this variability, structures with characteristics consistent with FRT epithelium were found in all grafts where both nMUM and hESC derived cell types were present ( $n = 30$ ) (Figure S2).

Immunofluorescence analysis indicated that the hESC derived FRT epithelium expressed human CK18 and CA125 (Figure 1D, Figure 1E). This result excludes the possibility that these structures represented luminal epithelium of the male reproductive tract or ependymal epithelium of the central nervous system, which do not express CA125 [20]. Following exogenous estrogen treatment, estrogen receptor- $\alpha$  (ER $\alpha$ ) was detected in the hESC derived FRT epithelium (Figure 1F, Figure S4A) albeit at a low frequency and variable intensity, comparable to ER $\alpha$  expression in human endometrial glands (Figure 1G, Figure S4C, Figure S4D). In recombinant grafts, ER $\alpha$  is only detected in mouse stromal cells and hESC derived FRT epithelium (Figure S4A, Figure S4B). To assess the functional capacity of the hESC derived FRT epithelium, we treated host mice with multiple estrogen injections over 5 days [9]. Estrogen induced epithelial proliferation, as demonstrated by Ki67 expression (Figure 1I), similarly, the hESC derived epithelia in estrogen treated animals expressed GdA in the cytoplasm (Figure 1K). We also observed morphological changes in response to exogenous hormonal stimulation, the hESC derived FRT epithelium increased in height, whilst the underlying stromal cells demonstrated edematous change (Figure 1M), mirroring changes that occur in normal cycling adult proliferative uterine epithelium and stroma (Figure 1N). In contrast, grafts from vehicle alone treated hosts contained low cuboidal epithelium and lacked stromal edema (Figure 1L). Furthermore evidence of reciprocal interaction between differentiated human epithelial cells and mouse endometrial stromal cells was indicated by the expression of alpha - smooth muscle actin ( $\alpha$ -SMA) in the latter (Figure 1O), consistent with previous studies [4,5]. Collectively, these results demonstrate that nMUM can direct hESCs to differentiate into hormonally responsive FRT epithelium.

### FRT epithelia arises from MIXL<sup>+</sup> embryoid bodies

Since MD is derived from primitive streak mesendoderm, we sought to determine if nMUM induced formation of mesendodermal cells in differentiating human EBs. To examine this process, we generated EBs with a *MIXL1*<sup>GFP/w</sup> hESC reporter line in which GFP expression has been placed under the control of the primitive streak gene, *MIXL1*. We detected GFP expression as early as day 3 in developing EBs cultured in serum-free-medium in the presence of nMUM (Figure 2A). Reporter activity in the recombinant EBs, which paralleled that seen in EBs treated with growth factors (BMP4 and ACTIVIN A), first appeared on day 3 and gradually diminished by day 7 (Figure 2A). Furthermore, in larger EBs (>4000 cells), reporter activity was localised to the area of contact between EB and mesenchyme (Figure 2B, Figure S3). When we recombined *MIXL1*<sup>GFP/w</sup> EBs with neonatal mouse uterine epithelial (nMUE) cells under serum free conditions, we observed no reporter activity (Figure 2C). These observations suggest close range morphogens from nMUM, but not nMUE, directed the differentiation of hESC to mesendodermal cells in *MIXL1*<sup>GFP/w</sup> EBs. These observations indicate that nMUM, but not nMUE, produced factors capable of directing the differentiation of hESCs to mesendodermal progenitors.

### Expression of mesoderm markers in EBs induced to differentiate with nMUM

We hypothesized that nMUM might induce the differentiation of *MIXL1*<sup>+</sup> mesendodermal progenitors to mesoderm with characteristics of lateral plate mesoderm. In the first instance, we

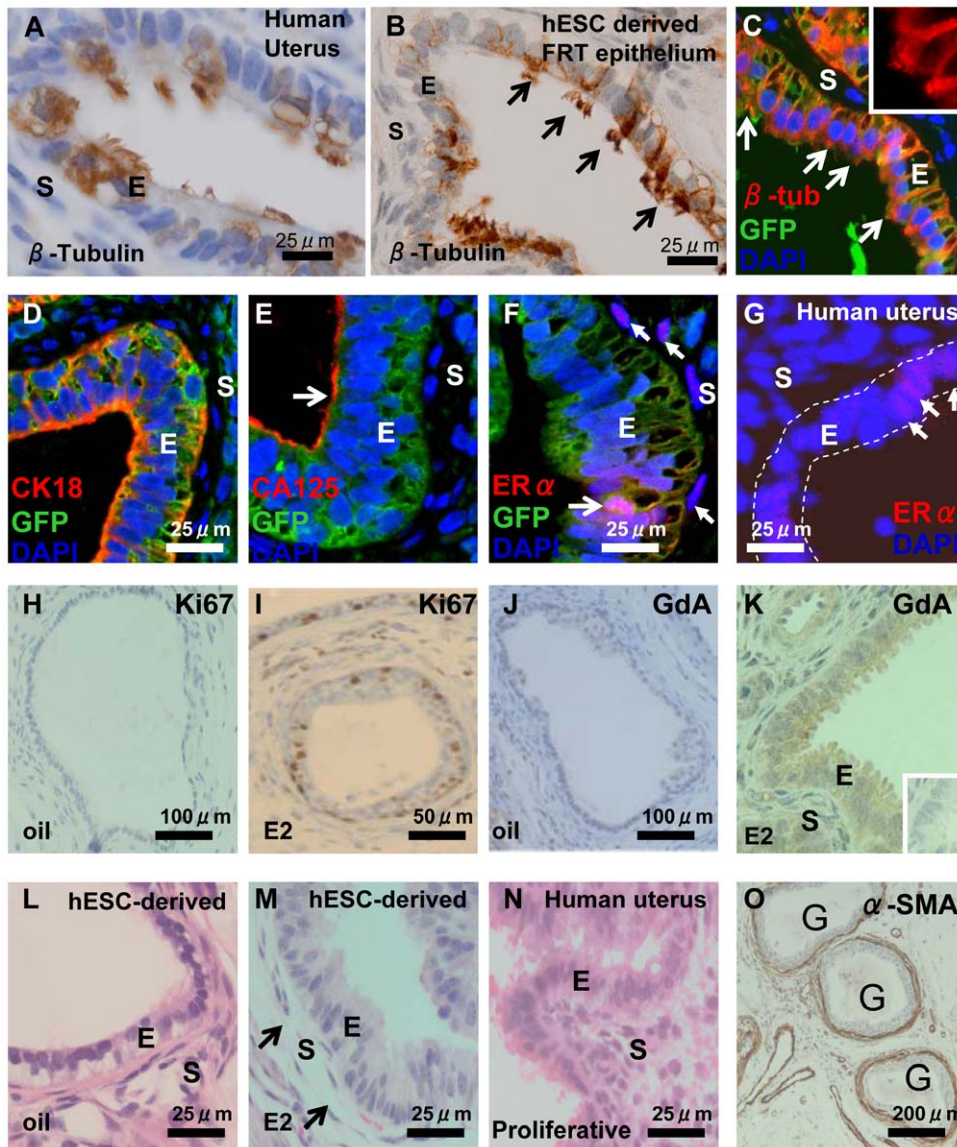


**Figure 1. Characterisation of hESC-derived FRT epithelium in GF treated heterotypic (nMUM) recombinant 8 week xenograft.**  $\beta$ -tubulin expression in (A) ciliated simple columnar epithelia of human adult proliferative endometrium and (B) in hESC derived ciliated, simple columnar FRT epithelium (arrows indicates cilia). (C) immunofluorescence analysis of hESC derived FRT epithelium (green) where  $\beta$ -tubulin (yellow orange) is expressed on cell surface (inset shows a close up view of the cilia), the hESC origin of epithelial cells was assigned on the basis of GFP expression. Note that adjacent mouse uterine stromal cells are GFP<sup>-</sup>. hESC derived FRT epithelium co-localised (D) cytoplasmic CK18, (E) CA125 on epithelial surface (arrow), and (F) ER $\alpha$  (pink) with GFP<sup>+</sup> hESC derived epithelial cells. Weak ER $\alpha$  expression was also evident in mouse uterine stromal cells (filled arrows). (G) ER $\alpha$  expression in human proliferative endometrial gland (full arrows), dotted line indicates epithelium. Ki67 expression in hESC derived FRT epithelium before (H) and after (I) estrogen injections showing estrogen-induced epithelial cell proliferation. The expression of GdA in hESC derived FRT epithelium without (J) and with (K) estrogen injections showing estrogen-induced cytoplasmic expression of GdA. H&E of hESC derived FRT epithelium lined by simple columnar cells without (L) and with (M) estrogen treatment, showing estrogen-induced increase in epithelial height and stromal oedema (arrows), classical hormonal responses of adult uterine epithelium (N). (O) Three hESC derived FRT epithelial structures surrounded by  $\alpha$ -SMA positive cells. Inset in (K) is concentration matched mouse IgG1 negative control. Hoechst stained serial sections corresponding to (I) and (K) are found in Figure S6E–F. Abbreviations:  $\alpha$ -SMA,  $\alpha$ -smooth muscle actin; CA125, cancer antigen 125; E, epithelium; ER $\alpha$ , estrogen receptor alpha; E2, estrogen; G, gland; GdA, glycodeilin A; S, stroma. doi:10.1371/journal.pone.0021136.g001

analysed the expression of genes which mark cells from the mesendoderm and mesoderm in the differentiating recombinant ENVY EBs from day 3 to day 9 using qRT-PCR. In the presence of growth factors (BMP4 and ACTIVIN A) alone, *MIXL1*, *Brachyury* (*T*), *PAX2*, were rapidly upregulated and slowly declined over time (Figure 3). *Gooseoid* (*GSC*), and *OSR1* increased over time compared to control (no growth factor). High levels of *MIXL1*, *GSC*, and *T* suggest differentiation of hESCs towards anterior

population of mesendodermal cells, consistent with the role of ACTIVIN A [21,22]. In addition, we also observed the upregulation of intermediate and lateral plate mesodermal markers *OSR1* and *PAX2*, consistent with a previous study, suggesting that under these conditions, EBs potentially harbour a precursor of MD [23]. nMUM upregulated *MIXL1*, *T*, and *GSC* as early as day 3, but there was delayed upregulation of *OSR1* compared to growth factor treated EBs (Figure 3). *PAX2* showed

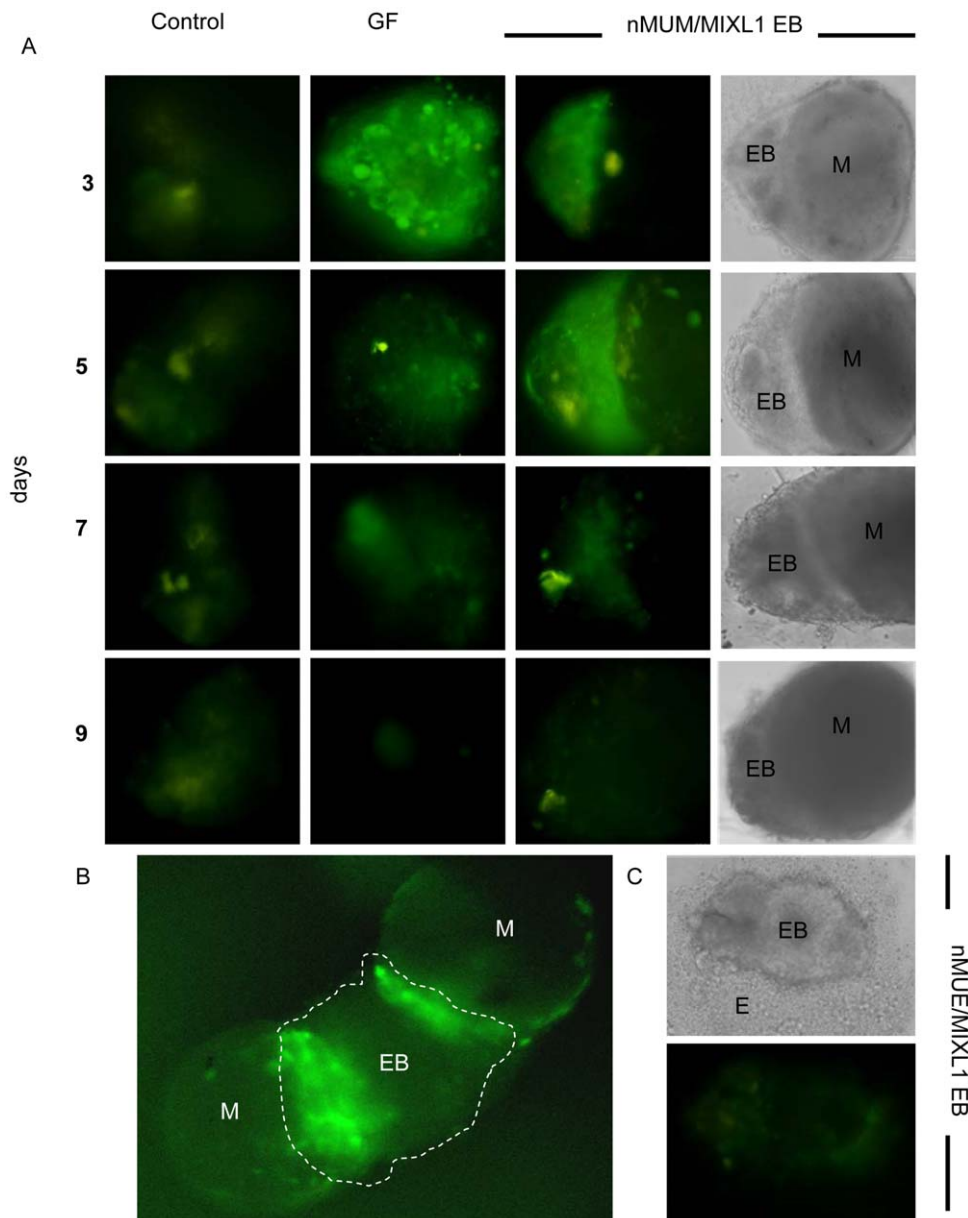


**Figure 2. Neonatal mouse uterine mesenchyme induces *MIXL1* expression in *MIXL1<sup>GFP/w</sup>* EBs.** (A) nMUM induced GFP expression in *MIXL1<sup>GFP/w</sup>* EB recombinants after three days of co-culture (3<sup>rd</sup> panel), representative example of  $n > 100$ . The duration of reporter activation is comparable to that observed in growth factor treated EBs (2<sup>nd</sup> panel, days 3,5), while little to no reporter activity was detected in the control (1<sup>st</sup> panel) ( $n > 100$ ) ( $\times 40$  magnification, first 3 panels are fluorescent images, images in 4<sup>th</sup> panel represent phase contrast images of recombinants in 3<sup>rd</sup> panel). (B) Co-culture of two nMUM pieces (0.5 mm) with a larger EB (>4000 cells) activated reporter activity locally (dotted area is the EB) ( $\times 20$  magnification). (C) No reporter activity was detected in embryoid bodies co-cultured with neonatal uterine epithelium (0.5 mm) ( $\times 40$  magnification). Areas marked as mesenchyme in recombinants are based on morphological evidence and recombination experiments using ENVY hESC (refer to Figure S2A–C). Abbreviations: EB, embryoid body; E, neonatal mouse uterine epithelium; GF, growth factors; M, neonatal mouse uterine mesenchyme. doi:10.1371/journal.pone.0021136.g002

little change compared to control over time. Gene expression profiles of recombinant EBs treated with growth factors were similar to that of EBs treated with growth factor alone, although the nMUM appeared to maintain higher levels of expression for *MIXL1*, and *T*, on day 9 compared to GF treated EBs (Figure 3). The pluripotency marker Oct4 decreased steadily over time in all groups except control. These results suggest that in the absence of growth factors, nMUM can promote hESC differentiation towards mesendoderm, albeit less efficiently than BMP4/ACTIVIN A. However, despite the similar gene expression profile of growth

factor only treated EBs and growth factor treated EB/nMUM recombinants, the former never developed FRT epithelium following transplantation.

#### nMUM induced differentiation of hESCs recapitulates aspects of rodent and human Müllerian Duct development

To investigate the kinetics of MD development following EB transplantation, we harvested recombinant grafts at 2 and 4 weeks. hESC-derived FRT epithelial structures were detected at both time points (Figure 4) and comprised of areas of pseudostratification



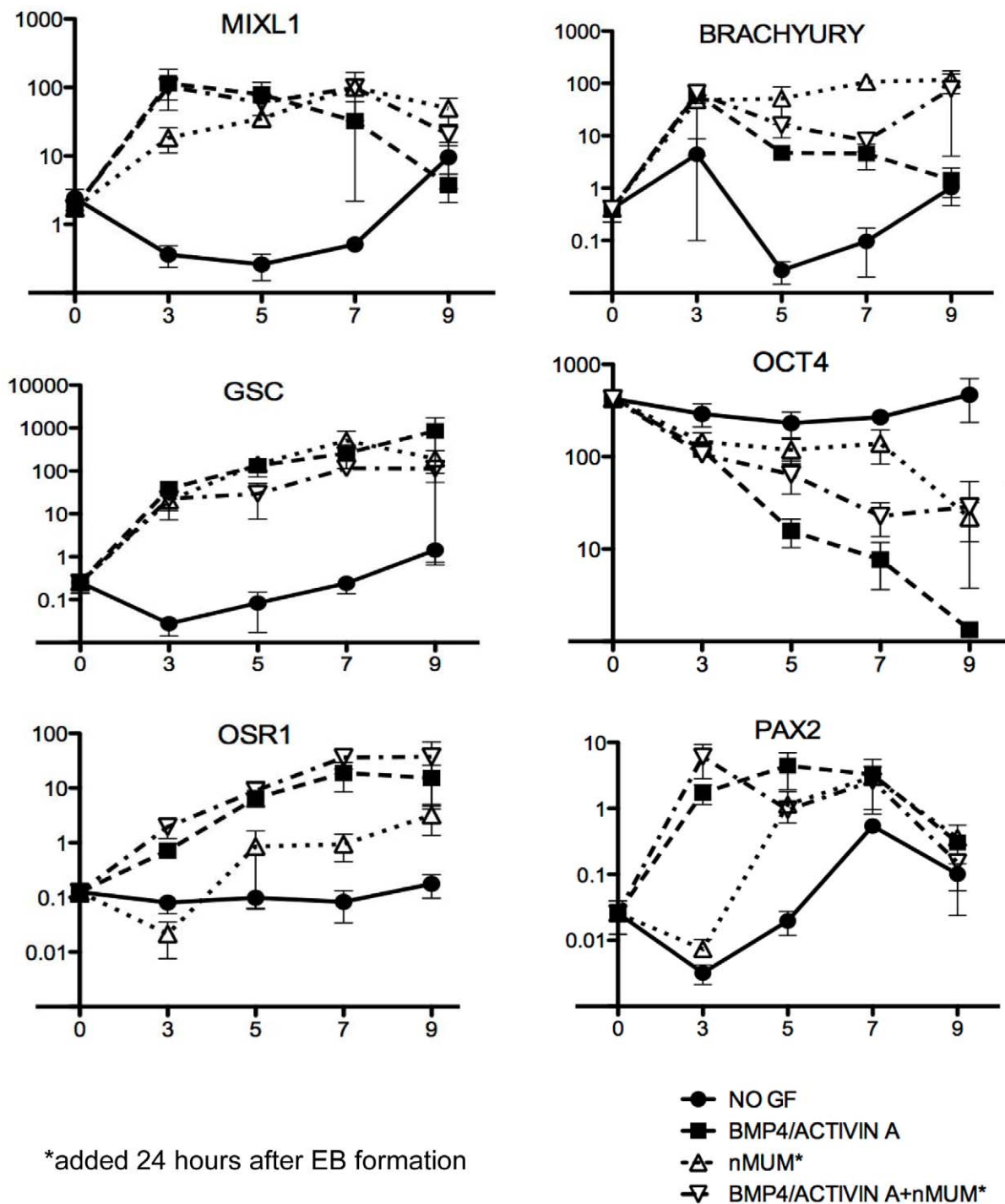


**Figure 3. Neonatal mouse uterine mesenchyme induces expression of primary germ layer markers in ENVI/nMUM recombinants.** Real time PCR analysis of RNA collected from EB and recombinants cultured in serum-free BPFL medium. Growth factors (BMP4, 50 ng.ml<sup>-1</sup> and ACTIVIN A, 20 ng.ml<sup>-1</sup>) were added immediately after forced aggregation of hESCs. Neonatal mouse uterine mesenchyme was added 24 hours after EB formation into either growth factor treated or untreated EB culture. Expression of genes relative to GAPDH were analysed by quantitative RT-PCR after 3, 5, 7 and 9 days incubation. Expression of target genes in undifferentiated hESCs is indicated as day 0 of differentiation (Data is plotted as mean ± s.e.m., n = 3 independent differentiation experiments). Abbreviations: GF, growth factor; nMUM, neonatal mouse uterine mesenchyme. doi:10.1371/journal.pone.0021136.g003

(Figure 4A), as described in a previous report of human MD epithelium [24]. To determine the stage of development, we examined expression of known MD developmental markers such as *PAX2* and *HOXA10* [25]. *PAX2* expression first appears after MD specification, during the elongation stage of development [26].

Although at 2 weeks, *PAX2* and *HOXA10* expression was not detected in the hESC derived FRT epithelium (Figure 4B–C), at 4 weeks, *HOXA10* and *PAX2* expression was observed in the developing hESC derived FRT epithelium (Figure 4D–E, Figure S5A, Figure S5B), consistent with the temporal expression pattern

previously reported for the elongation and differentiation stages of MD development in mice [25,27]. Co-expression of CK18 (Figure 4G) and Vimentin (Figure 4H, Figure S5C) in cells present on serial sections suggested that the hESC derived FRT epithelium was meso-epithelial in character. In addition, the expression of CA125 (Figure 4I, Figure S5D) supports our hypothesis that like human and rodent MD, hESC derived MD originates from a coelomic-like epithelia [12,28]. The complete absence of ER $\alpha$  in the hESC derived MD epithelium (Figure 4J) at this stage of development is consistent with previous reports showing human fetal MD lacks ER $\alpha$  expression [29]. Motile  $\beta$ -tubulin-expressing cilia were not detected on the hESC-derived FRT epithelium (data not shown). We then optically reconstructed a hESC derived FRT gland from stained serial sections (depicted from Figure 4E–J), and found it was ductal in character (Figure 4K). These data indicate that following in vitro differentiation, nMUM induced MD differentiation from hESCs recapitulated some of the known sequential stages MD ontogeny.

## Discussion

Very few studies have examined the developing human MD [24,30,31] and none have examined the differentiation of hESCs to mesoepithelial derivatives. In this study we established a model of MD development, providing an opportunity to investigate factors affecting the genesis of the human FRT. In contrast to recent work where nMUM was used to differentiate spermatogonial stem cells into murine uterine epithelium [10], developmental stages observed in our model are similar to normal Müllerian organogenesis, making it an ideal platform to study human FRT development (Figure 5). Our current protocol involves two distinct stages; hESCs were first differentiated towards cells expressing mesodermal markers in vitro, and then transplanted in vivo to form the hESC derived FRT epithelium expressing markers of the MD and its derivatives. To our knowledge, this is the first report of hESC differentiation into mesodermally derived epithelium, in this case the human FRT epithelium.

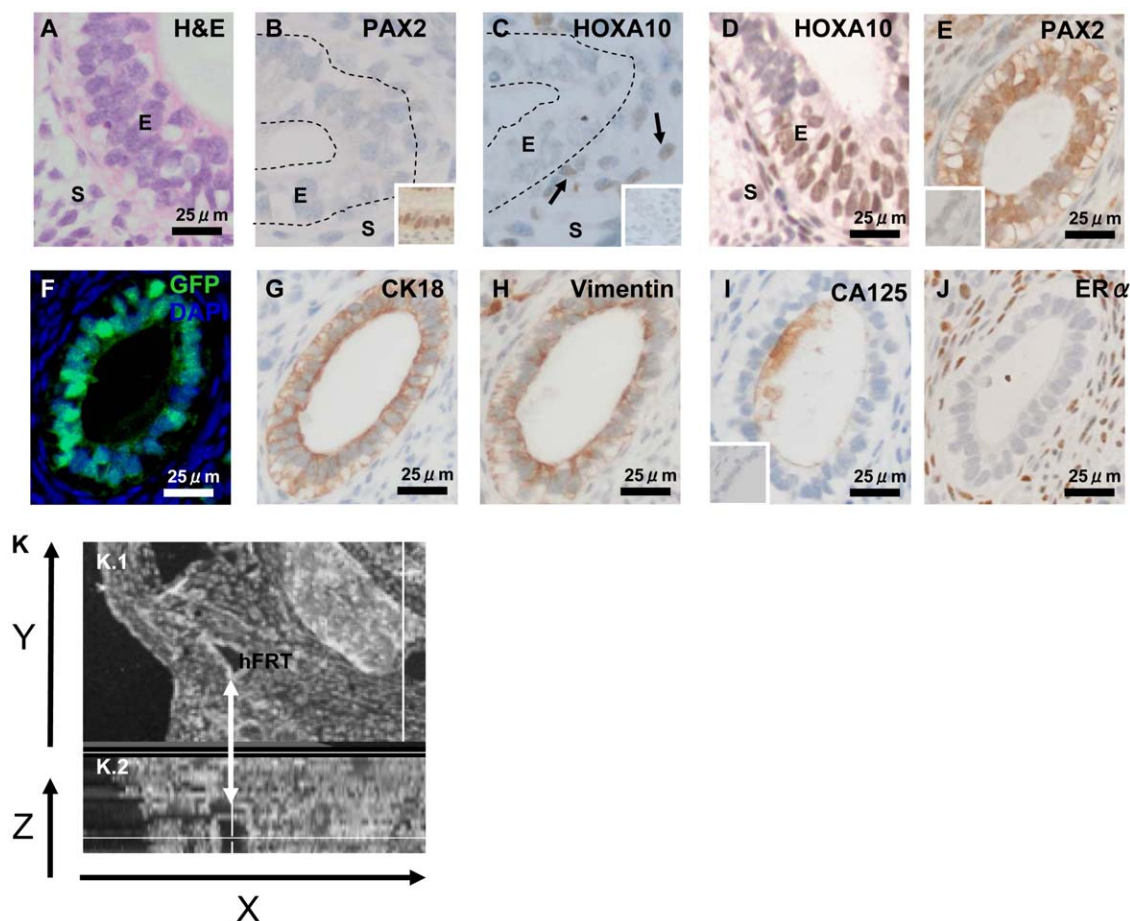


**Figure 4. Morphological and immunohistochemical characteristics of hESC derived FRT epithelial structures in grafted GF treated recombinants.** (A) H&E showing pseudostratification in the hESC derived FRT epithelium surrounded by co-transplanted mouse stroma in a 4 week graft. (B) no PAX2 or HOXA10 (C) expression in week 2 hESC derived FRT epithelium (B, C) were serial sections representative of two week 2 graft) (arrows point to HOXA10<sup>+</sup> mouse stromal cells). (D–I) Representative sections from two different 4 week grafts, (E–J) serial sections of a single gland (sectioned at 3  $\mu$ m), (D, E) Nuclear expression of HOXA10 and PAX2 in hESC derived FRT epithelium at 4 weeks. (F) representative serial sections of the same gland depicted from (E–J) showing GFP<sup>+</sup> hESC derived epithelium surrounded by GFP<sup>−</sup> mouse uterine stromal cells. The gland co-localised cytoplasmic expression of (G) CK18 and (H) Vimentin in hESC derived FRT epithelium. (I) CA125 expressed on hESC derived FRT epithelium surface. (J) ER $\alpha$  expressed in transplanted mouse stromal cells but absent from hESC derived FRT epithelium. Insets in (B) is a positive control of PAX2 expression in adult human endometrial epithelium, inset in (C) concentration matched goat IgG negative control, inset in (E) concentration matched rabbit IgG negative control, inset in (I) mouse IgG1 negative control for (G–I). (K.1–2) 3D reconstruction of hESC derived FRT epithelium from serial sections depicted in (E–J) (arrow) shown on the Y-axis, (K.2) shown on the Z-axis view as a duct. Abbreviations: E, epithelium; hFRT, hESC derived FRT; HOXA10, Homeobox A10; PAX2, Pair box gene 2; S, stroma.  
doi:10.1371/journal.pone.0021136.g004

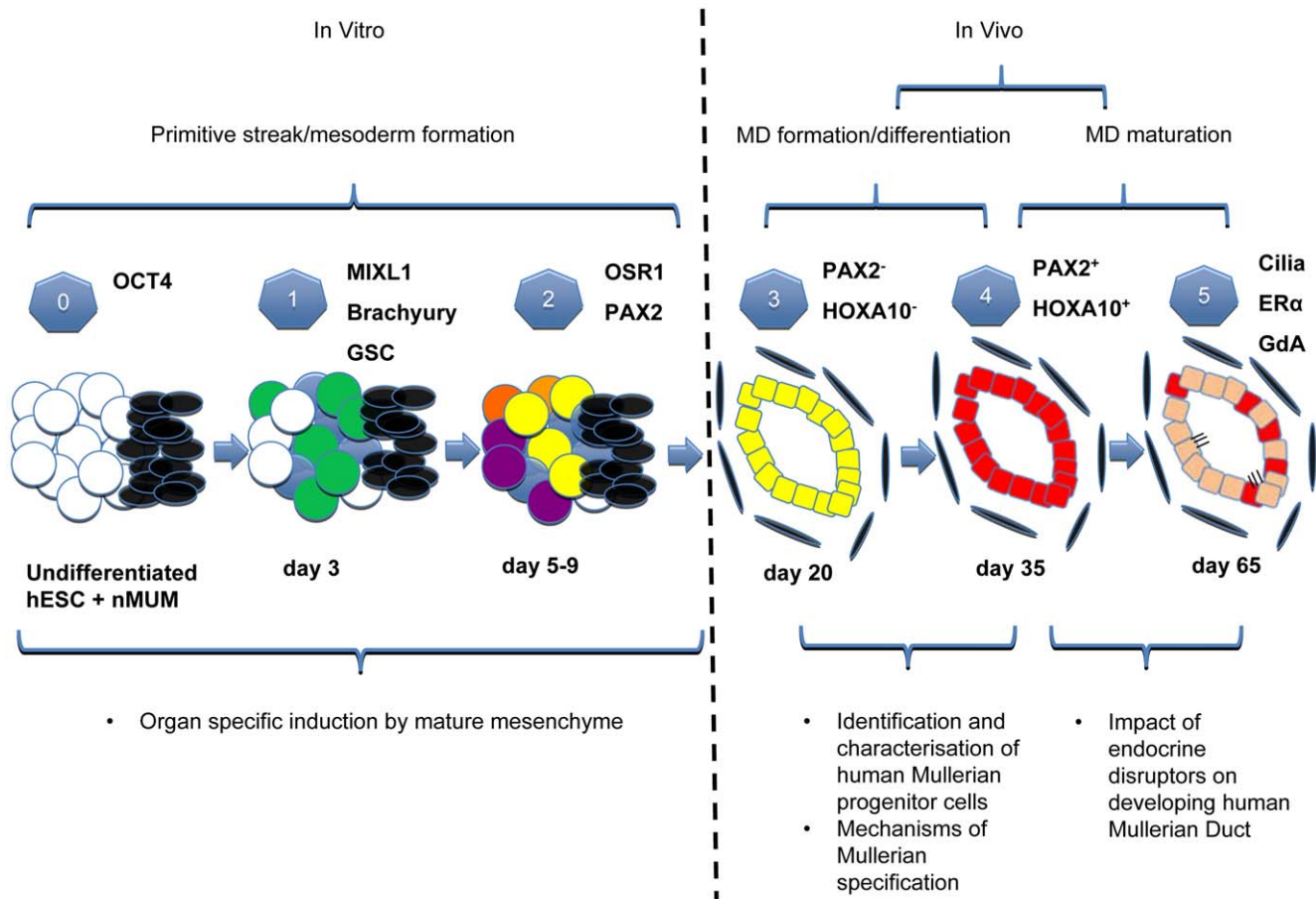


**Figure 5. Schematic of the proposed Human Müllerian Duct development model and its potential applications.** Stages of development of the hESCs/nMUM recombinant in vitro and in vivo. Key stages are numbered from 0–5 accompanied by some stage specific markers. (0): Undifferentiated hESC cells (white circles) were recombined with nMUM (black ovals), (1): primitive streak formation: nMUM (black ovals) induced some hESC to differentiate into MIXL1<sup>+</sup> mesendodermal cells (green circles) whilst the rest remained either as undifferentiated (white circles) or belonging to the ectodermal lineage (blue circles), (2): germ layer induction: mesodermal cells (yellow circles) derived from MIXL1<sup>+</sup> mesendodermal cells in the previous stage, other colored circles represent a variety of differentiated (purple, orange, blue) and undifferentiated cells (white circles), (3): in vivo differentiation, and formation of a pre-Müllerian epithelium (yellow) possibly derived from mesodermal cell types in the EB (the presence of tissues from other lineages is omitted from this figure for illustration purposes), (4): transition from the pre-Müllerian epithelium into MD epithelium (red), (5): maturation of MD epithelium into adult FRT epithelium (pink) containing residual MD epithelial cells (in red). Text boxes (below schematic) include potential applications of the model at different stages of development. doi:10.1371/journal.pone.0021136.g005

In order to identify MD epithelium and its derivatives in the recombinant grafts, we examined a short list of commonly known morphological and immunohistochemical markers of adult human female reproductive (oviduct/uterine) epithelium used in routine diagnostic laboratories and other tissue recombination studies [7,10]; cilia ( $\beta$ -tubulin), CK18, ER $\alpha$ , CA125 and GdA. Our results indicate only the hESC derived FRT epithelium in our recombinant grafts expressed this suite of epithelial markers. Several estrogen-induced functional responses of FRT epithelium were also demonstrated; increased epithelial proliferation, a defining feature of the uterine epithelium [8,9,10], and secretion of GdA. GdA is found in both oviduct (uterine tube) and uterine epithelium of the female reproductive tract and is produced by epithelium in response to estrogen or progesterone [13,32]. Low levels of ER $\alpha$  expression in the hESC derived FRT epithelium suggests that the action of estrogen on the recombinant structure may be mediated via ER $\alpha$  in the underlying mouse stroma by a paracrine mechanism, recapitulating a characteristic feature of stromal-epithelial interactions in mouse and human reproductive tract tissue [9]. Other evidence of stromal-epithelial interaction is

the smooth muscle differentiation of the mouse stromal cells, consistent with previous recombination studies using hESCs and other urogenital tissues [4,5]. One possible explanation for the weak expression of ER $\alpha$  is that our model developed in the absence of endogenous ovarian hormones. However, since MD development is an estrogen-independent process, the absence of ovarian hormones did not impair formation and differentiation of the MD, as expected [15,16]. Together these data suggest that nMUM directed differentiation of hESCs to become human FRT epithelium. However, as a recombinant model consisting of mouse and human cells, one would expect some functional differences between our hESC derived FRT epithelium and that of the normal human FRT epithelium especially in the area of hormone responsiveness of the tissue as demonstrated previously in other uterine recombinant models [9]. In future experiments, for further characterisation of the hESC derived FRT epithelium, we plan to compare the molecular signatures between our FRT epithelium with the normal human FRT epithelium.

Animal studies have shown that coelomic epithelium is specified to form the MD [28]. During embryogenesis, the coelom itself



derives from the lateral plate mesoderm that emanates from the primitive streak [33]. Similar to ontological development, our gene expression analysis indicated that nMUM first initiated mesendoderm differentiation and then influenced mesodermal lineage commitment in the differentiating human EBs. Rather than simply acting as an external cue to initiate EB self-organisation [34], our results suggest nMUM created morphogen gradients that influenced lineage commitment of differentiating hESCs, similar to other co-culture experiments [35]. Our previous microarray analysis in the nMUM (unpublished data) showed gene expression of several members of the TGF- $\beta$  super family of ligands (BMP, Activin) and Wnt family ligands consistent with other reports [36,37,38]. We propose that these and other morphogens in the nMUM initiated formation of mesendodermal cells and their subsequent differentiation in the EB. Further investigations are required to unravel the exact combination of mesenchymal soluble factors responsible for this induction. Following in vitro mesodermal lineage commitment, subsequent in vivo development of the hESC derived FRT epithelium at earlier time points mimicked known stages of MD development [27], both in morphological and molecular features previously described for human and mouse MD [24,28].

A persistent problem in developing both in vitro and in vivo human organogenesis models from hESCs is the heterogeneity of tissue types produced. Similar to recent tissue recombination studies involving pluripotent cells [4,5,10], our method employing organ specific mesenchyme for generation of human FRT epithelium also generated a large fraction of 'off target' cell types. Although, manipulating the ratio of mesenchyme and hESCs could enhance differentiation and reduce unwanted lineage differentiation [4], a more consistent and robust outcome might be achieved if the appropriate inductive growth factors could be identified. In this study, we combined both techniques by first pre-differentiating EBs in the presence of mesendoderm promoting factors and then recombining them with inductive mesenchyme. Future studies aimed at identifying mesenchymally derived inductive factors will enable further refinement and control over the direction and efficiency of differentiation.

Overall, we demonstrated for the first time that nMUM can direct differentiation of hESCs to form human FRT epithelium. The entire process can be dissected and studied over a period of 8 weeks (Figure 5), providing an avenue to investigate human MD development. Both host environment and mesenchyme can be manipulated to examine systemic and local factors involved in MD development and maturation. Furthermore, our model of human FRT development may also provide a platform for the characterisation of human endometrial stem/progenitor cells recently identified in human and mouse uterus [1,2,39]. Indirect evidence suggests that stem/progenitor cells reside in the basalis (non-shedding layer) of the endometrium and it is postulated that they are remnants of fetal MD epithelium [40]. However, the isolation and identification these cells have been hampered by lack of defining cell surface markers. In this context, the availability of hESC derived fetal human MD epithelium may facilitate the search for cell surface markers that can be used to locate rare adult stem cells residing in the adult human uterus. Identifying these cells has the potential to profoundly impact on understanding normal physiological processes and diseases affecting the female reproductive tract epithelium, such as endometriosis, endometrial hyperplasia and endometrial cancer [41,42].

## Materials and Methods

### Animals

Animals were obtained from Monash Animal Services. Day 1 nMUM and epithelium were obtained from female C57BL

/6JAsmu (F1) mice. Female NOD.CB17-prkdcscid/Asmu (NOD.Scid) and NOD/Scid IL-2R Gamma (NSG) mice 4–6 weeks old were housed under controlled environmental conditions at 20°C with 12-hour dark/light cycles and unlimited access to food and water. All animal handling and procedures were carried out in accordance with National Health and Medical Research Council of Australia guidelines for the Care and Use of Laboratory Animal Act and approval was obtained from the Monash University Animal Ethics Committee at Monash Medical Centre – A (MMC-A), Clayton, Australia. The approval numbers are 2006/44 and 2010/41.

### hESC Lines and Tissue Recombination

Two genetically modified hESC lines were used; the constitutively GFP<sup>+</sup> line, ENVY [18] and MIXL1<sup>GFP/wt</sup> reporter line [17], both of which were derived from HES3 (karyotype 46, XX) [43]. For differentiation experiments, 3000 hESCs per well were aggregated by centrifugation to form spin EBs in serum-free BPEL medium according to previously established protocols [44, 45]. In some experiments, the medium was supplemented with 50 ng.ml<sup>-1</sup> BMP4 and 20 ng.ml<sup>-1</sup> ACTIVIN A (both from R&D Systems). The uterine tubes of postnatal day 1 mice were mechanically dissected following enzymatic treatment as described in previous studies [7,46]. Two small pieces of epithelial-free mesenchyme measuring 0.5 mm were recombined with day 1 EBs by co-culture in serum-free BPEL medium with or without growth factors (BMP4, 50 ng.ml<sup>-1</sup>, ACTIVIN A 20 ng.ml<sup>-1</sup>). On day 3 or 5, recombinants were re-suspended in 10  $\mu$ l of neutralised rat tail collagen (a gift from Dr. Renea Taylor, Anatomy and Developmental Biology, Monash University, Australia) and placed on the surface of non-adherent Petri dishes for 10–15 minutes at 37°C to allow the gel to solidify. Medium was then added to the Petri dish and recombinants in collagen droplets were immersed in the medium and incubated at 37°C for 30 minutes prior to transplantation into NOD.Scid or NSG mice.

### Xenografting tissue recombinants

Tissue recombinants or mesenchyme alone and differentiated hESCs alone (EBs) were grafted under the renal capsule of female (5–6 weeks old) NOD.Scid or NSG mice for 2 to 8 weeks as previously described [5,47]. All mice were ovariectomized at the time of surgery. For experiments assessing the functional capacity of hESCs-derived reproductive tract epithelium, animals were subjected to hormonal treatment one week before harvesting. Hosts carrying tissue recombinants were injected daily with 500 ng estradiol valerate (E2) in 100  $\mu$ l corn oil (experiment group) or corn oil alone (control group) for 5 days. All grafts were harvested and fixed overnight in 4% paraformaldehyde (PFA), imaged, paraffin embedded and 3  $\mu$ m serial sections cut for histology and immunohistochemistry. Some recombinants were harvested on day 5 following in vitro incubation for histology. These grafts were first re-suspended in collagen and fixed with 4% PFA prior to processing.

### Real time PCR

Individual recombinants and EBs were harvested from in vitro culture for gene expression analysis on days 3, 5, and 7, and 9. Samples were incubated in TrypLE Select (Invitrogen) for 30 minutes at 37°C then disaggregated by mixing, and digested completely with Lysis Solution provided with the RNA extraction kit (Ambion, Applied Biosystems, CA.). Following RNA extraction, DNase treatment was performed to eliminate contaminating genomic DNA using RNeasy Micro DNase Treatment Kit (Ambion, Applied Biosystems). The quality and quantity of the

RNA was checked using a Nanodrop Spectrophotometer ND-1000 in conjunction with ND-1000 V3.3.1 computer software (ThermoFisher Scientific). Approximately 50 ng of total RNA from each sample was reverse transcribed to first strand cDNA with random hexamer primers using Superscript III reagents with RNase Inhibitor (Invitrogen). Real-time PCR was performed using Taqman gene expression probes, Taqman reagents and the 7900 HT Fast Real-Time PCR system absolute thermal cycler with software from Applied Biosystems. PCR reactions for all samples were run in triplicates. The comparative cycle threshold (Ct) method was used to analyse data. Gene expression levels were compared to the reference gene (REF), glyceraldehyde-3-phosphate dehydrogenase (GAPDH). Since gene expression is inversely proportional to the Ct, the expression for target gene relative to GAPDH was calculated according to previously described formula below [48,49].

$$\text{Gene expression} \propto \frac{1}{2^{C_t(\text{Gene}-\text{REF})}}$$

For purposes of presentation, we multiplied calculated values normalised to GAPDH by 1,000.

We tested for species cross reactivity of individual genes from information available on manufacturer's website; we performed a BLAST search using the amplicon to determine the gene's location in the human genome (GenBank mRNA reference numbers) against the mouse genome. The species specificity of each assay was tested by including neonatal uterine mesenchyme and human tissue in real time PCR reactions (data not shown). The inventoried Taqman Gene Expression Assays (Applied Biosystems) used in this study were: *GAPDH*: Hs99999905\_m1, *MIXL1*: Hs00430824\_g1, *BRACHYUR1*: Hs00610080\_m1, *GOOSECOID*: Hs00418279\_m1, *OSR1*: Hs00377071\_m1, *PAX2*: Hs01057415\_m1, *POU5F1* (*OCT4*): Hs03005111\_g1. The ID suffix “\_m” indicates the probe spans an exon junction and will not detect genomic DNA. “\_g” indicates an assay that may detect genomic DNA. The assay primers and probes may also be within a single exon. While genomic DNA amplification was possible for *MIXL1* and *POU5F1*, this was highly unlikely because of the DNase digestion step after RNA purification.

### Immunohistochemistry/Immunofluorescence

Sections were deparaffinized and hydrated through xylene and graded alcohols. Antigen retrieval was performed by microwaving sections in 0.01 M citrate buffer solution, pH-6 for 20 min, followed by cooling to room temperature. Sections stained with antibodies specific for nuclear proteins were permeabilized with 0.5% Triton-X 100 in PBS for 10 minutes. Endogenous peroxidase activity was blocked with 3% H<sub>2</sub>O<sub>2</sub> in methanol for 10 minutes at room temperature followed by 3 rinses with PBS. Protein Block was applied to minimise non-specific antibody binding (Serum-free protein block, DAKO, Denmark) for 10 minutes at room temperature. Concentration matched mouse IgG isotype negative controls were included in each run, rabbit IgG (DAKO) and goat IgG (Santa Cruz) were included in runs using polyclonal antibodies as negative controls. Following overnight incubation with primary antibodies at 4°C in a humidified chamber, slides were washed with PBS, and incubated with reagents from appropriate kits or stained with Alexa Fluor secondary antibodies (Table 1) at 1:200, RT for 30 minutes; Mouse or Rabbit ENVISION (DAKO), LSAB HRP for Mouse/Rabbit/Goat (DAKO) were used according to manufacturer's protocols. Immunoreactivity was detected by incubating with DAB (DAKO) for 10–15 minutes, then rinsing with distilled water,

**Table 1.** Primary antibody used in this study.

Primary Antibody	Species	Clone	Dilution	Source	Reference
α-SMA <sup>4</sup>	Mouse	1A4	1:100	Dako	[1]
Anti-GFP <sup>1</sup>	Mouse	N/A	1:500	Millipore	[50]
Anti-GFP <sup>2</sup>	Rabbit	N/A	1:500	Abcam	
Anti-β-Tubulin*	Mouse	TUB2.1	1:1000	Sigma-Aldrich	[51]
CA125 <sup>1</sup>	Mouse	OC125	1:200	Invitrogen	[12]
CK18 <sup>1</sup>	Mouse	DC10	1:500	Dako	[52]
ERα <sup>1</sup>	Mouse	6F11	1:50	Nova Castra	[53]
Glycodelin A <sup>4</sup>	Mouse	001-13	1:100	Abcam	[54]
HOXA10 <sup>3</sup>	Goat	N/A	1:1000	Santa Cruz	[55]
Ki67 <sup>4</sup>	Rabbit	SP6	1:200	ThermoScientific	[56]
PAX2 <sup>1</sup>	Rabbit	N/A	1:100	Invitrogen	[57,58]
Vimentin*	Mouse	V9	1:500	Sigma-Aldrich	[1]

<sup>1</sup>**secondary antibody:** goat anti-mouse IgG<sub>1</sub>-AlexaFluor 488 (Invitrogen) or goat anti-mouse IgG<sub>1</sub>-AlexaFluor 568.

<sup>2</sup>**secondary antibody:** donkey anti-rabbit AF 488 or donkey anti-rabbit AF 568 (Invitrogen).

<sup>3</sup>**secondary antibody:** donkey anti-goat AF568 (Invitrogen).

<sup>4</sup>**HRP kits:** mouse or rabbit envision (Dako) depending on the host species of the primary antibody.

\*primary antibody is CY3 conjugated.

doi:10.1371/journal.pone.0021136.t001

followed by haematoxylin counterstain. Refer to (Table 1) for a list of primary antibodies used in this study. Hoechst 33258 staining was performed for 30 seconds (Molecular Probes, Eugene, Oregon, USA). Bright field images were taken with an Olympus upright microscope (Olympus Corporation, Tokyo, Japan). Fluorescent images were taken with a Leica DMR upright fluorescence microscope (Leica Microsystems, Mannheim, Germany). Individual color images were merged using Image J analysis software. Adult human endometrial sections were included as positive controls for every staining run.

### 3D modelling of harvested tissue recombinant

Consecutive H&E and immunohistochemically stained serial sections of the tissue were imaged in their entirety using the Olympus DotSlide system (Olympus BX51, Olympus Corporation, Tokyo, Japan). The system utilised a 10× 0.3NA objective to image multiple connected fields-of-view and digitally joined the images together to form a single image covering the entire tissue section. The images of consecutive serial sections were then stacked into a 3D volume and aligned using AutoAligner v6.0.1 (Bitplane AG). The 3D tissue volume was then visualised and analysed using Imaris v7.0 (Bitplane AG).

### Supporting Information

**Figure S1 Xenograft size and hESC-derived FRT epithelium orientation.** (A) Size of grafts derived from EBs alone, growth factor (BMP4 and ACTIVIN A) treated EBs alone, recombinants and growth factor treated recombinants after 8 weeks in vivo incubation. Inset shows mean volume of three groups; GF EB, GF Recomb, Recomb, data plotted as mean ± s.e.m. (n = 4 per group, except for n = 2 for recombinant group). (B) H&E of a section from week 8 recombinant graft showing hESC derived epithelium grown in proximity to other epithelial and connective tissue structures (arrows indicate transplanted mouse stromal cells) (C) Composite image of a GF recombinant

graft. The Hoechst stain shows hESC derived FRT epithelium structure comprising human epithelial cells with smooth nuclei surrounded by mouse stromal cells with speckled nuclei (arrows). All images were captured on  $\times 4$  magnification, inset was captured on  $\times 40$ . (D) H&E of a section from week 4 recombinant graft showing two hESC derived epithelium in the same field of view (arrows indicate transplanted mouse stromal cells). Abbreviations: C, cartilage; E, epithelium; FC, Fluid-filled cavity; GF, growth factor; K, kidney; R, hESC derived FRT epithelium; S, stroma. (TIF)

**Figure S2 Histogram summarising the percentage of grafts that contained hESC derived FRT epithelium, asterix indicates that week 2 & 4 grafts are included.** (TIF)

**Figure S3 (A–B) representative ENVY hESC recombinant graft in vitro (C) representative H&E section of ENVY hESC recombinant graft consisting cells with distinct morphologies, two populations; ENVY hESC and nMUM.** Abbreviations: EB, embryoid body; M, neonatal mouse uterine mesenchyme. (TIF)

**Figure S4 (A–B) representative section demonstrating ER $\alpha$  expression in hESC derived epithelium in grafts with (A) or without (B) E2 treatment (arrows indicating weakly stained nuclei), full arrows in (A) indicate mouse uterine stromal cells (C, D) representative sections showing ER $\alpha$  expression in normal human adult proliferative uterine glands and stroma.** Abbreviations: E, epithelium; S, stroma. (TIF)

## References

- Chan RW, Gargett CE (2006) Identification of label-retaining cells in mouse endometrium. *Stem Cells* 24: 1529–1538.
- Gargett CE, Schwab KE, Zillwood RM, Nguyen HP, Wu D (2009) Isolation and Culture of Epithelial Progenitors and Mesenchymal Stem Cells from Human Endometrium. *Biol Reprod*.
- Chan RW, Schwab KE, Gargett CE (2004) Clonogenicity of human endometrial epithelial and stromal cells. *Biol Reprod* 70: 1738–1750.
- Oottamasathien S, Wang Y, Williams K, Franco OE, Wills ML, et al. (2007) Directed differentiation of embryonic stem cells into bladder tissue. *Dev Biol* 304: 556–566.
- Taylor RA, Cowin PA, Cunha GR, Pera M, Trounson AO, et al. (2006) Formation of human prostate tissue from embryonic stem cells. *Nat Methods* 3: 179–181.
- Cunha GR (1976) Stromal induction and specification of morphogenesis and cytodifferentiation of the epithelia of the Mullerian ducts and urogenital sinus during development of the uterus and vagina in mice. *J Exp Zool* 196: 361–370.
- Kurita T, Cooke PS, Cunha GR (2001) Epithelial-stromal tissue interaction in paramesonephric (Mullerian) epithelial differentiation. *Dev Biol* 240: 194–211.
- Kurita T, Lee KJ, Cooke PS, Taylor JA, Lubahn DB, et al. (2000) Paracrine regulation of epithelial progesterone receptor by estradiol in the mouse female reproductive tract. *Biol Reprod* 62: 821–830.
- Kurita T, Medina R, Schabel AB, Young P, Gama P, et al. (2005) The activation function-1 domain of estrogen receptor alpha in uterine stromal cells is required for mouse but not human uterine epithelial response to estrogen. *Differentiation* 73: 313–322.
- Simon L, Ekman GC, Kostereva N, Zhang Z, Hess RA, et al. (2009) Direct transdifferentiation of stem/progenitor spermatogonia into reproductive and nonreproductive tissues of all germ layers. *Stem Cells* 27: 1666–1675.
- Nicholas CR, Haston KM, Grewall AK, Longacre TA, Reijo Pera RA (2009) Transplantation directs oocyte maturation from embryonic stem cells and provides a therapeutic strategy for female infertility. *Hum Mol Genet* 18: 4376–4389.
- Bischof P (1993) What do we know about the origin of CA 125? *Eur J Obstet Gynecol Reprod Biol* 49: 93–98.
- Seppala M, Taylor RN, Koistinen H, Koistinen R, Milgrom E (2002) Glycodelin: a major lipocalin protein of the reproductive axis with diverse actions in cell recognition and differentiation. *Endocr Rev* 23: 401–430.
- Okada A, Ohta Y, Brody SL, Watanabe H, Krust A, et al. (2004) Role of foxj1 and estrogen receptor alpha in ciliated epithelial cell differentiation of the neonatal oviduct. *J Mol Endocrinol* 32: 615–625.
- Couse JF, Korach KS (2001) Contrasting phenotypes in reproductive tissues of female estrogen receptor null mice. *Ann N Y Acad Sci* 948: 1–8.
- Lydon JP, DeMayo FJ, Funk CR, Mani SK, Hughes AR, et al. (1995) Mice lacking progesterone receptor exhibit pleiotropic reproductive abnormalities. *Genes Dev* 9: 2266–2278.
- Przyborski SA (2005) Differentiation of human embryonic stem cells after transplantation in immune-deficient mice. *Stem Cells* 23: 1242–1250.
- Kishi Y, Tanaka Y, Shibata H, Nakamura S, Takeuchi K, et al. (2008) Variation in the incidence of teratomas after the transplantation of nonhuman primate ES cells into immunodeficient mice. *Cell Transplant* 17: 1095–1102.
- Moser FG, Dorman BP, Ruddle FH (1975) Mouse-human heterokaryon analysis with a 33258 Hoechst-Giemsa technique. *J Cell Biol* 66: 676–680.
- Wang Y, Cheon DJ, Lu Z, Cunningham SL, Chen CM, et al. (2008) MUC16 expression during embryogenesis, in adult tissues, and ovarian cancer in the mouse. *Differentiation* 76: 1081–1092.
- Gadue P, Huber TL, Paddison PJ, Keller GM (2006) Wnt and TGF-beta signaling are required for the induction of an in vitro model of primitive streak formation using embryonic stem cells. *Proc Natl Acad Sci U S A* 103: 16806–16811.
- Wiles MV, Johansson BM (1999) Embryonic stem cell development in a chemically defined medium. *Exp Cell Res* 247: 241–248.
- Batchelder CA, Lee CC, Matsell DG, Yoder MC, Tarantal AF (2009) Renal ontogeny in the rhesus monkey (*Macaca mulatta*) and directed differentiation of human embryonic stem cells towards kidney precursors. *Differentiation* 78: 45–56.
- Wang T (1989) Human fetal endometrium—light and electron microscopic study. *Arch Gynecol Obstet* 246: 169–179.
- Kobayashi A, Behringer RR (2003) Developmental genetics of the female reproductive tract in mammals. *Nat Rev Genet* 4: 969–980.
- Torres M, Gomez-Pardo E, Dressler GR, Gruss P (1995) Pax-2 controls multiple steps of urogenital development. *Development* 121: 4057–4065.
- Klattig J, Englert C (2007) The Mullerian duct: recent insights into its development and regression. *Sex Dev* 1: 271–278.
- Orvis GD, Behringer RR (2007) Cellular mechanisms of Mullerian duct formation in the mouse. *Dev Biol* 306: 493–504.
- Takeyama J, Suzuki T, Inoue S, Kaneko C, Nagura H, et al. (2001) Expression and cellular localization of estrogen receptors alpha and beta in the human fetus. *J Clin Endocrinol Metab* 86: 2258–2262.
- Barberini F, Makabe S, Franchitto G, Correr S, Relucanti M, et al. (2007) Ultrastructural dynamics of the human endometrium from 14 to 22 weeks of gestation. *Arch Histol Cytol* 70: 21–28.
- Okada A, Sato T, Ohta Y, Iguchi T (2005) Sex steroid hormone receptors in the developing female reproductive tract of laboratory rodents. *J Toxicol Sci* 30: 75–89.

**Figure S5 Immunofluorescent images showing co-localisation of GFP<sup>+</sup> hESC derived epithelium from 4 week grafts with (A) HOXA10 (arrows indicate nuclear staining), (B) PAX2 (arrows indicating partial/diffuse nuclear staining), (C) VIMENTIN, and (D) CA125 (arrows on cell surface).**

(TIF)

**Figure S6 (A–D) are constituents of the composite images in Figure 1C–F respectively.** DAPI stained images in (E) and (F) are serial sections corresponding to glandular structures depicted in Figure 1I and 1K respectively illustrating that hESC derived epithelium (smooth nuclei) is surrounded by mouse stromal cells (arrows, speckled nuclei). Abbreviations: CA125, Cancer Antigen 125; E, epithelium; HOX, Homeobox A10; PAX2, Pair box gene 2; S, stroma; Vim, VIMENTIN.

(TIF)

## Acknowledgments

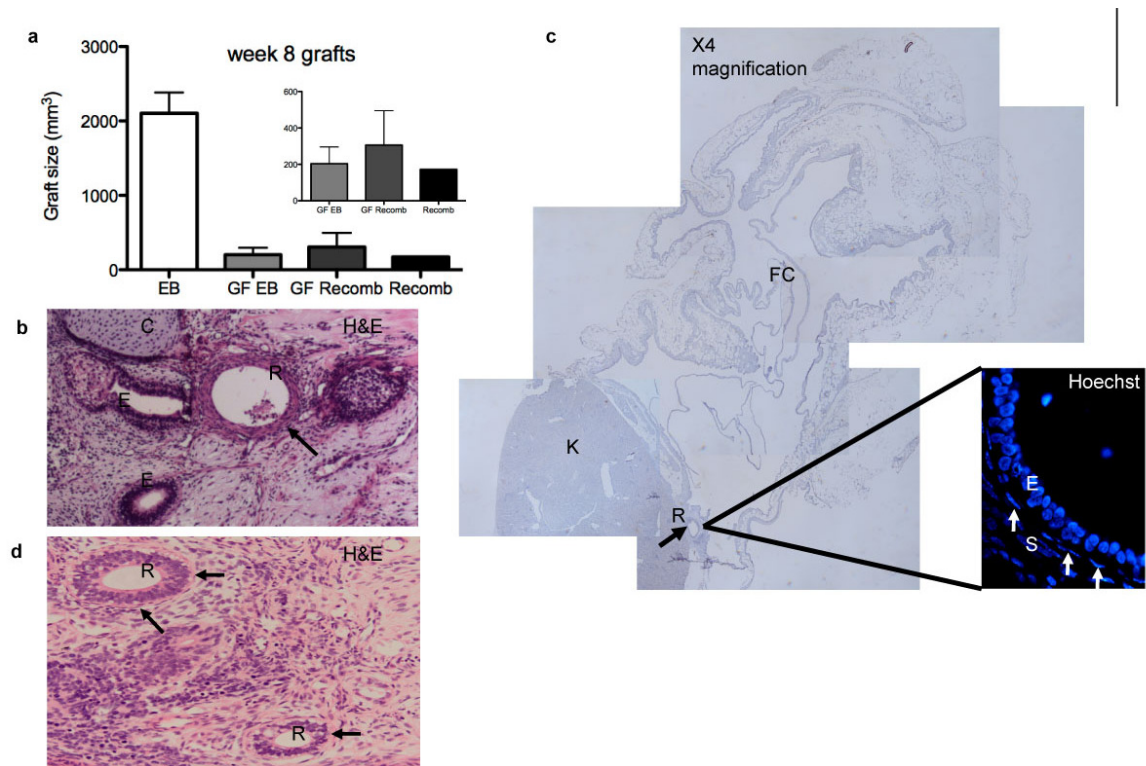
We thank Dr Renea Taylor and Dr Paul Verma for advice and technical assistance.

## Author Contributions

Conceived and designed the experiments: LY CEG AGE EGS. Performed the experiments: LY. Analyzed the data: LY CYL KLB. Contributed reagents/materials/analysis tools: CEG RM AGE EGS. Wrote the paper: LY CEG AGE EGS.

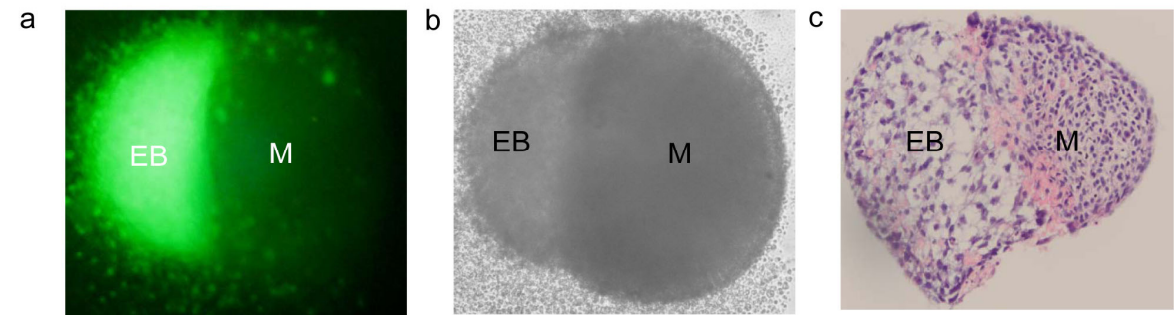
32. Laird SM, Hill CJ, Warren MA, Tuckerman EM, Li TC (1995) The production of placental protein 14 by human uterine tubal epithelial cells in culture. *Hum Reprod* 10: 1346–1351.
33. Funayama N, Sato Y, Matsumoto K, Ogura T, Takahashi Y (1999) Coelom formation: binary decision of the lateral plate mesoderm is controlled by the ectoderm. *Development* 126: 4129–4138.
34. ten Berge D, Koole W, Fuerer C, Fish M, Eroglu E, et al. (2008) Wnt signaling mediates self-organization and axis formation in embryoid bodies. *Cell Stem Cell* 3: 508–518.
35. Mummery C, Ward-van Oostwaard D, Doevendans P, Spijker R, van den Brink S, et al. (2003) Differentiation of human embryonic stem cells to cardiomyocytes: role of coculture with visceral endoderm-like cells. *Circulation* 107: 2733–2740.
36. Hu J, Gray CA, Spencer TE (2004) Gene expression profiling of neonatal mouse uterine development. *Biol Reprod* 70: 1870–1876.
37. Stoikos CJ, Harrison CA, Salamonson LA, Dimitriadis E (2008) A distinct cohort of the TGFbeta superfamily members expressed in human endometrium regulate decidualization. *Hum Reprod* 23: 1447–1456.
38. Tulac S, Nayak NR, Kao LC, Van Wae M, Huang J, et al. (2003) Identification, characterization, and regulation of the canonical Wnt signaling pathway in human endometrium. *J Clin Endocrinol Metab* 88: 3860–3866.
39. Masuda H, Matsuzaki Y, Hiratsu E, Ono M, Nagashima T, et al. Stem cell-like properties of the endometrial side population: implication in endometrial regeneration. *PLoS One* 5: e10387.
40. Gargett CE (2007) Uterine stem cells: what is the evidence? *Hum Reprod Update* 13: 87–101.
41. Gargett CE, Chan RW, Schwab KE (2008) Hormone and growth factor signaling in endometrial renewal: role of stem/progenitor cells. *Mol Cell Endocrinol* 288: 22–29.
42. Hubbard SA, Gargett CE A cancer stem cell origin for human endometrial carcinoma? *Reproduction* 140: 23–32.
43. Reubinoff BE, Pera MF, Fong CY, Trounson A, Bongso A (2000) Embryonic stem cell lines from human blastocysts: somatic differentiation in vitro. *Nat Biotechnol* 18: 399–404.
44. Ng ES, Davis R, Stanley EG, Elefanty AG (2008) A protocol describing the use of a recombinant protein-based, animal product-free medium (APEL) for human embryonic stem cell differentiation as spin embryoid bodies. *Nat Protoc* 3: 768–776.
45. Ng ES, Davis RP, Azzola L, Stanley EG, Elefanty AG (2005b) Forced aggregation of defined numbers of human embryonic stem cells into embryoid bodies fosters robust, reproducible hematopoietic differentiation. *Blood* 106: 1601–1603.
46. Bigsby RM, Cooke PS, Cunha GR (1986) A simple efficient method for separating murine uterine epithelial and mesenchymal cells. *Am J Physiol* 251: E630–E636.
47. Cunha GR, Donjacour A (1987) Mesenchymal-epithelial interactions: technical considerations. *Prog Clin Biol Res* 239: 273–282.
48. Pick M, Azzola L, Mossman A, Stanley EG, Elefanty AG (2007) Differentiation of human embryonic stem cells in serum-free medium reveals distinct roles for bone morphogenetic protein 4, vascular endothelial growth factor, stem cell factor, and fibroblast growth factor 2 in hematopoiesis. *Stem Cells* 25: 2206–2214.
49. Hatzistavrou T, Micallef SJ, Ng ES, Vadolas J, Stanley EG, et al. (2009) ErythRED, a hESC line enabling identification of erythroid cells. *Nat Methods* 6: 659–662.
50. Dai W, Field LJ, Rubart M, Reuter S, Hale SL, et al. (2007) Survival and maturation of human embryonic stem cell-derived cardiomyocytes in rat hearts. *J Mol Cell Cardiol* 43: 504–516.
51. Zhang Y, Huang G, Shornick LP, Roswit WT, Shipley JM, et al. (2007) A transgenic FOXJ1-Cre system for gene inactivation in ciliated epithelial cells. *Am J Respir Cell Mol Biol* 36: 515–519.
52. Merjava S, Neuwirth A, Mandys V, Jirsova K (2009) Cytokeratins 8 and 18 in adult human corneal endothelium. *Exp Eye Res* 89: 426–431.
53. Kaitu'u-Lino TJ, Ye L, Gargett CE Reepithelialization of the uterine surface arises from endometrial glands: evidence from a functional mouse model of breakdown and repair. *Endocrinology* 151: 3386–3395.
54. Wei Q, St Clair JB, Fu T, Stratton P, Nieman LK (2009) Reduced expression of biomarkers associated with the implantation window in women with endometriosis. *Fertil Steril* 91: 1686–1691.
55. Daftary GS, Kayisli U, Seli E, Bukulmez O, Arici A, et al. (2007) Salpingectomy increases peri-implantation endometrial HOXA10 expression in women with hydrosalpinx. *Fertil Steril* 87: 367–372.
56. Zabaglo L, Salter J, Anderson H, Quinn E, Hills M, et al. Comparative validation of the SP6 antibody to Ki67 in breast cancer. *J Clin Pathol* 63: 800–804.
57. Tong GX, Chiriboga L, Hamele-Bena D, Borczuk AC (2007) Expression of PAX2 in papillary serous carcinoma of the ovary: immunohistochemical evidence of fallopian tube or secondary Mullerian system origin? *Mod Pathol* 20: 856–863.
58. Mazal PR, Stichenwirth M, Koller A, Blach S, Haitel A, et al. (2005) Expression of aquaporins and PAX-2 compared to CD10 and cytokeratin 7 in renal neoplasms: a tissue microarray study. *Mod Pathol* 18: 535–540.

### 3.1 Supplementary Figures

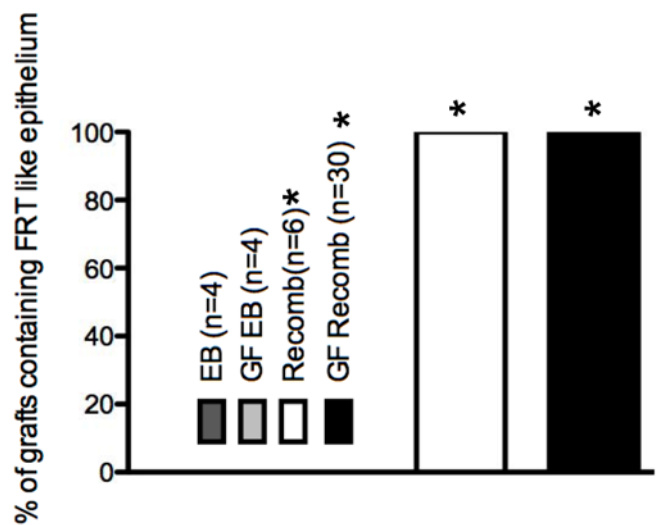


#### Supplementary Figure 3.1.1

(A) Size of grafts derived from EBs alone, growth factor (BMP4 and ACTIVIN A) treated EBs alone, recombinants and growth factor treated recombinants after 8 weeks in vivo incubation. Inset shows mean volume of three groups; GF EB, GF Recomb, Recomb, data plotted as mean  $\pm$  s.e.m. ( $n=4$  per group, except for  $n=2$  for recombinant group). (B) H&E of a section from week 8 recombinant graft showing hESC derived epithelium grown in proximity to other epithelial and connective tissue structures (arrows indicate transplanted mouse stromal cells) (C) Composite image of a GF recombinant graft. The Hoechst stain shows hESC derived FRT epithelium structure comprising human epithelial cells with smooth nuclei surrounded by mouse stromal cells with speckled nuclei (arrows). All images were captured on x4 magnification, inset was captured on x40. (d) H&E of a section from week 4 recombinant graft showing two hESC derived epithelium in the same field of view (arrows indicate transplanted mouse stromal cells). Abbreviations: C, cartilage; E, epithelium; FC,



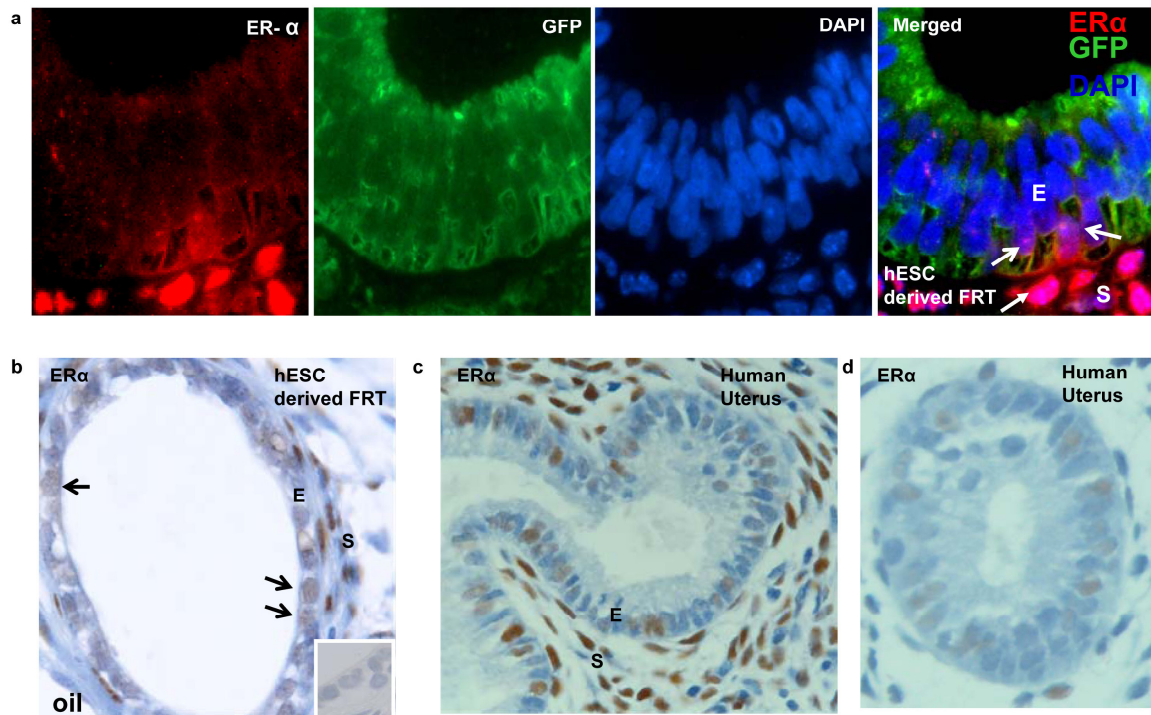
**Supplementary Figure 3.1.2**  
(A-B) representative ENVY hESC recombinant graft in vitro (C) representative H&E section of ENVY hESC recombinant graft consisting cells with distinct morphologies, two populations; ENVY hESC and nMUM. Abbreviations: EB, embryoid body; M, neonatal mouse uterine mesenchyme.



**Supplementary Figure 3.1.3**  
Histogram summarising the percentage of grafts that contained hESC derived FRT epithelium, asterix indicates that week 2 & 4 grafts are included.



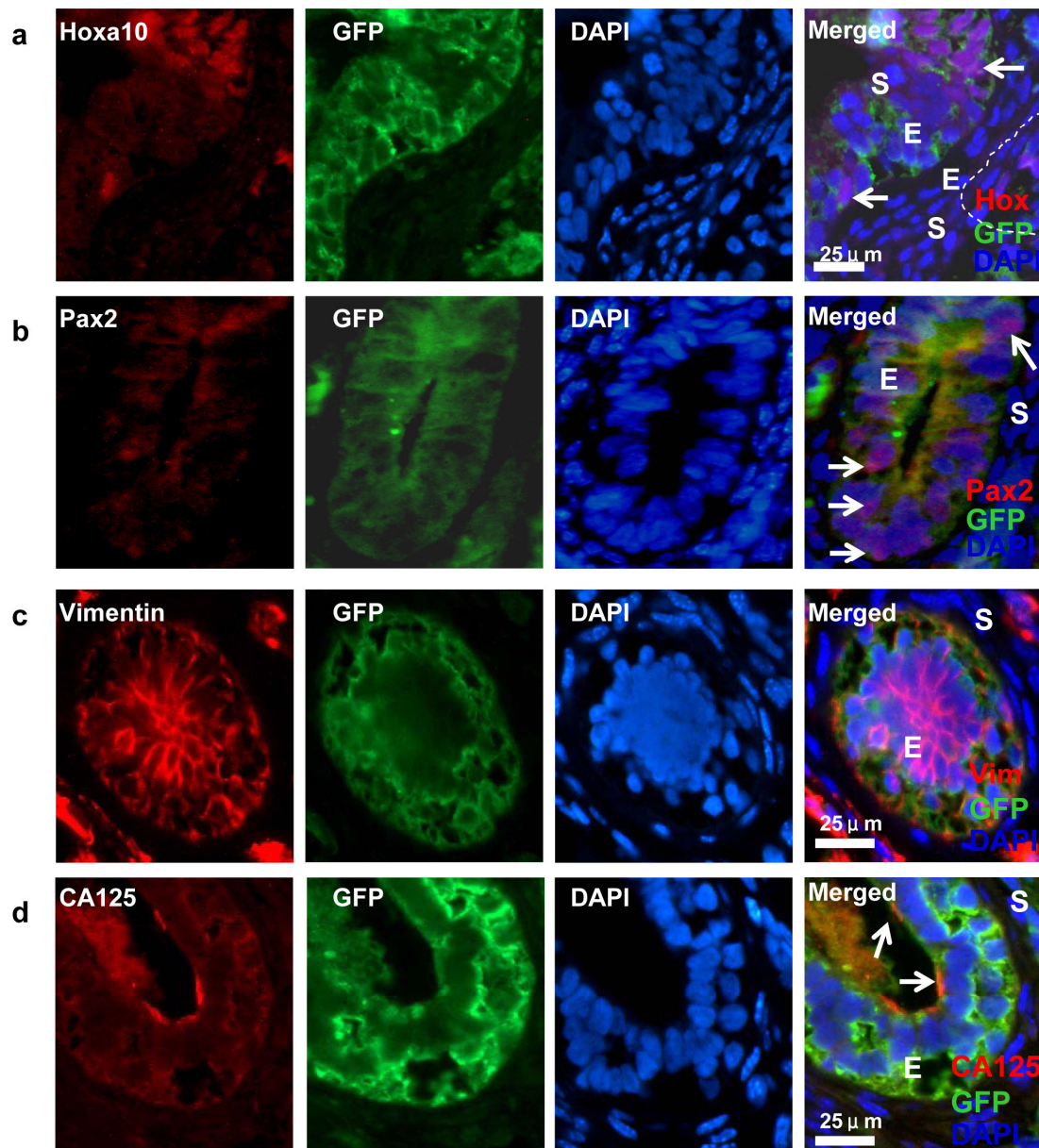
## Supplementary Figure 4



## Supplementary Figure 3.1.4

(A-B) representative section demonstrating ERα expression in hESC derived epithelium in grafts with (A) or without (B) E2 treatment (arrows indicating weakly stained nuclei), full arrows in (A) indicate mouse uterine stromal cells (C, D) representative sections showing ERα expression in normal human adult proliferative uterine glands and stroma. Abbreviations: E, epithelium; S, stroma.

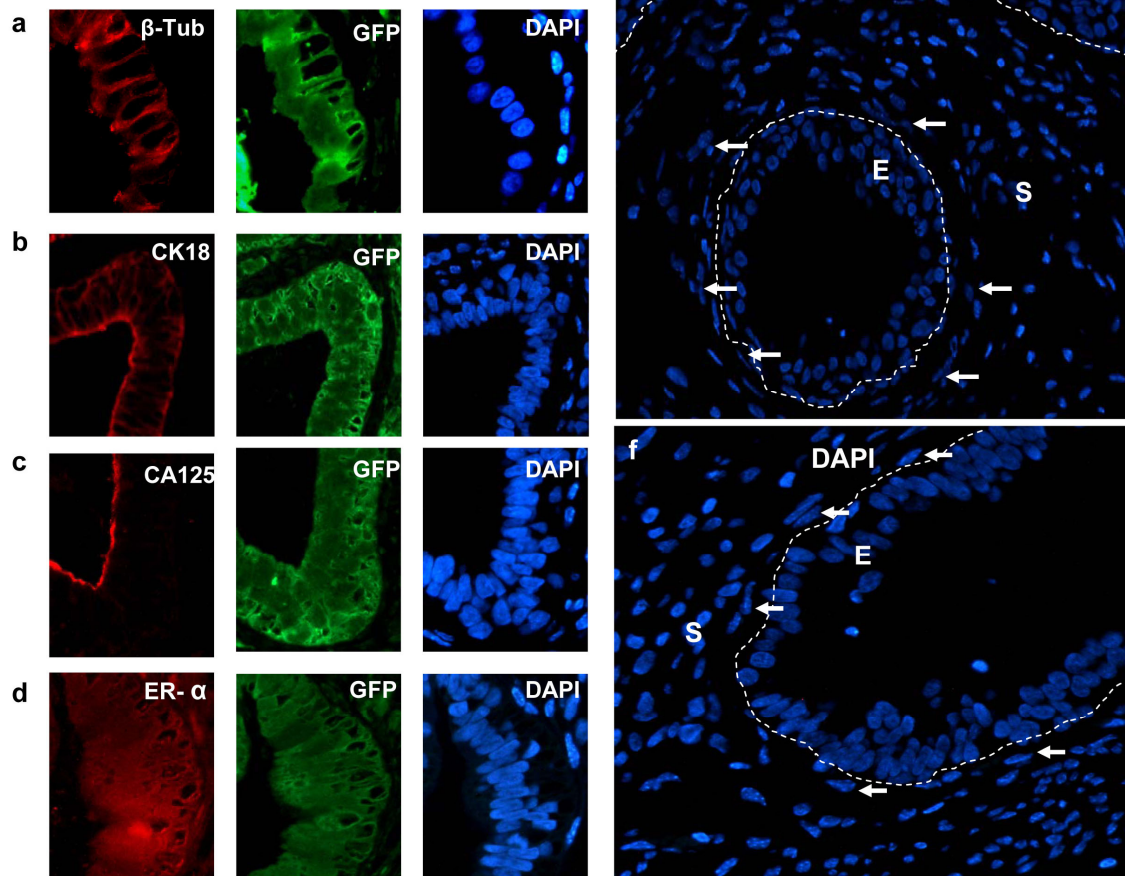
## Supplementary Figure 5

**Supplementary Figure 3.1.5**

Immunofluorescent images showing co-localisation of GFP<sup>+</sup> hESC derived epithelium from 4 week grafts with (A) HOXA10 (arrows indicate nuclear staining), (B) PAX2 (arrows indicating partial/diffuse nuclear staining), (C) VIMENTIN, and (D) CA125 (arrows on cell surface).



Supplementary Figure 6

**Supplementary Figure 3.1.6**

(A-D) are constituents of the composite images in Figure 1c-f respectively. DAPI stained images in (E) and (F) are serial sections corresponding to glandular structures depicted in Figure 1I and 1K respectively illustrating that hESC derived epithelium (smooth nuclei) is surrounded by mouse stromal cells (arrows, speckled nuclei). Abbreviations: CA125, Cancer Antigen 125; E, epithelium; HOX, Homeobox A10; PAX2, Pair box gene 2; S, stroma; Vim, VIMENTIN.

**PART B: Suggested Declaration for Thesis Chapter****Monash University****Declaration for Thesis Chapter 4****Declaration by candidate**

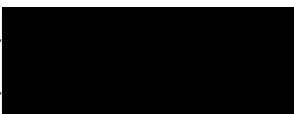
In the case of Chapter 4, the nature and extent of my contribution to the work was the following:

Nature of contribution	Extent of contribution (%)
I was involved in designing and performing the experiments, collecting and analysing the data for all figures and tables. I wrote the manuscript.	100

The following co-authors contributed to the work. Co-authors who are students at Monash University must also indicate the extent of their contribution in percentage terms:

Name	Nature of contribution	Extent of contribution (%) for student co-authors only
Caroline Gargett	Conception and design of experiments, editing of the manuscript, responsible for final approval of the manuscript	

Candidate's  
Signature


 Date 22/8/11

**Declaration by co-authors**

The undersigned hereby certify that:

- (1) the above declaration correctly reflects the nature and extent of the candidate's contribution to this work, and the nature of the contribution of each of the co-authors.
- (2) they meet the criteria for authorship in that they have participated in the conception, execution, or interpretation, of at least that part of the publication in their field of expertise;
- (3) they take public responsibility for their part of the publication, except for the responsible author who accepts overall responsibility for the publication;
- (4) there are no other authors of the publication according to these criteria;
- (5) potential conflicts of interest have been disclosed to (a) granting bodies, (b) the editor or publisher of journals or other publications, and (c) the head of the responsible academic unit; and
- (6) the original data are stored at the following location(s) and will be held for at least five years from the date indicated below:

Location(s) **Monash Institute of Medical Research (MIMR), Monash University, Clayton**

Signature 1  Date 22/8/11

.....

## **CHAPTER 4 Lim1/LIM1 is expressed in developing and adult mouse and human endometrium**

### **Abstract**

*Lim1* encodes a homeodomain transcription factor required for head, kidney and female reproductive tract development in the murine embryo. Recently, *Lim1* expression was documented in several adult murine and human organs. In the developing female reproductive tract, *Lim1* expression was first detected in the Müllerian ducts. Using immunofluorescence, we detected LIM1 expression in a developmental model of human female reproductive tract which was established by recombination of neonatal uterine mesenchyme with human embryonic stem cells. In addition, we report a dynamic expression of *Lim1/LIM1* in neonatal and adult mouse, and adult human endometrial epithelium and stroma as revealed by immunofluorescence and quantitative real time polymerase chain reaction. LIM1 expression was also observed in several endometrial epithelial cancer cell lines (ECC-1, Ishikawa, and HEC1A). These studies demonstrate previously unreported *Lim1/LIM1* expression in neonatal, adult mouse and human endometrium suggesting *Lim1/LIM1* may have a role in endometrial development and remodelling.

### **Key Words**

Lim1/LIM1 (LHX1), human endometrium, mouse endometrium, uterus

## 4.1 Introduction

The endometrium or lining of the uterus is one of few organs in the human body that undergoes cyclical degeneration and regeneration. This complex process of tissue remodelling in the adult endometrium coincides with the expression of several early developmental homeodomain transcription factors including *HOXA10*, *PAX2*, and *EMX2* [59, 60, 70, 263, 299]. The persistent expression of these development genes in adult uterine tissue is thought to be fundamental to the plasticity of the endometrium. Whilst these genes are temporally and spatially expressed in the endometrium, the role of another crucial female reproductive tract (FRT) developmental homeodomain transcription factor, *Lim1/LIM1* has not been reported in the adult human and mouse endometrium.

*LIM1* (also known as *LHX1*) is a member of the LIM homeodomain (LIM-HD) family, which encode nuclear transcription factors. Members of the LIM-HD family play a critical role in development of several organs during embryogenesis. *Lim1* is first expressed during gastrulation where it facilitates cell movements and is subsequently detected in both lateral and intermediate mesoderm [300, 301]. It is required for the development of the nervous system and urogenital organs [10, 12, 58, 302, 303]. Recently, *LIM1* has been implicated in uterine aplasia associated with Mayer-Rokitansky-Kuster-Hauser syndrome (MRKH) suggesting that it is indispensable for human FRT formation [40, 81].

It was previously shown that *Lim1* expression in the adult mouse was restricted to brain and kidney, and was not expressed in the uterus and testis [58]. More sensitive detection methods have revealed that *Lim1* is also expressed in other adult murine organs including the retina and testis [304, 305]. Human *LIM1* expression has been reported in the adult kidney, brain as well as organs and cells outside the nervous and urogenital systems including thymus, tonsil, and in leukemic cell lines [306, 307]. The LIM1 transcription factor has numerous functions in both undifferentiated and terminally differentiated cells ranging from cell specification, migration, differentiation and stem cell regulation in postnatal and adult tissue [305, 308-310]. We therefore hypothesized that LIM1 will also be expressed in adult human endometrium during the menstrual cycle where significant tissue remodelling occurs monthly.

We recently reported the differentiation of human embryonic stem cells (hESC) into Müllerian duct-like epithelium [311]. In the present study, our aim was to 1) localise LIM1 expression in our developmental model and 2) to examine Lim1/LIM1 expression in adult human and mouse endometrial tissue. We found LIM1 was expressed in our human female reproductive tract developmental model. For the first time, we report its expression in neonatal/adult mouse and human endometrial epithelial and stromal cells, as well as human endometrial cancer epithelial cells.

## **4.2 Methods**

### **4.2.1 Animals**

Animals were obtained from Monash Animal Services. Day 1 neonatal mouse uterine tissue was obtained from female C57BL/6JxCBA (F1) mice. Adult uteri were harvested from sexually mature 5-6 week old C57BL/6J mice (n=16). NOD/Scid II-2R Gamma (NSG) mice 4-6 weeks old were used as hosts for tissue recombinant transplants. All adult mice were housed under controlled environmental conditions at 20°C with 12-hour dark/light cycles and unlimited access to food and water. All animal handling and procedures were carried out in accordance with National Health and Medical Research Council of Australia guidelines for the Care and Use of Laboratory Animals and approval was obtained from the Monash University Animal Ethics Committee at Monash Medical Centre – A (MMC-A), Clayton, Australia. The approval numbers are 2006/44, 2008/12, and 2010/41.

### **4.2.2 Tissue recombination and graft transplantation**

ENVY hESC [201] were obtained from Stem Core (Australian Stem Cell Centre, Monash University). Embryoid bodies (EB) were generated by force aggregation in 96 well plates and individual EBs were subsequently recombined with dissected neonatal mouse uterine mesenchyme (P1) *in vitro* for several days before transplantation into mice as previously described [311].

### **4.2.3 Human and Mouse tissue collection**

Archival normal endometrial tissue paraffin blocks (n=15) were obtained from the Department of Obstetrics and Gynaecology, Monash University, Tissue Bank. The samples were originally collected from ovulating women aged 34–51 yr undergoing hysterectomy for fibroids or adenomyosis who had not taken exogenous hormones for 3 months before surgery. The full-thickness uterine samples were formalin fixed and paraffin embedded. The menstrual cycle stage was categorized into proliferative (n=4), early secretory (n=5), mid secretory (n=4), late secretory (n=2) by experienced pathologists according to established criteria [312]. Endometrial

adenocarcinoma sections (n=7) were obtained from the Victorian Cancer Biobank (approval number #09012). Tumours were graded by pathologists and comprised of 2 grade 1, 3 grade 2, 1 grade 3 (all type 1) and 1 type II endometrial carcinoma. Approximately 200,000 freshly isolated human endometrial epithelial cells were provided by Ms Hong Nguyen (The Ritchie Centre, Monash Institute of Medical Research) for tissue culture. Four snap-frozen normal curette samples were collected for RNA extraction. All samples were used with patients' written informed consent in accordance with ethics approval obtained from Southern Health Institutional Review Board.

Mouse uterine horns were collected without oviduct or ovarian tissue attached. The stage of estrus cycle was determined by assessing cell morphology and ratio in vaginal smears as previously described [313].

#### **4.2.4 Tissue culture**

Three human endometrial epithelial cancer cell lines were used; ECC-1 [314] (generous gifts from Professor Lois Salamonsen, Prince Henry's Institute), Ishikawa (ISH) [315], and HEC1A [316] were obtained from ATCC. Cells were grown in bicarbonate buffered DMEM/F-12 medium, containing 10% FCS (CSL Ltd.), 2 mM glutamine (Invitrogen), and antibiotic-antimycotic. Cells were passaged regularly and collected for either immunofluorescence or real-time PCR. For immunofluorescence, cells were cultured in 2 well chamber slides (20,000 cells per well)(Falcon, BD) to confluence over 48 hours then fixed in 4% PFA for 30 minutes followed by 3 rinses with PBS for immunofluorescence staining. Three independent experiments were performed by collecting cells from three different passages.

#### **4.2.5 Immunofluorescence**

Serial paraffin sections (3µm) from mouse and human uterine tissue, embryoid bodies as well as hESC-derived recombinant grafts were deparaffinized and hydrated through xylene and graded alcohols. Antigen retrieval was performed by microwaving sections in 0.01 M citrate buffer solution, at pH-6 for 20 min, followed by cooling to room temperature. Both cells on chamber

slides and paraffin sections were permeablized with 0.5% Triton-X 100 in PBS for 15 minutes. Endogenous peroxidase activity was blocked with 3% H<sub>2</sub>O<sub>2</sub> in methanol for 10 minutes at room temperature followed by 3 rinses with PBS. Protein Block was applied to minimise non-specific antibody binding (Serum-free protein block, DAKO, Denmark) for 10 minutes at room temperature. Concentration matched mouse IgG isotype and rabbit IgG (DAKO) were included in each run as negative controls for monoclonal and polyclonal antibodies respectively (refer to Supplementary Table 1 for the list of primary antibodies used in this study). A well characterised and widely published rabbit polyclonal Anti-LIM-1 (Millipore) was selected for the current study. Sections containing differentiating human embryoid bodies were included as positive controls for every staining run (Supplementary Figure 1L). Following overnight incubation with primary antibodies at 4°C in a humidified chamber, slides were washed with PBS, and incubated with Alexa Fluor secondary antibodies diluted 1:200 at RT for 30 minutes; Hoechst 33258 staining was then performed for 30 seconds (Molecular Probes, Eugene, Oregon, USA). Fluorescent images were taken with a Leica DMR upright fluorescence microscope (Leica Microsystems, Mannheim, Germany). Individual color images were merged using Image J analysis software.

#### **4.2.6 Quantification of LIM1<sup>+</sup> cells in human endometrium**

Five randomly selected glands from each endometrial region (ie. functionalis and basalis) were imaged from immunofluorescent stained sections. Glands were first selected in the DAPI filter and imaged. The same area was then imaged again using a FITC filter. The total number of glandular epithelial cells was counted in 5 randomly selected glands for each patient (at least 300 cells). The same number of stromal cells surrounding the glands was also counted. The percentages of the LIM1<sup>+</sup> cells were determined by dividing the number of labelled nuclei by the total number of nuclei counted in the selected regions. Only cells with full nuclear staining were counted as positive.

#### **4.2.7 Quantitative real time-PCR**

Total RNA was extracted using RNeasy Mini (Qiagen) or Trizol (Invitrogen) according to manufacturer's instructions. Following RNA extraction, DNase treatment was performed to eliminate contaminating genomic DNA using RNaqueous Micro DNase Treatment Kit (Ambion, Applied Biosystems). The quantity of the RNA was checked using a Nanodrop



Spectrophotometer ND-1000 in conjunction with ND-1000 V3.3.1 computer software (Thermofisher Scientific). 500ng-1µg of total RNA from each sample was reverse transcribed to first strand cDNA with oligoDT using Superscript III reagents with RNase Inhibitor (Invitrogen). PCR reactions were run in triplicates with primers using SYBR Green master mix (Applied Biosystems), alternatively, Taqman gene expression probes were used with Taqman Gene Expression master mix (Applied Biosystems) on the 7900 HT Fast Real-Time PCR system absolute thermal cycler with software from Applied Biosystems. PCR reactions for all samples were run in triplicates. The nucleotide sequences for human *LIM1* were obtained from a previous study [230]: TATA box binding protein (*TBP*), 5'-TGTGCACAGGAGCCAAGAGT-3' (Forward), 5'-ATTTTCTTGCTGCCAGTCTGG-3' (Reverse); *LIM1* 5'-TCCCCAATGGTCCCTTCTC-3' (Forward) and 5'-CGTAGTACTCGCTCTGGTAATCTCC-3' (Reverse). Taqman gene expression assay specific for mouse *Lim1* (Assay ID: Mm00521776\_m1) and *Tbp* (Assay ID: Mm00446971\_m1) were purchased from Applied Biosystems. *Tbp/TBP* was selected as the housekeeping gene as it is stable in the presence of ovarian hormones [317, 318]. The comparative cycle threshold (Ct) method was used to analyse data. Gene expression levels were compared to the reference gene (REF), *Tbp/TBP*. Since gene expression is inversely proportional to the Ct, the expression of the target gene relative to *Tbp/TBP* was calculated according to previously described formula below [206, 265]. RNA for endometrial carcinoma samples (n=2) was provided by Dr. Sonya Hubbard (The Ritchie Centre, MIMR)

$$\text{Gene expression} \propto \frac{1}{2^{C_t(\text{Gene}-\text{REF})}}$$

For purposes of presentation, we multiplied calculated values normalised to *Tbp/TBP* by 1,000.

#### 4.2.8 Statistical Analysis

Statistical analysis was performed using GraphPad Prism (version 5.00 for Windows, GraphPad Software, San Diego CA, USA). Statistical differences were assessed by One-way ANOVA (Kruskal Wallis) with Dunnett's post test.

### 4.3 Results

#### 4.3.1 LIM1 expression in the human developmental reproductive tract model

In a recent study, we demonstrated that neonatal uterine mesenchyme directs the differentiation hESC to form human FRT epithelium [311]. We investigated LIM1 expression in this developmental model of human FRT and found that whilst the expression of cancer antigen 125 (CA125) and CK18 increased over time as the Müllerian-like epithelium differentiated, the number of LIM1<sup>+</sup> hESC-derived epithelial cells diminished (Figure 4.1, Supplementary Figure 4.5.1A-F, 4.5.1I-K and 4.5.1M-O). We have previously shown that by week 8, the hESC-derived FRT have features resembling that of adult uterine epithelium [311]. The persistent LIM1 expression in week 8 hESC derived FRT epithelium suggests that it may also be expressed in adult FRT epithelium.

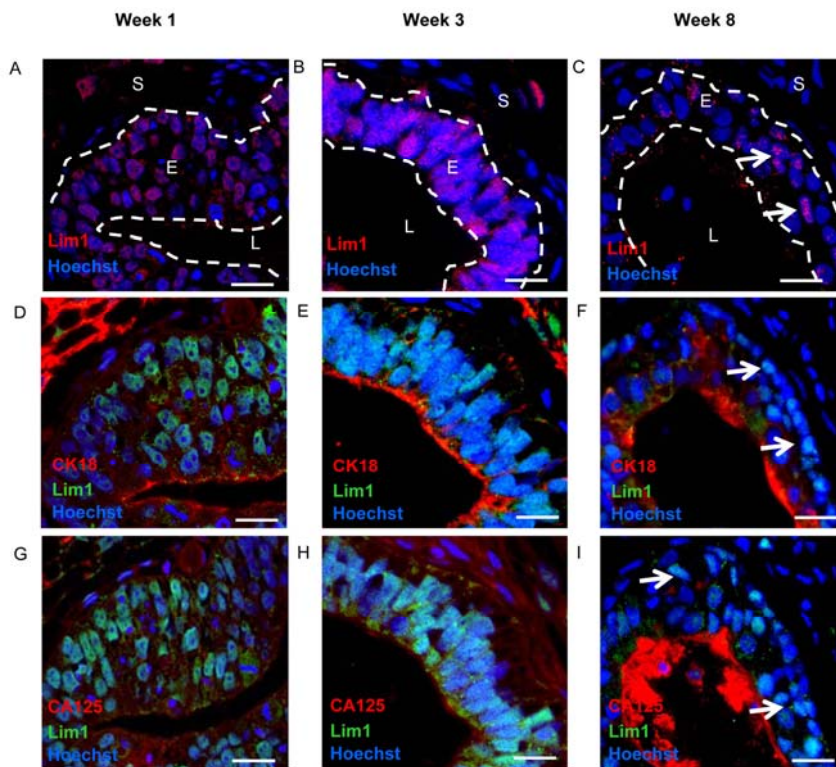


**Figure 4.1 LIM1 expression in hESC-derived human female reproductive epithelium**

Immunofluorescence photomicrographs of representative sections from three hESC-derived FRT glands after 1 (A, D, G), 3 (B, E, H), and 8 (C, F, I) weeks of *in vivo* incubation respectively (n=3, per time point) showing co-localisation of LIM1 with CK18 and CA125. (arrows point to LIM1<sup>+</sup> hESC-derived FRT epithelial cells). **Abbreviations:** E, epithelium; L, lumen; S, stroma. **Scale Bars:** 25µm

### 4.3.2 LIM1 expression in human uterine tissue

We then examined the expression of LIM1 in adult human uterine tissue. In normal human uterine samples, LIM1 was predominantly expressed in epithelial cells of the endometrium (including luminal epithelial cells) (Figure 4.2A-G, Supplementary Figure 4.5.1G-H, 4.5.1P-R) consistent with the observation that Lim1 expression is restricted to Müllerian epithelial cells in mouse [10]. Significantly more LIM1<sup>+</sup> cells were found in glandular epithelium of the functionalis than in the basalis epithelium (Figure 4.2A, 4.2H). Furthermore, the percentage of LIM1<sup>+</sup> cells varied across the menstrual cycle in the functionalis glandular epithelium, where significantly more LIM1<sup>+</sup> cells were observed in proliferative and mid-late secretory stages compared to early secretory endometrium (Figure 4.2B-D, 4.2I). LIM1<sup>+</sup> cells were barely detectable in early secretory endometrial samples (Figure 4.2C). It was previously demonstrated that ciliated endometrial epithelial cells are terminally differentiated [319]. LIM1<sup>+</sup> ciliated and non-ciliated epithelial cells were observed indicating that its expression was not restricted to terminally differentiated epithelial cells (Figure 4.2G, Supplementary Figure 4.5.1P-R). We also observed LIM1<sup>+</sup> stromal cells (Figure 4.2D, 4.2E). No LIM1<sup>+</sup> cells were detected in the myometrium (Figure 4.2A, 4.2F). *LIM1* mRNA expression in the endometrium was confirmed by quantitative real time PCR in human endometrial curettage samples (Supplementary Figure 4.2A).

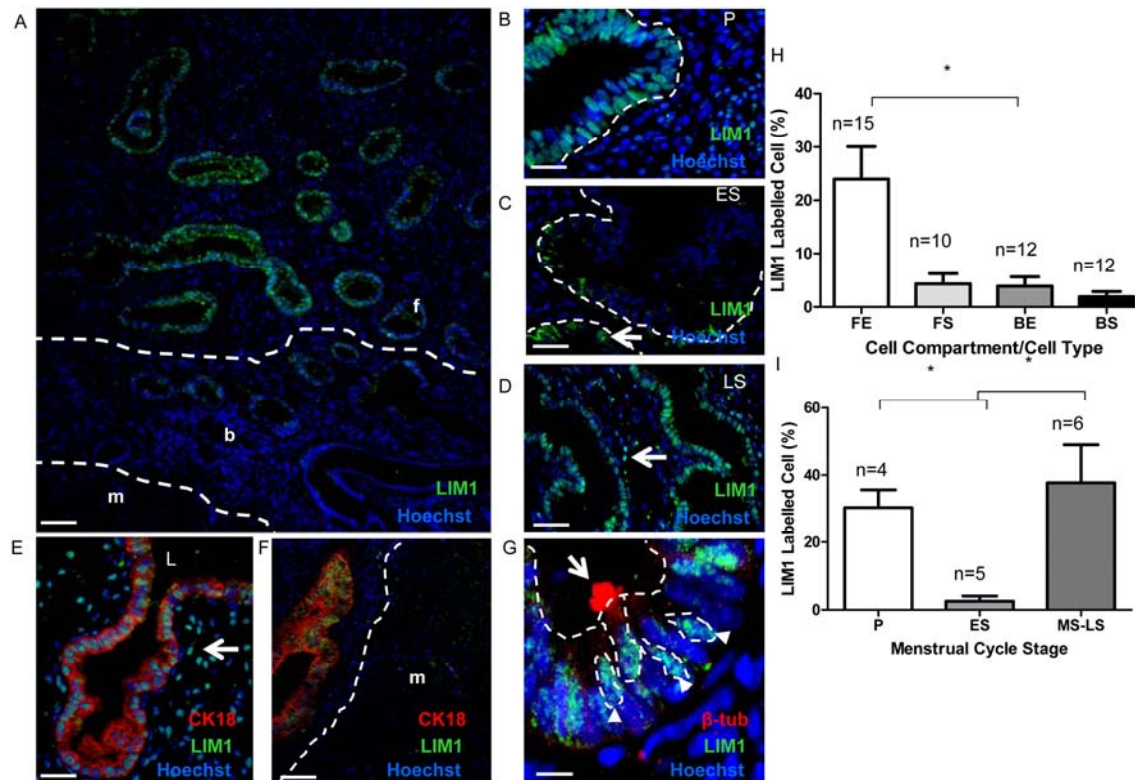


### Figure 4.2 LIM1 expression in normal adult human endometrial tissue

(A-G) Immunofluorescence photomicrographs of representative endometrial sections showing LIM1<sup>+</sup> epithelial cells located in the endometrial functionalis (f) and the basalis (b) (n=15) (arrow in (C) points to a single LIM1<sup>+</sup> epithelial cell, arrows in (D) and (E) point to LIM1<sup>+</sup> stromal cells). merged immunofluorescent images showing (E-F) co-localisation of LIM1 with CK18, (G) LIM1<sup>+</sup> ciliated and non-ciliated epithelial cells (arrow points to ciliated epithelial cells (red), arrow heads point to non-ciliated LIM1<sup>+</sup> cells). (H) Histogram showing the percentage of LIM1<sup>+</sup> cells in epithelial and stromal cells of functionalis and basalis in the endometrium (asterix denotes  $p < 0.05$  for functionalis epithelium vs functionalis stroma, functionalis vs basalis epithelium) (I) Histogram showing the percentage of LIM1<sup>+</sup> cells in the glandular epithelium of the functionalis at different stages of menstrual cycle (asterix denotes  $p < 0.05$  for P vs ES, ES vs MS-LS, data is presented as mean  $\pm$  s.e.m.). **Abbreviations:** b, basalis; BE, basalis epithelium; BS, basalis stroma; E, epithelium; f, functionalis; ES, early secretory; FE, functionalis epithelium; FS, functionalis stroma, MS, mid-secretory; LS, late secretory; F, functionalis; L, lumen; m, myometrium. P, proliferative; S, stroma. *Scale Bars:* (G) 10 $\mu$ m (B,C,E) 25 $\mu$ m, (D) 50 $\mu$ m, (F) 100 $\mu$ m, (A) 200 $\mu$ m

### 4.3.3 Lim1 expression in mouse uterine tissue

*Lim1* expression in uterine segment of the developing Müllerian ducts is downregulated during late stages of embryogenesis [10]. However, the murine uterus is not fully developed at birth since adenogenesis and myometrial development occur postnatally [24, 25]. Based on evidence of LIM1 expression in our human developmental model of the FRT, we examined the expression of *Lim1* in day 1 neonatal mouse uterus which comprises of luminal epithelium surrounded by differentiating mesenchyme (Figure 4.3). *Lim1*<sup>+</sup> cells were observed in luminal epithelial cells and the inner layer of mesenchymal cells (according to previously described morphological characteristics [24]) of the neonatal uterus (Figure 4.3A). In the cycling adult mouse endometrium, *Lim1*<sup>+</sup> cells were almost exclusively found in luminal and glandular epithelial cells (Figure 4.3B-C). Similar to the distribution of LIM<sup>+</sup> cells in the human uterus, *Lim1* expression was absent from the mouse uterine myometrium (Figure 4.3C), and the number *Lim1*<sup>+</sup> cells also appeared to vary between different stages of the estrus cycle (Figure 4.3B-C). Further quantitative analysis of *Lim1* mRNA in the adult mouse uterus revealed a dynamic pattern of expression during the estrus cycle; higher level of expression at proestrus and diestrus of the cycle, and lower level during estrus (Figure 4.3D). Neonatal uterine *Lim1* expression was significantly higher than the lowest level of expression detected at the estrus stage of the cycle (Figure 4.3D).

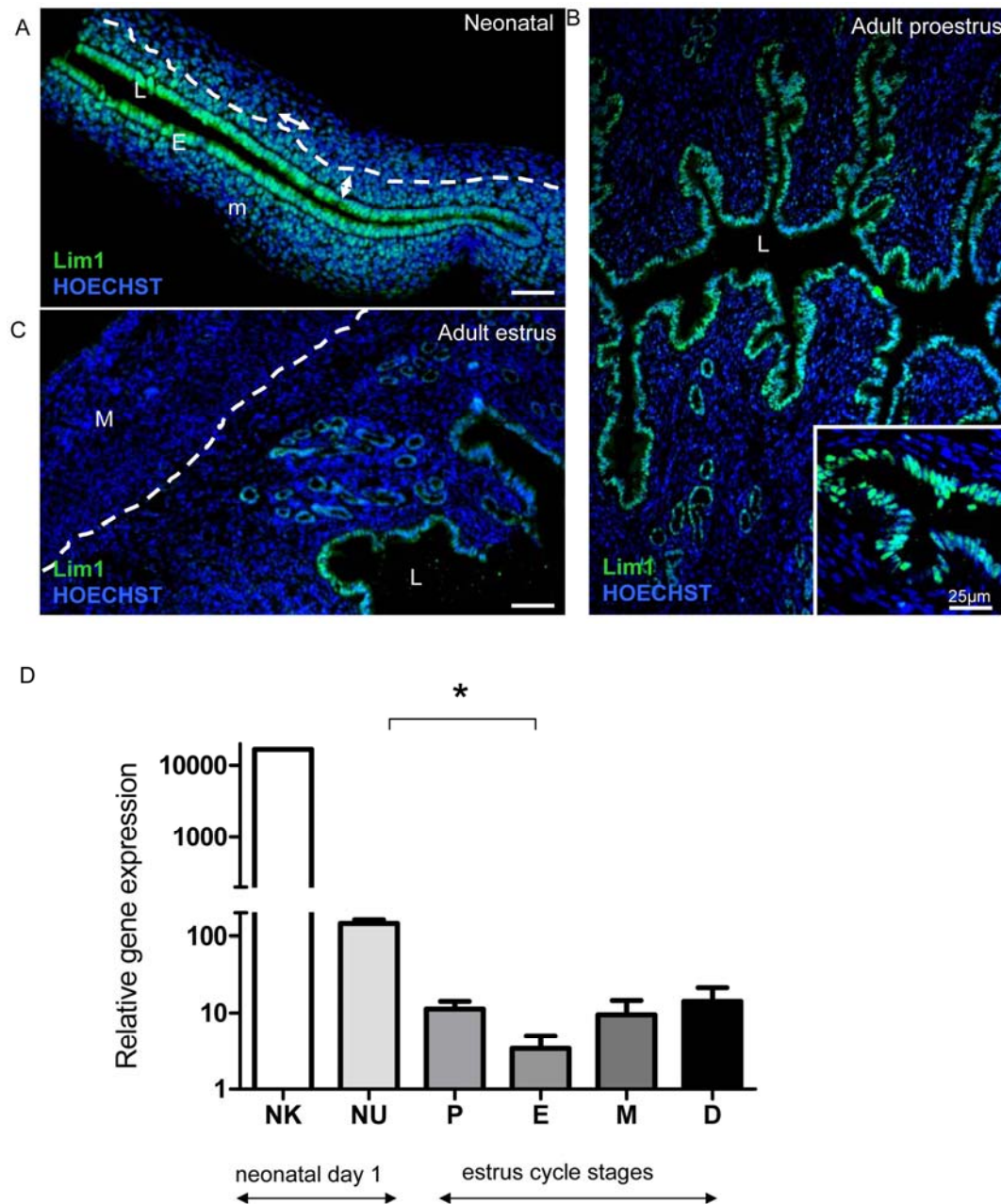


**Figure 4.3 *Lim1* expression in neonatal and adult mouse uterine tissue**

(A) Immunofluorescence photomicrographs of *Lim1*<sup>+</sup> endometrial epithelial and mesenchymal cells in a representative longitudinal section of the day 1 neonatal mouse uterine tissue (arrows indicate orientation of mesenchymal cells, dotted line show majority of the *Lim1*<sup>+</sup> cells are in the inner mesenchymal layer of the uterus). (B) Distribution of *Lim1*<sup>+</sup> cells in proestrus endometrium (inset shows higher magnification of endometrial glandular epithelium) (C) *Lim1*<sup>+</sup> cells in luminal and glandular epithelium but absent from the myometrium during estrus stage of the mouse cycle. (D) Real time PCR analysis of expression of *Lim1* in neonatal (Day 1) mouse kidney, and uterus, and in sexually mature adult uterus during the estrus cycle including proestrus (P), estrus (E), metestrus (M), and diestrus (D) relative to the housekeeping gene *Tbp*. Expression of target genes in kidney is included as a positive control for *Lim1* (data for uterine samples is presented as mean  $\pm$  s.e.m., n=4 per cycle stage asterix denotes p<0.05 for neonatal uterus (P1) vs estrus). **Abbreviations:** E, epithelium, L, lumen; m, mesenchyme; M, myometrium; NK, neonatal kidney; NU, neonatal uterus; Scale bars: 100 $\mu$ m



#### 4.3.4 LIM1 expression in human endometrial cancer tissue and cell lines

We further confirmed the expression of LIM1 in cultured normal human uterine epithelial cells as well as three human endometrial epithelial cancer cell lines (Figure 4.4A-D). We also observed that both Ishikawa and HEC1A cell lines had higher levels of LIM1 mRNA expression compared to ECC-1 although not statistically significant (Figure 4.4D). With limited samples, we confirmed *LIM1* mRNA expression in primary cancer samples (Supplementary Figure 4.5.2B). However, we did not detect LIM1<sup>+</sup> cells in any of the primary human endometrial cancer samples (data not shown, n=8).

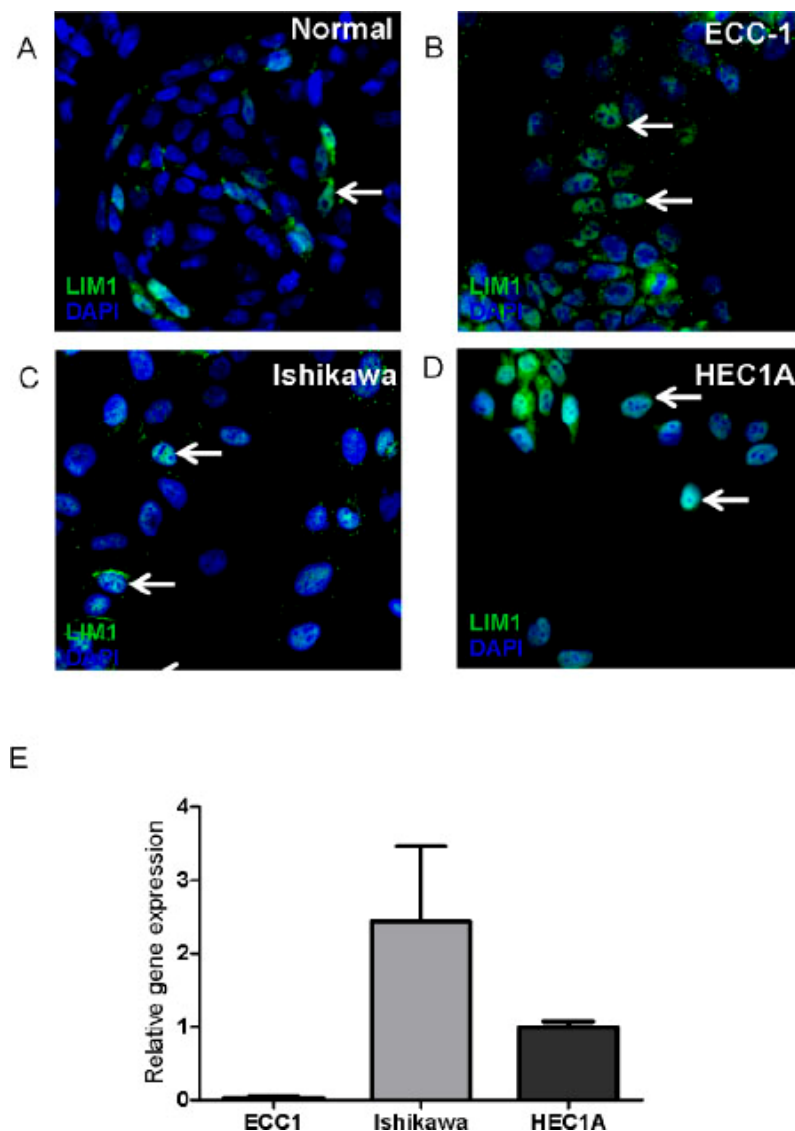


**Figure 4.4 LIM1 expression in human endometrial cancer cell lines**

(A-D) Representative photomicrographs showing the LIM1<sup>+</sup> cells in cultured normal human uterine epithelial cells and three cancer cell lines (arrows point at LIM1<sup>+</sup> nuclei). (E) Relative mRNA expression of *LIM1* in the cancer cell lines relative to the housekeeping gene *TBP* (Data is presented as mean±s.e.m., n=3 independent experiments).

## 4.4 Discussion

In the current study, we detected expression of the homeodomain transcription factor Lim1/LIM1 in developmental, postnatal, adult human and mouse endometrium. Furthermore, we demonstrated Lim1/LIM1 expression in human endometrial epithelial cancer cell lines.

The expression of LIM1 in the hESC-derived epithelium further confirmed the Müllerian identity of the epithelial duct like structures (surrounded by mouse endometrial stroma) demonstrated in our developmental model described in a previous study [311]. The diminishing level of LIM1<sup>+</sup> cells observed in the hESC-derived FRT epithelium is consistent with gradual decline of *Lim1* expression in the developing mouse Müllerian duct [10]. In the current study, we went a step further to characterise the expression of Lim1 in neonatal mouse uterus showing that its expression in endometrial epithelium and stroma coincides with postnatal epithelial development [25]. Furthermore, its expression in the inner layer of mesenchymal cells immediately adjacent to the epithelium suggests Lim1 may also be involved in mesenchymal cell fate specification and differentiation [24].

LIM1 expression has been demonstrated in normal adult human brain, kidney, tonsil, and thymus [306, 307]. An earlier study failed to detect *Lim1* in embryonic oviduct and adult mouse uterine tissue by Northern Blot analysis [58]. A subsequent study definitively demonstrated that *Lim1* was strongly expressed in the Müllerian ducts and its derivatives including embryonic oviduct and uterus [10]. In the current study we extend these findings and report the expression of Lim1/LIM1 in both adult mouse and human uterine tissue. We suspect the discrepancy observed between our study and the results described by the earlier study using Northern Blots may be attributed to differences in methodology.

Similar to other homeodomain transcription factors detected in neonatal and adult uterus [59, 60, 70], the persistent expression of Lim1/LIM1 in neonatal and adult endometrium suggests it may have a role in maintaining the organ's developmental plasticity during reproductive life. This plasticity is required since both the mouse and human adult endometrium undergo cyclical degeneration and regeneration during estrus/menstrual cycles. Recently, we and others have identified adult stem cells residing in the endometrium that may be responsible for its regenerative ability [143, 145, 146, 148, 320, 321]. LIM homeobox genes have been implicated

in the regulation of haemopoietic, testicular and hair follicle progenitor cells [305, 322-324]. It is possible that uterine Lim1/LIM1 is also involved in regulating endometrial stem/progenitor cells.

In addition to cyclical regeneration, extensive structural and functional differentiation also occurs in the endometrium during the window of implantation and early pregnancy. Coincidentally, the dynamic expression of Lim1/LIM1 observed in the current study suggests it may be involved in both regeneration of endometrium during the proestrus/proliferative stage of the cycle and tissue remodelling during mid/late secretory stage of the human cycle. The exact mechanisms that regulate Lim1/LIM1 expression in the endometrium is beyond the scope of the current study, although it is interesting to note that the pattern of Lim1/LIM1 expression observed in the current study parallels serum Activin A levels during the menstrual cycle [325]. Furthermore, high levels of Activin A have been reported in decidualized endometrial stromal cells during mid-late secretory stage of the menstrual cycle [113]. Given that *XLim/LIM1* has as an Activin A response element and can be upregulated by exogenous Activin A [230, 326, 327], we speculate that Activin A may regulate Lim1/LIM1 expression in the uterus.

A number of studies have reported LIM1 expression in human cancer cells including leukemic cells, renal carcinoma and ovarian cancer epithelial cells [306, 328, 329]. We also detected LIM1 expression in a number of uterine epithelial cancer cell lines and mRNA in primary cancer samples. However, we failed to detect LIM1<sup>+</sup> cells in primary human cancer tissue, possibly because protein expression in primary cancer samples may be regulated by an unknown posttranslational mechanism involving microRNAs (miRNAs). Recently, members of the miR-30 family have been identified amongst a list of upregulated miRNAs in endometrioid endometrial adenocarcinomas [330, 331]. Of interest, is that *XLim/Lim1* is negatively regulated by miR30a-p suggesting conservation of regulatory mechanisms across species and members of the miR-30 family may be involved in LIM1 regulation in human endometrial cancer cells [332].

In conclusion, we have demonstrated the expression of Lim1/LIM1 in human and mouse endometrial tissue at different stages of development, as well as in human primary and cancer epithelial cell lines. To our knowledge, this is the first report of Lim1/LIM1 expression in postnatal and adult FRT.



## 4.5 Supplementary Information

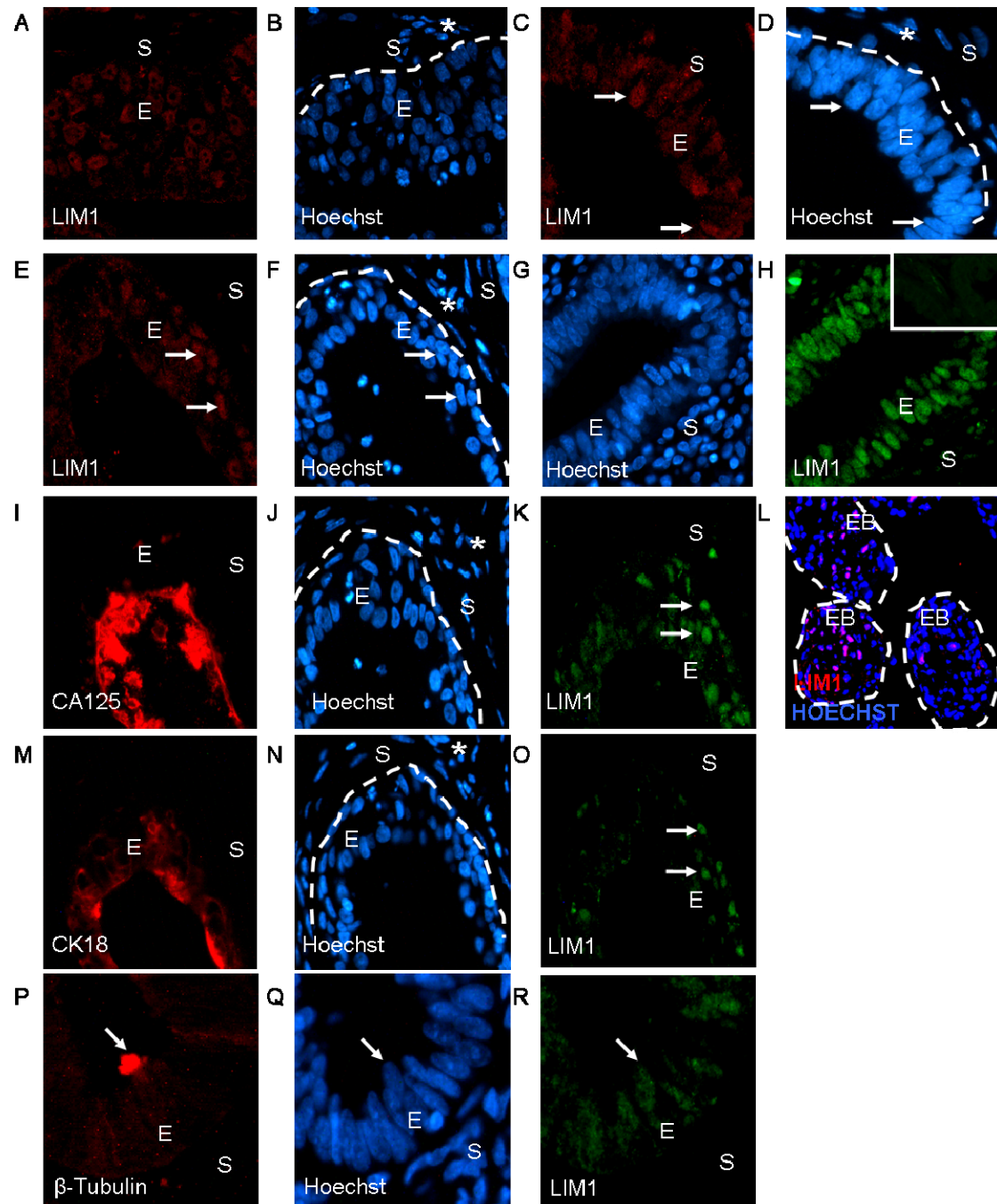
**Supplementary Table 4.5.1 Primary antibody**

Primary Antibody	Species	Clone	Dilution	Source	References
Anti- $\beta$ – Tubulin*	Mouse	TUB2.1	1:1000	Sigma-Aldrich	[311]
CA125 <sup>a</sup>	Mouse	OC125	1:200	Invitrogen	[311, 333]
CK18 <sup>a</sup>	Mouse	DC10	1:500	Dako	[311, 334]
Lim1 <sup>b</sup>	Rabbit	Polyclonal	1:200	Millipore	[307, 328, 335-337]

<sup>a</sup>**secondary antibody:** goat anti-mouse IgG<sub>1</sub>-AlexaFluor 568

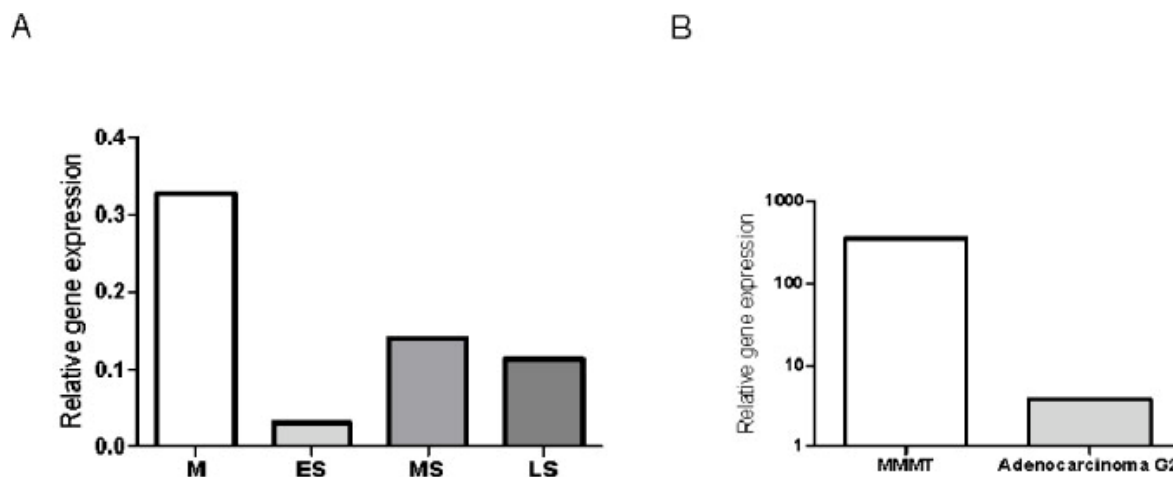
<sup>b</sup>**secondary antibody:** donkey anti-rabbit AlexaFluor 488 or donkey anti-rabbit AF 568 (Invitrogen)

\* primary antibody is CY3 conjugated



#### Supplementary Figure 4.5.1

(A-K, M-R) images of individual channels of the merged fluorescent images shown in Figures 1 and 2 (arrows from A-K, O point to LIM1<sup>+</sup> cells) (A-B) are images of individual channels of the merged image in Figure 1A (arrows point to LIM1<sup>+</sup> cells). (C-D) images of individual channels of the merged image in Figure 1B. (E-F) images of individual channels of the merged image in Figure 1C. (G-H) images of individual channels of the merged image in Figure 2B, inset in (H) represent a negative control section stained with rabbit IgG. (I-K, M-O) images of individual channels of the merged image in Figures 1I and 1F respectively. (L) merged image of positive control tissue. (P-R) images of individual channels of the merged image in Figure 2G (arrows point to a ciliated LIM1<sup>+</sup> cell). Asterisk in (B, D, F, J, N) indicate areas of mouse stromal cells with speckled nuclei. **Abbreviations:** EB, embryoid body; CA125, Cancer Antigen 125; E, epithelium; S, stroma.

**Supplementary Figure 4.5.2**

(A) Real time PCR analysis of *LIM1* expression in 4 samples of premenopausal normal human endometrial tissue relative to the housekeeping gene *TBP*. (B) Real time PCR analysis of *LIM1* expression in 2 samples of human endometrial cancer relative to the housekeeping gene *TBP*. **Abbreviations:** ES, early secretory; G2, Grade 2; LS, late secretory; M, menstrual; MS, mid-secretory; MMMT, malignant mixed Müllerian tumour.

## CHAPTER 5 Identification of mesenchyme-derived growth factors directing hESC differentiation

### 5.1 Introduction

Vertebrate embryo studies have demonstrated the complexity of organogenesis during development which relies heavily on finely orchestrated interactions between neighbouring cells and tissues. This interaction between different cell types is maintained in differentiating embryonic stem cells *in vitro* [238]. In order to generate clinically relevant cells and tissues from human embryonic stem cells (hESCs), various differentiation strategies have been devised to mimic embryogenesis. Conventionally, a cocktail of growth factors is added *in vitro* to stimulate differentiation of hESC towards a particular lineage. This approach generated a long list of cell types representing all three germ layers *in vitro* [164, 165, 168, 169, 171, 172, 338].

Other methods involve co-culturing hESC with mouse stroma or feeder layers derived from other cell types. For instance, mouse embryonic fibroblasts (MEF) interact with hESC to prevent hESC differentiation and maintain their pluripotency [217]. Various stromal niches induce mesoderm lineage specific differentiation. For example, mouse stromal cell lines S17, OP9, and the yolk sac endothelial cell line C166 and human bone marrow stromal cells induced haematopoietic-like cells from embryonic stem cells (ESCs) [339-341]. In addition, mouse visceral endoderm-like cells (END2) and bone marrow stromal cells directed differentiation of hESC to become cardiomyocytes [166, 342]. Murine OP9 stromal cells induced hESC to form mesenchymal precursors that gave rise to a number of connective tissue types [283].

ESC co-cultured with stromal cells also produce endodermally and ectodermally derived cell types. For instance, co-culture of mouse embryonic stem cells (mESC) with embryonic pulmonary mesenchyme generated pulmonary epithelial cell types [283]. Co-culture of hESC with a bone marrow-derived mouse stromal cell line (PA6) induced dopaminergic (DA) neurons [343]. Recently non-stromal feeder layers have also induced differentiation of ESC to form retinal epithelial cells [344].

There have been attempts to identify the soluble factors provided by mesenchyme/stroma that direct ESC differentiation. Bone marrow stromal cells (BMSC) have been screened for secreted

products using ELISA [345]. A more recent study used a microarray approach to interrogate the PA6 cell line for molecules important for induction of dopaminergic (DA) neurons [346]. Whilst several studies have shown the inductive capacity of neonatal mouse uterine mesenchyme (nMUM), none have identified specific growth factors involved in the process of induction [19, 22, 128]. However, a number of mesenchyme-derived growth factors and signalling molecules from both Wnt and TGF- $\beta$  families have been identified in nMUM which have roles in endometrial adenogenesis during postnatal development [26, 50, 52, 104, 106]. Collectively, these studies suggest that nMUM secretes morphogens that are also important during embryogenesis.

It has been shown previously that nMUM and hESC formed a heterospecific/heterotypic recombinants *in vitro* in Chapter 3 [311]. The nMUM induced the formation of primitive streak-like cells. In light of these findings, the aim of the current study was to use gene profiling approach to identify genes in nMUM coding for growth factors that may direct differentiation of hESC.

## **5.2 Methods**

### **5.2.1 Animals**

Animals were obtained from Monash Animal Services. Day 1 nMUM and epithelium were obtained from female C57BL/6JAsmu (F1) mice. All animal handling and procedures were carried out in accordance with National Health and Medical Research Council of Australia guidelines for the Care and Use of Laboratory Animal Act and approval was obtained from the Monash University Animal Ethics Committee at Monash Medical Centre – A (MMC-A), Clayton, Australia. The approval numbers are 2006/44 and 2010/41.

### **5.2.2 Tissue Recombination, RNA extraction and Microarray**

Experimental workflow of the current study is illustrated in Figure 5.1. ENVY hESCs were purchased from Stem Core (Australian Stem Cell Centre, Monash University). nMUM dissection, tissue recombination and embryoid body (EB) formation were performed as previously described under serum-free conditions [311]. The purity of separated nMUM (without epithelial contamination) was assessed by reverse transcription-polymerase chain reaction (RT-PCR) using calbindin-D28k, primers from a previous study [26]. For some experimental conditions, growth factors (BMP4, 50 ng.ml<sup>-1</sup>, ACTIVIN A 20ng.ml<sup>-1</sup>) were included in the culture medium. Each sample for microarray experiments consisted of a pool of 50-60 individual recombinants or mesenchyme(s) (consisted of two 0.5mm pieces in each well, up to 100 pieces altogether), cultured for 2 or 6 days at 37°C 5% O<sub>2</sub>. The hESC cells were micro-dissected from the mesenchyme in recombinant samples with a 30-gauge needle. It is possible that some hESC remained attached to the mesenchyme. All samples were incubated in TrypLE Select (Invitrogen) for 30 minutes at 37°C then disaggregated by mixing, and digested completely with Lysis Solution provided with the RNA extraction kit (Ambion, Applied Biosystems, CA). Following RNA extraction, DNase treatment was performed to eliminate contaminating genomic DNA using RNaqueous Micro DNase Treatment Kit (Ambion, Applied Biosystems). The quantity of the RNA was checked using a Nanodrop Spectrophotometer ND-1000 in conjunction with ND-1000 V3.3.1 computer software (Thermofisher Scientific). A total of 1µg of total RNA (per sample, n=12 samples) were sent to Australian Genome Research Facility (AGRF) for

quality assurance. Illumina platform was used to process the Mouse Sentrix WG6 v2.0 Beadchip. The procedure was carried out by staff at the AGRF and raw data were recorded onto a disc.

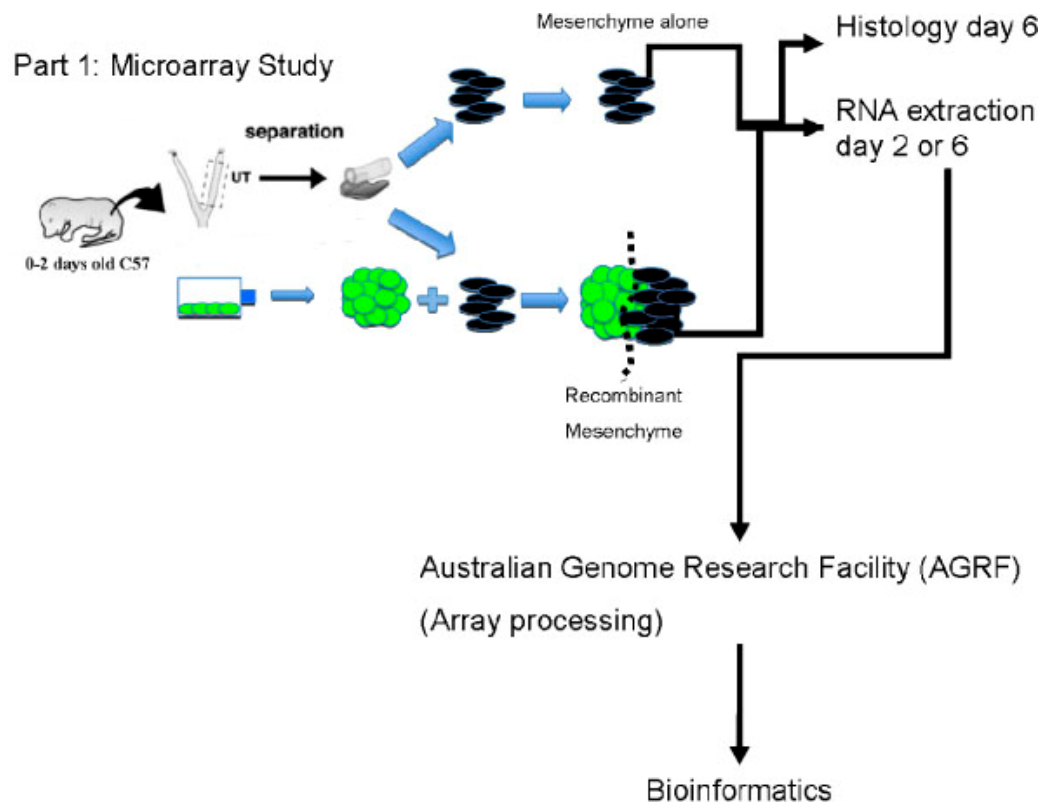


**Figure 5.1 Schematic diagram of experimental design: Part 1**

Recombinants were made by combining ENVY EBs (3000 cells) with two 0.5mm nMUM. Two sample types were harvested for RNA extraction 1) recombinant nMUM dissected from the recombinant (n=3 on day 2, n=3 on day 6) 2) nMUM cultured alone (n=3 on day 2, n=3 on day 6). All samples were sent to AGRF for further quality assurance and processing (n = 12) and raw data returned to Monash University for bioinformatics.

### 5.2.3 Microarray analysis

Raw array data analysis was performed with assistance from Dr. Kara Britt (Department of Anatomy and Developmental Biology, Monash University). Raw data was assessed in Genome Studio (Illumina) for array controls and then exported to R for further analysis using the Lumi Bioconductor package especially designed to process the Illumina microarray data [347]. Data was read using LumiR, background corrected using LumiB, transformed using variance-stabilizing transformation (VST) LumiT and then robust spline normalized (RSN) using LumiN [347]. Flagged data was removed and then differential gene expression was assessed using SAM analysis with a false discovery rate of 10%. Following SAM analysis, two lists were generated

including genes that changed between day 2 and day 6 in two experiment groups; recombinant mesenchyme or mesenchyme alone (ie. up in day 2 or up in day 6).

#### 5.2.4 Gene ontology (GO)

The enriched GO terms for recombinant mesenchyme or mesenchyme alone between day 2 and 6 was determined by uploading the combined gene list for each group individually on the Database for Annotation, Visualisation, and Integrated Discovery (DAVID) (<http://david.abcc.ncifcrf.gov>) and analysed according to published methodology [348, 349]. GO terms associated with biological process (GO-BP), molecular function (GO-MF) and cellular component (GO-CC) were all considered for analysis. Statistical significance of the GO terms was established by Fishers Exact T test. GO terms with p values <0.05 were considered statistically significant

#### 5.2.5 PCR

Approximately 200ng to 1µg of total RNA was reverse transcribed to first strand cDNA with Oligo-DT primers using Superscript III reagents in the presence of an RNase Inhibitor (Invitrogen). PCR reactions were run in triplicates with primers using SYBR Green master mix (Applied Biosystems), alternatively, Taqman gene expression probes (for genes including human specific *MIXL1*, *GSC*, *OSR1*, *GAPDH*) were used with Taqman Gene Expression master mix (Applied Biosystems) on the 7900 HT Fast Real-Time PCR system absolute thermal cycler with software from Applied Biosystems or Veriti Thermal Cycler (Applied Biosystems) for conventional PCR. Previously published primers were used in the current study [26, 350, 351]. A list of primer sequences can be found in Supplementary Table 3.5.2. The comparative cycle threshold (Ct) method was used to analyse data. Gene expression levels were compared to the reference gene (REF), glyceraldehyde-3-phosphate dehydrogenase (GAPDH). Since gene expression is inversely proportional to the Ct, the expression of the target gene relative to GAPDH was calculated according to previously described formula below [311].

$$\text{Gene expression} \propto \frac{1}{2^{C_t(\text{Gene}-\text{REF})}}$$



For purposes of presentation, calculated values normalised to GAPDH were multiplied by 1,000. For CTGF blocking experiments, results were calculated using the  $\Delta\Delta C_t$  method using rabbit IgG treated EBs as the calibrator (which had an arbitrary value of 1).

### **5.2.6 Immunohistochemistry**

All EBs were harvested and fixed overnight in 4% paraformaldehyde (PFA) then processed and paraffin embedded. 3  $\mu\text{m}$  serial sections were cut for immunohistochemistry. Sections were deparaffinized and hydrated through xylene and graded alcohols. Sections were stained with a rabbit polyclonal antibody specific for CTGF (1:200, Abcam). Endogenous peroxidase activity was blocked with 3%  $\text{H}_2\text{O}_2$  in methanol for 10 minutes at room temperature followed by 3 rinses with PBS. Protein Block was applied to minimise non-specific antibody binding (Serum-free protein block, DAKO, Denmark) for 10 minutes at room temperature. Concentration matched IgG isotype negative controls were included in each staining run. Following overnight incubation with primary antibodies at 4°C in a humidified chamber, slides were washed with PBS, and incubated with Alexa Fluor 488 goat anti-rabbit secondary antibody (1:200, Invitrogen) at RT for 30 minutes. Hoechst 33258 staining was performed for 30 seconds (Molecular Probes, Eugene, Oregon, USA). Fluorescent images were taken with a Leica DMR upright fluorescence microscope (Leica Microsystems, Mannheim, Germany). Individual color images were merged using Image J analysis software.

### **5.2.7 Statistical Analysis**

Statistical analysis was performed using GraphPad Prism (version 5.00 for Windows, GraphPad Software, San Diego CA, USA). Statistical differences were assessed by t-test (Mann-Whitney) and one-way ANOVA (Kruskal Wallis) with Dunnett's post test.

## 5.3 Results

### 5.3.1 Genes upregulated in mesenchyme during hESC differentiation

Previously, it was demonstrated that nMUM upregulated *MIXL1* expression in differentiating hESCs between days 3-7 *in vitro* [311]. Therefore, differentially upregulated genes in the nMUM during this incubation time may be involved in directing hESC differentiation, particularly genes coding for soluble growth factors. Total RNA was collected from the nMUM in recombinant samples (hereafter referred to as recombinant nMUM) cultured *in vitro* for 2 and 6 days (n=3 per time point). In addition, total RNA was also collected from cultured mesenchyme (nMUM alone) samples for comparison with recombinant nMUM to assess any influence hESC may have had in directing the nMUM to secrete unique growth factors.

Samples belonging to each group (Recombinant nMUM or nMUM alone) were placed on two separate Illumina Mouse WG-6 expression chips (6 samples per group, 2 time points). Euclidian distance hierarchical clustering of samples showed that the largest differences in gene expression occurred between day 2 and day 6 rather than between experimental groups tested (Figure 5.2). It should also be noted that variation existed within the experimental groups which may explain the lack of significant differences between sample types (ie. between recombinant nMUM and nMUM alone). Comparison between day 2 and 6 recombinant nMUM showed that 364 genes were upregulated assuming 10% false discovery rate (FDR) (Table 5.1). Similarly, 486 genes were upregulated between day 2 and 6 in mesenchyme cultured alone.

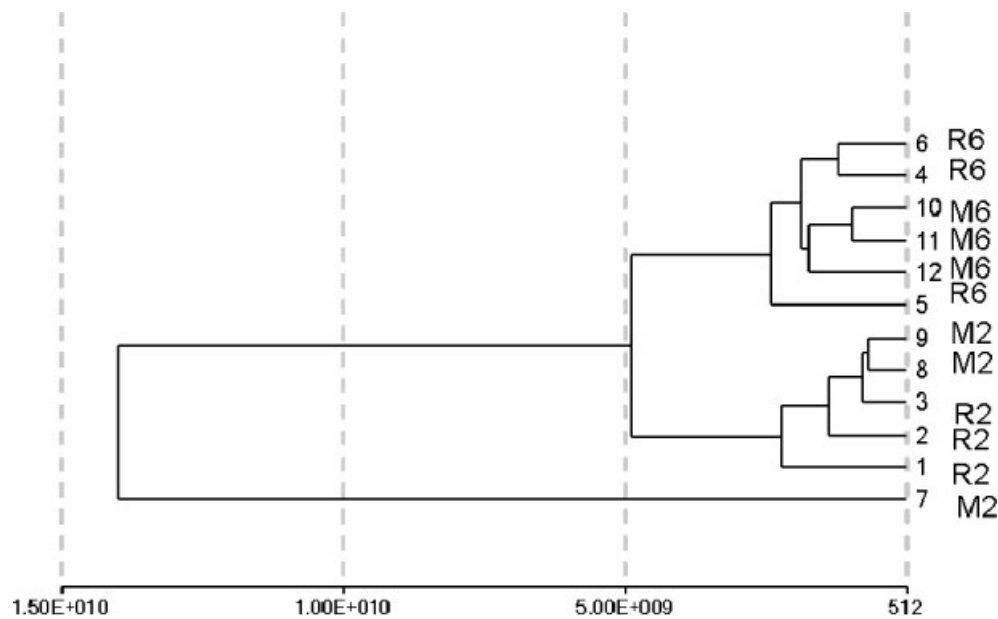


**Figure 5.2 Euclidian distance hierarchical clustering of samples**

Euclidian distance for 12 samples including recombinants nMUM and nMUM alone *in vitro*, each sample was assigned with a number (1-9). Abbreviation: M2, nMUM day 2; M6, nMUM day 6; R2, recombinant day 2; R6, recombinant day 6.

Gene Ontology (GO) pathway analysis was carried out to identify groups of genes (as defined by Gene Ontology) related to growth factors, extracellular matrix and cell differentiation from upregulated genes in recombinant nMUM or nMUM alone between day 2 and 6 (Table 5.2, Supplementary Table 5.5.1-showing only growth factor category). Despite the number of genes associated with these GO terms, only Connective Tissue Growth Factor (Ctgf) was selected as a potential factor involved in MIXL1 induction and hESC differentiation for several reasons, these include low FDR (<5%), greater than 2-fold change, relevant function in embryogenesis, as well as cellular location (Table 5.2). Other growth factors commonly found in early embryogenesis and uterine adenogenesis were not differentially expressed in either of the recombinant nMUM or nMUM alone groups. Quantitative real-time PCR was performed to confirm microarray gene expression changes using a mouse specific Ctgf primer. The fold-change in recombinant nMUM sample detected by RT-PCR was consistent with microarray data, although not statistically significant (Figure 5.3A). Ctgf protein expression in day 6 recombinant nMUM was further confirmed by immunofluorescence using Ctgf specific antibody which showed that Ctgf was found in both the nMUM as well as differentiating hESC (Figure 5.3B).

**Table 5.1 Number of differentially upregulated genes between time points**

	<b>Genes upregulated on Day 2</b>	<b>Genes upregulated on Day 6</b>	<b>FDR</b>
Mesenchyme (Day 2 vs Day 6)	139	347	10%, n=3 per group
Recombinant (Day 2 vs Day 6)	221	143	10%, n=3 per group

**Table 5.2 Candidate mouse genes expressed in Gene Ontology terms associated with growth factors, proteinaceous extracellular matrix and cell differentiation**

<b>Accession</b>	<b>Gene Symbol</b>	<b>Fold Change</b>	<b>FDR%</b>	<b>Description</b>
<b>Growth factor activity (GO:0008083) p &lt; 0.003</b>				
NM_011118.1	Prl2c3	6.90	1.73	prolactin family 2, subfamily c, member 3
NM_010217	Ctgf	4.18	4.48	connective tissue growth factor
	Ogn	11.66	6.91	osteoglycin
NM_00870.4				
NM_031191.1	Prl2c2	5.19	9.75	prolactin family 2, subfamily c, member 2
<b>Proteinaceous extracellular matrix (GO:0005578) p&lt; 0.0004</b>				
NM_010217	Ctgf	4.18	4.48	connective tissue growth factor
NM_009931.1	Col4a1	1.60	7.06	procollagen, type IV, alpha 1
NM_008760.2	Ogn	11.66	6.91	osteoglycin
XM_131451.2	Adamtsl1	1.45	5.09	ADAMTS-like protein 1
NM_021355.2	Fmod	1.16	6.50	KSPG fibromodulin
NM_019922.1	Crtap	1.32	9.54	cartilage associated protein
<b>Cell Differentiation (GO:0030154) p &lt; 0.001</b>				
AK077498	Robo1	1.24	2.57	roundabout homolog 1
AK078589	Sema3c	1.16	3.01	semaphorin-3C
NM_011145.3	Ppard	1.42	3.07	peroxisome proliferator activator receptor delta
NM_008597.3	Mgp	1.47	4.09	matrix Gla protein
NM_010217	Ctgf	4.18	4.48	connective tissue growth factor
NM_019867	Ngf	1.11	4.89	intraflagellar transport 81 homolog (Chlamydomonas)
NM_007921.1	Elf3	5.96	7.31	E74-like factor 3
NM_009879.2	Ift81	1.32	10.64	carnitine deficiency-associated gene expressed in ventricle 1

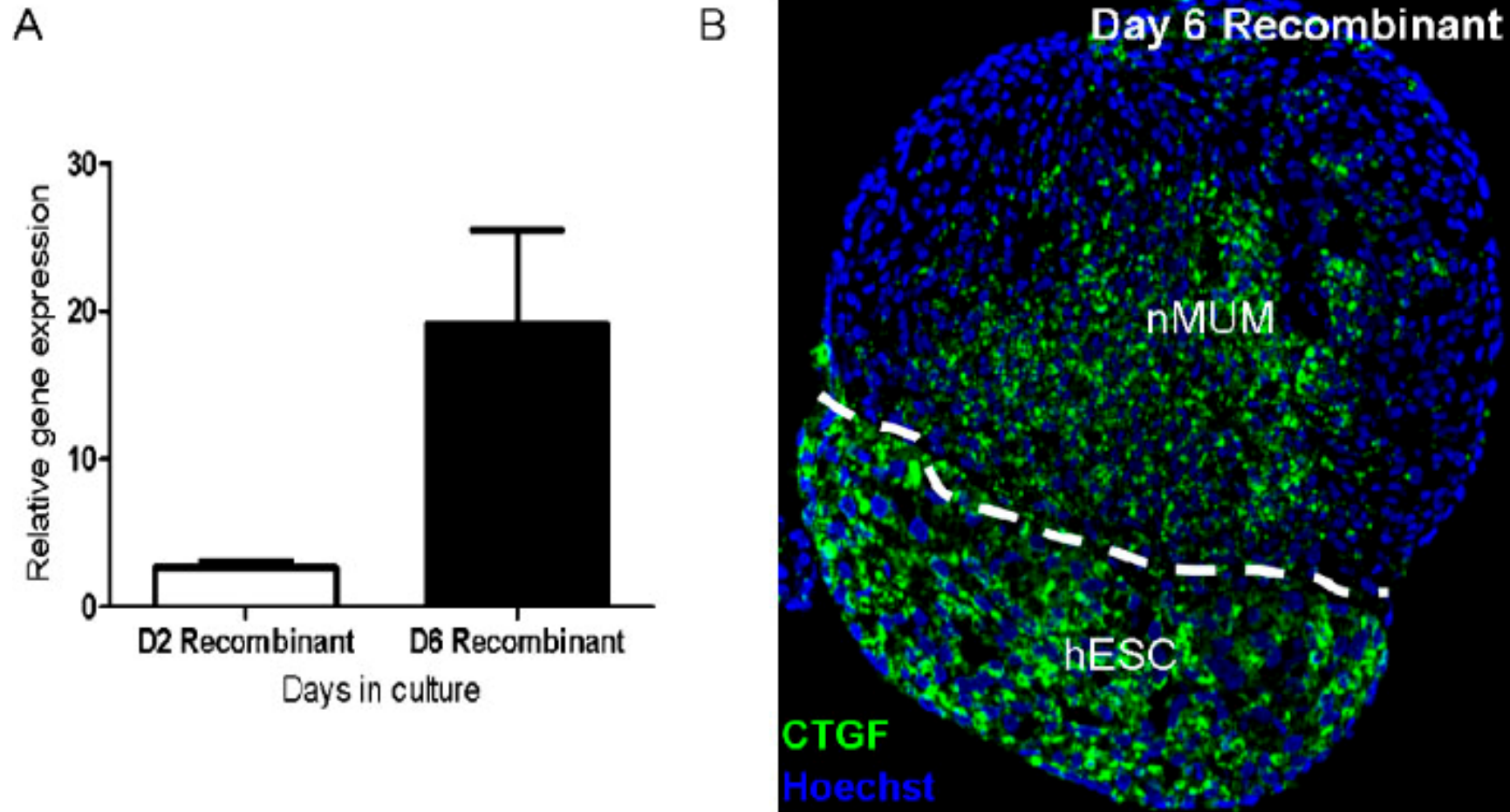


**Figure 5.3 Expression of CTGF in recombinant mesenchyme**

(A) Real time PCR analysis of *Ctgf* expression in recombinants on day 2 and day 6 relative to GAPDH (Data is presented mean $\pm$ s.e.m., n=3 per time point). (B) Expression of CTGF in day 6 recombinants (dotted lines marks the boundary between nMUM and hESC).

### 5.3.2 Endogenous CTGF is expressed in hESC derived embryoid body

The expression of CTGF in human developmental tissue has not been reported previously, however, *Ctgf* is found in embryonic mesoderm and endoderm of the developing murine embryo [100, 352]. Before examining the effects that exogenous *Ctgf* may have on hESC differentiation, the expression of endogenous CTGF in hESC derived embryoid bodies (EB) was assessed. The experimental workflow for the experiments that will be described in this section and 5.3.3 is illustrated in Figure 5.4.

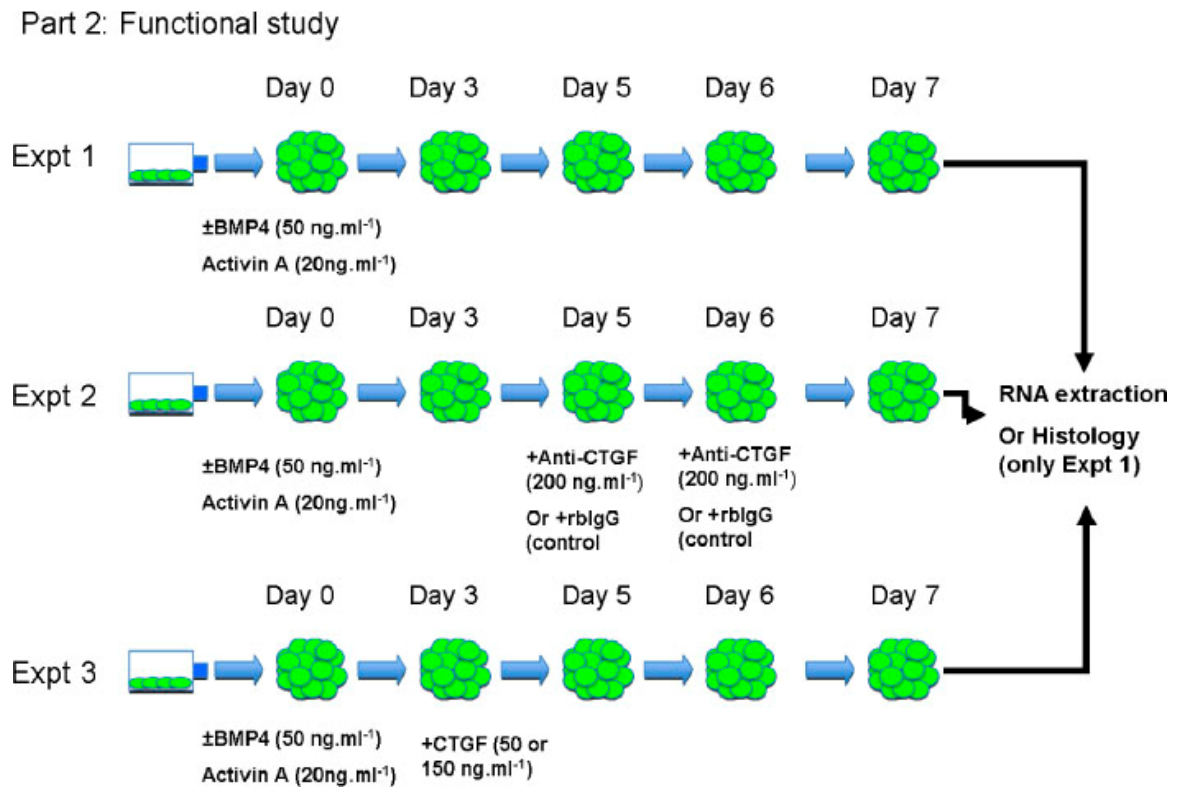


**Figure 5.4 Schematic diagram of experimental design: Part 2**

Investigations into the role of CTGF on hESC differentiation was separated into three different experiments. Experiment 1 (Expt 1) was designed to investigate endogenous CTGF in differentiating EBs. Experiment 2 (Expt 2) was performed to block endogenous CTGF in differentiating EBs. Experiment 3 (Expt 3) was completed to assess the influence exogenous CTGF had on hESC differentiation. Each experiment included untreated control groups (Expt 2 had rbIgG treated EBs as control group). Samples from Expt 2 and 3 were not collected for histology.

It was previously shown that MIXL1 induction in hESC was achieved by treatment with recombinant human BMP4 and Activin A as early as day 2 *in vitro* (Chapter 3) [311], consistent with other studies [204, 265]. In the current study, endogenous CTGF mRNA expression gradually decreased during MIXL1 induction suggesting that CTGF had little or no role in the formation of primitive streak-like cells in differentiating hESCs (Figure 5.5A. As demonstrated

previously, following the transient upregulation of *MIXL1* in differentiating EB (treated with BMP4, 50 ng.ml<sup>-1</sup>, ACTIVIN A 20ng.ml<sup>-1</sup>), there was gradual up-regulation of the mesodermal gene *OSR1* in differentiating hESC. The gradual increase in *OSR1* mRNA expression was confirmed and coincided with an increase in *CTGF* mRNA expression in growth factor treated group compared to the control group although not statistically significant (Figure 5.5A). Immunofluorescence demonstrated unequivocally that CTGF expression is found in the growth factor treated EBs but not controls (Figure 5.5B). Furthermore, *MIXL1* induction appears to be a pre-requisite for CTGF production by differentiating hESCs. Although, endogenous CTGF does not appear to be involved in *MIXL1* induction, it may have a role in mesoderm formation consistent with its localisation in embryonic mesoderm [100, 352].

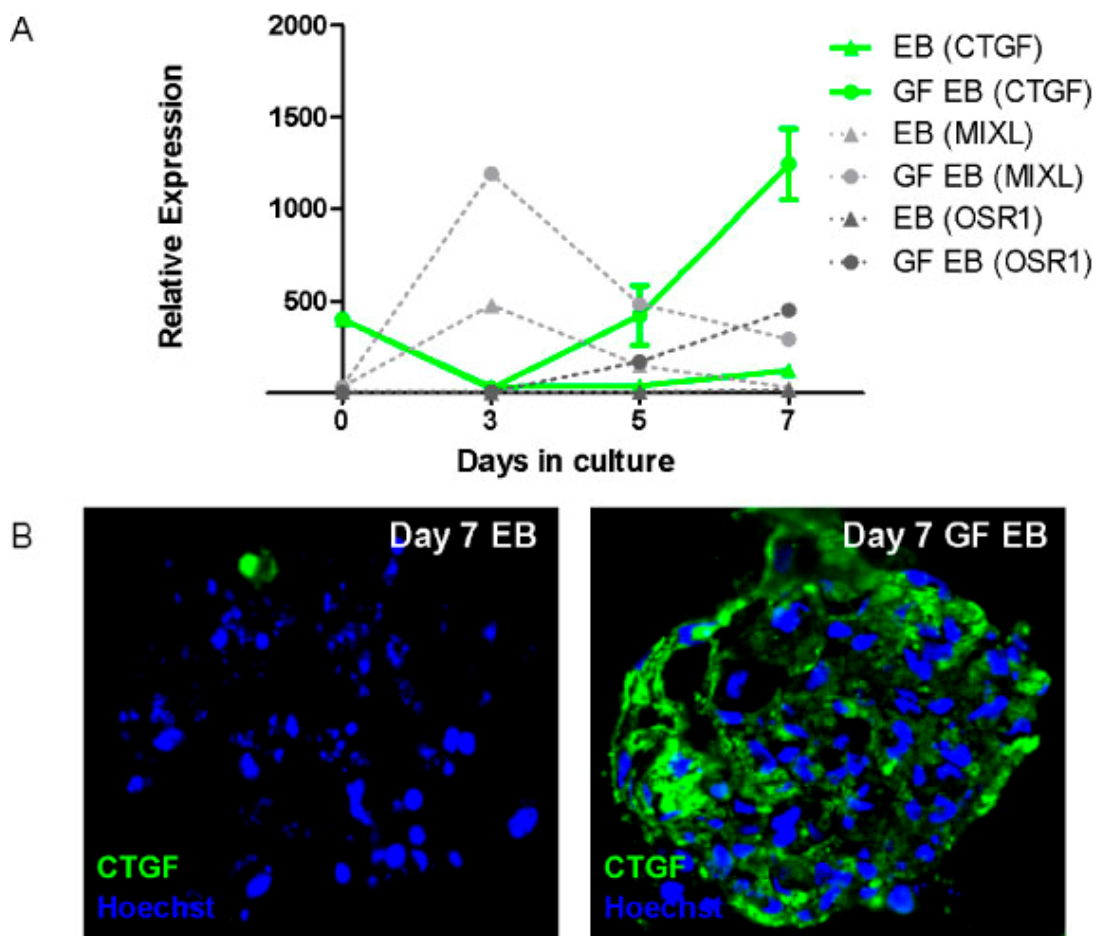


**Figure 5.5 Endogenous expression of CTGF in differentiating EBs**

(A) Real time PCR analysis of CTGF expression in growth factor treated EB versus untreated EB across time on days 0, 3, 5 and 7 relative to GAPDH. Expression of target genes in undifferentiated hESCs is indicated as day 0 of differentiation (Data for CTGF is presented as mean±s.e.m., n=3 independent experiments, statistical significances were not found, data for MIXL and OSR1 represent values from a single experiment for illustration purpose only, the expression level of MIXL and OSR1 is multiplied by 100,000 for illustration purpose). (B) Immunofluorescent expression of CTGF in untreated EB and growth factor treated EB on day 7.

Several studies have shown that anti-CTGF antibody inhibits CTGF activity *in vitro* [353-355]. Therefore, it was hypothesized that blocking CTGF with neutralising rabbit anti-CTGF antibody (200 ng.ml<sup>-1</sup>, Abcam) after MIXL1 induction may reduce mesodermal gene expression. Furthermore, since vertebrate primitive streak undergoes epithelial-mesenchymal transition (EMT) to form mesoderm and endoderm, it was hypothesized that several EMT related genes would also be down-regulated following treatment with anti-CTGF antibody [356]. EMT related genes were also included to assess the effectiveness of the anti-CTGF antibody treatment since previous studies have demonstrated the upregulation of EMT related genes following exogenous treatment with CTGF [357].

Since mesendoderm formation (marked by MIXL1 induction) may be a pre-requisite for the production of endogenous CTGF in differentiating hESC, EBs were treated on day 0 with 50 ng.ml<sup>-1</sup> BMP4, and 20ng.ml<sup>-1</sup> ACTIVIN A prior to addition of the neutralising CTGF antibody on both days 5 and 6 (Figure 5.4). The concentration of anti-CTGF antibody used in the current study was similar to a previous report [355]. Control samples were treated with rabbit IgG at a matching concentration to the neutralising rabbit anti-CTGF. RNA was harvested from EBs on day 7.

Real time quantitative PCR was performed to assess the expression of a mesoderm gene, *OSR1*; an endoderm gene, *GSC*; and a number of EMT related genes (*SNAI1*, *SLUG*, *VIMENTIN* and *ECAD*). Comparisons were made between control (EBs pre-treated with BMP4/ACTIVIN A on day 0, and then rabbit IgG on days 5 & 6) and experiment group (EBs pre-treated with BMP4/ACTIVIN A on day 0, and then polyclonal rabbit anti-CTGF antibody on days 5 & 6). A small increase in *GSC* expression coincides with a decrease in *OSR1*, and EMT related genes *SLUG*, *SNAI1* and *VIM* (not statistically significant) was observed suggesting that CTGF may be involved in the process EMT and mesoderm formation in differentiating EBs (Figure 5.6) [100, 352, 357].



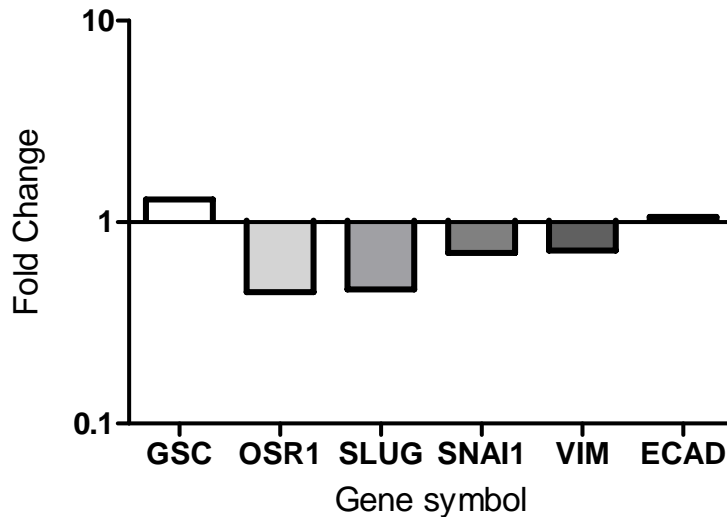


**Figure 5.6 Fold change of in gene expression in differentiating EBs following anti-CTGF antibody treatment**

Real time PCR analysis of expression of EMT (SLUG, SNAI1, VIM, ECAD), mesoderm (OSR1) and endoderm (GSC) related genes in growth factor treated EBs (BMP4, 50 ng.ml<sup>-1</sup>, ACTIVIN A 20ng.ml<sup>-1</sup> on day 0) followed by treatment with anti-CTGF antibody (200ng.ml<sup>-1</sup> on days 5 & 6) on day 7 of EB differentiation. The expression is relative to the calibrator (control group) which has an arbitrary value of 1 (Data is presented as mean from 2 independent experiments)

### 5.3.3 Role of exogenous CTGF on EB differentiation

To assess the role of exogenous CTGF on hESC differentiation, recombinant human CTGF (50 or 150 ng.ml<sup>-1</sup>, Invitrogen) was added to both BMP4/ACTIVIN A treated or untreated EB cultures on day 3 (when *MIXL1* expression in growth factor treated hESC is reduced, marking the end of primitive streak formation in EBs, Figure 5.5A, and Chapter 3-Figure 2) (Figure 5.4). Two concentrations of CTGF previously considered biologically active were used in the current study to detect a dose response from CTGF treatment [357, 358].

Several studies have shown that significant increase in the expression of *OSR1*, *GSC* and EMT related genes is achieved by addition of BMP4/ACTIVIN A to differentiating EBs [229, 265, 270, 311]. In the absence of these growth factors, hESC tend to remain undifferentiated or spontaneously commit to ectodermal lineages. In the current study, higher concentration of CTGF (150 ng.ml<sup>-1</sup>) failed to increase the expression *OSR1*, *GSC*, EMT related genes (SLUG, SNAI1, VIMENTIN) to the same level as that observed in growth factor treated groups at both time points (Figure 5.7). CTGF alone was comparable to the untreated EB culture indicating that CTGF alone was unable to induce differentiation of mesendodermal lineage consistent with the

previous results section (5.3.2). In contrast, both concentrations of CTGF (50 or 150 ng.ml<sup>-1</sup>) added into EB cultures pre-treated growth factors slightly increased expression of *SLUG*, *SNAI1*, *VIM*, *ECAD*, and *OSR1* gene whilst decreasing *GSC* in growth factor treated hESC on both days 5 and 7 compared to GF treated EBs (not statistically significant) in a dose dependent manner consistent with a previous report (Figure 5.7) [358]. It must be noted that there is an increase in *ECAD* expression similar to a previous study where CTGF induced partial EMT and temporarily increased *ECAD* expression [357]. These results suggest that CTGF may play a role in EMT induction and mesodermal formation during hESC differentiation.

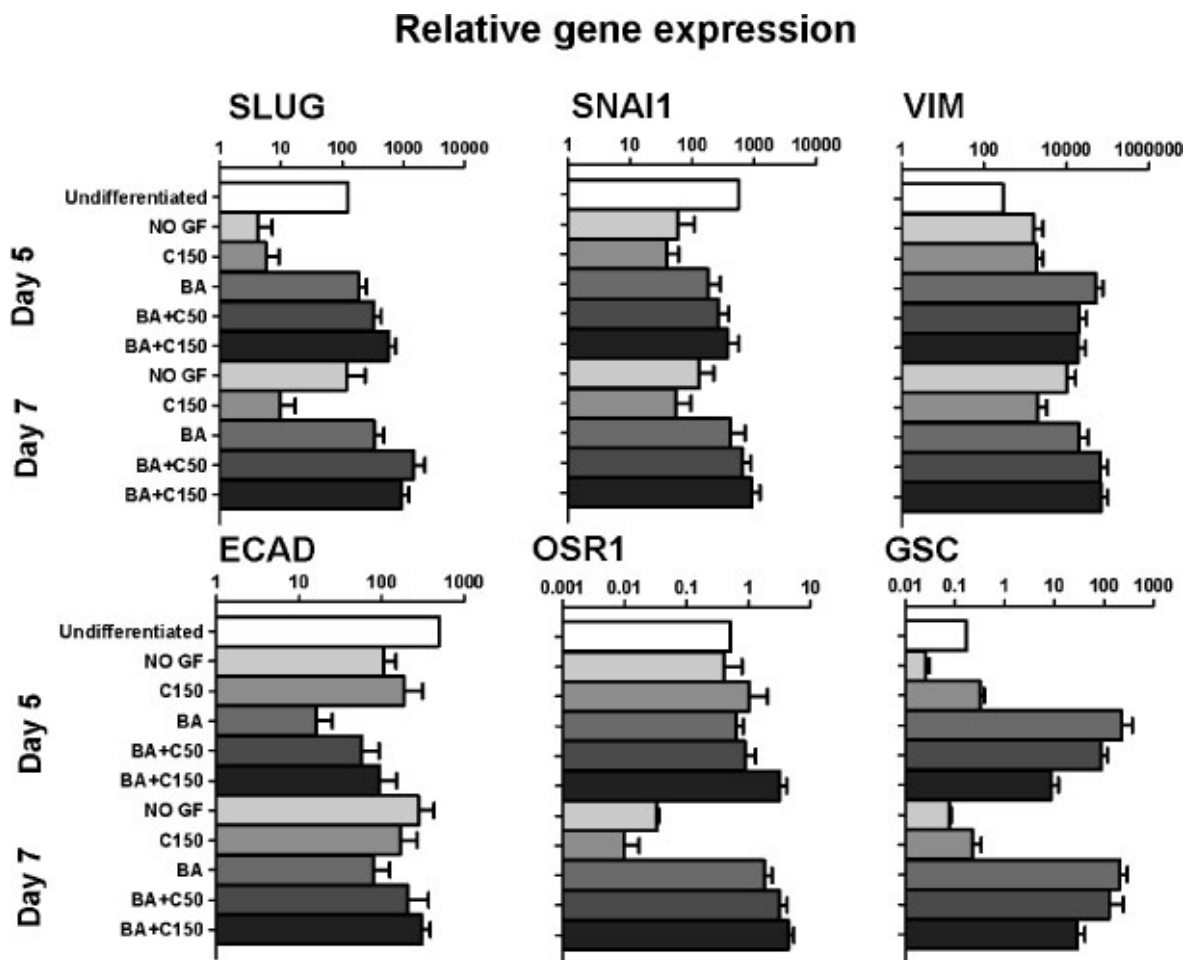


**Figure 5.7 Gene expression of differentiating EBs following treatment with CTGF**

Real time PCR analysis of expression of EMT, mesoderm and endoderm genes in differentiating hESC following treatment with various combinations of growth factors on day 5 and 7 relative to GAPDH. Expression of target genes in undifferentiated hESCs was from day 0 of differentiation (Data for samples on days 5 and 7 are presented as mean±s.e.m., n=3 independent experiments, statistical significances were not found). **Abbreviations:** BA, Bmp4/Activin A; C, CTGF; GF, growth factor

## 5.4 Discussion

In the current study, gene profiling of the inductive nMUM revealed Ctgf as a mesenchyme-derived growth factor that may have a role in mesendoderm differentiation of hESC. CTGF was also localised in differentiating human EBs for the first time. Furthermore, exogenous CTGF may induce EMT and mesoderm differentiation in hESC derived EBs.

### 5.4.1 Genes coding for mesenchyme-derived growth factors

In ESC differentiation systems, the addition of ligands from TGF- $\beta$  and Wnt families induced primitive streak-like cell formation *in vitro* [238, 265]. Uterine mesenchyme contains a variety of growth factors belonging the TGF- $\beta$  and Wnt families, and are upregulated during endometrial adenogenesis and decidulisation in both human and mouse [26, 48, 50, 113]. Surprisingly, genes coding for BMP and Wnt ligands in the nMUM were not upregulated in the current recombinant system [26, 50]. It is, however, possible that these growth factor and signalling molecules may have been revealed if the comparison had been made with a none inductive cell type. Therefore, the lack of differentially upregulated genes from the BMP and Wnt pathways does not rule out their potential involvement in hESC differentiation in the current model. Some growth factors are capable of inducing spontaneous differentiation of hESC to become primitive streak cells at very low concentrations.[238].

Only a small number of genes in the recombinant nMUM coding for proteins with growth factor activity were found to be differentially upregulated in the current study. Lack of significant differences between the control (nMUM alone) and recombinant nMUM groups suggest that differentially upregulated genes were more likely the result of culture related changes rather than reciprocal interaction between hESC and nMUM. More samples per group may have revealed more differences between the experimental conditions.

Genes coding for inducers of primitive streak were not upregulated in the nMUM in the current study. Genes coding for other mesenchyme-derived growth factors were identified, Lack of commercially available recombinant proteins and specific antibodies for most of factors made it difficult to investigate them further in the current study. Ctgf has not been identified as an inducer of primitive streak induction, however, developmental studies have identified Ctgf expression in murine embryos [100, 352].

### 5.4.2 Expression and role of CTGF in hESC differentiation

CTGF is a pleiotropic growth factor implicated in embryogenesis, implantation, angiogenesis, tumorigenesis, wound healing, differentiation, and transdifferentiation [359]. It was first described as a polypeptide growth factor secreted by human endothelial cells in culture [360] and later classified as one of six members of the CNN family of genes that code for cysteine-rich secreted proteins found in a wide variety of vertebrate tissues [361-363]. Increased CTGF production in tissue is primarily a response to injury [364-368]. It is possible that an increase of Ctgf in the nMUM was a result of epithelial/mesenchyme separation and *in vitro* culture conditions. Presence of TGF- $\beta$  in the hESC component of the recombinant may also upregulate CTGF production in nMUM [369]. The mechanisms underlying the induction of CTGF expression in both nMUM and hESC requires further investigation.

CTGF have been localised in maternal uterine tissue and fetal embryonic mouse tissue [100, 352]. The current study showed for the first time its expression in differentiating hESCs, and its potential role in directing hESC differentiation. It is known that primitive streak cells undergo EMT in the vertebrate embryos [356]. Recent studies have shown that hESC can form primitive streak-like cells (mesendodermal cells) in differentiating EBs that also undergo EMT *in vitro* to form endodermal and mesodermal cell types [229, 230, 370]. The addition of exogenous recombinant human CTGF had some positive influence on EMT related genes as well as on a mesoderm gene during hESC differentiation. By contrast, blocking endogenous CTGF had the opposite effect confirming previous reports of CTGF's role in EMT induction and highlighting its involvement in mesoderm formation [100, 352, 354, 357].

Further experiments would aim to demonstrate functional changes in differentiating EB by assessing changes in extracellular protein markers including fibronectin and collagen [354]. Whilst CTGF is important for EMT and therefore potentially impact the formation of mesoderm and endoderm from mesendodermal progenitors, its preferential localisation in the mesoderm and ability to induce differentiation of mesodermally derived progenitor cell types into various connective tissue cell types may explain the positive influence of exogenous CTGF on mesoderm gene and reduction in endodermal gene expression observed in the current study [100, 352, 371, 372]. Furthermore, CTGF has also been implicated in production of extracellular matrix (ECM) components both *in vitro* and *in vivo* [98, 99, 373]. Coincidentally, ECM production has also been linked to preferential mesoderm differentiation of hESC which further

highlights the role CTGF may have in mesoderm induction in hESC shown in the current study [224]. The exact interaction and mechanisms between exogenous CTGF with hESC development requires further investigations. CTGF has not been shown to bind to a specific receptor, its principle domains, however, bind to integrin that subsequently interact with extracellular and intracellular proteins [374]. Moreover, CTGF also antagonizes or enhances members of both the TGF- $\beta$  and Wnt family during development with implications in embryo patterning [375, 376]. In this context, CTGF may be seen as a modulator of endogenous morphogen gradients within the differentiating EB by interacting with ‘key regulators’ of TGF- $\beta$  and Wnt family members involved in the dorsal-ventral patterning of the primitive streak [377]. Further investigation may reveal how CTGF interacts with endogenous gradients in differentiating EB.

### 5.4.3 Limitations and future studies

An alternative way to screen novel secreted products involved in hESC differentiation would have been to compare inductive mesenchyme with non-inductive cell types such as uterine epithelial cells, or a known non-inductive cell line such as mouse embryonic fibroblast (MEF, commonly used as a feeder layer to maintain hESC pluripotency) [346]. Using such strategies would require explants to be cultured as a monolayer feeder to support hESC. Whilst this may easily be achieved with MEF, one would need to isolate a large amount of freshly dissected uterine mesenchyme to harvest enough stromal cells for *in vitro* culture, a costly and extremely labour intensive process that would have been impractical for the current study. Recently, a human uterine stromal cell line has been established [378]. The creation of a mouse uterine stromal cell line in the future would be ideal for this type of experiment as it may reveal a range of inductive growth factors that were not differentially upregulated using the current strategy. Since neonatal epithelial cells do not form recombinants with hESC [311], it is also inaccurate to compared uterine epithelial cells to nMUM. Extracting total RNA from recombinants and mesenchyme for comparison over time was a more efficient method. Whilst the current study revealed that a number of growth factors were upregulated in nMUM during hESC differentiation, for revelation of more organ specific induction, one could compare nMUM with embryonic or postnatal mesenchyme(s) from other organs following recombination with hESC or mESC [174, 175, 179].

Only limited number of mesodermal and endodermal genes were assessed in the current study due to financial and time constraints. Future studies could examine a panel of mesodermal genes for more definitive evidence of CTGF's role in mesoderm induction. Furthermore the recent discovery of surface markers for a multi-potent CD326-CD56+ mesoderm progenitor population [229], could become useful in future studies where mesodermal cell types may be quantified following treatment with rhCTGF.

Whilst the addition of exogenous recombinant human CTGF appears to influence hESC differentiation, the contribution of nMUM derived *Ctgf* has not been addressed in the current study. It appears from the previous study (Chapter 3), that nMUM in the presence of growth factors, also slightly enhanced expression of *OSR1* whilst reducing *GSC* although not at statistically significant levels [311]. The anti-CTGF antibody used in the current study was unsuitable to investigate the role of nMUM derived *Ctgf* on hESC differentiation. However, with the advances in siRNA technology, one could temporarily silence the *Ctgf* gene in the nMUM prior to tissue recombination with hESC. Future studies would aim to demonstrate that a reduction of *Ctgf* in the nMUM using siRNA technologies would reduce mesodermal differentiation of hESC.

#### **5.4.4 Conclusion**

In conclusion, the current study has identified CTGF as a factor that may have a role in mesendoderm differentiation especially towards the formation of mesoderm lineages. Since CTGF was found in both the nMUM and hESC, further investigation is required to ascertain the relative contribution of nMUM-derived CTGF in the differentiation of hESC.

## 5.5 Supplementary Information

**Supplementary Table 5.5.1 Candidate genes expressed in Gene Ontology terms associated with growth factor activity in nMUM alone group**

Accession	Gene Symbol	Fold Change	FDR%	Description
<b><i>Growth factor activity (GO:0008083) p&lt;0.000001</i></b>				
NM_008808	Pdgfa	1.88	0	N/A
NM_008760.2	Ogn	10.45	0	osteoglycin
NM_010275.2	Gdnf	3.31	0	glial cell line derived neurotrophic factor
NM_001039537.1	Lif	1.20	0.4	leukemia inhibitory factor
NM_007778.3	Csf1	1.37	4.41	colony stimulating factor 1
NM_001048141.1	Bdnf	1.38	5.81	brain derived neurotrophic factor
NM_010217.1	Ctgf	3.98	5.93	connective tissue growth factor
NM_010216.1	Figf	2.25	9.93	c-fos induced growth factor

**Supplementary Table 5.5.2 Primer Sequences**

Gene Name	Gene Symbol	Expression Domains				Refs	Forward	Reverse
		PS	Ecto	Meso	Endo			
Connective tissue growth factor	CTGF (H)	N/A				[350]	AGGCAGTTGGCTCTAATCAT AGTTG	GCCCTCGCGGCTTACC
	Ctgf (M)	-	+	+	+	[100, 350, 352]	CCGCCAACCGCAAGATC	ACCGACCCACCGAAGACA
E-Cadherin	ECAD	-	+	-	+/-	[229, 351, 379]	GTCAGTTCAGACTCCAGCCC	AAATTCACCTCTGCCCAGGACG
Goosecoid	GSC	+	-	+	+	[380]	ABI Taqman assay# Hs00418279_m1	
Mix1 homeobox-like 1	MIXL1	+	-	+	-	[381, 382]	ABI Taqman assay# Hs00430824_g1	
Odd-skipped-1	OSR1	+	-	+	-	[270, 383, 384]	ABI Taqman assay# Hs00377071_m1	
Snail homolog 1	SNAI1	+	+	+	+	[229, 351, 385]	ACCACTATGCCGCGCTCTT	GGTCGTAGGGCTGCTGGAA
Snail homolog 2	SLUG	+	+	+	-	[229, 351, 386]	TGTTGCAGTGAGGGCAAGAA	GACCCTGGTTGCTTCAAGGA
Vimentin	VIM	-	-	+	+	[229, 351, 387, 388]	TCTACGAGGAGGAGATGCGG	GGTCAAGACGTGCCAGAGAC
Glyceraldehyde-3-phosphate dehydrogenase	GAPDH	Housekeeping gene					ACCACAGTCCATGCCATCAC	TCCACCCTGTTGCTGTA
-	GAPDH	Housekeeping gene					ABI Taqman assay# Hs99999905_m1	
Calbindin-D28k	Calb1	N/A				[26]	CCCACATGTAACCTCTGTTTCG TGTA	TCACAATAAAGAATCCAGGC AATTAA



## CHAPTER 6 General Discussion

In this study, I developed a 2 stage *in vitro* and *in vivo* model of hESC differentiation. I demonstrated for the first time, neonatal mouse uterine mesenchyme (nMUM) direct human embryonic stem cells (hESC) to form human female reproductive tract (FRT) epithelium. This is also the first report of mesodermally-derived epithelial structure differentiated from hESC. The ability of nMUM to direct hESC differentiation was confirmed using three separate hESC cell lines (MEL-1, ENVY and MIXL1). The model provided a platform on which two other discoveries were made 1) LIM1 expression in the uterine tissue and 2) involvement of connective tissue growth factor (CTGF) in hESC differentiation.

At the commencement of this study, no experimental models existed for developing human FRT. Fetal tissues obtained from miscarriage or stillborn babies were the primary source of human tissue for investigations into human Müllerian duct development [15, 36-38, 129]. In **Chapter 2**, a novel method was developed using tissue recombination of hESC with nMUM to generate human FRT-like epithelium *in vivo*. The interaction between hESC and nMUM corroborates previous reports with regards to the capacity of nMUM to form recombinants and communicate with various epithelial cell types [22, 60, 175, 184, 190]. In **Chapter 3**, morphological and functional markers in the hESC-derived FRT-like epithelium matched features in adult human upper FRT epithelium whilst earlier time points recapitulated events during fetal development. Evidence suggests that hESC-derived epithelial cells belong to a mesodermal lineage with characteristics of the human FRT. Collectively, **Chapter 2 & 3** reports the establishment and characterisation of a novel experimental model of the human FRT development. Subsequent chapters described several studies conducted using this experimental model. In **Chapter 4**, the expression of the homeodomain transcription factor LIM1 in both early and late developmental stages of the current model contradicted a previous report of Lim1 expression in mouse FRT [58]. Further investigation of Lim1/LIM1 in mouse and human uterine tissue revealed for the first time that its expression is not restricted to the Müllerian ducts and its derivatives during late fetal development, but is also present in adult uterine tissue, where its function is currently unknown [10].

In a separate investigation into the role of nMUM-derived growth factors on hESC differentiation (continuation from findings described in **Chapter 3**), a mesenchyme-derived

growth factor known as the CTGF was identified that may have had some influence on hESC differentiation *in vitro* (**Chapter 5**). Further studies examining the role of CTGF and other short listed growth factors may reveal the mechanism by which nMUM induced hESC differentiation.

## **6.1 Development of methods to differentiate human FRT epithelium from hESC**

Instructive capacity of the nMUM was first discovered several decades ago when nMUM was shown to transdifferentiate the mouse vaginal epithelium to form uterine epithelium [22]. The primary hypothesis of the current study was that nMUM will induce hESC differentiation into epithelial cells of the human FRT. The primary aim of the study was to establish a model for generating heterospecific/heterotypic recombinants consisting of hESC and nMUM for transplantation *in vivo* for further development into human FRT epithelium. Other important considerations for the experimental model were reproducibility, applicability to several hESC cell lines, and adaptability for cell tracking methods.

Co-culture of hESC with mouse stromal feeder layers or embryonic mesenchyme explants *in vitro* is more commonly used for hESC differentiation [272]. Alternatively, pre-differentiation of hESC into a homogenous cell population has become a more desirable option for experiments involving transplantation of cells directly into host organs [180, 181]. Recombination of embryonic stem cells with organ specific mesenchyme to produce an organ development model *in vivo* is a relatively new concept. The first demonstration of this technology was the differentiation of hESC into human prostate epithelial structures *in vivo* by tissue recombination with embryonic urogenital mesenchyme [174]. Later, the differentiation of mouse embryonic stem cells (mESC) into bladder epithelial cell types *in vivo* was demonstrated [175].

In **Chapter 2**, a novel method was developed for recombination of nMUM and hESC. When the recombinant grafts were transplanted *in vivo*, hESC formed ductal structures lined with epithelium reminiscent of the human upper female reproductive tract epithelium (oviduct/uterine) based on morphological assessments. Differentiation was achieved with two separate hESC cell lines (MEL-1 and ENVY), one of which can be tracked non-invasively by *in vivo* imaging techniques (ENVY). To our knowledge, this was the first study attempting to produce human FRT from hESC and only the second study ever to differentiate hESC using tissue recombination methods *in vivo*. The results are consistent with the inductive capacity of the nMUM demonstrated previously [22]. During the course my PhD studies, another study was published further demonstrating nMUM's instructive capacity for transdifferentiating mouse spermatogonial stem cells into uterine epithelium [190]. The current study concurs with the

concept that instructive postnatal organ specific mesenchyme can guide the differentiation of pluripotent stem cells to form organ specific epithelium *in vivo*.

Like others, we also encountered problems associated with success rate and off-target differentiation (in the form of teratoma formation) of hESC. Nevertheless, we managed to identify cell type of interest within teratoma-like tissue developed from the recombinant grafts. However, basic morphological features were insufficient to draw a conclusion with regards to the identity of the hESC derived epithelium. A comprehensive analysis of the established model was carried out in Chapter 3.

During the course of the study, the NOD.SCID gamma strain of immunodeficient mice was demonstrated as a better host with a greater take rate for cynomolgus ES cells than the NOD/SCIDs used in the current investigation [281]. The challenge for the next investigation (**Chapter 3**) was to reduce off-target differentiation and improve hESC survival by using a new strain of immunodeficient mice and supplementing the serum-free culture with growth factors.

## **6.2 Generation of human female reproductive tract epithelium from hESC**

In Chapter 2 of the current study, a novel method was established for generating tissue recombinants and their transplantation *in vivo* where hESC differentiated into human FRT-like epithelial structures. The hypotheses of the current investigation were 1) exogenous growth factors in conjunction with nMUM would reduce off-target differentiation 2) use of another strain of immunodeficient mice would slightly improve hESC survival *in vivo* 3) hESC derived epithelium was FRT in nature. The aims of the investigation described in **Chapter 3** were to improve the methods established in **Chapter 2** and prove that the hESC-derived epithelium has characteristics of human FRT epithelium.

It was found in the current investigation that inclusion of mesoderm-inducing growth factors dramatically reduced off-target differentiation (measured by size of the teratoma formed) and NOD.SCID gamma mice lacking functional B and T cells improved viability of recombinants *in vivo* consistent with a previous study [281]. A panel of morphological and functional markers (including those used by another study to identify spermatogonial stem cell-derived mouse FRT epithelium) confirmed the FRT nature of the hESC-derived epithelium in the current investigation [190]. Furthermore, the expression of several stage-specific Müllerian developmental transcription factors suggested that hESC underwent key developmental stages recapitulating aspects of normal FRT organogenesis. A similar phenomenon was also reported in a previous study differentiating hESC towards prostate epithelium [174].

In conclusion, human FRT epithelium was generated from hESCs, and the model may be particularly useful for investigations into the earliest stages of human Müllerian Duct development. The model was used in the current study to investigate other areas of interest include 1) expression of the LIM1 gene in the developing and mature human reproductive tract epithelium and 2) the growth factors involved in the induction of hESC by nMUM during early *in vitro* differentiation.

### **6.3 Expression of transcription factor *Lim1/LIM1* in mouse and human endometrium**

*Lim1* is a homeodomain transcription factor critical to the development of central nervous system and urogenital organs [389, 390]. Some inconsistencies exist within the literature with regards to *Lim1* expression in Müllerian Duct derivatives. Whilst an earlier study found *Lim1* absent in the embryonic oviduct and adult mouse uterus [58], it was later detected in the Müllerian ducts [10]. No study to our knowledge, has examined LIM1 expression in mature human female reproductive tract.

In the current investigation, *Lim1/LIM1* was detected in our experimental FRT model, and for the first time in wild type postnatal, adult mouse, and in both normal and malignant endometrial cells. *Lim1/LIM1* is dynamically expressed across the menstrual/estrus cycle. The expression of *Lim1/LIM1* in the aforementioned tissue/cell types contradicts a previous study that failed to detect *Lim1* expression in adult uterus. It further confirms the FRT identity of the hESC derived epithelium in our model [58]. The findings in the current investigation confirms and extends previous observations of *Lim1* expression in the Müllerian duct during fetal development, and various human studies implicating LIM1 with uterine aplasia [40, 81]. Furthermore, detection of LIM1 in the adult uterus is consistent with its expression in several other adult organs [304, 305, 307]. Some of these studies have demonstrated the significant roles that *Lim1/LIM1* transcription factor plays in stem cell regulation, cell differentiation and specification as well as disease progression [304, 305, 328].

The FRT model established in earlier chapters facilitated this investigation by providing a more comprehensive view of LIM1 expression in human FRT tissue. In conclusion, expression of *Lim1/LIM1* in both fetal and adult FRT uterine tissues suggests that it may have a range of functions in development, remodelling and cell differentiation in human FRT.

#### **6.4 Identification of mesenchyme-derived growth factors involved in hESC differentiation**

The most widely used approach to differentiate hESC towards a desired lineage uses exogenous growth factors [226]. Alternatively, co-culture of stromal feeder layers with hESCs has been used to guide hESC differentiation *in vitro* [223, 340, 346, 391]. The model developed in Chapters 2 and 3 included a pre-differentiation stage of hESC differentiation [311]. In Chapter 3, primitive streak-like cells formed *in vitro* in differentiating EBs briefly after recombination with nMUM in the absence of exogenous growth factors indicating nMUM may have provided morphogens for hESC differentiation [311].

Gene profiling in this current investigation led to the discovery of the potential inductive capacity of CTGF on hESC differentiation *in vitro*, consistent with its roles in embryogenesis [374]. The current investigation is the first report describing the expression of CTGF in nMUM and human EBs. The finding corroborates a previous report describing the localisation of CTGF in similar cell types *in vivo* during early embryonic development [100]. In combination with known inductive growth factors (BMP4 and Activin A), CTGF influenced the differentiation of primitive streak-like cells towards cells expressing mesodermal genes, consistent with its preferential localisation in the embryonic mesoderm [352]. Moreover, CTGF has also been implicated in production of extracellular matrix (ECM) which may enhance hESC differentiation towards mesodermal lineages [98, 224].

In summary, the FRT model developed in earlier chapters has facilitated another investigation, revealing growth factors involved in induction of hESC differentiation. The exact contribution of nMUM-derived CTGF requires further investigation using siRNA technologies. Further studies are required to quantify and characterised the cell types produced from differentiating hESC resulting from the addition of exogenous CTGF.

## 6.5 Limitations of this investigation

Both logistical and technical challenges were encountered whilst establishing the hESC derived human FRT model, some of which have been addressed in previous chapters. The most notable limitation was the survival rate of the transplanted recombinants *in vivo*. This common issue associated with transplanting small numbers of hESC has also been reported in another study [174]. Another technical issue relates to residual uterine epithelial fragments in the nMUM tube resulting in differentiation of mouse uterine epithelium in the recombinant graft in a previous report [184]. In the current study, recombinant grafts containing both mouse uterine gland and hESC derived human FRT glands were excluded from analysis, further reducing take rate of the model. A number of strategies were devised to overcome these technical issues. The exogenous growth factors BMP4 and Activin A were included in recombinant cultures to improve hESC survival *in vitro* [205]. To improve hESC survival *in vivo*, recombinant grafts were transplanted into severely immunocompromised NSG mice (lacking functional B, T and NK cells). In addition, a non-invasive *in vivo* imaging approach was used to monitor graft growth. In order to reduce the impact of contaminating remnant mouse uterine epithelial cells in recombinant grafts, ovariectomies were performed on host mice at the time of graft transplantation.

Logistical limiting factors faced in conducting the current studies included the initial sporadic supply of the hESCs. Culturing hESC is an expensive and labour intensive undertaking for most laboratories. In the first year of my PhD studies (2008), I spent considerable time learning how to culture and maintain hESC (MEL-1) for experimentation. Limited quantities of hESCs were available for small numbers of experiments with high failure rates. The establishment of Stem Core (a Core Facility offering a wide variety stem cells and related services at Monash University) in the second year of my PhD studies enabled a reliable and more frequent supply of hESCs. Despite the establishment of the core facility, the unpredictability of hESC growth and its dependence on other cell lines (MEFs) to maintain pluripotency meant that hESCs were not always available for experiments. To further complicate the supply issue, most of the experiments in the current studies depended on availability of both hESCs and nMUM. When neonatal mice were not born on days planned, experiments were also postponed. Despite these challenges, a total of more than 36 recombinant grafts were harvested over the course of my PhD studies. 15 out of 112 recombinants grafts transplanted into NSG mouse hosts successfully developed into small tumours containing human FRT epithelium representing success rate of 13%.



Other limitations concerned the identity and functional similarities of the hESC derived FRT model to actual human FRT epithelium. Even though defining features of the upper female reproductive tract (including the oviduct and uterus which have overlapping features) were identified, whether or not the epithelium is oviductal or uterine requires further investigation. We suspect there would be some functional differences between our model and the normal human FRT epithelium since the model has murine stroma supporting human epithelia, similar to the human prostate epithelium generated from hESC in a previous study [174]. However, further characterisation may not be necessary for the mature version of the current model (i.e. 8 weeks) since its purpose was purely to confirm that the epithelium was a Müllerian derivative. The more important components of the current human FRT model are the developmental stages observed at the earlier time points. These stages may be most useful for investigations into the earliest events of human Müllerian duct formation and development, a time before regional specification of the Müllerian duct into oviducts and uterine segments. Collectively, the methods developed in this thesis for generation of hESC-derived FRT epithelium is reproducible and can be used as a model to conduct further investigations in the biology of hESC differentiation and human FRT development.

The availability of primary human samples was the main limitation for investigations described in **Chapter 4**. The high demand for primary human endometrial samples by other researchers in my laboratory meant limited supply of human tissue for the current investigations. In addition, during the course of my PhD, changes to organisational structure of the research institute through which I was enrolled meant I had limited access to archival (paraffin) human patient endometrial tissue. As a result of these factors, only a limited number of human patient samples were examined for LIM1 expression in **Chapter 4**. In spite of limited access to human patient samples, we confidently conclude that LIM1 is expressed in human adult endometrium.

As mentioned previously during the discussion of **Chapter 5**, within the usual financial and time constraints of conducting PhD studies in 3½ years, certain experiments were not performed for the final chapter of this thesis. It is recommended that gene profiling experiments to be extended to compare non-inductive tissue types with nMUM which may reveal uterine specific inductive growth factors. Future studies might consider altering the current *in vitro* model by culturing nMUM as a feeder layer which will allow comparison with other cell lines and feeder layers. To ensure that exogenous recombinant CTGF treatment and anti-CTGF antibody treatments were

effective, biologically relevant concentrations described in previous studies were used. The effects of CTGF were indirectly assessed by mRNA expression of genes involved in epithelial-mesenchymal transition [357]. With regards to blocking experiments, future studies would utilise ELISA to measure CTGF level after anti-CTGF treatment.

## 6.6 Future applications and further studies

The implications of this study relates to hESC differentiation, developmental biology of the human FRT as well as adult mouse and human uterine physiology. The study described a novel model of human FRT epithelial development from hESCs and nMUM [311]. The model provides a platform for future studies investigating various aspects of human FRT development and hESC differentiation.

The detection of Lim1/LIM1 in adult uterine tissue opens a new area for further investigation to reveal its functional roles in adult uterine tissue. Of particular interest is the role Lim1/LIM1 may have in the regulation of recently discovered uterine stem/progenitor populations [144, 145]. In addition, its expression in endometrial cell lines would allow the design of future *in vitro* studies aimed to understand the regulation of Lim1/LIM1 and its downstream targets in uterine cells.

In terms of using the FRT model to study hESC differentiation, a mesenchyme derived growth factor, CTGF was identified in the current study, which may influence hESC differentiation *in vitro*. Nevertheless, exogenous CTGF may be used in future hESC differentiation strategies to complement the use of other growth factors used to produce clinically relevant cell types. Most current hESC differentiation strategies attempt to recreate stage specific embryonic niche environments associated with the induction of particular cell types by addition of exogenous growth factors [226]. In contrast, the current model utilised mouse postnatal niche environment to guide early embryonic events, resulting in the formation of Müllerian-like epithelium from hESC after merely one week of *in vivo* incubation with nMUM following *in vitro* mesodermal differentiation. The current model provides a platform for alternative *in vitro* hESC differentiation strategies modelled on postnatal mesenchyme's interaction with hESC. Future experiments aiming to examine in more detail the interaction between nMUM and hESC *in vitro* and *in vivo* will reveal mechanisms and signalling pathways of this and other similar differentiation models.

Better understanding of mesenchyme derived molecules and their role in differentiation of hESC may lead to the creation of a more defined *in vitro* differentiation system capable of producing Müllerian duct epithelial cells and their derivatives in culture in the absence of nMUM. Pure populations of human Müllerian epithelial cells may have clinical applications for endometrial

regeneration in patients suffering from Asherman's syndrome (characterised by complete obliteration of uterine cavity with adhesions) [392]. Other applications of cultured Müllerian epithelial cells would allow screening for environmental agents that may impact on Müllerian development. Furthermore, comparison of hESC-derived Müllerian epithelial cells with endometrial epithelial stem/progenitor cells by gene or epigenetic profiling will determine their relationship.

It has been known for decades that adult FRT disease has a fetal origin [151]. Animal studies have shown that exposure to endocrine disruptors such as DES or other estradiol analogs mimics during fetal/neonatal uterine development may cause permanent damage by permanently altering signalling pathways critical to normal development [162]. Administration of DES and other endocrine disruptors into hosts carrying heterospecific recombinant grafts would allow researchers to examine changes in human Müllerian duct development for comparison with animal data since only a small percentage of experiments conducted in laboratory rodents actually translates to human situations.

The model would also facilitate investigations into the development of human Müllerian duct epithelium. With advances in genetic manipulation technologies, future studies would aim to modify gene expression in the uterine mesenchyme prior to recombination with hESC to understand effects of specific paracrine pathways on differentiation of hESC to form the Müllerian duct epithelium. Manipulation of the mesenchyme can be achieved by transfection methods [191], or alternatively, one could utilise mesenchyme with targeted gene deletion from knockout mice [186, 192, 194].

## **6.7 Conclusion**

In this study, I have demonstrated that nMUM directed hESC differentiation into human FRT-like epithelium using two separate cell lines. Further examination at key time points indicated that the FRT-like epithelium expressed all the hall marks (morphological and functional markers) of mature upper FRT epithelium. Further characterisations revealed features recapitulating key events of the FRT development observed during embryogenesis. The versatility of the model was further demonstrated where it led to the discovery of Lim1/LIM1 expression in adult mouse and human endometrium and also implicated CTGF in differentiation of hESC. Overall, this study lays the ground work for future studies that will provide a better understanding of human FRT development as well as new strategies for hESC differentiation towards Müllerian duct cells which may have implications in regenerative medicine.

## Bibliography

1. Kaufman, M.H.a.B., J. B. L. : , *The Anatomical Basis of Mouse Development*. 1999, San Diego, CA: Academic Press.
2. Funayama, N., Y. Sato, K. Matsumoto, T. Ogura, and Y. Takahashi, *Coelom formation: binary decision of the lateral plate mesoderm is controlled by the ectoderm*. Development, 1999. **126**(18): p. 4129-38.
3. Cochard, L.R. and F.H. Netter, *Netter's atlas of human embryology*. 1st ed. 2002, Teterboro, N.J.: Icon Learning Systems. xx, 267 p.
4. Balfour, F.M. and A. Sedgewick, *On the existence of a head-kidney in the embryo chick, and on certain points in the development of the Müllerian duct*. Q. J. Microsc. Sci, 1879. **19**: p. 1-19.
5. Dohr, G., T. Tarmann, and H. Schiechl, *Different antigen expression on Wolffian and Mullerian cells in rat embryos as detected by monoclonal antibodies*. Anat Embryol (Berl), 1987. **176**(2): p. 239-42.
6. Inomata, T., Y. Eguchi, and T. Nakamura, *Origin of mullerian duct and its later developmental changes in relation to wolffian duct in bovine fetuses*. Zentralbl Veterinarmed A, 1989. **36**(3): p. 166-74.
7. Guioli, S., R. Sekido, and R. Lovell-Badge, *The origin of the Mullerian duct in chick and mouse*. Dev Biol, 2007. **302**(2): p. 389-98.
8. Orvis, G.D. and R.R. Behringer, *Cellular mechanisms of Mullerian duct formation in the mouse*. Dev Biol, 2007. **306**(2): p. 493-504.
9. Kabawat, S.E., R.C. Bast, Jr., A.K. Bhan, W.R. Welch, R.C. Knapp, and R.B. Colvin, *Tissue distribution of a coelomic-epithelium-related antigen recognized by the monoclonal antibody OC125*. Int J Gynecol Pathol, 1983. **2**(3): p. 275-85.
10. Kobayashi, A., W. Shawlot, A. Kania, and R.R. Behringer, *Requirement of Lim1 for female reproductive tract development*. Development, 2004. **131**(3): p. 539-49.
11. Vainio, S., M. Heikkila, A. Kispert, N. Chin, and A.P. McMahon, *Female development in mammals is regulated by Wnt-4 signalling*. Nature, 1999. **397**(6718): p. 405-9.
12. Kobayashi, A., K.M. Kwan, T.J. Carroll, A.P. McMahon, C.L. Mendelsohn, and R.R. Behringer, *Distinct and sequential tissue-specific activities of the LIM-class homeobox gene Lim1 for tubular morphogenesis during kidney development*. Development, 2005. **132**(12): p. 2809-23.

13. Miyamoto, N., M. Yoshida, S. Kuratani, I. Matsuo, and S. Aizawa, *Defects of urogenital development in mice lacking Emx2*. Development, 1997. **124**(9): p. 1653-64.
14. Torres, M., E. Gomez-Pardo, G.R. Dressler, and P. Gruss, *Pax-2 controls multiple steps of urogenital development*. Development, 1995. **121**(12): p. 4057-65.
15. Hashimoto, R., *Development of the human Mullerian duct in the sexually undifferentiated stage*. Anat Rec A Discov Mol Cell Evol Biol, 2003. **272**(2): p. 514-9.
16. Josso, N., I. Lamarre, J.Y. Picard, P. Berta, N. Davies, N. Morichon, M. Peschanski, and R. Jeny, *Anti-mullerian hormone in early human development*. Early Hum Dev, 1993. **33**(2): p. 91-9.
17. Kobayashi, A. and R.R. Behringer, *Developmental genetics of the female reproductive tract in mammals*. Nat Rev Genet, 2003. **4**(12): p. 969-80.
18. Spencer, T.E., K. Hayashi, J. Hu, and K.D. Carpenter, *Comparative developmental biology of the mammalian uterus*. Curr Top Dev Biol, 2005. **68**: p. 85-122.
19. Kurita, T., P.S. Cooke, and G.R. Cunha, *Epithelial-stromal tissue interaction in paramesonephric (Mullerian) epithelial differentiation*. Dev Biol, 2001. **240**(1): p. 194-211.
20. Spencer, T.E., K.D. Carpenter, K. Hayashi, and J. Hu, *Uterine gland*, in *Molecular Biology Intelligence Unit*. 2005, Eurekah.com and Springer Science+Business Media, Inc.: Boston, MA.
21. Cunha, G.R., *The dual origin of vaginal epithelium*. Am J Anat, 1975. **143**(3): p. 387-92.
22. Cunha, G.R., *Stromal induction and specification of morphogenesis and cytodifferentiation of the epithelia of the Mullerian ducts and urogenital sinus during development of the uterus and vagina in mice*. J Exp Zool, 1976. **196**(3): p. 361-70.
23. Cunha, G.R., *Epithelial-stromal interactions in development of the urogenital tract*. Int Rev Cytol, 1976. **47**: p. 137-94.
24. Brody, J.R. and G.R. Cunha, *Histologic, morphometric, and immunocytochemical analysis of myometrial development in rats and mice: I. Normal development*. Am J Anat, 1989. **186**(1): p. 1-20.
25. Gray, C.A., F.F. Bartol, B.J. Tarleton, A.A. Wiley, G.A. Johnson, F.W. Bazer, and T.E. Spencer, *Developmental biology of uterine glands*. Biol Reprod, 2001. **65**(5): p. 1311-23.
26. Hu, J., C.A. Gray, and T.E. Spencer, *Gene expression profiling of neonatal mouse uterine development*. Biol Reprod, 2004. **70**(6): p. 1870-6.

27. Branham, W.S., D.M. Sheehan, D.R. Zehr, E. Ridlon, and C.J. Nelson, *The postnatal ontogeny of rat uterine glands and age-related effects of 17 beta-estradiol*. Endocrinology, 1985. **117**(5): p. 2229-37.
28. Komatsu, M. and H. Fujita, *Electron-microscopic studies on the development and aging of the oviduct epithelium of mice*. Anat Embryol (Berl), 1978. **152**(3): p. 243-59.
29. Okada, A., Y. Ohta, S.L. Brody, H. Watanabe, A. Krust, P. Chambon, and T. Iguchi, *Role of foxj1 and estrogen receptor alpha in ciliated epithelial cell differentiation of the neonatal oviduct*. J Mol Endocrinol, 2004. **32**(3): p. 615-25.
30. Bartol, F.F., A.A. Wiley, J.G. Floyd, T.L. Ott, F.W. Bazer, C.A. Gray, and T.E. Spencer, *Uterine differentiation as a foundation for subsequent fertility*. J Reprod Fertil Suppl, 1999. **54**: p. 287-302.
31. Spencer, T.E., F.F. Bartol, A.A. Wiley, D.A. Coleman, and D.F. Wolfe, *Neonatal porcine endometrial development involves coordinated changes in DNA synthesis, glycosaminoglycan distribution, and 3H-glucosamine labeling*. Biol Reprod, 1993. **48**(4): p. 729-40.
32. Carpenter, K.D., C.A. Gray, T.M. Bryan, T.H. Welsh, Jr., and T.E. Spencer, *Estrogen and antiestrogen effects on neonatal ovine uterine development*. Biol Reprod, 2003. **69**(2): p. 708-17.
33. Gray, C.A., K.M. Taylor, F.W. Bazer, and T.E. Spencer, *Mechanisms regulating norgestomet inhibition of endometrial gland morphogenesis in the neonatal ovine uterus*. Mol Reprod Dev, 2000. **57**(1): p. 67-78.
34. Gray, C.A., F.W. Bazer, and T.E. Spencer, *Effects of neonatal progestin exposure on female reproductive tract structure and function in the adult ewe*. Biol Reprod, 2001. **64**(3): p. 797-804.
35. Kurita, T.N., H., *Endometrium: Embryology of the uterus*. 2nd ed. 2008, London: Informa Healthcare.
36. Barberini, F., S. Makabe, G. Franchitto, S. Correr, M. Relucenti, R. Heyn, and G. Familiari, *Ultrastructural dynamics of the human endometrium from 14 to 22 weeks of gestation*. Arch Histol Cytol, 2007. **70**(1): p. 21-8.
37. Wang, T., *Human fetal endometrium--light and electron microscopic study*. Arch Gynecol Obstet, 1989. **246**(3): p. 169-79.
38. Huber, A., S. Michael, and K. Feik, *[Functional changes in the fetal and infantile endometrium]*. Arch Gynakol, 1971. **211**(4): p. 583-94.



39. Coffinier, C., J. Barra, C. Babinet, and M. Yaniv, *Expression of the vHNF1/HNF1beta homeoprotein gene during mouse organogenesis*. Mech Dev, 1999. **89**(1-2): p. 211-3.
40. Bernardini, L., S. Gimelli, C. Gervasini, M. Carella, A. Baban, G. Frontino, G. Barbano, M.T. Divizia, L. Fedele, A. Novelli, F. Bena, F. Lalatta, M. Miozzo, and B. Dallapiccola, *Recurrent microdeletion at 17q12 as a cause of Mayer-Rokitansky-Kuster-Hauser (MRKH) syndrome: two case reports*. Orphanet J Rare Dis, 2009. **4**: p. 25.
41. Bingham, C., S. Ellard, T.R. Cole, K.E. Jones, L.I. Allen, J.A. Goodship, T.H. Goodship, D. Bakalnova-Pugh, G.I. Russell, A.S. Woolf, A.J. Nicholls, and A.T. Hattersley, *Solitary functioning kidney and diverse genital tract malformations associated with hepatocyte nuclear factor-1beta mutations*. Kidney Int, 2002. **61**(4): p. 1243-51.
42. Lindner, T.H., P.R. Njolstad, Y. Horikawa, L. Bostad, G.I. Bell, and O. Sovik, *A novel syndrome of diabetes mellitus, renal dysfunction and genital malformation associated with a partial deletion of the pseudo-POU domain of hepatocyte nuclear factor-1beta*. Hum Mol Genet, 1999. **8**(11): p. 2001-8.
43. Davis, R.J., M. Harding, Y. Moayed, and G. Mardon, *Mouse Dach1 and Dach2 are redundantly required for Mullerian duct development*. Genesis, 2008. **46**(4): p. 205-13.
44. Cadigan, K.M. and R. Nusse, *Wnt signaling: a common theme in animal development*. Genes Dev, 1997. **11**(24): p. 3286-305.
45. Nusse, R. and H.E. Varmus, *Wnt genes*. Cell, 1992. **69**(7): p. 1073-87.
46. Wodarz, A. and R. Nusse, *Mechanisms of Wnt signaling in development*. Annu Rev Cell Dev Biol, 1998. **14**: p. 59-88.
47. Bhanot, P., M. Brink, C.H. Samos, J.C. Hsieh, Y. Wang, J.P. Macke, D. Andrew, J. Nathans, and R. Nusse, *A new member of the frizzled family from Drosophila functions as a Wingless receptor*. Nature, 1996. **382**(6588): p. 225-30.
48. Hayashi, K., D.W. Erikson, S.A. Tilford, B.M. Bany, J.A. Maclean, 2nd, E.B. Rucker, 3rd, G.A. Johnson, and T.E. Spencer, *Wnt genes in the mouse uterus: potential regulation of implantation*. Biol Reprod, 2009. **80**(5): p. 989-1000.
49. Hayashi, K. and T.E. Spencer, *WNT pathways in the neonatal ovine uterus: potential specification of endometrial gland morphogenesis by SFRP2*. Biol Reprod, 2006. **74**(4): p. 721-33.
50. Hayashi, K., S. Yoshioka, S.N. Reardon, E.B. Rucker, 3rd, T.E. Spencer, F.J. DeMayo, J.P. Lydon, and J.A. MacLean, 2nd, *WNTs in the neonatal mouse uterus: potential regulation of endometrial gland development*. Biol Reprod, 2010. **84**(2): p. 308-19.

51. Tulac, S., N.R. Nayak, L.C. Kao, M. Van Waes, J. Huang, S. Lobo, A. Germeyer, B.A. Lessey, R.N. Taylor, E. Suchanek, and L.C. Giudice, *Identification, characterization, and regulation of the canonical Wnt signaling pathway in human endometrium*. J Clin Endocrinol Metab, 2003. **88**(8): p. 3860-6.
52. Miller, C., A. Pavlova, and D.A. Sassoon, *Differential expression patterns of Wnt genes in the murine female reproductive tract during development and the estrous cycle*. Mech Dev, 1998. **76**(1-2): p. 91-9.
53. Biason-Lauber, A., D. Konrad, F. Navratil, and E.J. Schoenle, *A WNT4 mutation associated with Mullerian-duct regression and virilization in a 46,XX woman*. N Engl J Med, 2004. **351**(8): p. 792-8.
54. Carroll, T.J., J.S. Park, S. Hayashi, A. Majumdar, and A.P. McMahon, *Wnt9b plays a central role in the regulation of mesenchymal to epithelial transitions underlying organogenesis of the mammalian urogenital system*. Dev Cell, 2005. **9**(2): p. 283-92.
55. Mendelsohn, C., D. Lohnes, D. Decimo, T. Lufkin, M. LeMeur, P. Chambon, and M. Mark, *Function of the retinoic acid receptors (RARs) during development (II). Multiple abnormalities at various stages of organogenesis in RAR double mutants*. Development, 1994. **120**(10): p. 2749-71.
56. Iizuka-Kogo, A., T. Ishida, T. Akiyama, and T. Senda, *Abnormal development of urogenital organs in Dlg1-deficient mice*. Development, 2007. **134**(9): p. 1799-807.
57. Fujino, A., N.A. Arango, Y. Zhan, T.F. Manganaro, X. Li, D.T. MacLaughlin, and P.K. Donahoe, *Cell migration and activated PI3K/AKT-directed elongation in the developing rat Mullerian duct*. Dev Biol, 2009. **325**(2): p. 351-62.
58. Fujii, T., J.G. Pichel, M. Taira, R. Toyama, I.B. Dawid, and H. Westphal, *Expression patterns of the murine LIM class homeobox gene lim1 in the developing brain and excretory system*. Dev Dyn, 1994. **199**(1): p. 73-83.
59. Tong, G.X., L. Chiriboga, D. Hamele-Bena, and A.C. Borczuk, *Expression of PAX2 in papillary serous carcinoma of the ovary: immunohistochemical evidence of fallopian tube or secondary Mullerian system origin?* Mod Pathol, 2007. **20**(8): p. 856-63.
60. Taylor, H.S. and X. Fei, *Emx2 regulates mammalian reproduction by altering endometrial cell proliferation*. Mol Endocrinol, 2005. **19**(11): p. 2839-46.
61. Jeong, J.W., I. Kwak, K.Y. Lee, T.H. Kim, M.J. Large, C.L. Stewart, K.H. Kaestner, J.P. Lydon, and F.J. DeMayo, *Foxa2 is essential for mouse endometrial gland development and fertility*. Biol Reprod, 2010. **83**(3): p. 396-403.

62. Mericskay, M., J. Kitajewski, and D. Sassoon, *Wnt5a is required for proper epithelial-mesenchymal interactions in the uterus*. Development, 2004. **131**(9): p. 2061-72.
63. Dunlap, K.A., J. Filant, K. Hayashi, E.B. Rucker, 3rd, G. Song, J.M. Deng, R.R. Behringer, F.J. Demayo, J. Lydon, J.W. Jeong, and T.E. Spencer, *Postnatal deletion of wnt7a inhibits uterine gland morphogenesis and compromises adult fertility in mice*. Biol Reprod, 2011. **85**(2): p. 386-96.
64. Miller, C., K. Degenhardt, and D.A. Sassoon, *Fetal exposure to DES results in de-regulation of Wnt7a during uterine morphogenesis*. Nat Genet, 1998. **20**(3): p. 228-30.
65. Miller, C. and D.A. Sassoon, *Wnt-7a maintains appropriate uterine patterning during the development of the mouse female reproductive tract*. Development, 1998. **125**(16): p. 3201-11.
66. Carta, L. and D. Sassoon, *Wnt7a is a suppressor of cell death in the female reproductive tract and is required for postnatal and estrogen-mediated growth*. Biol Reprod, 2004. **71**(2): p. 444-54.
67. Parr, B.A., E.J. Avery, J.A. Cygan, and A.P. McMahon, *The classical mouse mutant postaxial hemimelia results from a mutation in the Wnt 7a gene*. Dev Biol, 1998. **202**(2): p. 228-34.
68. Mendelsohn, C., S. Larkin, M. Mark, M. LeMeur, J. Clifford, A. Zelent, and P. Chambon, *RAR beta isoforms: distinct transcriptional control by retinoic acid and specific spatial patterns of promoter activity during mouse embryonic development*. Mech Dev, 1994. **45**(3): p. 227-41.
69. Benson, G.V., H. Lim, B.C. Paria, I. Satokata, S.K. Dey, and R.L. Maas, *Mechanisms of reduced fertility in Hoxa-10 mutant mice: uterine homeosis and loss of maternal Hoxa-10 expression*. Development, 1996. **122**(9): p. 2687-96.
70. Taylor, H.S., G.B. Vanden Heuvel, and P. Igarashi, *A conserved Hox axis in the mouse and human female reproductive system: late establishment and persistent adult expression of the Hoxa cluster genes*. Biol Reprod, 1997. **57**(6): p. 1338-45.
71. Gendron, R.L., H. Paradis, H.M. Hsieh-Li, D.W. Lee, S.S. Potter, and E. Markoff, *Abnormal uterine stromal and glandular function associated with maternal reproductive defects in Hoxa-11 null mice*. Biol Reprod, 1997. **56**(5): p. 1097-105.
72. Wang, L.F., H.Z. Luo, Z.M. Zhu, and J.D. Wang, *Expression of HOXA11 gene in human endometrium*. Am J Obstet Gynecol, 2004. **191**(3): p. 767-72.
73. Warot, X., C. Fromental-Ramain, V. Fraulob, P. Chambon, and P. Dolle, *Gene dosage-dependent effects of the Hoxa-13 and Hoxd-13 mutations on morphogenesis of the*

- terminal parts of the digestive and urogenital tracts*. Development, 1997. **124**(23): p. 4781-91.
74. McGinnis, W. and R. Krumlauf, *Homeobox genes and axial patterning*. Cell, 1992. **68**(2): p. 283-302.
  75. Zhao, Y. and S.S. Potter, *Functional specificity of the Hoxa13 homeobox*. Development, 2001. **128**(16): p. 3197-207.
  76. Du, H. and H.S. Taylor, *Molecular regulation of mullerian development by Hox genes*. Ann N Y Acad Sci, 2004. **1034**: p. 152-65.
  77. Parr, B.A. and A.P. McMahon, *Sexually dimorphic development of the mammalian reproductive tract requires Wnt-7a*. Nature, 1998. **395**(6703): p. 707-10.
  78. Kurita, T., A.A. Mills, and G.R. Cunha, *Roles of p63 in the diethylstilbestrol-induced cervicovaginal adenosis*. Development, 2004. **131**(7): p. 1639-49.
  79. Jeong, J.W., H.S. Lee, H.L. Franco, R.R. Broaddus, M.M. Taketo, S.Y. Tsai, J.P. Lydon, and F.J. DeMayo, *beta-catenin mediates glandular formation and dysregulation of beta-catenin induces hyperplasia formation in the murine uterus*. Oncogene, 2009. **28**(1): p. 31-40.
  80. Franco, H.L., D. Dai, K.Y. Lee, C.A. Rubel, D. Roop, D. Boerboom, J.W. Jeong, J.P. Lydon, I.C. Bagchi, M.K. Bagchi, and F.J. DeMayo, *WNT4 is a key regulator of normal postnatal uterine development and progesterone signaling during embryo implantation and decidualization in the mouse*. FASEB J, 2010. **25**(4): p. 1176-87.
  81. Cheroki, C., A.C. Krepischi-Santos, K. Szuhai, V. Brenner, C.A. Kim, P.A. Otto, and C. Rosenberg, *Genomic imbalances associated with mullerian aplasia*. J Med Genet, 2008. **45**(4): p. 228-32.
  82. Mortlock, D.P. and J.W. Innis, *Mutation of HOXA13 in hand-foot-genital syndrome*. Nat Genet, 1997. **15**(2): p. 179-80.
  83. Belville, C., N. Josso, and J.Y. Picard, *Persistence of Mullerian derivatives in males*. Am J Med Genet, 1999. **89**(4): p. 218-23.
  84. Boutin, E.L., E. Battle, and G.R. Cunha, *The response of female urogenital tract epithelia to mesenchymal inductors is restricted by the germ layer origin of the epithelium: prostatic inductions*. Differentiation, 1991. **48**(2): p. 99-105.
  85. Cunha, G.R., *Alterations in the developmental properties of stroma during the development of the urogenital ridge into ductus deferens and uterus in embryonic and neonatal mice*. J Exp Zool, 1976. **197**(3): p. 375-88.

86. Cunha, G.R., P. Young, and J.R. Brody, *Role of uterine epithelium in the development of myometrial smooth muscle cells*. Biol Reprod, 1989. **40**(4): p. 861-71.
87. Okulicz, W.C., C.I. Ace, and R. Scarrell, *Zonal changes in proliferation in the rhesus endometrium during the late secretory phase and menses*. Proc Soc Exp Biol Med, 1997. **214**(2): p. 132-8.
88. Padykula, H.A., L.G. Coles, J.A. McCracken, N.W. King, Jr., C. Longcope, and I.R. Kaiserman-Abramof, *A zonal pattern of cell proliferation and differentiation in the rhesus endometrium during the estrogen surge*. Biol Reprod, 1984. **31**(5): p. 1103-18.
89. Taylor, K.M., C.A. Gray, M.M. Joyce, M.D. Stewart, F.W. Bazer, and T.E. Spencer, *Neonatal ovine uterine development involves alterations in expression of receptors for estrogen, progesterone, and prolactin*. Biol Reprod, 2000. **63**(4): p. 1192-204.
90. Bartol, F.F., A.A. Wiley, and D.R. Goodlett, *Ovine uterine morphogenesis: histochemical aspects of endometrial development in the fetus and neonate*. J Anim Sci, 1988. **66**(5): p. 1303-13.
91. Afify, A.M., S. Craig, and A.F. Paulino, *Temporal variation in the distribution of hyaluronic acid, CD44s, and CD44v6 in the human endometrium across the menstrual cycle*. Appl Immunohistochem Mol Morphol, 2006. **14**(3): p. 328-33.
92. Afify, A.M., S. Craig, A.F. Paulino, and R. Stern, *Expression of hyaluronic acid and its receptors, CD44s and CD44v6, in normal, hyperplastic, and neoplastic endometrium*. Ann Diagn Pathol, 2005. **9**(6): p. 312-8.
93. Zagorianakou, N., E. Ioachim, A. Mitselou, E. Kitsou, P. Zagorianakou, S. Stefanaki, G. Makrydimas, and N.J. Agnantis, *Glycoprotein CD44 expression in normal, hyperplastic and neoplastic endometrium. An immunohistochemical study including correlations with p53, steroid receptor status and proliferative indices (PCNA, MIB1)*. Eur J Gynaecol Oncol, 2003. **24**(6): p. 500-4.
94. Curry, T.E., Jr. and K.G. Osteen, *Cyclic changes in the matrix metalloproteinase system in the ovary and uterus*. Biol Reprod, 2001. **64**(5): p. 1285-96.
95. Salamonsen, L.A., *Current concepts of the mechanisms of menstruation: a normal process of tissue destruction*. Trends Endocrinol Metab, 1998. **9**(8): p. 305-9.
96. Hu, J., X. Zhang, W.B. Nothnick, and T.E. Spencer, *Matrix metalloproteinases and their tissue inhibitors in the developing neonatal mouse uterus*. Biol Reprod, 2004. **71**(5): p. 1598-604.

97. Nothnick, W.B., *Disruption of the tissue inhibitor of metalloproteinase-1 gene results in altered reproductive cyclicity and uterine morphology in reproductive-age female mice.* Biol Reprod, 2000. **63**(3): p. 905-12.
98. Frazier, K., S. Williams, D. Kothapalli, H. Klapper, and G.R. Grotendorst, *Stimulation of fibroblast cell growth, matrix production, and granulation tissue formation by connective tissue growth factor.* J Invest Dermatol, 1996. **107**(3): p. 404-11.
99. Mori, T., S. Kawara, M. Shinozaki, N. Hayashi, T. Kakinuma, A. Igarashi, M. Takigawa, T. Nakanishi, and K. Takehara, *Role and interaction of connective tissue growth factor with transforming growth factor-beta in persistent fibrosis: A mouse fibrosis model.* J Cell Physiol, 1999. **181**(1): p. 153-9.
100. Surveyor, G.A., A.K. Wilson, and D.R. Brigstock, *Localization of connective tissue growth factor during the period of embryo implantation in the mouse.* Biol Reprod, 1998. **59**(5): p. 1207-13.
101. Bellusci, S., J. Grindley, H. Emoto, N. Itoh, and B.L. Hogan, *Fibroblast growth factor 10 (FGF10) and branching morphogenesis in the embryonic mouse lung.* Development, 1997. **124**(23): p. 4867-78.
102. Rubin, J.S., D.P. Bottaro, M. Chedid, T. Miki, D. Ron, G. Cheon, W.G. Taylor, E. Fortney, H. Sakata, P.W. Finch, and et al., *Keratinocyte growth factor.* Cell Biol Int, 1995. **19**(5): p. 399-411.
103. Weidner, K.M., G. Hartmann, L. Naldini, P.M. Comoglio, M. Sachs, C. Fonatsch, H. Rieder, and W. Birchmeier, *Molecular characteristics of HGF-SF and its role in cell motility and invasion.* EXS, 1993. **65**: p. 311-28.
104. Hom, Y.K., P. Young, A.A. Thomson, and G.R. Cunha, *Keratinocyte growth factor injected into female mouse neonates stimulates uterine and vaginal epithelial growth.* Endocrinology, 1998. **139**(9): p. 3772-9.
105. Taylor, K.M., C. Chen, C.A. Gray, F.W. Bazer, and T.E. Spencer, *Expression of messenger ribonucleic acids for fibroblast growth factors 7 and 10, hepatocyte growth factor, and insulin-like growth factors and their receptors in the neonatal ovine uterus.* Biol Reprod, 2001. **64**(4): p. 1236-46.
106. Gu, Y., W.S. Branham, D.M. Sheehan, P.J. Webb, C.L. Moland, and R.D. Streck, *Tissue-specific expression of messenger ribonucleic acids for insulin-like growth factors and insulin-like growth factor-binding proteins during perinatal development of the rat uterus.* Biol Reprod, 1999. **60**(5): p. 1172-82.

107. Hayashi, K., K.D. Carpenter, and T.E. Spencer, *Neonatal estrogen exposure disrupts uterine development in the postnatal sheep*. Endocrinology, 2004. **145**(7): p. 3247-57.
108. Hayashi, K., K.D. Carpenter, T.H. Welsh, Jr., R.C. Burghardt, L.J. Spicer, and T.E. Spencer, *The IGF system in the neonatal ovine uterus*. Reproduction, 2005. **129**(3): p. 337-47.
109. Zhou, J., B.A. Dsupin, L.C. Giudice, and C.A. Bondy, *Insulin-like growth factor system gene expression in human endometrium during the menstrual cycle*. J Clin Endocrinol Metab, 1994. **79**(6): p. 1723-34.
110. Teh, M.T., D. Blaydon, L.R. Ghali, V. Briggs, S. Edmunds, E. Pantazi, M.R. Barnes, I.M. Leigh, D.P. Kelsell, and M.P. Philpott, *Role for WNT16B in human epidermal keratinocyte proliferation and differentiation*. J Cell Sci, 2007. **120**(Pt 2): p. 330-9.
111. Yamaguchi, T.P., A. Bradley, A.P. McMahon, and S. Jones, *A Wnt5a pathway underlies outgrowth of multiple structures in the vertebrate embryo*. Development, 1999. **126**(6): p. 1211-23.
112. Bui, T.D., L. Zhang, M.C. Rees, R. Bicknell, and A.L. Harris, *Expression and hormone regulation of Wnt2, 3, 4, 5a, 7a, 7b and 10b in normal human endometrium and endometrial carcinoma*. Br J Cancer, 1997. **75**(8): p. 1131-6.
113. Stoikos, C.J., C.A. Harrison, L.A. Salamonsen, and E. Dimitriadis, *A distinct cohort of the TGFbeta superfamily members expressed in human endometrium regulate decidualization*. Hum Reprod, 2008. **23**(6): p. 1447-56.
114. Li, Q., A. Kannan, W. Wang, F.J. Demayo, R.N. Taylor, M.K. Bagchi, and I.C. Bagchi, *Bone morphogenetic protein 2 functions via a conserved signaling pathway involving Wnt4 to regulate uterine decidualization in the mouse and the human*. J Biol Chem, 2007. **282**(43): p. 31725-32.
115. Mylonas, I., U. Jeschke, I. Wiest, A. Hoeing, J. Vogl, N. Shabani, C. Kuhn, S. Schulze, M.S. Kupka, and K. Friese, *Inhibin/activin subunits alpha, beta-A and beta-B are differentially expressed in normal human endometrium throughout the menstrual cycle*. Histochem Cell Biol, 2004. **122**(5): p. 461-71.
116. Ying, Y. and G.Q. Zhao, *Detection of multiple bone morphogenetic protein messenger ribonucleic acids and their signal transducer, Smad1, during mouse decidualization*. Biol Reprod, 2000. **63**(6): p. 1781-6.
117. Erickson, G.F., L. Fuqua, and S. Shimasaki, *Analysis of spatial and temporal expression patterns of bone morphogenetic protein family members in the rat uterus over the estrous cycle*. J Endocrinol, 2004. **182**(2): p. 203-17.

118. Jones, R.L., C. Stoikos, J.K. Findlay, and L.A. Salamonsen, *TGF-beta superfamily expression and actions in the endometrium and placenta*. Reproduction, 2006. **132**(2): p. 217-32.
119. Yi, S.E., P.S. LaPolt, B.S. Yoon, J.Y. Chen, J.K. Lu, and K.M. Lyons, *The type I BMP receptor Bmpr1B is essential for female reproductive function*. Proc Natl Acad Sci U S A, 2001. **98**(14): p. 7994-9.
120. Carpenter, K.D., C.A. Gray, S. Noel, A. Gertler, F.W. Bazer, and T.E. Spencer, *Prolactin regulation of neonatal ovine uterine gland morphogenesis*. Endocrinology, 2003. **144**(1): p. 110-20.
121. Jabbour, H.N. and H.O. Critchley, *Potential roles of decidual prolactin in early pregnancy*. Reproduction, 2001. **121**(2): p. 197-205.
122. Branham, W.S. and D.M. Sheehan, *Ovarian and adrenal contributions to postnatal growth and differentiation of the rat uterus*. Biol Reprod, 1995. **53**(4): p. 863-72.
123. Clark, J.H. and J. Gorski, *Ontogeny of the estrogen receptor during early uterine development*. Science, 1970. **169**(940): p. 76-8.
124. Tarleton, B.J., A.A. Wiley, T.E. Spencer, A.G. Moss, and F.F. Bartol, *Ovary-independent estrogen receptor expression in neonatal porcine endometrium*. Biol Reprod, 1998. **58**(4): p. 1009-19.
125. Fisher, C.R., K.H. Graves, A.F. Parlow, and E.R. Simpson, *Characterization of mice deficient in aromatase (ArKO) because of targeted disruption of the cyp19 gene*. Proc Natl Acad Sci U S A, 1998. **95**(12): p. 6965-70.
126. Jost, A., B. Vigier, J. Prepin, and J.P. Perchellet, *Studies on sex differentiation in mammals*. Recent Prog Horm Res, 1973. **29**: p. 1-41.
127. Couse, J.F. and K.S. Korach, *Contrasting phenotypes in reproductive tissues of female estrogen receptor null mice*. Ann N Y Acad Sci, 2001. **948**: p. 1-8.
128. Everett, L.M., A. Caperell-Grant, and R.M. Bigsby, *Mesenchymal-epithelial interactions in an in vitro model of neonatal mouse uterus*. Proc Soc Exp Biol Med, 1997. **214**(1): p. 49-53.
129. Takeyama, J., T. Suzuki, S. Inoue, C. Kaneko, H. Nagura, N. Harada, and H. Sasano, *Expression and cellular localization of estrogen receptors alpha and beta in the human fetus*. J Clin Endocrinol Metab, 2001. **86**(5): p. 2258-62.
130. Jamieson, J.S.S.a.M.A., *Puberty, menarche and the endometrium*, in *The Endometrium*. 2008. p. 19-24.



131. Gargett, C.E., R.W. Chan, and K.E. Schwab, *Hormone and growth factor signaling in endometrial renewal: role of stem/progenitor cells*. Mol Cell Endocrinol, 2008. **288**(1-2): p. 22-9.
132. Dockery, B.J.M., *The fine structure of the mature human endometrium*, in *The Endometrium*. 2008. p. 47-65.
133. Eun Kwon, H. and H.S. Taylor, *The role of HOX genes in human implantation*. Ann N Y Acad Sci, 2004. **1034**: p. 1-18.
134. Salamonsen, L.A., *Menstrual and estrous cycles*, in *The Endometrium*. 2008, informa healthcare.
135. Zhang, Y., G. Huang, L.P. Shornick, W.T. Roswit, J.M. Shipley, S.L. Brody, and M.J. Holtzman, *A transgenic FOXJ1-Cre system for gene inactivation in ciliated epithelial cells*. Am J Respir Cell Mol Biol, 2007. **36**(5): p. 515-9.
136. Cornillie, F.J., J.M. Lauweryns, and I.A. Brosens, *Normal human endometrium. An ultrastructural survey*. Gynecol Obstet Invest, 1985. **20**(3): p. 113-29.
137. Wynn, R., *The human endometrium: cyclic and gestational changes*  
2nd ed. Biology of the uterus  
1989.
138. Bentin-Ley, U., A. Sjogren, L. Nilsson, L. Hamberger, J.F. Larsen, and T. Horn, *Presence of uterine pinopodes at the embryo-endometrial interface during human implantation in vitro*. Hum Reprod, 1999. **14**(2): p. 515-20.
139. Bakkum-Gamez, J.N., G. Aletti, K.A. Lewis, G.L. Keeney, B.M. Thomas, I. Navarro-Teulon, and W.A. Cliby, *Mullerian inhibiting substance type II receptor (MISIIR): a novel, tissue-specific target expressed by gynecologic cancers*. Gynecol Oncol, 2008. **108**(1): p. 141-8.
140. Padykula, H.A., *Regeneration in the primate uterus: the role of stem cells*. Ann N Y Acad Sci, 1991. **622**: p. 47-56.
141. Prianishnikov, V.A., *On the concept of stem cell and a model of functional-morphological structure of the endometrium*. Contraception, 1978. **18**(3): p. 213-23.
142. Gargett, C.E., *Review article: stem cells in human reproduction*. Reprod Sci, 2007. **14**(5): p. 405-24.
143. Chan, R.W., K.E. Schwab, and C.E. Gargett, *Clonogenicity of human endometrial epithelial and stromal cells*. Biol Reprod, 2004. **70**(6): p. 1738-50.

144. Schwab, K.E. and C.E. Gargett, *Co-expression of two perivascular cell markers isolates mesenchymal stem-like cells from human endometrium*. Hum Reprod, 2007. **22**(11): p. 2903-11.
145. Chan, R.W. and C.E. Gargett, *Identification of label-retaining cells in mouse endometrium*. Stem Cells, 2006. **24**(6): p. 1529-38.
146. Kaitu'u-Lino, T.J., L. Ye, and C.E. Gargett, *Reepithelialization of the uterine surface arises from endometrial glands: evidence from a functional mouse model of breakdown and repair*. Endocrinology, 2010. **151**(7): p. 3386-95.
147. Cervello, I., J.A. Martinez-Conejero, J.A. Horcajadas, A. Pellicer, and C. Simon, *Identification, characterization and co-localization of label-retaining cell population in mouse endometrium with typical undifferentiated markers*. Hum Reprod, 2007. **22**(1): p. 45-51.
148. Cervello, I., C. Gil-Sanchis, A. Mas, F. Delgado-Rosas, J.A. Martinez-Conejero, A. Galan, A. Martinez-Romero, S. Martinez, I. Navarro, J. Ferro, J.A. Horcajadas, F.J. Esteban, J.E. O'Connor, A. Pellicer, and C. Simon, *Human endometrial side population cells exhibit genotypic, phenotypic and functional features of somatic stem cells*. PLoS One, 2010. **5**(6): p. e10964.
149. Katoh, M., *WNT signaling in stem cell biology and regenerative medicine*. Curr Drug Targets, 2008. **9**(7): p. 565-70.
150. Wang, Y., M. van der Zee, R. Fodde, and L.J. Blok, *Wnt/Beta-catenin and sex hormone signaling in endometrial homeostasis and cancer*. Oncotarget, 2011. **1**(7): p. 674-84.
151. Herbst, A.L., H. Ulfelder, and D.C. Poskanzer, *Adenocarcinoma of the vagina. Association of maternal stilbestrol therapy with tumor appearance in young women*. N Engl J Med, 1971. **284**(15): p. 878-81.
152. Kaufman, R.H., E. Adam, E.E. Hatch, K. Noller, A.L. Herbst, J.R. Palmer, and R.N. Hoover, *Continued follow-up of pregnancy outcomes in diethylstilbestrol-exposed offspring*. Obstet Gynecol, 2000. **96**(4): p. 483-9.
153. Verloop, J., F.E. van Leeuwen, T.J. Helmerhorst, H.H. van Boven, and M.A. Rookus, *Cancer risk in DES daughters*. Cancer Causes Control, 2010. **21**(7): p. 999-1007.
154. Couse, J.F. and K.S. Korach, *Estrogen receptor-alpha mediates the detrimental effects of neonatal diethylstilbestrol (DES) exposure in the murine reproductive tract*. Toxicology, 2004. **205**(1-2): p. 55-63.

155. Newbold, R.R., B.C. Bullock, and J.A. McLachlan, *Uterine adenocarcinoma in mice following developmental treatment with estrogens: a model for hormonal carcinogenesis*. Cancer Res, 1990. **50**(23): p. 7677-81.
156. Suzuki, A., A. Sugihara, K. Uchida, T. Sato, Y. Ohta, Y. Katsu, H. Watanabe, and T. Iguchi, *Developmental effects of perinatal exposure to bisphenol-A and diethylstilbestrol on reproductive organs in female mice*. Reprod Toxicol, 2002. **16**(2): p. 107-16.
157. McLachlan, J.A., R.R. Newbold, H.C. Shah, M.D. Hogan, and R.L. Dixon, *Reduced fertility in female mice exposed transplacentally to diethylstilbestrol (DES)*. Fertil Steril, 1982. **38**(3): p. 364-71.
158. McLachlan, J.A., R.R. Newbold, and B.C. Bullock, *Long-term effects on the female mouse genital tract associated with prenatal exposure to diethylstilbestrol*. Cancer Res, 1980. **40**(11): p. 3988-99.
159. Newbold, R.R., E.P. Banks, B. Bullock, and W.N. Jefferson, *Uterine adenocarcinoma in mice treated neonatally with genistein*. Cancer Res, 2001. **61**(11): p. 4325-8.
160. Newbold, R.R., W.N. Jefferson, and E. Padilla-Banks, *Long-term adverse effects of neonatal exposure to bisphenol A on the murine female reproductive tract*. Reprod Toxicol, 2007. **24**(2): p. 253-8.
161. Ma, L., G.V. Benson, H. Lim, S.K. Dey, and R.L. Maas, *Abdominal B (AbdB) Hoxa genes: regulation in adult uterus by estrogen and progesterone and repression in mullerian duct by the synthetic estrogen diethylstilbestrol (DES)*. Dev Biol, 1998. **197**(2): p. 141-54.
162. Newbold, R.R., W.N. Jefferson, S.F. Grissom, E. Padilla-Banks, R.J. Snyder, and E.K. Lobenhofer, *Developmental exposure to diethylstilbestrol alters uterine gene expression that may be associated with uterine neoplasia later in life*. Mol Carcinog, 2007. **46**(9): p. 783-96.
163. Thomson, J.A., J. Itskovitz-Eldor, S.S. Shapiro, M.A. Waknitz, J.J. Swiergiel, V.S. Marshall, and J.M. Jones, *Embryonic stem cell lines derived from human blastocysts*. Science, 1998. **282**(5391): p. 1145-7.
164. Barberi, T., L.M. Willis, N.D. Socci, and L. Studer, *Derivation of multipotent mesenchymal precursors from human embryonic stem cells*. PLoS Med, 2005. **2**(6): p. e161.
165. Chadwick, K., L. Wang, L. Li, P. Menendez, B. Murdoch, A. Rouleau, and M. Bhatia, *Cytokines and BMP-4 promote hematopoietic differentiation of human embryonic stem cells*. Blood, 2003. **102**(3): p. 906-15.

166. Mummery, C., D. Ward-van Oostwaard, P. Doevendans, R. Spijker, S. van den Brink, R. Hassink, M. van der Heyden, T. Opthof, M. Pera, A.B. de la Riviere, R. Passier, and L. Tertoolen, *Differentiation of human embryonic stem cells to cardiomyocytes: role of coculture with visceral endoderm-like cells*. *Circulation*, 2003. **107**(21): p. 2733-40.
167. Kehat, I., D. Kenyagin-Karsenti, M. Snir, H. Segev, M. Amit, A. Gepstein, E. Livne, O. Binah, J. Itskovitz-Eldor, and L. Gepstein, *Human embryonic stem cells can differentiate into myocytes with structural and functional properties of cardiomyocytes*. *J Clin Invest*, 2001. **108**(3): p. 407-14.
168. Laflamme, M.A., K.Y. Chen, A.V. Naumova, V. Muskheli, J.A. Fugate, S.K. Dupras, H. Reinecke, C. Xu, M. Hassanipour, S. Police, C. O'Sullivan, L. Collins, Y. Chen, E. Minami, E.A. Gill, S. Ueno, C. Yuan, J. Gold, and C.E. Murry, *Cardiomyocytes derived from human embryonic stem cells in pro-survival factors enhance function of infarcted rat hearts*. *Nat Biotechnol*, 2007. **25**(9): p. 1015-24.
169. Li, N., A. Hornbruch, R. Klafke, B. Katzenberger, and A. Wizenmann, *Specification of dorsoventral polarity in the embryonic chick mesencephalon and its presumptive role in midbrain morphogenesis*. *Dev Dyn*, 2005. **233**(3): p. 907-20.
170. Aberdam, E., E. Barak, M. Rouleau, S. de LaForest, S. Berrih-Aknin, D.M. Suter, K.H. Krause, M. Amit, J. Itskovitz-Eldor, and D. Aberdam, *A pure population of ectodermal cells derived from human embryonic stem cells*. *Stem Cells*, 2008. **26**(2): p. 440-4.
171. Agarwal, S., K.L. Holton, and R. Lanza, *Efficient differentiation of functional hepatocytes from human embryonic stem cells*. *Stem Cells*, 2008. **26**(5): p. 1117-27.
172. D'Amour, K.A., A.G. Bang, S. Eliazar, O.G. Kelly, A.D. Agulnick, N.G. Smart, M.A. Moorman, E. Kroon, M.K. Carpenter, and E.E. Baetge, *Production of pancreatic hormone-expressing endocrine cells from human embryonic stem cells*. *Nat Biotechnol*, 2006. **24**(11): p. 1392-401.
173. Wang, D., D.L. Haviland, A.R. Burns, E. Zsigmond, and R.A. Wetsel, *A pure population of lung alveolar epithelial type II cells derived from human embryonic stem cells*. *Proc Natl Acad Sci U S A*, 2007. **104**(11): p. 4449-54.
174. Taylor, R.A., P.A. Cowin, G.R. Cunha, M. Pera, A.O. Trounson, J. Pedersen, and G.P. Risbridger, *Formation of human prostate tissue from embryonic stem cells*. *Nat Methods*, 2006. **3**(3): p. 179-81.
175. Oottamasathien, S., Y. Wang, K. Williams, O.E. Franco, M.L. Wills, J.C. Thomas, K. Saba, A.R. Sharif-Afshar, J.H. Makari, N.A. Bhowmick, R.T. DeMarco, S. Hipkens, M. Magnuson, J.W. Brock, 3rd, S.W. Hayward, J.C.t. Pope, and R.J. Matusik, *Directed*

- differentiation of embryonic stem cells into bladder tissue*. Dev Biol, 2007. **304**(2): p. 556-66.
176. Haffen, K., M. Kedinger, and P. Simon-Assmann, *Mesenchyme-dependent differentiation of epithelial progenitor cells in the gut*. J Pediatr Gastroenterol Nutr, 1987. **6**(1): p. 14-23.
  177. Cunha, G.R., M. Sekkingstad, and B.A. Meloy, *Heterospecific induction of prostatic development in tissue recombinants prepared with mouse, rat, rabbit and human tissues*. Differentiation, 1983. **24**(2): p. 174-80.
  178. Neubauer, B.L., L.W. Chung, K.A. McCormick, O. Taguchi, T.C. Thompson, and G.R. Cunha, *Epithelial-mesenchymal interactions in prostatic development. II. Biochemical observations of prostatic induction by urogenital sinus mesenchyme in epithelium of the adult rodent urinary bladder*. J Cell Biol, 1983. **96**(6): p. 1671-6.
  179. Taylor, R.A., H. Wang, S.E. Wilkinson, M.G. Richards, K.L. Britt, F. Vaillant, G.J. Lindeman, J.E. Visvader, G.R. Cunha, J. St John, and G.P. Risbridger, *Lineage enforcement by inductive mesenchyme on adult epithelial stem cells across developmental germ layers*. Stem Cells, 2009. **27**(12): p. 3032-42.
  180. Nicholas, C.R., K.M. Haston, A.K. Grewall, T.A. Longacre, and R.A. Reijo Pera, *Transplantation directs oocyte maturation from embryonic stem cells and provides a therapeutic strategy for female infertility*. Hum Mol Genet, 2009. **18**(22): p. 4376-89.
  181. Dai, W., L.J. Field, M. Rubart, S. Reuter, S.L. Hale, R. Zweigerdt, R.E. Graichen, G.L. Kay, A.J. Jyrala, A. Colman, B.P. Davidson, M. Pera, and R.A. Kloner, *Survival and maturation of human embryonic stem cell-derived cardiomyocytes in rat hearts*. J Mol Cell Cardiol, 2007. **43**(4): p. 504-16.
  182. Hubbard, S.A., A.M. Friel, B. Kumar, L. Zhang, B.R. Rueda, and C.E. Gargett, *Evidence for cancer stem cells in human endometrial carcinoma*. Cancer Res, 2009. **69**(21): p. 8241-8.
  183. Masuda, H., T. Maruyama, E. Hiratsu, J. Yamane, A. Iwanami, T. Nagashima, M. Ono, H. Miyoshi, H.J. Okano, M. Ito, N. Tamaoki, T. Nomura, H. Okano, Y. Matsuzaki, and Y. Yoshimura, *Noninvasive and real-time assessment of reconstructed functional human endometrium in NOD/SCID/gamma c(null) immunodeficient mice*. Proc Natl Acad Sci U S A, 2007. **104**(6): p. 1925-30.
  184. Kurita, T., R. Medina, A.B. Schabel, P. Young, P. Gama, T.V. Parekh, J. Brody, G.R. Cunha, K.G. Osteen, K.L. Bruner-Tran, and L.I. Gold, *The activation function-1 domain of estrogen receptor alpha in uterine stromal cells is required for mouse but not human uterine epithelial response to estrogen*. Differentiation, 2005. **73**(6): p. 313-22.

185. Bowsher, W., A. Carter, and Ebooks Corporation., *Challenges in prostate cancer*. 2006, Blackwell Pub.: Malden, Mass. ; Oxford. p. xii, 282 p., [4] p. of plates.
186. Kurita, T., K.J. Lee, P.S. Cooke, J.A. Taylor, D.B. Lubahn, and G.R. Cunha, *Paracrine regulation of epithelial progesterone receptor by estradiol in the mouse female reproductive tract*. Biol Reprod, 2000. **62**(4): p. 821-30.
187. Cunha, G.R. and A. Donjacour, *Mesenchymal-epithelial interactions: technical considerations*. Prog Clin Biol Res, 1987. **239**: p. 273-82.
188. Bigsby, R.M., P.S. Cooke, and G.R. Cunha, *A simple efficient method for separating murine uterine epithelial and mesenchymal cells*. Am J Physiol, 1986. **251**(5 Pt 1): p. E630-6.
189. Bowsher, W., *Challenges in prostate cancer*. 2000, Malden, MA: Blackwell Science.
190. Simon, L., G.C. Ekman, N. Kostereva, Z. Zhang, R.A. Hess, M.C. Hofmann, and P.S. Cooke, *Direct transdifferentiation of stem/progenitor spermatogonia into reproductive and nonreproductive tissues of all germ layers*. Stem Cells, 2009. **27**(7): p. 1666-75.
191. Oottamasathien, S., K. Williams, O.E. Franco, M.L. Wills, J.C. Thomas, A.R. Sharif-Afshar, R.T. DeMarco, J.W. Brock, 3rd, N.A. Bhowmick, S.W. Hayward, and J.C.t. Pope, *Urothelial inhibition of transforming growth factor-beta in a bladder tissue recombination model*. J Urol, 2007. **178**(4 Pt 2): p. 1643-9.
192. Li, X., Y. Wang, A.R. Sharif-Afshar, C. Uwamariya, A. Yi, K. Ishii, S.W. Hayward, R.J. Matusik, and N.A. Bhowmick, *Urothelial transdifferentiation to prostate epithelia is mediated by paracrine TGF-beta signaling*. Differentiation, 2009. **77**(1): p. 95-102.
193. Buchanan, D.L., T. Kurita, J.A. Taylor, D.B. Lubahn, G.R. Cunha, and P.S. Cooke, *Role of stromal and epithelial estrogen receptors in vaginal epithelial proliferation, stratification, and cornification*. Endocrinology, 1998. **139**(10): p. 4345-52.
194. Kurita, T., P. Young, J.R. Brody, J.P. Lydon, B.W. O'Malley, and G.R. Cunha, *Stromal progesterone receptors mediate the inhibitory effects of progesterone on estrogen-induced uterine epithelial cell deoxyribonucleic acid synthesis*. Endocrinology, 1998. **139**(11): p. 4708-13.
195. Trounson, A., *The production and directed differentiation of human embryonic stem cells*. Endocr Rev, 2006. **27**(2): p. 208-19.
196. Pera, M.F., B. Reubinoff, and A. Trounson, *Human embryonic stem cells*. J Cell Sci, 2000. **113** ( Pt 1): p. 5-10.
197. Avery, S., K. Inniss, and H. Moore, *The regulation of self-renewal in human embryonic stem cells*. Stem Cells Dev, 2006. **15**(5): p. 729-40.

198. Hyslop, L.A., L. Armstrong, M. Stojkovic, and M. Lako, *Human embryonic stem cells: biology and clinical implications*. Expert Rev Mol Med, 2005. **7**(19): p. 1-21.
199. Mountford, J.C., *Human embryonic stem cells: origins, characteristics and potential for regenerative therapy*. Transfus Med, 2008. **18**(1): p. 1-12.
200. Osafune, K., L. Caron, M. Borowiak, R.J. Martinez, C.S. Fitz-Gerald, Y. Sato, C.A. Cowan, K.R. Chien, and D.A. Melton, *Marked differences in differentiation propensity among human embryonic stem cell lines*. Nat Biotechnol, 2008. **26**(3): p. 313-5.
201. Costa, M., M. Dottori, E. Ng, S.M. Hawes, K. Sourris, P. Jamshidi, M.F. Pera, A.G. Elefanty, and E.G. Stanley, *The hESC line Envy expresses high levels of GFP in all differentiated progeny*. Nat Methods, 2005. **2**(4): p. 259-60.
202. Wolvetang, E.J., M.F. Pera, and K.S. Zuckerman, *Gap junction mediated transport of shRNA between human embryonic stem cells*. Biochem Biophys Res Commun, 2007. **363**(3): p. 610-5.
203. Davis, R.P., M. Costa, C. Grandela, A.M. Holland, T. Hatzistavrou, S.J. Micallef, X. Li, A.L. Goulburn, L. Azzola, A.G. Elefanty, and E.G. Stanley, *A protocol for removal of antibiotic resistance cassettes from human embryonic stem cells genetically modified by homologous recombination or transgenesis*. Nat Protoc, 2008. **3**(10): p. 1550-8.
204. Davis, R.P., E.S. Ng, M. Costa, A.K. Mossman, K. Sourris, A.G. Elefanty, and E.G. Stanley, *Targeting a GFP reporter gene to the MIXL1 locus of human embryonic stem cells identifies human primitive streak-like cells and enables isolation of primitive hematopoietic precursors*. Blood, 2008. **111**(4): p. 1876-84.
205. Ng, E.S., R. Davis, E.G. Stanley, and A.G. Elefanty, *A protocol describing the use of a recombinant protein-based, animal product-free medium (APEL) for human embryonic stem cell differentiation as spin embryoid bodies*. Nat Protoc, 2008. **3**(5): p. 768-76.
206. Hatzistavrou, T., S.J. Micallef, E.S. Ng, J. Vadolas, E.G. Stanley, and A.G. Elefanty, *ErythRED, a hESC line enabling identification of erythroid cells*. Nat Methods, 2009. **6**(9): p. 659-62.
207. Bretzner, F., F. Gilbert, F. Baylis, and R.M. Brownstone, *Target populations for first-in-human embryonic stem cell research in spinal cord injury*. Cell Stem Cell, 2011. **8**(5): p. 468-75.
208. Ellerstrom, C., R. Strehl, K. Noaksson, J. Hyllner, and H. Semb, *Facilitated expansion of human embryonic stem cells by single-cell enzymatic dissociation*. Stem Cells, 2007. **25**(7): p. 1690-6.

209. Costa, M., K. Sourris, T. Hatzistavrou, A.G. Elefanty, and E.G. Stanley, *Expansion of human embryonic stem cells in vitro*. Curr Protoc Stem Cell Biol, 2008. **Chapter 1**: p. Unit 1C 1 1-1C 1 7.
210. Amit, M., M.K. Carpenter, M.S. Inokuma, C.P. Chiu, C.P. Harris, M.A. Waknitz, J. Itskovitz-Eldor, and J.A. Thomson, *Clonally derived human embryonic stem cell lines maintain pluripotency and proliferative potential for prolonged periods of culture*. Dev Biol, 2000. **227**(2): p. 271-8.
211. Xu, C., M.S. Inokuma, J. Denham, K. Golds, P. Kundu, J.D. Gold, and M.K. Carpenter, *Feeder-free growth of undifferentiated human embryonic stem cells*. Nat Biotechnol, 2001. **19**(10): p. 971-4.
212. Amit, M., V. Margulets, H. Segev, K. Shariki, I. Laevsky, R. Coleman, and J. Itskovitz-Eldor, *Human feeder layers for human embryonic stem cells*. Biol Reprod, 2003. **68**(6): p. 2150-6.
213. Hovatta, O., M. Mikkola, K. Gertow, A.M. Stromberg, J. Inzunza, J. Hreinsson, B. Rozell, E. Blennow, M. Andang, and L. Ahrlund-Richter, *A culture system using human foreskin fibroblasts as feeder cells allows production of human embryonic stem cells*. Hum Reprod, 2003. **18**(7): p. 1404-9.
214. Inzunza, J., K. Gertow, M.A. Stromberg, E. Matilainen, E. Blennow, H. Skottman, S. Wolbank, L. Ahrlund-Richter, and O. Hovatta, *Derivation of human embryonic stem cell lines in serum replacement medium using postnatal human fibroblasts as feeder cells*. Stem Cells, 2005. **23**(4): p. 544-9.
215. Amit, M., C. Shariki, V. Margulets, and J. Itskovitz-Eldor, *Feeder layer- and serum-free culture of human embryonic stem cells*. Biol Reprod, 2004. **70**(3): p. 837-45.
216. Ludwig, T.E., M.E. Levenstein, J.M. Jones, W.T. Berggren, E.R. Mitchen, J.L. Frane, L.J. Crandall, C.A. Daigh, K.R. Conard, M.S. Piekarczyk, R.A. Llanas, and J.A. Thomson, *Derivation of human embryonic stem cells in defined conditions*. Nat Biotechnol, 2006. **24**(2): p. 185-7.
217. Reubinoff, B.E., M.F. Pera, C.Y. Fong, A. Trounson, and A. Bongso, *Embryonic stem cell lines from human blastocysts: somatic differentiation in vitro*. Nat Biotechnol, 2000. **18**(4): p. 399-404.
218. Itskovitz-Eldor, J., M. Schuldiner, D. Karsenti, A. Eden, O. Yanuka, M. Amit, H. Soreq, and N. Benvenisty, *Differentiation of human embryonic stem cells into embryoid bodies compromising the three embryonic germ layers*. Mol Med, 2000. **6**(2): p. 88-95.



219. Sachlos, E. and D.T. Auguste, *Embryoid body morphology influences diffusive transport of inductive biochemicals: a strategy for stem cell differentiation*. Biomaterials, 2008. **29**(34): p. 4471-80.
220. Kurosawa, H., *Methods for inducing embryoid body formation: in vitro differentiation system of embryonic stem cells*. J Biosci Bioeng, 2007. **103**(5): p. 389-98.
221. Wartenberg, M., J. Gunther, J. Hescheler, and H. Sauer, *The embryoid body as a novel in vitro assay system for antiangiogenic agents*. Lab Invest, 1998. **78**(10): p. 1301-14.
222. Ng, E.S., R.P. Davis, L. Azzola, E.G. Stanley, and A.G. Elefanty, *Forced aggregation of defined numbers of human embryonic stem cells into embryoid bodies fosters robust, reproducible hematopoietic differentiation*. Blood, 2005b. **106**(5): p. 1601-3.
223. Mummery, C., D. Ward, C.E. van den Brink, S.D. Bird, P.A. Doevendans, T. Opthof, A. Brutel de la Riviere, L. Tertoolen, M. van der Heyden, and M. Pera, *Cardiomyocyte differentiation of mouse and human embryonic stem cells*. J Anat, 2002. **200**(Pt 3): p. 233-42.
224. Chen, S.S., W. Fitzgerald, J. Zimmerberg, H.K. Kleinman, and L. Margolis, *Cell-cell and cell-extracellular matrix interactions regulate embryonic stem cell differentiation*. Stem Cells, 2007. **25**(3): p. 553-61.
225. Tam, P.P. and R.R. Behringer, *Mouse gastrulation: the formation of a mammalian body plan*. Mech Dev, 1997. **68**(1-2): p. 3-25.
226. Murry, C.E. and G. Keller, *Differentiation of embryonic stem cells to clinically relevant populations: lessons from embryonic development*. Cell, 2008. **132**(4): p. 661-80.
227. Parameswaran, M. and P.P. Tam, *Regionalisation of cell fate and morphogenetic movement of the mesoderm during mouse gastrulation*. Dev Genet, 1995. **17**(1): p. 16-28.
228. Kinder, S.J., T.E. Tsang, G.A. Quinlan, A.K. Hadjantonakis, A. Nagy, and P.P. Tam, *The orderly allocation of mesodermal cells to the extraembryonic structures and the anteroposterior axis during gastrulation of the mouse embryo*. Development, 1999. **126**(21): p. 4691-701.
229. Evseenko, D., Y. Zhu, K. Schenke-Layland, J. Kuo, B. Latour, S. Ge, J. Scholes, G. Dravid, X. Li, W.R. MacLellan, and G.M. Crooks, *Mapping the first stages of mesoderm commitment during differentiation of human embryonic stem cells*. Proc Natl Acad Sci U S A, 2010. **107**(31): p. 13742-7.
230. D'Amour, K.A., A.D. Agulnick, S. Eliazer, O.G. Kelly, E. Kroon, and E.E. Baetge, *Efficient differentiation of human embryonic stem cells to definitive endoderm*. Nat Biotechnol, 2005. **23**(12): p. 1534-41.

231. Gadue, P., T.L. Huber, M.C. Nostro, S. Kattman, and G.M. Keller, *Germ layer induction from embryonic stem cells*. Exp Hematol, 2005. **33**(9): p. 955-64.
232. Winnier, G., M. Blessing, P.A. Labosky, and B.L. Hogan, *Bone morphogenetic protein-4 is required for mesoderm formation and patterning in the mouse*. Genes Dev, 1995. **9**(17): p. 2105-16.
233. Mishina, Y., A. Suzuki, N. Ueno, and R.R. Behringer, *Bmpr encodes a type I bone morphogenetic protein receptor that is essential for gastrulation during mouse embryogenesis*. Genes Dev, 1995. **9**(24): p. 3027-37.
234. Beppu, H., M. Kawabata, T. Hamamoto, A. Chytil, O. Minowa, T. Noda, and K. Miyazono, *BMP type II receptor is required for gastrulation and early development of mouse embryos*. Dev Biol, 2000. **221**(1): p. 249-58.
235. Davis, S., S. Miura, C. Hill, Y. Mishina, and J. Klingensmith, *BMP receptor IA is required in the mammalian embryo for endodermal morphogenesis and ectodermal patterning*. Dev Biol, 2004. **270**(1): p. 47-63.
236. Finley, M.F., S. Devata, and J.E. Huettner, *BMP-4 inhibits neural differentiation of murine embryonic stem cells*. J Neurobiol, 1999. **40**(3): p. 271-87.
237. Gratsch, T.E. and K.S. O'Shea, *Noggin and chordin have distinct activities in promoting lineage commitment of mouse embryonic stem (ES) cells*. Dev Biol, 2002. **245**(1): p. 83-94.
238. ten Berge, D., W. Koole, C. Fuerer, M. Fish, E. Eroglu, and R. Nusse, *Wnt signaling mediates self-organization and axis formation in embryoid bodies*. Cell Stem Cell, 2008. **3**(5): p. 508-18.
239. Johansson, B.M. and M.V. Wiles, *Evidence for involvement of activin A and bone morphogenetic protein 4 in mammalian mesoderm and hematopoietic development*. Mol Cell Biol, 1995. **15**(1): p. 141-51.
240. Ng, E.S., L. Azzola, K. Sourris, L. Robb, E.G. Stanley, and A.G. Elefanty, *The primitive streak gene Mixl1 is required for efficient haematopoiesis and BMP4-induced ventral mesoderm patterning in differentiating ES cells*. Development, 2005a. **132**(5): p. 873-84.
241. Nostro, M.C., X. Cheng, G.M. Keller, and P. Gadue, *Wnt, activin, and BMP signaling regulate distinct stages in the developmental pathway from embryonic stem cells to blood*. Cell Stem Cell, 2008. **2**(1): p. 60-71.
242. Park, C., I. Afrikanova, Y.S. Chung, W.J. Zhang, E. Arentson, G. Fong Gh, A. Rosendahl, and K. Choi, *A hierarchical order of factors in the generation of FLK1- and*

- SCL-expressing hematopoietic and endothelial progenitors from embryonic stem cells.* Development, 2004. **131**(11): p. 2749-62.
243. Ying, Q.L., M. Stavridis, D. Griffiths, M. Li, and A. Smith, *Conversion of embryonic stem cells into neuroectodermal precursors in adherent monoculture.* Nat Biotechnol, 2003. **21**(2): p. 183-6.
  244. Bruce, S.J., R.W. Rea, A.L. Steptoe, M. Busslinger, J.F. Bertram, and A.C. Perkins, *In vitro differentiation of murine embryonic stem cells toward a renal lineage.* Differentiation, 2007. **75**(5): p. 337-49.
  245. Mae, S., S. Shirasawa, S. Yoshie, F. Sato, Y. Kanoh, H. Ichikawa, T. Yokoyama, F. Yue, D. Tomotsune, and K. Sasaki, *Combination of small molecules enhances differentiation of mouse embryonic stem cells into intermediate mesoderm through BMP7-positive cells.* Biochem Biophys Res Commun, 2010. **393**(4): p. 877-82.
  246. Liu, P., M. Wakamiya, M.J. Shea, U. Albrecht, R.R. Behringer, and A. Bradley, *Requirement for Wnt3 in vertebrate axis formation.* Nat Genet, 1999. **22**(4): p. 361-5.
  247. Kelly, O.G., K.I. Pinson, and W.C. Skarnes, *The Wnt co-receptors Lrp5 and Lrp6 are essential for gastrulation in mice.* Development, 2004. **131**(12): p. 2803-15.
  248. Tran, H.T., B. Sekkali, G. Van Imschoot, S. Janssens, and K. Vleminckx, *Wnt/beta-catenin signaling is involved in the induction and maintenance of primitive hematopoiesis in the vertebrate embryo.* Proc Natl Acad Sci U S A, 2010. **107**(37): p. 16160-5.
  249. Aubert, J., H. Dunstan, I. Chambers, and A. Smith, *Functional gene screening in embryonic stem cells implicates Wnt antagonism in neural differentiation.* Nat Biotechnol, 2002. **20**(12): p. 1240-5.
  250. Lindsley, R.C., J.G. Gill, M. Kyba, T.L. Murphy, and K.M. Murphy, *Canonical Wnt signaling is required for development of embryonic stem cell-derived mesoderm.* Development, 2006. **133**(19): p. 3787-96.
  251. Naito, A.T., I. Shiojima, H. Akazawa, K. Hidaka, T. Morisaki, A. Kikuchi, and I. Komuro, *Developmental stage-specific biphasic roles of Wnt/beta-catenin signaling in cardiomyogenesis and hematopoiesis.* Proc Natl Acad Sci U S A, 2006. **103**(52): p. 19812-7.
  252. Ueno, S., G. Weidinger, T. Osugi, A.D. Kohn, J.L. Golob, L. Pabon, H. Reinecke, R.T. Moon, and C.E. Murry, *Biphasic role for Wnt/beta-catenin signaling in cardiac specification in zebrafish and embryonic stem cells.* Proc Natl Acad Sci U S A, 2007. **104**(23): p. 9685-90.

253. Gadue, P., T.L. Huber, P.J. Paddison, and G.M. Keller, *Wnt and TGF-beta signaling are required for the induction of an in vitro model of primitive streak formation using embryonic stem cells*. Proc Natl Acad Sci U S A, 2006. **103**(45): p. 16806-11.
254. Lowe, L.A., S. Yamada, and M.R. Kuehn, *Genetic dissection of nodal function in patterning the mouse embryo*. Development, 2001. **128**(10): p. 1831-43.
255. Conlon, F.L., K.M. Lyons, N. Takaesu, K.S. Barth, A. Kispert, B. Herrmann, and E.J. Robertson, *A primary requirement for nodal in the formation and maintenance of the primitive streak in the mouse*. Development, 1994. **120**(7): p. 1919-28.
256. Schier, A.F. and M.M. Shen, *Nodal signalling in vertebrate development*. Nature, 2000. **403**(6768): p. 385-9.
257. Kubo, A., K. Shinozaki, J.M. Shannon, V. Kouskoff, M. Kennedy, S. Woo, H.J. Fehling, and G. Keller, *Development of definitive endoderm from embryonic stem cells in culture*. Development, 2004. **131**(7): p. 1651-62.
258. Ben-Haim, N., C. Lu, M. Guzman-Ayala, L. Pescatore, D. Mesnard, M. Bischofberger, F. Naef, E.J. Robertson, and D.B. Constam, *The nodal precursor acting via activin receptors induces mesoderm by maintaining a source of its convertases and BMP4*. Dev Cell, 2006. **11**(3): p. 313-23.
259. Fassler, R. and M. Meyer, *Consequences of lack of beta 1 integrin gene expression in mice*. Genes Dev, 1995. **9**(15): p. 1896-908.
260. Hynes, R.O., *Integrins: versatility, modulation, and signaling in cell adhesion*. Cell, 1992. **69**(1): p. 11-25.
261. Rohwedel, J., K. Guan, W. Zuschratter, S. Jin, G. Ahnert-Hilger, D. Furst, R. Fassler, and A.M. Wobus, *Loss of beta1 integrin function results in a retardation of myogenic, but an acceleration of neuronal, differentiation of embryonic stem cells in vitro*. Dev Biol, 1998. **201**(2): p. 167-84.
262. Cerdan, C., A. Rouleau, and M. Bhatia, *VEGF-A165 augments erythropoietic development from human embryonic stem cells*. Blood, 2004. **103**(7): p. 2504-12.
263. Daftary, G.S., U. Kayisli, E. Seli, O. Bukulmez, A. Arici, and H.S. Taylor, *Salpingectomy increases peri-implantation endometrial HOXA10 expression in women with hydrosalpinx*. Fertil Steril, 2007. **87**(2): p. 367-72.
264. Kennedy, M., S.L. D'Souza, M. Lynch-Kattman, S. Schwantz, and G. Keller, *Development of the hemangioblast defines the onset of hematopoiesis in human ES cell differentiation cultures*. Blood, 2007. **109**(7): p. 2679-87.

265. Pick, M., L. Azzola, A. Mossman, E.G. Stanley, and A.G. Elefanty, *Differentiation of human embryonic stem cells in serum-free medium reveals distinct roles for bone morphogenetic protein 4, vascular endothelial growth factor, stem cell factor, and fibroblast growth factor 2 in hematopoiesis*. Stem Cells, 2007. **25**(9): p. 2206-14.
266. Zhang, P., J. Li, Z. Tan, C. Wang, T. Liu, L. Chen, J. Yong, W. Jiang, X. Sun, L. Du, M. Ding, and H. Deng, *Short-term BMP-4 treatment initiates mesoderm induction in human embryonic stem cells*. Blood, 2008. **111**(4): p. 1933-41.
267. Woll, P.S., J.K. Morris, M.S. Painschab, R.K. Marcus, A.D. Kohn, T.L. Biechele, R.T. Moon, and D.S. Kaufman, *Wnt signaling promotes hematoendothelial cell development from human embryonic stem cells*. Blood, 2008. **111**(1): p. 122-31.
268. Evseenko, D., K. Schenke-Layland, G. Dravid, Y. Zhu, Q.L. Hao, J. Scholes, X.C. Wang, W.R. Maclellan, and G.M. Crooks, *Identification of the critical extracellular matrix proteins that promote human embryonic stem cell assembly*. Stem Cells Dev, 2009. **18**(6): p. 919-28.
269. Dambrot, C., R. Passier, D. Atsma, and C.L. Mummery, *Cardiomyocyte differentiation of pluripotent stem cells and their use as cardiac disease models*. Biochem J, 2011. **434**(1): p. 25-35.
270. Batchelder, C.A., C.C. Lee, D.G. Matsell, M.C. Yoder, and A.F. Tarantal, *Renal ontogeny in the rhesus monkey (Macaca mulatta) and directed differentiation of human embryonic stem cells towards kidney precursors*. Differentiation, 2009. **78**(1): p. 45-56.
271. Lin, S.A., G. Kolle, S.M. Grimmond, Q. Zhou, E. Doust, M.H. Little, B. Aronow, S.D. Ricardo, M.F. Pera, J.F. Bertram, and A.L. Laslett, *Subfractionation of differentiating human embryonic stem cell populations allows the isolation of a mesodermal population enriched for intermediate mesoderm and putative renal progenitors*. Stem Cells Dev, 2010. **19**(10): p. 1637-48.
272. Vazin, T. and W.J. Freed, *Human embryonic stem cells: derivation, culture, and differentiation: a review*. Restor Neurol Neurosci, 2010. **28**(4): p. 589-603.
273. Eritja, N., D. Llobet, M. Domingo, M. Santacana, A. Yeramian, X. Matias-Guiu, and X. Dolcet, *A novel three-dimensional culture system of polarized epithelial cells to study endometrial carcinogenesis*. Am J Pathol, 2010. **176**(6): p. 2722-31.
274. Kurita, T. and G.R. Cunha, *Roles of p63 in differentiation of Mullerian duct epithelial cells*. Ann N Y Acad Sci, 2001. **948**: p. 9-12.

275. Liu, J., K.L. Jones, H. Sumer, and P.J. Verma, *Stable transgene expression in human embryonic stem cells after simple chemical transfection*. Mol Reprod Dev, 2009. **76**(6): p. 580-6.
276. Zeng, Y., K. Opeskin, J. Goad, and E.D. Williams, *Tumor-induced activation of lymphatic endothelial cells via vascular endothelial growth factor receptor-2 is critical for prostate cancer lymphatic metastasis*. Cancer Res, 2006. **66**(19): p. 9566-75.
277. Cai, J., J. Chen, Y. Liu, T. Miura, Y. Luo, J.F. Loring, W.J. Freed, M.S. Rao, and X. Zeng, *Assessing self-renewal and differentiation in human embryonic stem cell lines*. Stem Cells, 2006. **24**(3): p. 516-30.
278. Draper, J.S., C. Pigott, J.A. Thomson, and P.W. Andrews, *Surface antigens of human embryonic stem cells: changes upon differentiation in culture*. J Anat, 2002. **200**(Pt 3): p. 249-58.
279. Cooke, M.J., M. Stojkovic, and S.A. Przyborski, *Growth of teratomas derived from human pluripotent stem cells is influenced by the graft site*. Stem Cells Dev, 2006. **15**(2): p. 254-9.
280. Przyborski, S.A., *Differentiation of human embryonic stem cells after transplantation in immune-deficient mice*. Stem Cells, 2005. **23**(9): p. 1242-50.
281. Kishi, Y., Y. Tanaka, H. Shibata, S. Nakamura, K. Takeuchi, S. Masuda, T. Ikeda, S. Muramatsu, and Y. Hanazono, *Variation in the incidence of teratomas after the transplantation of nonhuman primate ES cells into immunodeficient mice*. Cell Transplant, 2008. **17**(9): p. 1095-102.
282. Watanabe, K., M. Ueno, D. Kamiya, A. Nishiyama, M. Matsumura, T. Wataya, J.B. Takahashi, S. Nishikawa, K. Muguruma, and Y. Sasai, *A ROCK inhibitor permits survival of dissociated human embryonic stem cells*. Nat Biotechnol, 2007. **25**(6): p. 681-6.
283. Van Vranken, B.E., H.M. Romanska, J.M. Polak, H.J. Rippon, J.M. Shannon, and A.E. Bishop, *Coculture of embryonic stem cells with pulmonary mesenchyme: a microenvironment that promotes differentiation of pulmonary epithelium*. Tissue Eng, 2005. **11**(7-8): p. 1177-87.
284. Moser, F.G., B.P. Dorman, and F.H. Ruddle, *Mouse-human heterokaryon analysis with a 33258 Hoechst-Giemsa technique*. J Cell Biol, 1975. **66**(3): p. 676-80.
285. Young, B. and P.R. Wheater, *Wheater's functional histology : a text and colour atlas*. 5th ed. 2006, Edinburgh ; New York: Churchill Livingstone. x, 437 p.

286. Gertow, K., S. Wolbank, B. Rozell, R. Sugars, M. Andang, C.L. Parish, M.P. Imreh, M. Wendel, and L. Ahrlund-Richter, *Organized development from human embryonic stem cells after injection into immunodeficient mice*. Stem Cells Dev, 2004. **13**(4): p. 421-35.
287. Kolle, G., M. Ho, Q. Zhou, H.S. Chy, K. Krishnan, N. Cloonan, I. Bertoncello, A.L. Laslett, and S.M. Grimmond, *Identification of human embryonic stem cell surface markers by combined membrane-polysome translation state array analysis and immunotranscriptional profiling*. Stem Cells, 2009. **27**(10): p. 2446-56.
288. Hoffman, R.M., *In vivo imaging of metastatic cancer with fluorescent proteins*. Cell Death Differ, 2002. **9**(8): p. 786-9.
289. Bradley, J.A., E.M. Bolton, and R.A. Pedersen, *Stem cell medicine encounters the immune system*. Nat Rev Immunol, 2002. **2**(11): p. 859-71.
290. Drukker, M., G. Katz, A. Urbach, M. Schuldiner, G. Markel, J. Itskovitz-Eldor, B. Reubinoff, O. Mandelboim, and N. Benvenisty, *Characterization of the expression of MHC proteins in human embryonic stem cells*. Proc Natl Acad Sci U S A, 2002. **99**(15): p. 9864-9.
291. Koch, C.A., P. Geraldles, and J.L. Platt, *Immunosuppression by embryonic stem cells*. Stem Cells, 2008. **26**(1): p. 89-98.
292. Li, L., M.L. Baroja, A. Majumdar, K. Chadwick, A. Rouleau, L. Gallacher, I. Ferber, J. Lebkowski, T. Martin, J. Madrenas, and M. Bhatia, *Human embryonic stem cells possess immune-privileged properties*. Stem Cells, 2004. **22**(4): p. 448-56.
293. Drukker, M., H. Katchman, G. Katz, S. Even-Tov Friedman, E. Shezen, E. Hornstein, O. Mandelboim, Y. Reisner, and N. Benvenisty, *Human embryonic stem cells and their differentiated derivatives are less susceptible to immune rejection than adult cells*. Stem Cells, 2006. **24**(2): p. 221-9.
294. Swijnenburg, R.J., M. Tanaka, H. Vogel, J. Baker, T. Kofidis, F. Gunawan, D.R. Lebl, A.D. Caffarelli, J.L. de Bruin, E.V. Fedoseyeva, and R.C. Robbins, *Embryonic stem cell immunogenicity increases upon differentiation after transplantation into ischemic myocardium*. Circulation, 2005. **112**(9 Suppl): p. I166-72.
295. Matsune, H., D. Sakurai, Y. Niidome, S. Takenaka, and M. Kishida, *Relationship between degree of dynamic morphological change and proliferative potential of murine embryonic stem cells*. J Biosci Bioeng, 2008. **105**(1): p. 58-60.
296. Tanaka, Y., S. Nakamura, H. Shibata, Y. Kishi, T. Ikeda, S. Masuda, K. Sasaki, T. Abe, S. Hayashi, Y. Kitano, Y. Nagao, and Y. Hanazono, *Sustained macroscopic engraftment*

- of cynomolgus embryonic stem cells in xenogeneic large animals after in utero transplantation.* Stem Cells Dev, 2008. **17**(2): p. 367-81.
297. Choy, G., S. O'Connor, F.E. Diehn, N. Costouros, H.R. Alexander, P. Choyke, and S.K. Libutti, *Comparison of noninvasive fluorescent and bioluminescent small animal optical imaging.* Biotechniques, 2003. **35**(5): p. 1022-6, 1028-30.
  298. Sun, H., O.X. Shen, X.R. Wang, L. Zhou, S.Q. Zhen, and X.D. Chen, *Anti-thyroid hormone activity of bisphenol A, tetrabromobisphenol A and tetrachlorobisphenol A in an improved reporter gene assay.* Toxicol In Vitro, 2009. **23**(5): p. 950-4.
  299. Sarno, J.L., H.J. Kliman, and H.S. Taylor, *HOXA10, Pbx2, and Meis1 protein expression in the human endometrium: formation of multimeric complexes on HOXA10 target genes.* J Clin Endocrinol Metab, 2005. **90**(1): p. 522-8.
  300. Barnes, J.D., J.L. Crosby, C.M. Jones, C.V. Wright, and B.L. Hogan, *Embryonic expression of Lim-1, the mouse homolog of Xenopus Xlim-1, suggests a role in lateral mesoderm differentiation and neurogenesis.* Dev Biol, 1994. **161**(1): p. 168-78.
  301. Hukriede, N.A., T.E. Tsang, R. Habas, P.L. Khoo, K. Steiner, D.L. Weeks, P.P. Tam, and I.B. Dawid, *Conserved requirement of Lim1 function for cell movements during gastrulation.* Dev Cell, 2003. **4**(1): p. 83-94.
  302. Shawlot, W. and R.R. Behringer, *Requirement for Lim1 in head-organizer function.* Nature, 1995. **374**(6521): p. 425-30.
  303. Kania, A., R.L. Johnson, and T.M. Jessell, *Coordinate roles for LIM homeobox genes in directing the dorsoventral trajectory of motor axons in the vertebrate limb.* Cell, 2000. **102**(2): p. 161-73.
  304. Liu, W., J.H. Wang, and M. Xiang, *Specific expression of the LIM/homeodomain protein Lim-1 in horizontal cells during retinogenesis.* Dev Dyn, 2000. **217**(3): p. 320-5.
  305. Oatley, J.M., M.R. Avarbock, and R.L. Brinster, *Glial cell line-derived neurotrophic factor regulation of genes essential for self-renewal of mouse spermatogonial stem cells is dependent on Src family kinase signaling.* J Biol Chem, 2007. **282**(35): p. 25842-51.
  306. Dong, W.F., H.H. Heng, R. Lowsky, Y. Xu, J.F. DeCoteau, X.M. Shi, L.C. Tsui, and M.D. Minden, *Cloning, expression, and chromosomal localization to 11p12-13 of a human LIM/HOMEBOX gene, hLim-1.* DNA Cell Biol, 1997. **16**(6): p. 671-8.
  307. Dormoy, V., S. Danilin, V. Lindner, L. Thomas, S. Rothhut, C. Coquard, J.J. Helwig, D. Jacqmin, H. Lang, and T. Massfelder, *The sonic hedgehog signaling pathway is reactivated in human renal cell carcinoma and plays orchestral role in tumor growth.* Mol Cancer, 2009. **8**: p. 123.



308. Poche, R.A., K.M. Kwan, M.A. Raven, Y. Furuta, B.E. Reese, and R.R. Behringer, *Lim1 is essential for the correct laminar positioning of retinal horizontal cells*. J Neurosci, 2007. **27**(51): p. 14099-107.
309. Suga, A., M. Taira, and S. Nakagawa, *LIM family transcription factors regulate the subtype-specific morphogenesis of retinal horizontal cells at post-migratory stages*. Dev Biol, 2009. **330**(2): p. 318-28.
310. Pillai, A., A. Mansouri, R. Behringer, H. Westphal, and M. Goulding, *Lhx1 and Lhx5 maintain the inhibitory-neurotransmitter status of interneurons in the dorsal spinal cord*. Development, 2007. **134**(2): p. 357-66.
311. Ye, L., R. Mayberry, C.Y. Lo, K.L. Britt, E.G. Stanley, A.G. Elefanty, and C.E. Gargett, *Generation of human female reproductive tract epithelium from human embryonic stem cells*. PLoS One, 2011. **6**(6): p. e21136.
312. Noyes, R.W., A.T. Hertig, and J. Rock, *Dating the endometrial biopsy*. Am J Obstet Gynecol, 1975. **122**(2): p. 262-3.
313. Hubscher, C.H., D.L. Brooks, and J.R. Johnson, *A quantitative method for assessing stages of the rat estrous cycle*. Biotech Histochem, 2005. **80**(2): p. 79-87.
314. Mo, B., A.E. Vendrov, W.A. Palomino, B.R. DuPont, K.B. Apparao, and B.A. Lessey, *ECC-1 cells: a well-differentiated steroid-responsive endometrial cell line with characteristics of luminal epithelium*. Biol Reprod, 2006. **75**(3): p. 387-94.
315. Nishida, M., K. Kasahara, M. Kaneko, H. Iwasaki, and K. Hayashi, *[Establishment of a new human endometrial adenocarcinoma cell line, Ishikawa cells, containing estrogen and progesterone receptors]*. Nippon Sanka Fujinka Gakkai Zasshi, 1985. **37**(7): p. 1103-11.
316. Kuramoto, H., S. Tamura, and Y. Notake, *Establishment of a cell line of human endometrial adenocarcinoma in vitro*. Am J Obstet Gynecol, 1972. **114**(8): p. 1012-9.
317. Fu, J., L. Bian, L. Zhao, Z. Dong, X. Gao, H. Luan, Y. Sun, and H. Song, *Identification of genes for normalization of quantitative real-time PCR data in ovarian tissues*. Acta Biochim Biophys Sin (Shanghai), 2010. **42**(8): p. 568-74.
318. Hvid, H., C.T. Ekstrom, S. Vienberg, M.B. Oleksiewicz, and R. Klopfeisch, *Identification of stable and oestrus cycle-independent housekeeping genes in the rat mammary gland and other tissues*. Vet J, 2010.
319. Conti, C.J., E.A. Conner, I.B. Gimenez-Conti, S.G. Silverberg, and L.E. Gerschenson, *Regulation of ciliogenesis and proliferation of uterine epithelium by 20 alpha-hydroxy-*

- pregn-4-en-3-one administration and withdrawal in ovariectomized rabbits*. Biol Reprod, 1981. **24**(4): p. 903-11.
320. Masuda, H., Y. Matsuzaki, E. Hiratsu, M. Ono, T. Nagashima, T. Kajitani, T. Arase, H. Oda, H. Uchida, H. Asada, M. Ito, Y. Yoshimura, T. Maruyama, and H. Okano, *Stem cell-like properties of the endometrial side population: implication in endometrial regeneration*. PLoS One, 2010. **5**(4): p. e10387.
  321. Gargett, C.E., K.E. Schwab, R.M. Zillwood, H.P. Nguyen, and D. Wu, *Isolation and Culture of Epithelial Progenitors and Mesenchymal Stem Cells from Human Endometrium*. Biol Reprod, 2009.
  322. Dahl, L., K. Richter, A.C. Hagglund, and L. Carlsson, *Lhx2 expression promotes self-renewal of a distinct multipotential hematopoietic progenitor cell in embryonic stem cell-derived embryoid bodies*. PLoS One, 2008. **3**(4): p. e2025.
  323. Rhee, H., L. Polak, and E. Fuchs, *Lhx2 maintains stem cell character in hair follicles*. Science, 2006. **312**(5782): p. 1946-9.
  324. Tornqvist, G., A. Sandberg, A.C. Hagglund, and L. Carlsson, *Cyclic expression of lhx2 regulates hair formation*. PLoS Genet, 2010. **6**(4): p. e1000904.
  325. Muttukrishna, S., P.A. Fowler, L. George, N.P. Groome, and P.G. Knight, *Changes in peripheral serum levels of total activin A during the human menstrual cycle and pregnancy*. J Clin Endocrinol Metab, 1996. **81**(9): p. 3328-34.
  326. Drews, C., S. Senkel, and G.U. Ryffel, *The nephrogenic potential of the transcription factors *osr1*, *osr2*, *hnf1b*, *lhx1* and *pax8* assessed in *Xenopus* animal caps*. BMC Dev Biol, 2011. **11**: p. 5.
  327. Rebbert, M.L. and I.B. Dawid, *Transcriptional regulation of the *Xlim-1* gene by activin is mediated by an element in intron I*. Proc Natl Acad Sci U S A, 1997. **94**(18): p. 9717-22.
  328. Dormoy, V., C. Beraud, V. Lindner, L. Thomas, C. Coquard, M. Barthelmebs, D. Jacqmin, H. Lang, and T. Massfelder, *LIM-class homeobox gene *Lim1*, a novel oncogene in human renal cell carcinoma*. Oncogene, 2010. **30**(15): p. 1753-63.
  329. Bowen, N.J., L.D. Walker, L.V. Matyunina, S. Logani, K.A. Totten, B.B. Benigno, and J.F. McDonald, *Gene expression profiling supports the hypothesis that human ovarian surface epithelia are multipotent and capable of serving as ovarian cancer initiating cells*. BMC Med Genomics, 2009. **2**: p. 71.
  330. Chung, T.K., T.H. Cheung, N.Y. Huen, K.W. Wong, K.W. Lo, S.F. Yim, N.S. Siu, Y.M. Wong, P.T. Tsang, M.W. Pang, M.Y. Yu, K.F. To, S.C. Mok, V.W. Wang, C. Li, A.Y. Cheung, G. Doran, M.J. Birrer, D.I. Smith, and Y.F. Wong, *Dysregulated microRNAs*

- and their predicted targets associated with endometrioid endometrial adenocarcinoma in Hong Kong women.* Int J Cancer, 2009. **124**(6): p. 1358-65.
331. Boren, T., Y. Xiong, A. Hakam, R. Wenham, S. Apte, Z. Wei, S. Kamath, D.T. Chen, H. Dressman, and J.M. Lancaster, *MicroRNAs and their target messenger RNAs associated with endometrial carcinogenesis.* Gynecol Oncol, 2008. **110**(2): p. 206-15.
  332. Agrawal, R., U. Tran, and O. Wessely, *The miR-30 miRNA family regulates Xenopus pronephros development and targets the transcription factor Xlim1/Lhx1.* Development, 2009. **136**(23): p. 3927-36.
  333. Bischof, P., *What do we know about the origin of CA 125?* Eur J Obstet Gynecol Reprod Biol, 1993. **49**(1-2): p. 93-8.
  334. Merjava, S., A. Neuwirth, V. Mandys, and K. Jirsova, *Cytokeratins 8 and 18 in adult human corneal endothelium.* Exp Eye Res, 2009. **89**(3): p. 426-31.
  335. Acampora, D., L.G. Di Giovannantonio, M. Di Salvio, P. Mancuso, and A. Simeone, *Selective inactivation of Otx2 mRNA isoforms reveals isoform-specific requirement for visceral endoderm anteriorization and head morphogenesis and highlights cell diversity in the visceral endoderm.* Mech Dev, 2009. **126**(10): p. 882-97.
  336. Karavanov, A.A., J.P. Saint-Jeannet, I. Karavanova, M. Taira, and I.B. Dawid, *The LIM homeodomain protein Lim-1 is widely expressed in neural, neural crest and mesoderm derivatives in vertebrate development.* Int J Dev Biol, 1996. **40**(2): p. 453-61.
  337. Basak, O. and V. Taylor, *Identification of self-replicating multipotent progenitors in the embryonic nervous system by high Notch activity and Hes5 expression.* Eur J Neurosci, 2007. **25**(4): p. 1006-22.
  338. Reubinoff, B.E., P. Itsykson, T. Turetsky, M.F. Pera, E. Reinhardt, A. Itzik, and T. Ben-Hur, *Neural progenitors from human embryonic stem cells.* Nat Biotechnol, 2001. **19**(12): p. 1134-40.
  339. Kaufman, D.S., E.T. Hanson, R.L. Lewis, R. Auerbach, and J.A. Thomson, *Hematopoietic colony-forming cells derived from human embryonic stem cells.* Proc Natl Acad Sci U S A, 2001. **98**(19): p. 10716-21.
  340. Kim, S.J., B.S. Kim, S.W. Ryu, J.H. Yoo, J.H. Oh, C.H. Song, S.H. Kim, D.S. Choi, J.H. Seo, C.W. Choi, S.W. Shin, Y.H. Kim, and J.S. Kim, *Hematopoietic differentiation of embryoid bodies derived from the human embryonic stem cell line SNUhES3 in co-culture with human bone marrow stromal cells.* Yonsei Med J, 2005. **46**(5): p. 693-9.

341. Vodyanik, M.A., J.A. Bork, J.A. Thomson, and Slukvin, II, *Human embryonic stem cell-derived CD34+ cells: efficient production in the coculture with OP9 stromal cells and analysis of lymphohematopoietic potential*. Blood, 2005. **105**(2): p. 617-26.
342. Yue, F., K. Johkura, D. Tomotsune, S. Shirasawa, T. Yokoyama, M. Nagai, and K. Sasaki, *Bone marrow stromal cells as an inducer for cardiomyocyte differentiation from mouse embryonic stem cells*. Ann Anat, 2010. **192**(5): p. 314-21.
343. Zeng, X., T. Miura, Y. Luo, B. Bhattacharya, B. Condie, J. Chen, I. Ginis, I. Lyons, J. Mejido, R.K. Puri, M.S. Rao, and W.J. Freed, *Properties of pluripotent human embryonic stem cells BG01 and BG02*. Stem Cells, 2004. **22**(3): p. 292-312.
344. Gong, J., O. Sagiv, H. Cai, S.H. Tsang, and L.V. Del Priore, *Effects of extracellular matrix and neighboring cells on induction of human embryonic stem cells into retinal or retinal pigment epithelial progenitors*. Exp Eye Res, 2008. **86**(6): p. 957-65.
345. Xu, M., R. Uemura, Y. Dai, Y. Wang, Z. Pasha, and M. Ashraf, *In vitro and in vivo effects of bone marrow stem cells on cardiac structure and function*. J Mol Cell Cardiol, 2007. **42**(2): p. 441-8.
346. Vazin, T., K.G. Becker, J. Chen, C.E. Spivak, C.R. Lupica, Y. Zhang, L. Worden, and W.J. Freed, *A novel combination of factors, termed SPIE, which promotes dopaminergic neuron differentiation from human embryonic stem cells*. PLoS One, 2009. **4**(8): p. e6606.
347. Du, P., W.A. Kibbe, and S.M. Lin, *lumi: a pipeline for processing Illumina microarray*. Bioinformatics, 2008. **24**(13): p. 1547-8.
348. Dennis, G., Jr., B.T. Sherman, D.A. Hosack, J. Yang, W. Gao, H.C. Lane, and R.A. Lempicki, *DAVID: Database for Annotation, Visualization, and Integrated Discovery*. Genome Biol, 2003. **4**(5): p. P3.
349. Huang da, W., B.T. Sherman, and R.A. Lempicki, *Systematic and integrative analysis of large gene lists using DAVID bioinformatics resources*. Nat Protoc, 2009. **4**(1): p. 44-57.
350. Blaney Davidson, E.N., E.L. Vitters, F.M. Mooren, N. Oliver, W.B. Berg, and P.M. van der Kraan, *Connective tissue growth factor/CCN2 overexpression in mouse synovial lining results in transient fibrosis and cartilage damage*. Arthritis Rheum, 2006. **54**(5): p. 1653-61.
351. Medici, D., E.D. Hay, and B.R. Olsen, *Snail and Slug promote epithelial-mesenchymal transition through beta-catenin-T-cell factor-4-dependent expression of transforming growth factor-beta3*. Mol Biol Cell, 2008. **19**(11): p. 4875-87.

352. Surveyor, G.A. and D.R. Brigstock, *Immunohistochemical localization of connective tissue growth factor (CTGF) in the mouse embryo between days 7.5 and 14.5 of gestation*. Growth Factors, 1999. **17**(2): p. 115-24.
353. Yin, Q., H.Y. Nan, W.H. Zhang, L.F. Yan, G.B. Cui, X.F. Huang, and J.G. Wei, *Pulmonary microvascular endothelial cells from bleomycin-induced rats promote the transformation and collagen synthesis of fibroblasts*. J Cell Physiol, 2010.
354. Zhou, G., C. Li, and L. Cai, *Advanced glycation end-products induce connective tissue growth factor-mediated renal fibrosis predominantly through transforming growth factor beta-independent pathway*. Am J Pathol, 2004. **165**(6): p. 2033-43.
355. Heng, N.H., P.D. N'Guessan, B.M. Kleber, J.P. Bernimoulin, and N. Pischon, *Enamel matrix derivative induces connective tissue growth factor expression in human osteoblastic cells*. J Periodontol, 2007. **78**(12): p. 2369-79.
356. Shook, D. and R. Keller, *Mechanisms, mechanics and function of epithelial-mesenchymal transitions in early development*. Mech Dev, 2003. **120**(11): p. 1351-83.
357. Burns, W.C., S.M. Twigg, J.M. Forbes, J. Pete, C. Tikellis, V. Thallas-Bonke, M.C. Thomas, M.E. Cooper, and P. Kantharidis, *Connective tissue growth factor plays an important role in advanced glycation end product-induced tubular epithelial-to-mesenchymal transition: implications for diabetic renal disease*. J Am Soc Nephrol, 2006. **17**(9): p. 2484-94.
358. McLennan, S.V., X.Y. Wang, V. Moreno, D.K. Yue, and S.M. Twigg, *Connective tissue growth factor mediates high glucose effects on matrix degradation through tissue inhibitor of matrix metalloproteinase type 1: implications for diabetic nephropathy*. Endocrinology, 2004. **145**(12): p. 5646-55.
359. Moussad, E.E. and D.R. Brigstock, *Connective tissue growth factor: what's in a name?* Mol Genet Metab, 2000. **71**(1-2): p. 276-92.
360. Bradham, D.M., A. Igarashi, R.L. Potter, and G.R. Grotendorst, *Connective tissue growth factor: a cysteine-rich mitogen secreted by human vascular endothelial cells is related to the SRC-induced immediate early gene product CEF-10*. J Cell Biol, 1991. **114**(6): p. 1285-94.
361. Bork, P., *The modular architecture of a new family of growth regulators related to connective tissue growth factor*. FEBS Lett, 1993. **327**(2): p. 125-30.
362. Brigstock, D.R., *The connective tissue growth factor/cysteine-rich 61/nephroblastoma overexpressed (CCN) family*. Endocr Rev, 1999. **20**(2): p. 189-206.

363. Lau, L.F. and S.C. Lam, *The CCN family of angiogenic regulators: the integrin connection*. Exp Cell Res, 1999. **248**(1): p. 44-57.
364. Grotendorst, G.R., H. Okochi, and N. Hayashi, *A novel transforming growth factor beta response element controls the expression of the connective tissue growth factor gene*. Cell Growth Differ, 1996. **7**(4): p. 469-80.
365. Igarashi, A., H. Okochi, D.M. Bradham, and G.R. Grotendorst, *Regulation of connective tissue growth factor gene expression in human skin fibroblasts and during wound repair*. Mol Biol Cell, 1993. **4**(6): p. 637-45.
366. Okada, H., T. Kikuta, T. Kobayashi, T. Inoue, Y. Kanno, M. Takigawa, T. Sugaya, J.B. Kopp, and H. Suzuki, *Connective tissue growth factor expressed in tubular epithelium plays a pivotal role in renal fibrogenesis*. J Am Soc Nephrol, 2005. **16**(1): p. 133-43.
367. Conrad, F.G., H.R. Bales, Jr., M.F. Allen, and R.G. Rossing, *Hazard rate of recurrence in germinal cell tumors of the testis*. Aerosp Med, 1972. **43**(8): p. 893-7.
368. Schwab, J.M., R. Beschoner, T.D. Nguyen, R. Meyermann, and H.J. Schluesener, *Differential cellular accumulation of connective tissue growth factor defines a subset of reactive astrocytes, invading fibroblasts, and endothelial cells following central nervous system injury in rats and humans*. J Neurotrauma, 2001. **18**(4): p. 377-88.
369. Han, Y., N. Li, X. Tian, J. Kang, C. Yan, and Y. Qi, *Endogenous transforming growth factor (TGF) beta1 promotes differentiation of smooth muscle cells from embryonic stem cells: stable plasmid-based siRNA silencing of TGF beta1 gene expression*. J Physiol Sci, 2009. **60**(1): p. 35-41.
370. Hughes, J.N., J.M. Washington, Z. Zheng, X.K. Lau, C. Yap, P.D. Rathjen, and J. Rathjen, *Manipulation of cell:cell contacts and mesoderm suppressing activity direct lineage choice from pluripotent primitive ectoderm-like cells in culture*. PLoS One, 2009. **4**(5): p. e5579.
371. Lee, C.H., E.K. Moiola, and J.J. Mao, *Fibroblastic differentiation of human mesenchymal stem cells using connective tissue growth factor*. Conf Proc IEEE Eng Med Biol Soc, 2006. **1**: p. 775-8.
372. Wang, J.J., F. Ye, L.J. Cheng, Y.J. Shi, J. Bao, H.Q. Sun, W. Wang, P. Zhang, and H. Bu, *Osteogenic differentiation of mesenchymal stem cells promoted by overexpression of connective tissue growth factor*. J Zhejiang Univ Sci B, 2009. **10**(5): p. 355-67.
373. Riser, B.L., M. Denichilo, P. Cortes, C. Baker, J.M. Grondin, J. Yee, and R.G. Narins, *Regulation of connective tissue growth factor activity in cultured rat mesangial cells and*

- its expression in experimental diabetic glomerulosclerosis*. J Am Soc Nephrol, 2000. **11**(1): p. 25-38.
374. Katsube, K., K. Sakamoto, Y. Tamamura, and A. Yamaguchi, *Role of CCN, a vertebrate specific gene family, in development*. Dev Growth Differ, 2009. **51**(1): p. 55-67.
  375. Abreu, J.G., N.I. Ketpura, B. Reversade, and E.M. De Robertis, *Connective-tissue growth factor (CTGF) modulates cell signalling by BMP and TGF-beta*. Nat Cell Biol, 2002. **4**(8): p. 599-604.
  376. Mercurio, S., B. Latinkic, N. Itasaki, R. Krumlauf, and J.C. Smith, *Connective-tissue growth factor modulates WNT signalling and interacts with the WNT receptor complex*. Development, 2004. **131**(9): p. 2137-47.
  377. Alev, C., Y. Wu, T. Kasukawa, L.M. Jakt, H.R. Ueda, and G. Sheng, *Transcriptomic landscape of the primitive streak*. Development, 2010. **137**(17): p. 2863-74.
  378. Krikun, G., G. Mor, A. Alvero, S. Guller, F. Schatz, E. Sapi, M. Rahman, R. Caze, M. Qumsiyeh, and C.J. Lockwood, *A novel immortalized human endometrial stromal cell line with normal progestational response*. Endocrinology, 2004. **145**(5): p. 2291-6.
  379. Stemmler, M.P., A. Hecht, B. Kinzel, and R. Kemler, *Analysis of regulatory elements of E-cadherin with reporter gene constructs in transgenic mouse embryos*. Dev Dyn, 2003. **227**(2): p. 238-45.
  380. Blum, M., S.J. Gaunt, K.W. Cho, H. Steinbeisser, B. Blumberg, D. Bittner, and E.M. De Robertis, *Gastrulation in the mouse: the role of the homeobox gene goosecoid*. Cell, 1992. **69**(7): p. 1097-106.
  381. Hart, A.H., L. Hartley, K. Sourris, E.S. Stadler, R. Li, E.G. Stanley, P.P. Tam, A.G. Elefanty, and L. Robb, *Mixl1 is required for axial mesendoderm morphogenesis and patterning in the murine embryo*. Development, 2002. **129**(15): p. 3597-608.
  382. Pearce, J.J. and M.J. Evans, *Mml, a mouse Mix-like gene expressed in the primitive streak*. Mech Dev, 1999. **87**(1-2): p. 189-92.
  383. Mugford, J.W., P. Sipila, J.A. McMahon, and A.P. McMahon, *Osrl expression demarcates a multi-potent population of intermediate mesoderm that undergoes progressive restriction to an Osrl-dependent nephron progenitor compartment within the mammalian kidney*. Dev Biol, 2008. **324**(1): p. 88-98.
  384. Wang, Q., Y. Lan, E.S. Cho, K.M. Maltby, and R. Jiang, *Odd-skipped related 1 (Odd 1) is an essential regulator of heart and urogenital development*. Dev Biol, 2005. **288**(2): p. 582-94.

385. Nieto, M.A., M.F. Bennett, M.G. Sargent, and D.G. Wilkinson, *Cloning and developmental expression of Sna, a murine homologue of the Drosophila snail gene*. Development, 1992. **116**(1): p. 227-37.
386. Nieto, M.A., M.G. Sargent, D.G. Wilkinson, and J. Cooke, *Control of cell behavior during vertebrate development by Slug, a zinc finger gene*. Science, 1994. **264**(5160): p. 835-9.
387. Franke, W.W., C. Grund, C. Kuhn, B.W. Jackson, and K. Illmensee, *Formation of cytoskeletal elements during mouse embryogenesis. III. Primary mesenchymal cells and the first appearance of vimentin filaments*. Differentiation, 1982. **23**(1): p. 43-59.
388. Lane, E.B., B.L. Hogan, M. Kurkinen, and J.I. Garrels, *Co-expression of vimentin and cytokeratins in parietal endoderm cells of early mouse embryo*. Nature, 1983. **303**(5919): p. 701-4.
389. Hobert, O. and H. Westphal, *Functions of LIM-homeobox genes*. Trends Genet, 2000. **16**(2): p. 75-83.
390. Hunter, C.S. and S.J. Rhodes, *LIM-homeodomain genes in mammalian development and human disease*. Mol Biol Rep, 2005. **32**(2): p. 67-77.
391. Zeng, X., J. Cai, J. Chen, Y. Luo, Z.B. You, E. Fotter, Y. Wang, B. Harvey, T. Miura, C. Backman, G.J. Chen, M.S. Rao, and W.J. Freed, *Dopaminergic differentiation of human embryonic stem cells*. Stem Cells, 2004. **22**(6): p. 925-40.
392. Gargett, C.E. and D.L. Healy, *Generating receptive endometrium in Asherman's syndrome*. J Hum Reprod Sci, 2011. **4**(1): p. 49-52.